Electronic Thesis and Dissertation Repository

7-3-2014 12:00 AM

Sox9 conditional knockdown reduces chondroitin sulphate proteoglycan expression, increases neuroplasticity, and improves motor function in a mouse model of spinal cord injury

William M. McKillop
The University of Western Ontario

Supervisor
Dr. Arthur Brown
The University of Western Ontario

Graduate Program in Anatomy and Cell Biology
A thesis submitted in partial fulfillment of the requirements for the degree in Doctor of Philosophy
© William M. McKillop 2014

SOX9 CONDITIONAL KNOCKDOWN REDUCES CHONDROITIN SULFATE
PROTEOGLYCAN EXPRESSION, INCREASES NEUROPLASTICITY, AND IMPROVES
MOTOR FUNCTION IN A MOUSE MODEL OF SPINAL CORD INJURY

(Thesis format: Integrated-Article)

by

William M. McKillop

Graduate Program in Anatomy and Cell Biology

A thesis submitted in partial fulfillment

of the requirements for the degree of

Doctor of Philosophy

The School of Graduate and Postdoctoral Studies

The University of Western Ontario

London, Ontario, Canada

Abstract

      This thesis investigates the effect of *Sox9* knockdown on anti-regenerative scar gene expression, neuroplasticity, and hind limb functional recovery following mouse spinal cord injury. We hypothesized that *Sox9* knockdown would reduce expression of anti-regenerative chondroitin sulfate proteoglycans both at the lesion site and at sites distant to the injury, thus providing an avenue for increased neuroplasticity and locomotor recovery after spinal cord injury. The first chapter provides a general introduction to the biological problem of spinal cord injury. The development of the glial scar and expression of the anti-regenerative chondroitin sulfate proteoglycan (CSPG) extracellular matrix is introduced, and *Sox9* is identified as a transcription factor that may control expression of these anti-regenerative genes. The second chapter is a manuscript that describes the molecular changes and improved locomotor function seen when *Sox9* knockdown is carried out just prior to spinal cord injury. The third chapter is more clinically relevant as it is a manuscript detailing the effects of *Sox9* knockdown after spinal cord injury on the recovery of hind limb motor function. The fourth chapter is a manuscript investigating the neuro-anatomical mechanism of the improved functional recovery seen in *Sox9* knockdown mice after spinal cord injury. The fifth chapter reflects on the findings presented herein, and suggests possible future plans of study. This dissertation demonstrates that inhibition of *Sox9* leads to reduced CSPG expression, improved hind limb function, and increased total locomotion. It further provides compelling evidence that increased neuroplasticity as evidenced by increased reactive sprouting and increased expression of the presynaptic markers synaptophysin and VGLUT1 caudal to the injury site underlies the improved neurological recovery observed in spinal cord injured *Sox9* conditional knockdown mice.

Key words: spinal cord injury, *Sox9*, chondroitin sulfate proteoglycans, neuroplasticity, reactive sprouting

Co-authorship

Chapter 2 of this dissertation was co-authored for publication by myself, Magda Dragan, Dr. Andreas Schedl, and Dr. Arthur Brown. Magda Dragan was instrumental in developing astrocyte cell culture techniques. Chapter 3 of this dissertation has been submitted for publication co-authored by myself, Eli York, and Dr. Arthur Brown. Eli York assisted in the day to day care of the mice used for the delayed knockdown experiment, the evaluation of their locomotor activity, and the spinal tissue cryosectioning as well as GFAP and CSPG immunostaining of sectioned spinal cords. Chapter 4 of this dissertation has been prepared for publication co-authored by myself, Dr. Todd Hryciw, Dr. Kathy Xu, Dr. Nicole Geremia, and Dr. Arthur Brown. Dr. Todd Hryciw performed the BDA injections into the mouse primary motor cortex. Dr. Kathy Xu helped to develop the BDA and fluorogold quantification techniques. Dr. Nicole Geremia helped to develop the fluorogold administration technique. In each of these studies, I planned and executed the experiments and completed the analysis of results with the aforementioned assistance. Dr. Andreas Schedl contributed the $Sox9^{flox/flox}$ mice for our usage. Dr. Arthur Brown conceptualized much of the experimental design, provided appropriate guidance, assisted with technical problems, and edited manuscripts. Dr. Arthur Brown also secured the funding and provided the facilities required to complete this work.

Acknowledgements

Thank you to my supervisor and mentor Dr. Arthur Brown and to the members of my advisory committee, Dr. Vania Prado, Dr. Nagalingam Rajakumar, and Dr. Lique Coolen for their guidance and assistance. I would also like to thank Dr. Greg Dekaban for all of his assistance over the years, and Dr. Lynne Weaver for help with manuscript preparation.

I must extend a special thank you to Anna Pniak, Eli York, Dr. Kathy Xu, Dr. Todd Hryciw, and Dr. Nicole Geremia who each directly affected this project. Thank you to the Brown laboratory personnel; Stephen McDonald, Bethany Bass, Trina Rosenzweig, Vanessa Omaña, John Pierce, Daniel Bottner, and Luc Rubinger, Dekaban laboratory personnel; Dr. Kemi Adeyanju, Christy Willert, Sonali de Chickera, Ryan Buensuceso, Bryan Au, Robarts Research Institute students; Arthur Lau, Cynthia Tang, and Peter Mitsopoulos, and finally my friends from outside Western; Susan Sheng, Arash Behravan, Kevin Tsin, and Howard Fung. Each of these people contributed something important to this project along the way.

Finally I would like to thank my parents Brian and Renee McKillop for their guidance, love, and support.

This work could not have been completed without funding from the National Science and Education Research Council of Canada, the Ontario Graduate Scholarship program, the Canadian Institutes of Health Research, and the University of Western Ontario.

Dedication

This work is dedicated to anyone with a spinal cord injury

Table of Contents

Chapter 4: Sox9 knockdown promotes neuroplasticity after spinal cord injury

List of Abbreviations

AANS/CNS – American Association of Neurological Surgeons/Congress of Neurological Surgeons

ANOVA – analysis of variance

BBB – blood brain barrier

BMS – Basso Mouse Scale

BDNF – brain derived neurotrophic factor

C4ST – Chondroitin-4 sulfotransferase

CNS – central nervous system

CPG – central pattern generator

CSPG – chondroitin sulfate proteoglycans

DRG – dorsal root ganglion

ECM – extracellular matrix

GAG – glycosaminoglycans

GalNAc – N-acetylgalactosamine

GFAP – glial fibrillary acidic protein

GFP – green fluorescent protein

GlcA – glucuronic acid

HMG – high-mobility-group

HRP – horse radish peroxidase

HSPG – heparin sulfate proteoglycans

IL – interleukin

LAR - leukocyte common antigen-related phosphatase receptor

MAG – myelin associated glycoprotein

MBP – myelin basic protein

MP – methylprednisolone

NASCIS – National Acute Spinal Cord Injury Study

PDGF – platelet derived growth factor

PGC-1alpha – Peroxisome proliferator-activated receptor gamma co-activator 1alpha

PNN – perineuronal net

PNS – peripheral nervous system

RPTPσ – receptor protein tyrosine phosphatase sigma

RT-PCR – real time PCR

SCI – spinal cord injury

SOX – Sry-type HMG box transcription factor

SDS-PAGE – Sodium dodecyl sulphate polyacrylamide gel electrophoresis

TGF – transforming growth factor

VGAT – vesicular GABA transporter

VGLUT – vesicular glutamate transporter

XT – xylosyltransferase

YFP – yellow fluorescent protein

Chapter 1: Introduction

1.0 Spinal cord injury

The spinal cord serves as the communication relay between the brain and the periphery. It conveys messages from the brain to control movement, breathing, and other bodily functions, and messages from sensory organs to the brain to allow us to interpret and act on those sensations. These messages are transmitted by long extensions of neurons called axons. The spinal cord is surrounded by vertebrae that protect it. If these bones are damaged, the spinal cord and the axons therein may be injured and vital information that needs to be transmitted to, or from, the brain does not reach its destination.

Spinal cord injury (SCI) is a devastating event resulting in immediate life-altering consequences for not only the affected individual but their family and friends. SCI can result in motor, sensory, and autonomic dysfunctions [1]. Depending on the severity of injury, SCI may leave patients with lifetime disability [1]. Although paralysis is the symptom most people associate with SCI, those who suffer a SCI may also develop numerous other debilitating symptoms including chronic pain [2], muscle spasticity [3], poor control of bladder and bowel function [4], and decreased sexual function [5, 6]. SCI resulting in permanent paralysis or significant neurological deficit occurs with an annual incidence between 25 and 93 cases per million North Americans [7]; in Canada this translates to over 1,000 new cases a year. SCI often has a profound socio-economic impact on people as they may be forced to leave their jobs, require ongoing medical care for the duration of their lives, and incur massive patient health care

costs [8]. This socio-economic burden is exacerbated by the fact that these injures are most common in young adults [7].

SCI occurs in a two-stage process. The initial stage is known as the primary SCI which occurs at the time of injury due to physical trauma to the spinal cord [9]. Examples of primary injury include hyperextension of the cord, destruction due to sheering or twisting of the cord, vertebral fracture and contact with the side of the cord, and laceration due to a direct cut of the cord by sharp object, or projectile [10]. Most often these injuries also result in reduction of blood flow to the spinal cord resulting in ischemia [11] that contributes significantly to the destruction of the grey matter which requires considerable oxygen supply [10]. Damage to the spinal cord is not limited to this initial physical injury. A secondary phase of SCI begins in the hours following the initial trauma to the cord. This secondary SCI is characterized by the body's activation of inter-related processes that lead to an expansion of the lesion and contribute to neuronal loss and increased functional defect [12]. Such secondary processes contributing to SCI include ischemia-reperfusion [13], edema [14], excitotoxicity [15], oxidative damage [16], inflammation [17], and glial scarring [18].

The debilitating neurological damage that results as a consequence of SCI has long been considered to be irreversible. Currently, there are no effective pharmacological treatments for SCI [19]. Thus, improved therapeutic strategies for the treatment of SCI need to be developed. A beneficial treatment for SCI will need to limit neuronal damage and subsequent functional degeneration, or promote axonal regeneration culminating in significant functional recovery. The project described herein focuses on the promotion of axonal regeneration post-SCI.

1.1 Nervous system plasticity

Embryonic central nervous system (CNS) neurons display significant plasticity, however in the adult CNS this intrinsic ability to grow becomes suppressed to maintain proper synaptic organization [20]. Unlike embryonic CNS neurons, mature CNS neurons display minimal neurite outgrowth, do not respond readily to neurotrophic stimuli, are significantly inhibited by myelin-associated inhibitors, and form few growth cones [21, 22]. Much like CNS neurons, peripheral neurons undergo similar reduction in their growth properties over time, but their intrinsic growth capabilities can be reactivated by peripheral nerve injury that may result in increased expression of pro-regeneration transcription factors and growth associated proteins thus allowing for considerable peripheral nerve regeneration [20, 23, 24]. This type of reactivation of pro-regenerative transcription factors is not seen in response to CNS injuries, and thus CNS neurons do not regenerate to the same extent as peripheral nervous system (PNS) neurons post-injury. However, this is not the sole reason why CNS neurons do not regenerate to the same extent as PNS neurons. The PNS contains Schwann cells, and axons from both PNS and CNS neurons grow well in a Schwann cell rich environment [25-27]. The CNS, however, contains astrocytes and oligodendrocytes rather than Schwann cells, and culture experiments have shown that both PNS and CNS axons grow poorly across astrocyte and oligodendrocyte rich environments [28-30]. Following CNS damage, axonal and glial debris remains for a significant period of time, often months, and has been suggested to act as a source of axonal growth inhibition. In comparison, post-injury debris is cleared much faster in the PNS [31, 32]. Perhaps the most significant impediment to axonal growth in the CNS is the response of cells located at the local site of injury. Unlike in the periphery [33], the adult CNS experiences the activation of astrocytes, and development of a subsequent astroglial scar. CNS trauma often results in a

disruption of the blood–brain barrier, which allows neutrophils and macrophage to extravasate from the blood to assist endogenous microglia with antigen recognition and phagocytic functions. Fibroblasts from the meninges converge with the inflammatory cells to the injury site and release various cytokines and chemokines [34, 35]. These small molecules activate reactive astrocytes to induce further gliosis and glial scar formation. This glial scar consists of a number of growth inhibiting molecules that contribute to the failure of axon regeneration [18, 36-42]. Many of the molecules (semaphorins, ephrins, netrins and slit) that are expressed after injury in the glial scar induce axonal growth cone collapse. Studies investigating the inhibition of these molecules have demonstrated some promise for the functional recovery after CNS injuries including SCI [43, 44]. There are also many myelin-derived inhibitors such as Nogo, myelin-associated glycoprotein, repulsive guidance molecule, and oligodendrocyte myelin glycoprotein each of which inhibit neurite outgrowth *in vitro* [45]. However, their contribution *in vivo* is still under investigation as Nogo, myelin-associated glycoprotein, and oligodendrocyte myelin glycoprotein triple knockout mice do not display improved recovery post-SCI [46, 47]. In 1990 Silver *et al.* found that a major component of the glial scar, chondroitin sulfate proteoglycans (CSPGs) that are up-regulated post-neurotrauma [48], prevent axonal growth as cultured axons from the E9 chick dorsal ganglia would not grow across a strip of CSPGs coated on nitrocellulose [49]. CSPG digestion abolished this inhibition and allowed the chick axons to grow across the plate. Thus, CSPGs became a focus for the investigation of axonal growth inhibitory molecules.

1.2 Chondroitin Sulfate Proteoglycans (CSPGs)

CSPGs are a class of extracellular matrix macromolecules that share a common structure consisting of a central core protein with a number of chondroitin sulfate side chains attached [50]. More than 10 enzymes participate in the complex synthesis of a completed CSPG. First, the CSPG core protein is produced. Next a tetrasaccharide linker is synthesized. The rate limiting step in CSPG synthesis is the attachment of this tetrasaccharide linker to the CSPG core protein by way of a serine-xyline interaction catalyzed by the enzyme xylosyltransferase (XT) isoforms I and II (XT-I, XT-II) [51]. Chondroitin sulfate N-acetylgalactosaminyltransferase adds *N*-acetylgalactosamine (GalNAc) to the tetrasaccharide linker [52], and chondroitin sulfate synthase, as well as chondroitin polymerizing factor, add glucuronic acid (GlcA) to the available *N*-acetylgalactosamine [53, 54]. This polymerization process repeats with the addition of subsequent (GalNAc-GlcA) disaccharides one after another to form a long carbohydrate chain. Finally, these side chains are sulfated by chondroitin 4-sulfotransferase (C4ST) [55] to make a complete CSPG.

There are many different types of CSPGs, each defined by their core protein. There are large aggregating proteoglycans including aggrecan [56] and versican [57] localized in most smooth muscle tissues and in fibrous and elastic cartilage as well as the CNS, and CNS-specific proteoglycans neurocan [58], brevican[59], NG2 [60], and phosphacan [61]. These CSPGs exist abundantly within the CNS and interact with a variety of other ECM components including laminin, fibronectin, tenascin, hyaluronic acid and several collagens by way of interaction through their core protein, or sugar side chain [57, 62-65].

CSPG expression is tightly controlled in the embryonic brain, with expression restricted during development to highly specialized and organized regions such as neural crest pathways and the spinal cord where they act as axon guidance molecules [66, 67]. The removal of these CSPGs results in abnormally formed axonal pathways [68]. In the adult CNS, the normal expression patterns of CSPGs become more diffuse. Neurocan (produced by astrocytes and oligodendrocyte precursor cells) is generally found in the white matter of the adult CNS [69]. NG2 is distributed throughout the adult brain existing on oligodendrocyte precursor cells [70], on blood vessels and meningeal cells [50]; and is often cleaved and secreted into the ECM [71]. Phosphacan is present throughout the CNS and at particularly high levels in the cerebellum [72]. Versican is produced by oligodendrocyte precursor cells and is found in high concentration in the white matter, [73]. Brevican is distributed throughout the CNS [74] and is produced predominantly by astrocytes [75]. CSPGs also amass in extracellular matrix structures which surround synapses on the neuronal surface known as perineuronal networks (PNNs) [76]. This CSPG recruitment into PNN structures coincides with the end of the critical period of plasticity which occurs in the transition to adulthood [76]. These CSPGs exist normally within the adult CNS [77], but following SCI, their expression levels markedly increase [37, 78]. CSPGs become up-regulated to play a beneficial role post-injury as they surround the lesion site and disrupted blood-brain barrier to seal off the damaged tissue, limit the secondary inflammatory response, and prevent increased cavitation [79]. However, as previously mentioned, CSPGs both in the lesion site and in PNNs also pose a significant impediment to regeneration post neurotrauma.

1.3 Regenerative failure post-SCI – CSPGs in the glial scar

Following SCI, axonal regeneration in the adult CNS is poor. However, axons do have an intrinsic ability to grow in both the CNS tissue and degenerating white matter. Davies et al. [42] demonstrated that adult dorsal root ganglion (DRG) sensory neurons transplanted into the white matter tracts of adult rats could grow in the CNS. If the transplantation procedure caused minimal damage to the local transplantation site, considerable numbers of regenerating adult axons rapidly extended through the white matter and eventually invaded the grey matter. If the surgical procedure caused considerable damage to the local area, failure in long range regeneration was noted. Increased CSPG expression was seen within the extracellular matrix at the transplant interface in those animals that displayed abortive regeneration, and minimal CSPG expression was noted in animals which displayed successfully regenerating transplants [42]. In a follow up study Davies et al. [36] transplanted DRG sensory neurons into degenerating white matter of the adult rat spinal cord several millimeters rostral to a severe lesion of the dorsal columns. DRG axonal growth away from the transplantation site, in both the rostral and caudal directions, was noted. Upon reaching the lesion site the rapidly extending axons stopped their growth, experienced growth cone collapse, and became dystrophic. High concentrations of CSPGs were found at the site of cessation of growth in the reactive glial matrix. These results suggested that the major impediment to axonal regeneration in the adult CNS was the molecular barrier found in the glial scar that forms at the lesion site, and that inhibition of axon growth correlates directly with elevated CSPG expression.

In vitro studies have shown that explanted glial tissue expressing CSPGs do not permit neurite extension [37]. In cultures of primary astrocytes, neurites avoid patches of cells

expressing CSPGs [80]. Specific CSPGs have also been shown to inhibit neurite outgrowth including: aggrecan [81], neurocan [82], phosphocan [83], brevican [75], versican [84], and NG2 [85]. Neurocan in particular has been identified as a major impediment to recovery post-SCI [86]. Importantly, following mid-thoracic SCI neurocan expression is increased throughout the lesion site both in the cervical dorsal columns and in the lumbar ventral horn much longer than other CSPGs [86]. The long lasting increase of neurocan in gray matter regions at distal levels of the spinal cord may contribute to the restriction of plasticity in the chronic phase after SCI.

The mechanism behind CSPG inhibition of axonal growth is believed to be due to both the physical and molecular barrier that CSPGs impose at the glial scar. The negatively charged sulfates present on the sugar side chains are repellent to axon fibers [87] and CSPGs sterically inhibit access to substrate adhesion molecules [88]. Recently, the transmembrane receptor protein tyrosine phosphatase sigma (RPTPσ) has been identified as an axonal high affinity receptor for CNS CSPGs [89]. Following interaction with CSPGs, RPTPσ signals growth cone collapse and cessation of axonal growth [90-92]. *In vitro* work demonstrated that cerebellar granule neurons from RPTPσ knockdown mice display reduced sensitivity to CSPG growth inhibition [93]. *In vivo*, corticospinal tract axons were found to regenerate through the injury site and extend for long distances after a dorsal hemisection or contusion injury of the thoracic spinal cord in RPTPσ deficient mice [93]. Transmembrane leukocyte common antigen-related phosphatase receptor (LAR), another member of the RPTP family, has also been identified as a receptor for CSPGs [94]. Functional blockade of LAR reversed neurite growth inhibition induced by CSPGs and induced significant descending axonal growth and locomotor functional recovery in mice with thoracic SCI [94].

CSPG up-regulation in the glial scar at the local injury site is certainly an obstacle to regeneration post-SCI; however, CSPG inhibition of axonal regeneration does not only occur at the glial scar. CSPGs also act as natural endogenous regulators of synaptic plasticity and experience-dependent neural plasticity as the principle component of the perineuronal network at sites distant to injury, and can thus restrict axonal plasticity throughout the CNS [95-97].

1.4 The perineuronal network

PNNs are composed of a highly condensed extracellular matrix that exists around the end feet of astrocytes surrounding the cell bodies and dendrites of CNS neurons [98]. PNNs were originally reported by Camillo Golgi in 1898 [99], and have since been confirmed to be produced by both neurons [100] and glia [101, 102]. PNNs are believed to play a number of functions in the adult brain; they maintain cellular positioning [103]; they modulate the chemotactic gradient of growth factors around neurons [98]; and they generate a polyanionic ion-buffering microenvironment to promote cell survival [104]. PNNs contain CSPGs, and tenascin-R [105], both non-permissive strata for axonal growth or attachment [106, 107]. This suggests that PNNs impede the formation of new synaptic contacts, and restrict axonal plasticity. In fact, PNNs play a crucial role in regulation of what is referred to as the critical period of synaptic plasticity in the brain.

As the juvenile brain develops, particular systems display critical periods of plasticity where the neuronal circuitry controlling these systems shows significantly increased sensitivity to experience [108-110]. Experience during these critical periods is believed to have a significant effect on how these neuronal systems interconnect; thus contributing to learning specific skills

and behaviors including interpretation of one's senses and emotional processing [110, 111]. This critical period comes to an end with a dramatic up-regulation of PNNs around neuronal cell bodies and dendritic synapses bringing to a close this period of increased plasticity [98], finalizing the adaptations to the neuronal network acquired during the critical period [112-114]. The PNNs contain CSPGs that stabilize those synapses formed by critical period experience, preventing the formation of inappropriate synapses in the future by stunting axonal sprouting onto incorrect targets after appropriate connections have been made [97, 101, 115-117]. This mechanism appears to function as a method to retain proper understanding of sensation and optimized motor behaviors without need for continual maintenance, as constantly plastic synapses might leave individuals unable to use that circuitry optimally, and thus would be unable to interact optimally with their environment. Multiple studies have shown that reducing CSPG levels at the lesion site and/or in PNNs results in increased structural neuroplasticity [118-122]. Thus, therapies targeting a reduction in CSPGs both near and far from the lesion epicenter may present an interesting strategy for improved recovery post-SCI.

1.5 Anti-CSPG strategies show promise for the treatment of SCI

Thus far, three strategies have been devised to have broad effects on CSPGs and have been shown to improve axonal regeneration after SCI. The first strategy makes use of enzymatic digestion of the chondroitin sulfate side chains found on all CSPGs using the enzyme chondroitinase ABC. Chondroitinase treatment renders glia permissive to neurite outgrowth *in vitro* [118], and intrathecal chondroitinase treatment in the rat resulted in minor improvements in recovery and regeneration of ascending axonal tracts post-SCI [119], Axonal regeneration

following chondroitinase treatment of the injured spinal cord was modest. The lack of extensive improvement was attributed to the carbohydrate stubs left on the CSPG core proteins after chondroitinase treatment [123]. Another strategy was devised to block glycosylation of proteoglycan core proteins using an anti-XT-I ribozyme administered after SCI, and resulted in improved axonal regeneration [124]. A third approach investigated mice carrying a gene knockdown for Chondroitin sulfate N-acetylgalactosaminyltransferase-1, a key enzyme in CSPG biosynthesis. N-acetylgalactosaminyltransferase-1 knockdown mice displayed reduced CSPG expression, and recovered more completely from SCI than both wild-type mice or chondroitinase treated mice [125]. Thus, strategies targeting CSPG expression are particularly interesting as potential therapeutics for the treatment of SCI.

1.6 Existing therapies for SCI

Currently, there are remarkably few treatments for SCI. Spinal cord decompression is widely practiced as a surgical intervention designed to relieve the physical pressure applied to a compressed spine and to reduce secondary damage. Spinal decompression leads to improved neurological function, reduced hospital stay, fewer secondary complications, earlier mobilization, and quicker transfer to rehabilitation centers [126-130]. However, the decompression surgery needs to occur immediately after SCI as studies have demonstrated that no significant neurologic benefit was seen when spinal cord decompression was performed just over 24 hours post-injury (mean 1.8 days) or during a more chronic time point (mean, 16.8 days) [131].

A pharmacological treatment for SCI also exists; methylprednisolone (MP) has been used as an approved anti-inflammatory clinical treatment for SCI due to its promising immunosuppressive effects [132] and profound anti-oxidant properties [133] in pre-clinical models. However, MP treatment is not without its detractors. In 1979 a multicenter, randomized, double-blinded clinical trial referred to as National Acute Spinal Cord Injury Study (NASCIS) analyzed 330 patients treated with MP or placebo and found no beneficial effect of MP treatment on neurological recovery, motor function, or sensory function, at 6 weeks or 6 months after injury [134]. However, animal studies suggested that the MP dose used in NASCIS I was not sufficient to confer neuroprotection [135, 136]. Thus, a second multicenter trial (NASCIS II) was initiated in 1985 using a higher MP dose, and 487 participants. The administration of a higher dose of MP within 8 hours after injury was associated with a statistically significant improvement in motor and sensory function at the 6-month follow up compared with patients receiving placebo or MP at later time-points [137]. However, there were no functional outcome measures designed to assess whether the statistical improvements noted with MP treatment were indeed clinically relevant. As a whole, this trial was criticized for methodological, scientific, and statistical design issues [138-141]. These criticisms resulted in the development of a third NASCIS trial. The study began in 1991 and followed 499 patients, this time also assessing self-care, mobility, locomotion, sphincter control, communication and social cognition in acute SCI patients. Any benefit of MP treatment was only observed at the 6 week and 6 month follow-ups and no positive effect was noted beyond 1 year [142, 143]. Importantly, all NASCIS trials reported a statistically significant increase in adverse side effects, including: infections, gastrointestinal hemorrhages, sepsis, pulmonary embolism, severe pneumonia, and death [140, 141].

In 2002, the American Association of Neurological Surgeons/Congress of Neurological Surgeons (AANS/CNS) released a statement indicating that the harmful side effects of MP treatment outweighed the potential for clinical benefit [144]. In Canada, administration of MP was common practice following NASCISII (administered in 76% of acute SCI cases) and, following the AANS/CNS recommendations, Canadian clinicians dramatically reduced MP usage for treatment of SCI (administered in only 24% of acute SCI) [145]. As MP is losing favor among clinicians treating SCI, and spinal decompression intervention must occur in the very acute stages after injury, there is clearly a need to develop new efficacious treatments for SCI.

1.7 *Sox9* was identified as a potential regulator of CSPG biosynthesis

Given that CSPGs are such a potent obstacle to regeneration post-SCI the regulation of XT-I, XT-II and C4ST, the enzymes that synthesize the chondroitin sulfate side chains on CSPGs, was investigated. Following SCI, XT-I, XT-II and C4ST all show similar temporal patterns of up-regulated gene expression [146], and are followed by the detection of increased CSPG levels [146]. As the formation of the glial scar is a process that does not occur in the undamaged adult spinal cord, it seemed reasonable to presume that a genetic program for the elaboration of the glial scar would be activated post-SCI to up-regulate the expression of CSPGs and other relevant genes. Thus, researchers in the Brown laboratory conducted an *in silico* phylogenetic footprinting analyses [147] to identify transcription factors that could potentially activate XT-I, XT-II, and C4ST expression. Genomatix software identified five transcription factors which have putative binding sites within the promoters of human, rat, and mouse, XT-I, XT-II and C4ST. Of the five, *Sox9* was particularly interesting as it plays a key role in astrocyte

development [148, 149] and positively regulates the expression of proteoglycans during chondrogenesis in the periphery [150-152].

1.8 Transcription factor *Sox9*

SOX (SRY-type HMG box) transcription factors are part of a DNA-binding protein subfamily with a high-mobility-group (HMG) domain [153]. Individual members of the SOX family show greater than 50% identity in their HMG domain to SRY, the testes-determining factor, and thus it is not surprising that SOX transcription factors play roles in sex determination [153, 154]. However, SOX transcription factors are involved in a wide range of developmental processes beyond sex determination, including neurogenesis, hematopoiesis, lens development, and skeleton formation [153, 155-161].

Sox9 has two essential functions: it regulates the activity of genes required for testes development, and it regulates essential genes required for cartilage and bone development. Mutations to SOX9 have significant consequences for those afflicted. Disrupting *Sox9* results in sex reversal, in which a genetically male (XY) individual will appear phenotypically female as *Sox9* is unable to carry out its normal role in testes development [162, 163]. Mutations to *Sox9* also result in a genetically dominant skeletal condition known as campomelic dysplasia that presents alongside sex reversal [162, 163]. It is characterized by bone and cartilage abnormalities causing short arms and legs, short digits, bowing of the legs, dislocated hips, feet that are abnormally rotated, and small chest size. The condition is life threatening during the newborn period, with death often resulting from breathing problems as a result of underdeveloped chest or lungs [164]. A few individuals have survived with campomelic dysplasia past infancy. As they

age they develop further orthopedic problems and hearing loss [165, 166]. Mutations to the regions near the SOX9 locus may disrupt enhancer elements that normally regulate the activity of *Sox9*. If this leads to reduced *Sox9* activity an inability to properly control the development of facial structures known as isolated Pierre Robin sequence may result [167]. These skeletal abnormalities result from the individual's inability to form proper cartilaginous structures due to *Sox9* mutation. *Sox9*'s role in cartilage development is particularly important to this study as proteoglycans are required for proper cartilage formation.

1.9 The role of *Sox9* in cartilage formation

Cartilage formation is an essential process during development. Cartilages do not only constitute permanent skeletal structures in the respiratory tract, articular joints, and other organs, but are also essential templates for the formation of endochondral bones. Cartilage is created by chondrocytes secreting specific extracellular matrix components such as various collagens and proteoglycans. *Sox9* is expressed in all chondroprogenitors and differentiated active chondrocytes [168]. *In vitro* studies have shown that *Sox9* binds and activates chondrocyte-specific enhancer elements for the *Col2a1, Col11a2, Aggrecan*, and *CD-RAP* genes *in vitro*, demonstrating that these genes are targets of *Sox9* [169-172]. *Sox9* can also directly activate type 2 collagen expression when ectopically expressed in some non-cartilaginous sites in transgenic mice [173].

Studies using mouse embryo chimeras derived from *Sox9* knockdown embryonic stem (ES) cells demonstrated that *Sox9* null mutant cells were excluded from chondrogenic mesenchymal condensations and did not express chondrocyte-specific markers for collagen

expression or aggrecan proteoglycan expression [174]. To elucidate further the role of *Sox9* in chondrogenesis and chondrocytic differentiation, Akiyama et al. [175] developed a *Sox9* conditional knockdown line using the Cre recombinase system. Embryos, in which *Sox9* was deleted after mesenchymal condensations, exhibited a severe generalized chondrodysplasia. Most cells were arrested as condensed mesenchymal cells and did not undergo overt differentiation into chondrocytes. Furthermore, chondrocyte proliferation was severely inhibited and joint formation was defective. Embryos missing *Sox9* from undifferentiated mesenchymal cells of limb buds displayed the complete absence of both cartilage and bone, and developed chondrodysplasia. This was associated with dramatically reduced expression of *Runx2*, a transcription factor needed for osteoblast differentiation, as well as an absence of *Sox5*/*Sox6* expression [175]. *Sox5* and *Sox6* work alongside *Sox9* to play a crucial role in chondrocytic differentiation [176]. *Sox5* and *Sox6* are co-expressed with *Sox9* in all chondroprogenitors and all differentiated chondrocytes, and cooperate with *Sox9* to activate the *Col2a1* enhancer and the *Col2a1* gene [177]. *Sox9*'s involvement in the control of so many genes that contribute to expression of the extracellular matrix, including collagen and proteoglycan genes, suggested that *Sox9* may be a master regulator of many genes required for scar formation. Thus, *Sox9* was chosen as the first transcription factor to be investigated in search of a putative CSPG modulator in glial scarring post-SCI.

1.10 *Sox9* modulates enzymes essential for CSPG production

Researchers in the Brown laboratory have carried out chromatin immunoprecipitation (ChIP) assays to determine whether *Sox9* directly binds XT-I, XT-II and C4ST. Mouse genomic DNA from developing testes that express *Sox9* was immunoprecipitated with an anti-SOX9 antibody. The *Sox9*-immunoprecipitated DNA was purified and subsequently amplified by PCR using primers that flank the Genomatix predicted *Sox9* binding sites in the XT-I, XT-II, and C4ST promoters. The ChIP experiments demonstrate *in vivo* binding of *Sox9* to the XT-I and C4ST promoters. Experiments are ongoing to identify *Sox9* binding sites in the XT-II promoter region.

To investigate the effects of *Sox9* on astrocyte-produced XT-I, XT-II, and C4ST, a primary rat astrocyte tissue culture model was used. Over-expression of *Sox9* was accomplished by transient transfection of a *Sox9* expression cassette and demonstrated increased astrocyte XT-I, XT-II, and C4ST expression. *Sox9* knockdown in primary rat astrocyte cultures, accomplished by treatment with anti-*Sox9* siRNA, demonstrated decreased astrocyte XT-I, XT-II, and C4ST expression along with increased laminin and fibronectin expression [146]. These findings suggested that *Sox9* plays a role in up-regulating anti-regenerative CSPG production as well as down-regulating pro-regenerative laminin and fibronectin expression [146].

A second, seemingly unrelated, experimental strategy to promote recovery post-SCI, is the intravenous administration of anti-CD11d monoclonal antibody. This anti-inflammatory treatment that blocks leukocytes from infiltrating into the damaged spinal cord has been shown to decrease lesion size, improve neurological recovery after rodent SCI, and indirectly result in reduced levels of *Sox9* at the lesion epicenter [178]. The observed reduction in *Sox9* was

accompanied by a reduction in XT-I, XT-II, and C4ST expression as well as an increase in laminin and fibronectin expression [179]. Consistent with these mRNA changes, CSPGs were reduced by approximately one half in the lesions of anti-CD11d-treated rats, and laminin was increased. These results are in keeping with our previous observation that pro-inflammatory cytokines (IL-6, TGF-β2 and PDGF) up-regulate the expression of SOX9 [146]. We conjectured that these changes in *Sox9*, CSPG, and laminin/fibronectin expression in the scars of anti-CD11d mAb-treated rats greatly contributed to the increase in axonal growth and sprouting as well as functional recovery observed [178]. We were thus interested in investigating CSPG expression, recovery of hind limb motor function, and neuroplasticity in *Sox9* knockdown mice.

1.11 The dorsal contusion spinal cord injury model used in these studies

The SCI model used in this dissertation is a thoracic spinal cord dorsal contusion. Mice are anesthetized, restrained in a mechanical device which stabilizes their spinal cord, and a laminectomy is performed to expose the 9th thoracic spinal segment. A computer controlled injury is induced by the Infinite Horizons Impactor mechanically delivering a blunt contusion to the exposed spinal cord (without disruption of the dura) [180]. The device records precise force delivered and displacement of spinal tissue, thus allowing for consistent and reproducible injuries. This contusion model of SCI produces primary mechanical trauma to the cord as well as significant secondary damage [181]. The resulting injury generates motor and behavioral deficits similar in morphology and pathology to common human SCI [182, 183]. Following SCI, motor function is evaluated using the Basso Mouse Scale (BMS) for scoring hind limb function [184] as well as locomotor activity box for assessment of total locomotion over a given period of time.

1.12 Conditional *Sox9* knockdown mouse breeding strategy

Conventional *Sox9* knockdown embryos have been generated but are unsuitable for studies of SCI as *Sox9* knockdown embryos do not survive to birth [174, 185]. Thus, to study the effect of *Sox9* knockdown in adult mice which develop with normal *Sox9* activity, we bred two existing mouse strains together. The first mouse strain used was *Sox9^{flox/flox}*, a transgenic strain carrying floxed *Sox9* alleles (exons 2 and 3 of *Sox9* surrounded by loxP sites) which has been used successfully for the conditional knockdown of *Sox9* in various cell types [148, 175]. The second mouse strain used was CAGGCre-ER, a transgenic line that ubiquitously expresses Cre recombinase fused to the mutated ligand binding domain of the mouse estrogen receptor under the control of the chicken beta actin promoter/enhancer coupled to the Cytomegalovirus (CMV) immediate early enhancer [186]. The mutated estrogen receptor ligand binding domain does not bind endogenous estradiol but rather binds to exogenously administered tamoxifen. Cre recombinase expressed in these animals is trapped outside the nucleus by the mutated estrogen receptor until tamoxifen administration releases Cre allowing for its transport to the nucleus where it excises floxed regions of DNA. By breeding the *Sox9^{flox/flox}* mice to the CAGGCre-ER mice we generate *Sox9^{flox/flox}*;CAGGCre-ER offspring (*Sox9^{flox/flox};Cre)*. The F1 pups of *Sox9^{flox/flox};Cre* genotype were backcrossed with the *Sox9^{flox/flox}* mice for more than 5 generations to attain the *Sox9^{flox/flox};Cre* and their *Sox9^{flox/flox}* littermates described herein. In these *Sox9^{flox/flox};Cre* mice, tamoxifen administration allows us to examine the molecular, cellular, and neurological responses to SCI in the presence of greatly reduced expression levels of *Sox9*. In all of our studies *Sox9^{flox/flox}* littermates that do not carry the CAGGCre-ER allele serve as controls as they express normal levels of *Sox9* (even after tamoxifen administration). These *Sox9*

conditional knockdown (*Sox9^{flox/flox};Cre*) and control mice expressing normal levels of Sox9 (*Sox9^{flox/flox}*) were used to evaluate the following specific goals for this thesis.

1.13 Specific goals

This thesis had three major goals: 1) to determine if the transcription factor *Sox9* controls chondroitin sulfate proteoglycan gene expression, 2) to determine if *Sox9* conditional knockdown mice display improved hind limb functional recovery post-SCI, and 3) to determine if *Sox9* conditional knockdown mice display increased neuroplasticity post-SCI.

I set out the following seven objectives to investigate these goals:

1) To breed *Sox9* conditional knockdown mice for use in studying the effect of *Sox9* knockdown on recovery post-SCI in the mouse.

2) To determine if *Sox9* conditional knockdown mice display decreased CSPG expression *in vitro*.

3) To determine if *Sox9* conditional knockdown mice display decreased CSPG expression *in vivo*.

4) To determine if *Sox9* conditional knockdown mice display increased hind limb function post-SCI.

5) To determine if *Sox9* conditional knockdown mice display increased locomotion post-SCI.

6) To determine if *Sox9* conditional knockdown mice display increased axonal regeneration post-SCI.

7) To determine if *Sox9* conditional knockdown mice display increased synapse plasticity post-SCI.

The first objective was accomplished by breeding *Sox9^{flox/flox}* mice to CAGGCre-ER mice to generate *Sox9^{flox/flox};Cre* and their *Sox9^{flox/flox}* littermates. On tamoxifen administration the *Sox9^{flox/flox};Cre* mice lose expression of *Sox9* while the *Sox9^{flox/flox}* littermates will still express wild type levels of *Sox9^{flox/flox}*. By comparing *Sox9^{flox/flox};Cre* and *Sox9^{flox/flox}* littermates we can ascertain the effect of *Sox9* knockdown on mouse physiology post-SCI. The second objective was accomplished by using real time PCR to monitor mRNA changes in *Sox9* knockdown and control primary astrocyte cultures. The third objective was accomplished by using western blot and immunohistochemistry to monitor protein changes in *Sox9* knockdown and control mice. The fourth objective evaluated hind limb functional recovery in both a proof of principle model, as well as a more clinically relevant delayed knockdown model. Hind limb functional recovery from a T9 dorsal contusion SCI was evaluated in both models by way of Basso mouse scale hind limb function scoring. The fifth objective was accomplished by use of rodent activity box locomotion testing performed on *Sox9* knockdown and control mice in both a proof of principle model, as well as a more clinically relevant delayed knockdown model. The sixth objective was accomplished by neuronal labeling techniques including retrograde labeling to assess for sparing and long range regeneration of axons through the injury site, and anterograde labeling to assess for axonal sprouting caudal to the injury site. The seventh and final objective was investigated using synapse markers to assess synaptic plasticity.

1.14 Summary

The failure of CNS axons to undergo significant regeneration following injury is considered to be the main reason why most animals do not display significant functional recovery post-neurotrauma. One of the most detrimental causes of this failure of CNS axons to undergo significant regeneration is the expression of CSPG extracellular matrix post-injury. We have previously identified *Sox9* as a transcription factor which may up-regulate expression of this anti-regenerative CSPG extracellular matrix. This thesis will attempt to determine if *Sox9* ablation will inhibit CSPG extracellular matrix production both *in vitro* and *in vivo*, result in increased neuroplasticity and axonal regeneration, and lead to improved hind limb motor function post-SCI. **Chapter 2** of this thesis contains our proof of principle study in which we show that, following SCI, *Sox9* knockdown mice display reduced CSPG expression and improved hind limb functional recovery. **Chapter 3** of this thesis details a more clinically relevant injury model in which *Sox9* is knocked down approximately 2 weeks post-injury, and still results in reduced CSPG expression and improved hind limb functional recovery. **Chapter 4** of this thesis investigates the neuronal mechanism behind this improved hind limb functional recovery and finds evidence for increased neuroplasticity, revealed as reactive sprouting and increased synaptic plasticity, in *Sox9* knockdown mice post-SCI.

1.15 References

1.   Fehlings, M.G. and D.C. Baptiste, *Current status of clinical trials for acute spinal cord injury.* Injury, 2005. **36 Suppl 2**: p. B113-22.
2.   Siddall, P.J., D. Taylor, and M.J. Cousins, *Pain associated with spinal cord injury.* Curr Opin Neurol, 1995. **8**(6): p. 447-50.
3.   Krause, J.S., *Factors associated with risk for subsequent injuries after traumatic spinal cord injury.* Arch Phys Med Rehabil, 2004. **85**(9): p. 1503-8.
4.   Lynch, A.C., et al., *Bowel dysfunction following spinal cord injury.* Spinal Cord, 2001. **39**(4): p. 193-203.
5.   Dahlberg, A., et al., *Sexual activity and satisfaction in men with traumatic spinal cord lesion.* J Rehabil Med, 2007. **39**(2): p. 152-5.
6.   Allard, J., et al., *Spinal cord control of ejaculation.* World J Urol, 2005. **23**(2): p. 119-26.
7.   Pickett, G.E., et al., *Epidemiology of traumatic spinal cord injury in Canada.* Spine, 2006. **31**(7): p. 799-805.
8.   Krueger, H., et al., *The economic burden of traumatic spinal cord injury in Canada.* Chronic diseases and injuries in Canada, 2013. **33**(3): p. 113-22.
9.   Taoka, Y. and K. Okajima, *Spinal cord injury in the rat.* Prog Neurobiol, 1998. **56**(3): p. 341-58.
10.   Dumont, R.J., et al., *Acute spinal cord injury, part I: pathophysiologic mechanisms.* Clinical neuropharmacology, 2001. **24**(5): p. 254-64.
11.   Taoka, Y. and K. Okajima, *Spinal cord injury in the rat.* Progress in neurobiology, 1998. **56**(3): p. 341-58.
12.   Carlson, S.L., et al., *Acute inflammatory response in spinal cord following impact injury.* Exp Neurol, 1998. **151**(1): p. 77-88.
13.   Reece, T.B., et al., *The evolution of ischemic spinal cord injury in function, cytoarchitecture, and inflammation and the effects of adenosine A2A receptor activation.* J Thorac Cardiovasc Surg, 2004. **128**(6): p. 925-32.
14.   Joseph, G., et al., *Spinal cord infarction due to a self-inflicted needle stick injury.* Spinal Cord, 2004. **42**(11): p. 655-8.
15.   Agrawal, S.K. and M.G. Fehlings, *Role of NMDA and non-NMDA ionotropic glutamate receptors in traumatic spinal cord axonal injury.* J Neurosci, 1997. **17**(3): p. 1055-63.
16.   Demopoulos, H.B., et al., *The free radical pathology and the microcirculation in the major central nervous system disorders.* Acta Physiol Scand Suppl, 1980. **492**: p. 91-119.
17.   Popovich, P.G., P. Wei, and B.T. Stokes, *Cellular inflammatory response after spinal cord injury in Sprague-Dawley and Lewis rats.* J Comp Neurol, 1997. **377**(3): p. 443-64.
18.   Fawcett, J.W. and R.A. Asher, *The glial scar and central nervous system repair.* Brain Res Bull, 1999. **49**(6): p. 377-91.
19.   Conti, A., et al., *Role of inflammation in the secondary injury following experimental spinal cord trauma.* J Neurosurg Sci, 2003. **47**(2): p. 89-94.
20.   Abe, N. and V. Cavalli, *Nerve injury signaling.* Current opinion in neurobiology, 2008. **18**(3): p. 276-83.
21.   Sun, F. and Z. He, *Neuronal intrinsic barriers for axon regeneration in the adult CNS.* Current opinion in neurobiology, 2010. **20**(4): p. 510-8.

22.   Yang, P. and Z. Yang, *Enhancing intrinsic growth capacity promotes adult CNS regeneration.* Journal of the neurological sciences, 2012. **312**(1-2): p. 1-6.

23.   Smith, D.S. and J.H. Skene, *A transcription-dependent switch controls competence of adult neurons for distinct modes of axon growth.* J Neurosci, 1997. **17**(2): p. 646-58.

24.   Stam, F.J., et al., *Identification of candidate transcriptional modulators involved in successful regeneration after nerve injury.* Eur J Neurosci, 2007. **25**(12): p. 3629-37.

25.   Richardson, P.M., V.M. Issa, and A.J. Aguayo, *Regeneration of long spinal axons in the rat.* Journal of neurocytology, 1984. **13**(1): p. 165-82.

26.   Richardson, P.M., U.M. McGuinness, and A.J. Aguayo, *Axons from CNS neurons regenerate into PNS grafts.* Nature, 1980. **284**(5753): p. 264-5.

27.   David, S. and A.J. Aguayo, *Axonal elongation into peripheral nervous system "bridges" after central nervous system injury in adult rats.* Science, 1981. **214**(4523): p. 931-3.

28.   Fawcett, J.W., et al., *The growth of axons in three-dimensional astrocyte cultures.* Dev Biol, 1989. **135**(2): p. 449-58.

29.   Fawcett, J.W., J. Rokos, and I. Bakst, *Oligodendrocytes repel axons and cause axonal growth cone collapse.* Journal of cell science, 1989. **92 (Pt 1)**: p. 93-100.

30.   Bandtlow, C., T. Zachleder, and M.E. Schwab, *Oligodendrocytes arrest neurite growth by contact inhibition.* J Neurosci, 1990. **10**(12): p. 3837-48.

31.   Perry, V.H., M.C. Brown, and S. Gordon, *The macrophage response to central and peripheral nerve injury. A possible role for macrophages in regeneration.* The Journal of experimental medicine, 1987. **165**(4): p. 1218-23.

32.   Stoll, G., B.D. Trapp, and J.W. Griffin, *Macrophage function during Wallerian degeneration of rat optic nerve: clearance of degenerating myelin and Ia expression.* J Neurosci, 1989. **9**(7): p. 2327-35.

33.   Berry, M., et al., *Deposition of scar tissue in the central nervous system.* Acta neurochirurgica. Supplementum, 1983. **32**: p. 31-53.

34.   Silver, J. and J.H. Miller, *Regeneration beyond the glial scar.* Nat Rev Neurosci, 2004. **5**(2): p. 146-56.

35.   Brouty-Boye, D., et al., *Chemokines and CD40 expression in human fibroblasts.* European journal of immunology, 2000. **30**(3): p. 914-9.

36.   Davies, S.J., et al., *Robust regeneration of adult sensory axons in degenerating white matter of the adult rat spinal cord.* J Neurosci, 1999. **19**(14): p. 5810-22.

37.   McKeon, R.J., et al., *Reduction of neurite outgrowth in a model of glial scarring following CNS injury is correlated with the expression of inhibitory molecules on reactive astrocytes.* J Neurosci, 1991. **11**(11): p. 3398-411.

38.   Reier, P.J. and J.D. Houle, *The glial scar: its bearing on axonal elongation and transplantation approaches to CNS repair.* Adv Neurol, 1988. **47**: p. 87-138.

39.   Bahr, M., C. Przyrembel, and M. Bastmeyer, *Astrocytes from adult rat optic nerves are nonpermissive for regenerating retinal ganglion cell axons.* Exp Neurol, 1995. **131**(2): p. 211-20.

40.   Jones, L.L., et al., *NG2 is a major chondroitin sulfate proteoglycan produced after spinal cord injury and is expressed by macrophages and oligodendrocyte progenitors.* J Neurosci, 2002. **22**(7): p. 2792-803.

41.   Eddleston, M. and L. Mucke, *Molecular profile of reactive astrocytes--implications for their role in neurologic disease.* Neuroscience, 1993. **54**(1): p. 15-36.

42. Davies, S.J., et al., *Regeneration of adult axons in white matter tracts of the central nervous system.* Nature, 1997. **390**(6661): p. 680-3.

43. Hata, K., et al., *RGMa inhibition promotes axonal growth and recovery after spinal cord injury.* The Journal of cell biology, 2006. **173**(1): p. 47-58.

44. Kaneko, S., et al., *A selective Sema3A inhibitor enhances regenerative responses and functional recovery of the injured spinal cord.* Nature medicine, 2006. **12**(12): p. 1380-9.

45. Kyoto, A., K. Hata, and T. Yamashita, *Synapse formation of the cortico-spinal axons is enhanced by RGMa inhibition after spinal cord injury.* Brain Research, 2007. **1186**: p. 74-86.

46. Cafferty, W.B., et al., *MAG and OMgp synergize with Nogo-A to restrict axonal growth and neurological recovery after spinal cord trauma.* J Neurosci, 2010. **30**(20): p. 6825-37.

47. Lee, J.K., et al., *Assessing spinal axon regeneration and sprouting in Nogo-, MAG-, and OMgp-deficient mice.* Neuron, 2010. **66**(5): p. 663-70.

48. Rudge, J.S., G.M. Smith, and J. Silver, *An in vitro model of wound healing in the CNS: analysis of cell reaction and interaction at different ages.* Experimental neurology, 1989. **103**(1): p. 1-16.

49. Snow, D.M., et al., *Sulfated proteoglycans in astroglial barriers inhibit neurite outgrowth in vitro.* Experimental neurology, 1990. **109**(1): p. 111-30.

50. Morgenstern, D.A., R.A. Asher, and J.W. Fawcett, *Chondroitin sulphate proteoglycans in the CNS injury response.* Prog Brain Res, 2002. **137**: p. 313-32.

51. Gotting, C., et al., *Molecular cloning and expression of human UDP-d-Xylose:proteoglycan core protein beta-d-xylosyltransferase and its first isoform XT-II.* J Mol Biol, 2000. **304**(4): p. 517-28.

52. Gotoh, M., et al., *Enzymatic synthesis of chondroitin with a novel chondroitin sulfate N-acetylgalactosaminyltransferase that transfers N-acetylgalactosamine to glucuronic acid in initiation and elongation of chondroitin sulfate synthesis.* J Biol Chem, 2002. **277**(41): p. 38189-96.

53. Kitagawa, H., T. Uyama, and K. Sugahara, *Molecular cloning and expression of a human chondroitin synthase.* J Biol Chem, 2001. **276**(42): p. 38721-6.

54. Kitagawa, H., et al., *Molecular cloning of a chondroitin polymerizing factor that cooperates with chondroitin synthase for chondroitin polymerization.* J Biol Chem, 2003. **278**(26): p. 23666-71.

55. Yamauchi, S., et al., *Molecular cloning and expression of chondroitin 4-sulfotransferase.* J Biol Chem, 2000. **275**(12): p. 8975-81.

56. Paulsson, M., et al., *Extended and globular protein domains in cartilage proteoglycans.* The Biochemical journal, 1987. **245**(3): p. 763-72.

57. Krusius, T., K.R. Gehlsen, and E. Ruoslahti, *A fibroblast chondroitin sulfate proteoglycan core protein contains lectin-like and growth factor-like sequences.* J Biol Chem, 1987. **262**(27): p. 13120-5.

58. Oohira, A., et al., *Developmentally regulated expression of a brain specific species of chondroitin sulfate proteoglycan, neurocan, identified with a monoclonal antibody IG2 in the rat cerebrum.* Neuroscience, 1994. **60**(1): p. 145-57.

59. Yamada, H., et al., *Molecular cloning of brevican, a novel brain proteoglycan of the aggrecan/versican family.* J Biol Chem, 1994. **269**(13): p. 10119-26.

60.   Stallcup, W.B. and L. Beasley, *Bipotential glial precursor cells of the optic nerve express the NG2 proteoglycan.* J Neurosci, 1987. **7**(9): p. 2737-44.

61.   Maurel, P., et al., *Phosphacan, a chondroitin sulfate proteoglycan of brain that interacts with neurons and neural cell-adhesion molecules, is an extracellular variant of a receptor-type protein tyrosine phosphatase.* Proc Natl Acad Sci U S A, 1994. **91**(7): p. 2512-6.

62.   Schmidt, G., H. Hausser, and H. Kresse, *Interaction of the small proteoglycan decorin with fibronectin. Involvement of the sequence NKISK of the core protein.* The Biochemical journal, 1991. **280 (Pt 2)**: p. 411-4.

63.   Grumet, M., et al., *Interactions with tenascin and differential effects on cell adhesion of neurocan and phosphacan, two major chondroitin sulfate proteoglycans of nervous tissue.* J Biol Chem, 1994. **269**(16): p. 12142-6.

64.   Bidanset, D.J., et al., *Binding of the proteoglycan decorin to collagen type VI.* J Biol Chem, 1992. **267**(8): p. 5250-6.

65.   Hedbom, E. and D. Heinegard, *Binding of fibromodulin and decorin to separate sites on fibrillar collagens.* J Biol Chem, 1993. **268**(36): p. 27307-12.

66.   Snow, D.M., D.A. Steindler, and J. Silver, *Molecular and cellular characterization of the glial roof plate of the spinal cord and optic tectum: a possible role for a proteoglycan in the development of an axon barrier.* Dev Biol, 1990. **138**(2): p. 359-76.

67.   Oakley, R.A. and K.W. Tosney, *Peanut agglutinin and chondroitin-6-sulfate are molecular markers for tissues that act as barriers to axon advance in the avian embryo.* Dev Biol, 1991. **147**(1): p. 187-206.

68.   Brittis, P.A., D.R. Canning, and J. Silver, *Chondroitin sulfate as a regulator of neuronal patterning in the retina.* Science, 1992. **255**(5045): p. 733-6.

69.   Asher, R.A., et al., *Neurocan is upregulated in injured brain and in cytokine-treated astrocytes.* J Neurosci, 2000. **20**(7): p. 2427-38.

70.   Levine, J.M. and J.P. Card, *Light and electron microscopic localization of a cell surface antigen (NG2) in the rat cerebellum: association with smooth protoplasmic astrocytes.* J Neurosci, 1987. **7**(9): p. 2711-20.

71.   Nishiyama, A., X.H. Lin, and W.B. Stallcup, *Generation of truncated forms of the NG2 proteoglycan by cell surface proteolysis.* Molecular biology of the cell, 1995. **6**(12): p. 1819-32.

72.   Meyer-Puttlitz, B., et al., *Chondroitin sulfate proteoglycans in the developing central nervous system. II. Immunocytochemical localization of neurocan and phosphacan.* J Comp Neurol, 1996. **366**(1): p. 44-54.

73.   Asher, R.A., et al., *Versican is upregulated in CNS injury and is a product of oligodendrocyte lineage cells.* J Neurosci, 2002. **22**(6): p. 2225-36.

74.   Seidenbecher, C.I., et al., *Brevican, a chondroitin sulfate proteoglycan of rat brain, occurs as secreted and cell surface glycosylphosphatidylinositol-anchored isoforms.* J Biol Chem, 1995. **270**(45): p. 27206-12.

75.   Yamada, H., et al., *The brain chondroitin sulfate proteoglycan brevican associates with astrocytes ensheathing cerebellar glomeruli and inhibits neurite outgrowth from granule neurons.* J Neurosci, 1997. **17**(20): p. 7784-95.

76.   Kwok, J.C., et al., *Extracellular matrix and perineuronal nets in CNS repair.* Developmental neurobiology, 2011. **71**(11): p. 1073-89.

77.   Bignami, A., R. Asher, and G. Perides, *The extracellular matrix of rat spinal cord: a comparative study on the localization of hyaluronic acid, glial hyaluronate-binding protein, and chondroitin sulfate proteoglycan.* Exp Neurol, 1992. **117**(1): p. 90-3.

78.   Lemons, M.L., D.R. Howland, and D.K. Anderson, *Chondroitin sulfate proteoglycan immunoreactivity increases following spinal cord injury and transplantation.* Exp Neurol, 1999. **160**(1): p. 51-65.

79.   Fitch, M.T., et al., *Cellular and molecular mechanisms of glial scarring and progressive cavitation: in vivo and in vitro analysis of inflammation-induced secondary injury after CNS trauma.* J Neurosci, 1999. **19**(19): p. 8182-98.

80.   Meiners, S., E.M. Powell, and H.M. Geller, *A distinct subset of tenascin/CS-6-PG-rich astrocytes restricts neuronal growth in vitro.* J Neurosci, 1995. **15**(12): p. 8096-108.

81.   Condic, M.L., D.M. Snow, and P.C. Letourneau, *Embryonic neurons adapt to the inhibitory proteoglycan aggrecan by increasing integrin expression.* J Neurosci, 1999. **19**(22): p. 10036-43.

82.   Friedlander, D.R., et al., *The neuronal chondroitin sulfate proteoglycan neurocan binds to the neural cell adhesion molecules Ng-CAM/L1/NILE and N-CAM, and inhibits neuronal adhesion and neurite outgrowth.* J Cell Biol, 1994. **125**(3): p. 669-80.

83.   Milev, P., et al., *Interactions of the chondroitin sulfate proteoglycan phosphacan, the extracellular domain of a receptor-type protein tyrosine phosphatase, with neurons, glia, and neural cell adhesion molecules.* J Cell Biol, 1994. **127**(6 Pt 1): p. 1703-15.

84.   Schmalfeldt, M., et al., *Brain derived versican V2 is a potent inhibitor of axonal growth.* J Cell Sci, 2000. **113 (Pt 5)**: p. 807-16.

85.   Dou, C.L. and J.M. Levine, *Inhibition of neurite growth by the NG2 chondroitin sulfate proteoglycan.* J Neurosci, 1994. **14**(12): p. 7616-28.

86.   Andrews, E.M., et al., *Alterations in chondroitin sulfate proteoglycan expression occur both at and far from the site of spinal contusion injury.* Exp Neurol, 2011.

87.   Gilbert, R.J., et al., *CS-4,6 is differentially upregulated in glial scar and is a potent inhibitor of neurite extension.* Molecular and cellular neurosciences, 2005. **29**(4): p. 545-58.

88.   McKeon, R.J., A. Hoke, and J. Silver, *Injury-induced proteoglycans inhibit the potential for laminin-mediated axon growth on astrocytic scars.* Experimental neurology, 1995. **136**(1): p. 32-43.

89.   Shen, Y., et al., *PTPsigma is a receptor for chondroitin sulfate proteoglycan, an inhibitor of neural regeneration.* Science, 2009. **326**(5952): p. 592-6.

90.   Johnson, K.G. and D. Van Vactor, *Receptor protein tyrosine phosphatases in nervous system development.* Physiological reviews, 2003. **83**(1): p. 1-24.

91.   Dunah, A.W., et al., *LAR receptor protein tyrosine phosphatases in the development and maintenance of excitatory synapses.* Nature neuroscience, 2005. **8**(4): p. 458-67.

92.   Rashid-Doubell, F., et al., *Chick PTPsigma regulates the targeting of retinal axons within the optic tectum.* J Neurosci, 2002. **22**(12): p. 5024-33.

93.   Fry, E.J., et al., *Corticospinal tract regeneration after spinal cord injury in receptor protein tyrosine phosphatase sigma deficient mice.* Glia, 2010. **58**(4): p. 423-33.

94.   Fisher, D., et al., *Leukocyte common antigen-related phosphatase is a functional receptor for chondroitin sulfate proteoglycan axon growth inhibitors.* J Neurosci, 2011. **31**(40): p. 14051-66.

95.   Frischknecht, R., et al., *Brain extracellular matrix affects AMPA receptor lateral mobility and short-term synaptic plasticity.* Nature neuroscience, 2009. **12**(7): p. 897-904.

96.   Gogolla, N., et al., *Perineuronal nets protect fear memories from erasure.* Science, 2009. **325**(5945): p. 1258-61.

97.   Pizzorusso, T., et al., *Reactivation of ocular dominance plasticity in the adult visual cortex.* Science, 2002. **298**(5596): p. 1248-51.

98.   Celio, M.R. and I. Blumcke, *Perineuronal nets--a specialized form of extracellular matrix in the adult nervous system.* Brain research. Brain research reviews, 1994. **19**(1): p. 128-45.

99.   Golgi, C., *Intorno alla struttura delle cellule nervose.* Boll Soc Med-chir Pavia, 1898. **1**: p. 1-14.

100.   Lander, C., H. Zhang, and S. Hockfield, *Neurons produce a neuronal cell surface-associated chondroitin sulfate proteoglycan.* J Neurosci, 1998. **18**(1): p. 174-83.

101.   Galtrey, C.M. and J.W. Fawcett, *The role of chondroitin sulfate proteoglycans in regeneration and plasticity in the central nervous system.* Brain research reviews, 2007. **54**(1): p. 1-18.

102.   Maleski, M. and S. Hockfield, *Glial cells assemble hyaluronan-based pericellular matrices in vitro.* Glia, 1997. **20**(3): p. 193-202.

103.   Hockfield, S. and R.D. McKay, *A surface antigen expressed by a subset of neurons in the vertebrate central nervous system.* Proc Natl Acad Sci U S A, 1983. **80**(18): p. 5758-61.

104.   Bruckner, G., et al., *Perineuronal nets provide a polyanionic, glia-associated form of microenvironment around certain neurons in many parts of the rat brain.* Glia, 1993. **8**(3): p. 183-200.

105.   Wintergerst, E.S., et al., *Temporal and spatial appearance of the membrane cytoskeleton and perineuronal nets in the rat neocortex.* Neuroscience letters, 1996. **209**(3): p. 173-6.

106.   Xiao, Z.C., et al., *Distinct effects of recombinant tenascin-R domains in neuronal cell functions and identification of the domain interacting with the neuronal recognition molecule F3/11.* Eur J Neurosci, 1996. **8**(4): p. 766-82.

107.   Apostolova, I., A. Irintchev, and M. Schachner, *Tenascin-R restricts posttraumatic remodeling of motoneuron innervation and functional recovery after spinal cord injury in adult mice.* J Neurosci, 2006. **26**(30): p. 7849-59.

108.   Hensch, T.K., *Critical period regulation.* Annu Rev Neurosci, 2004. **27**: p. 549-79.

109.   Knudsen, E.I., *Sensitive periods in the development of the brain and behavior.* Journal of cognitive neuroscience, 2004. **16**(8): p. 1412-25.

110.   Wiesel, T.N., *Postnatal development of the visual cortex and the influence of environment.* Nature, 1982. **299**(5884): p. 583-91.

111.   Akers, K.G., et al., *Ontogeny of contextual fear memory formation, specificity, and persistence in mice.* Learning & memory, 2012. **19**(12): p. 598-604.

112.   Kim, J.H. and R. Richardson, *A developmental dissociation in reinstatement of an extinguished fear response in rats.* Neurobiology of learning and memory, 2007. **88**(1): p. 48-57.

113.   Kim, J.H. and R. Richardson, *New findings on extinction of conditioned fear early in development: theoretical and clinical implications.* Biological psychiatry, 2010. **67**(4): p. 297-303.

114.   Wu, C. and D.G. Hunter, *Amblyopia: diagnostic and therapeutic options.* American journal of ophthalmology, 2006. **141**(1): p. 175-184.

115. Berardi, N., et al., *Molecular basis of plasticity in the visual cortex.* Trends in neurosciences, 2003. **26**(7): p. 369-78.

116. Lander, C., et al., *A family of activity-dependent neuronal cell-surface chondroitin sulfate proteoglycans in cat visual cortex.* J Neurosci, 1997. **17**(6): p. 1928-39.

117. Pizzorusso, T., et al., *Structural and functional recovery from early monocular deprivation in adult rats.* Proc Natl Acad Sci U S A, 2006. **103**(22): p. 8517-22.

118. Zuo, J., et al., *Degradation of chondroitin sulfate proteoglycan enhances the neurite-promoting potential of spinal cord tissue.* Exp Neurol, 1998. **154**(2): p. 654-62.

119. Bradbury, E.J., et al., *Chondroitinase ABC promotes functional recovery after spinal cord injury.* Nature, 2002. **416**(6881): p. 636-40.

120. Barritt, A.W., et al., *Chondroitinase ABC promotes sprouting of intact and injured spinal systems after spinal cord injury.* J Neurosci, 2006. **26**(42): p. 10856-67.

121. Corvetti, L. and F. Rossi, *Degradation of chondroitin sulfate proteoglycans induces sprouting of intact purkinje axons in the cerebellum of the adult rat.* J Neurosci, 2005. **25**(31): p. 7150-8.

122. Garcia-Alias, G., et al., *Chondroitinase ABC treatment opens a window of opportunity for task-specific rehabilitation.* Nat Neurosci, 2009. **12**(9): p. 1145-51.

123. Lemons, M.L., et al., *Intact aggrecan and chondroitin sulfate-depleted aggrecan core glycoprotein inhibit axon growth in the adult rat spinal cord.* Exp Neurol, 2003. **184**(2): p. 981-90.

124. Grimpe, B. and J. Silver, *A novel DNA enzyme reduces glycosaminoglycan chains in the glial scar and allows microtransplanted dorsal root ganglia axons to regenerate beyond lesions in the spinal cord.* J Neurosci, 2004. **24**(6): p. 1393-7.

125. Takeuchi, K., et al., *Chondroitin sulphate N-acetylgalactosaminyl-transferase-1 inhibits recovery from neural injury.* Nature communications, 2013. **4**: p. 2740.

126. Fehlings, M.G. and B. Arvin, *The timing of surgery in patients with central spinal cord injury.* Journal of neurosurgery. Spine, 2009. **10**(1): p. 1-2.

127. Papadopoulos, S.M., et al., *Immediate spinal cord decompression for cervical spinal cord injury: feasibility and outcome.* The Journal of trauma, 2002. **52**(2): p. 323-32.

128. Chipman, J.G., W.E. Deuser, and G.J. Beilman, *Early surgery for thoracolumbar spine injuries decreases complications.* The Journal of trauma, 2004. **56**(1): p. 52-7.

129. Croce, M.A., et al., *Does optimal timing for spine fracture fixation exist?* Annals of surgery, 2001. **233**(6): p. 851-8.

130. Furlan, J.C., et al., *Timing of decompressive surgery of spinal cord after traumatic spinal cord injury: an evidence-based examination of pre-clinical and clinical studies.* Journal of neurotrauma, 2011. **28**(8): p. 1371-99.

131. Vaccaro, A.R., et al., *Neurologic outcome of early versus late surgery for cervical spinal cord injury.* Spine, 1997. **22**(22): p. 2609-13.

132. Rosenberg, J.C. and K. Lysz, *Suppression of the immune response by steroids. Comparative potency of hydrocortisone, methylprednisolone, and dexamethasone.* Transplantation, 1980. **29**(5): p. 425-8.

133. Hall, E.D., et al., *Biochemistry and pharmacology of lipid antioxidants in acute brain and spinal cord injury.* J Neurotrauma, 1992. **9 Suppl 2**: p. S425-42.

134. Bracken, M.B., et al., *Efficacy of methylprednisolone in acute spinal cord injury.* JAMA : the journal of the American Medical Association, 1984. **251**(1): p. 45-52.

135.	Braughler, J.M. and E.D. Hall, *Effects of multi-dose methylprednisolone sodium succinate administration on injured cat spinal cord neurofilament degradation and energy metabolism.* Journal of neurosurgery, 1984. **61**(2): p. 290-5.

136.	Hall, E.D. and J.M. Braughler, *Effects of intravenous methylprednisolone on spinal cord lipid peroxidation and Na+ + K+)-ATPase activity. Dose-response analysis during 1st hour after contusion injury in the cat.* Journal of neurosurgery, 1982. **57**(2): p. 247-53.

137.	Bracken, M.B., et al., *A randomized, controlled trial of methylprednisolone or naloxone in the treatment of acute spinal-cord injury. Results of the Second National Acute Spinal Cord Injury Study.* The New England journal of medicine, 1990. **322**(20): p. 1405-11.

138.	Coleman, W.P., et al., *A critical appraisal of the reporting of the National Acute Spinal Cord Injury Studies (II and III) of methylprednisolone in acute spinal cord injury.* Journal of spinal disorders, 2000. **13**(3): p. 185-99.

139.	Hanigan, W.C. and R.J. Anderson, *Commentary on NASCIS-2.* Journal of spinal disorders, 1992. **5**(1): p. 125-31; discussion 132-3.

140.	Hurlbert, R.J., *Methylprednisolone for acute spinal cord injury: an inappropriate standard of care.* Journal of neurosurgery, 2000. **93**(1 Suppl): p. 1-7.

141.	Short, D.J., W.S. El Masry, and P.W. Jones, *High dose methylprednisolone in the management of acute spinal cord injury - a systematic review from a clinical perspective.* Spinal Cord, 2000. **38**(5): p. 273-86.

142.	Bracken, M.B., et al., *Administration of methylprednisolone for 24 or 48 hours or tirilazad mesylate for 48 hours in the treatment of acute spinal cord injury. Results of the Third National Acute Spinal Cord Injury Randomized Controlled Trial. National Acute Spinal Cord Injury Study.* JAMA : the journal of the American Medical Association, 1997. **277**(20): p. 1597-604.

143.	Bracken, M.B., et al., *Methylprednisolone or tirilazad mesylate administration after acute spinal cord injury: 1-year follow up. Results of the third National Acute Spinal Cord Injury randomized controlled trial.* Journal of neurosurgery, 1998. **89**(5): p. 699-706.

144.	Surgeons, A.A.o.N.S.C.o.N., *Pharmacological therapy after acute cervical spinal cord injury.* Neurosurgery, 2002. **50**(3 Suppl): p. S63-72.

145.	Hurlbert, R.J. and M.G. Hamilton, *Methylprednisolone for acute spinal cord injury: 5-year practice reversal.* The Canadian journal of neurological sciences. Le journal canadien des sciences neurologiques, 2008. **35**(1): p. 41-5.

146.	Gris, P., et al., *Transcriptional regulation of scar gene expression in primary astrocytes.* Glia, 2007. **55**(11): p. 1145-55.

147.	Dermitzakis, E.T. and A.G. Clark, *Evolution of transcription factor binding sites in Mammalian gene regulatory regions: conservation and turnover.* Molecular biology and evolution, 2002. **19**(7): p. 1114-21.

148.	Stolt, C.C., et al., *The Sox9 transcription factor determines glial fate choice in the developing spinal cord.* Genes Dev, 2003. **17**(13): p. 1677-89.

149.	Kordes, U., Y.C. Cheng, and P.J. Scotting, *Sox group E gene expression distinguishes different types and maturational stages of glial cells in developing chick and mouse.* Brain Res Dev Brain Res, 2005. **157**(2): p. 209-13.

150.	Kawakami, Y., et al., *Transcriptional coactivator PGC-1alpha regulates chondrogenesis via association with Sox9.* Proc Natl Acad Sci U S A, 2005. **102**(7): p. 2414-9.

151. Furumatsu, T., et al., *Smad3 induces chondrogenesis through the activation of SOX9 via CREB-binding protein/p300 recruitment.* J Biol Chem, 2005. **280**(9): p. 8343-50.

152. Wehrli, B.M., et al., *Sox9, a master regulator of chondrogenesis, distinguishes mesenchymal chondrosarcoma from other small blue round cell tumors.* Hum Pathol, 2003. **34**(3): p. 263-9.

153. Laudet, V., D. Stehelin, and H. Clevers, *Ancestry and diversity of the HMG box superfamily.* Nucleic Acids Res, 1993. **21**(10): p. 2493-501.

154. Bergstrom, D.E., et al., *Related function of mouse SOX3, SOX9, and SRY HMG domains assayed by male sex determination.* Genesis, 2000. **28**(3-4): p. 111-24.

155. Southard-Smith, E.M., L. Kos, and W.J. Pavan, *Sox10 mutation disrupts neural crest development in Dom Hirschsprung mouse model.* Nat Genet, 1998. **18**(1): p. 60-4.

156. Oosterwegel, M., M. van de Wetering, and H. Clevers, *HMG box proteins in early T-cell differentiation.* Thymus, 1993. **22**(2): p. 67-81.

157. Schilham, M.W. and H. Clevers, *HMG box containing transcription factors in lymphocyte differentiation.* Seminars in immunology, 1998. **10**(2): p. 127-32.

158. Hargrave, M., et al., *Expression of the Sox11 gene in mouse embryos suggests roles in neuronal maturation and epithelio-mesenchymal induction.* Developmental dynamics : an official publication of the American Association of Anatomists, 1997. **210**(2): p. 79-86.

159. Uwanogho, D., et al., *Embryonic expression of the chicken Sox2, Sox3 and Sox11 genes suggests an interactive role in neuronal development.* Mechanisms of development, 1995. **49**(1-2): p. 23-36.

160. Kamachi, Y., et al., *Involvement of SOX proteins in lens-specific activation of crystallin genes.* The EMBO journal, 1995. **14**(14): p. 3510-9.

161. Ng, L.J., et al., *SOX9 binds DNA, activates transcription, and coexpresses with type II collagen during chondrogenesis in the mouse.* Dev Biol, 1997. **183**(1): p. 108-21.

162. Wagner, T., et al., *Autosomal sex reversal and campomelic dysplasia are caused by mutations in and around the SRY-related gene SOX9.* Cell, 1994. **79**(6): p. 1111-20.

163. Foster, J.W., et al., *Campomelic dysplasia and autosomal sex reversal caused by mutations in an SRY-related gene.* Nature, 1994. **372**(6506): p. 525-30.

164. Khoshhal, K. and R.M. Letts, *Orthopaedic manifestations of campomelic dysplasia.* Clinical orthopaedics and related research, 2002(401): p. 65-74.

165. Noyal, P., et al., *[Camptomelic dysplasia. A case of survival for more than 4 years].* Archives francaises de pediatrie, 1982. **39**(8): p. 621-4.

166. Ray, S. and J.R. Bowen, *Orthopaedic problems associated with survival in campomelic dysplasia.* Clinical orthopaedics and related research, 1984(185): p. 77-82.

167. R, S. and M.P. A, *Role of SOX9 in the Etiology of Pierre-Robin Syndrome.* Iranian journal of basic medical sciences, 2013. **16**(5): p. 700-4.

168. Pacifici, M., et al., *Hypertrophic chondrocytes. The terminal stage of differentiation in the chondrogenic cell lineage?* Annals of the New York Academy of Sciences, 1990. **599**: p. 45-57.

169. Lefebvre, V., et al., *SOX9 is a potent activator of the chondrocyte-specific enhancer of the pro alpha1(II) collagen gene.* Mol Cell Biol, 1997. **17**(4): p. 2336-46.

170. Bridgewater, L.C., V. Lefebvre, and B. de Crombrugghe, *Chondrocyte-specific enhancer elements in the Col11a2 gene resemble the Col2a1 tissue-specific enhancer.* J Biol Chem, 1998. **273**(24): p. 14998-5006.

171. Sekiya, I., et al., *SOX9 enhances aggrecan gene promoter/enhancer activity and is up-regulated by retinoic acid in a cartilage-derived cell line, TC6.* J Biol Chem, 2000. **275**(15): p. 10738-44.

172. Xie, W.F., et al., *Trans-activation of the mouse cartilage-derived retinoic acid-sensitive protein gene by Sox9.* Journal of bone and mineral research : the official journal of the American Society for Bone and Mineral Research, 1999. **14**(5): p. 757-63.

173. Bell, D.M., et al., *SOX9 directly regulates the type-II collagen gene.* Nat Genet, 1997. **16**(2): p. 174-8.

174. Bi, W., et al., *Sox9 is required for cartilage formation.* Nat Genet, 1999. **22**(1): p. 85-9.

175. Akiyama, H., et al., *The transcription factor Sox9 has essential roles in successive steps of the chondrocyte differentiation pathway and is required for expression of Sox5 and Sox6.* Genes Dev, 2002. **16**(21): p. 2813-28.

176. Smits, P., et al., *The transcription factors L-Sox5 and Sox6 are essential for cartilage formation.* Developmental cell, 2001. **1**(2): p. 277-90.

177. Lefebvre, V., P. Li, and B. de Crombrugghe, *A new long form of Sox5 (L-Sox5), Sox6 and Sox9 are coexpressed in chondrogenesis and cooperatively activate the type II collagen gene.* EMBO J, 1998. **17**(19): p. 5718-33.

178. Gris, D., et al., *Transient blockade of the CD11d/CD18 integrin reduces secondary damage after spinal cord injury, improving sensory, autonomic, and motor function.* J Neurosci, 2004. **24**(16): p. 4043-51.

179. Gris, P., et al., *Gene expression profiling in anti-CD11d mAb-treated spinal cord-injured rats.* J Neuroimmunol, 2009. **209**(1-2): p. 104-13.

180. Scheff, S.W., et al., *Experimental modeling of spinal cord injury: characterization of a force-defined injury device.* J Neurotrauma, 2003. **20**(2): p. 179-93.

181. Jakeman, L.B., et al., *Traumatic spinal cord injury produced by controlled contusion in mouse.* J Neurotrauma, 2000. **17**(4): p. 299-319.

182. Kakulas, B.A., *A review of the neuropathology of human spinal cord injury with emphasis on special features.* J Spinal Cord Med, 1999. **22**(2): p. 119-24.

183. Anderson, T.E. and B.T. Stokes, *Experimental models for spinal cord injury research: physical and physiological considerations.* Journal of neurotrauma, 1992. **9 Suppl 1**: p. S135-42.

184. Basso, D.M., M.S. Beattie, and J.C. Bresnahan, *A sensitive and reliable locomotor rating scale for open field testing in rats.* J Neurotrauma, 1995. **12**(1): p. 1-21.

185. Bi, W., et al., *Haploinsufficiency of Sox9 results in defective cartilage primordia and premature skeletal mineralization.* Proc Natl Acad Sci U S A, 2001. **98**(12): p. 6698-703.

186. Hayashi, S. and A.P. McMahon, *Efficient recombination in diverse tissues by a tamoxifen-inducible form of Cre: a tool for temporally regulated gene activation/inactivation in the mouse.* Dev Biol, 2002. **244**(2): p. 305-18.

Chapter 2: Conditional SOX9 ablation reduces chondroitin sulfate proteoglycan expression and improves motor function following spinal cord injury

William M. McKillop[a,b], Magdalena Dragan[a], Anna Pniak[a], Andreas Schedl[c], Arthur Brown[a,b]

Corresponding Author: Dr. Arthur Brown

Robarts Research Institute, Schulich School of Medicine,

University of Western Ontario

100 Perth Drive, London, Ontario, Canada, N6A 5K8

Email: abrown@robarts.ca

Telephone: 519-663-3776 ext. 24308

[a] Robarts Research Institute, University of Western Ontario, London, Canada

[b] Department of Anatomy and Cell Biology, University of Western Ontario, London, Canada

[c] INSERM U636, Centre de Biochimie, and University of Nice/Sophia-Antipolis, Nice, France

2.0 Abstract

Chondroitin sulfate proteoglycans (CSPGs) found in perineuronal nets and in the glial scar after spinal cord injury have been shown to inhibit axonal growth and plasticity. Since we have previously identified SOX9 as a transcription factor that up-regulates the expression of a battery of genes associated with glial scar formation in primary astrocyte cultures, we predicted that conditional *Sox9* ablation would result in reduced CSPG expression after spinal cord injury and that this would lead to increased neuroplasticity and improved locomotor recovery. Control and *Sox9* conditional knockdown mice were subject to a 70 kdyne contusion spinal cord injury at thoracic level 9. One week after injury, *Sox9* conditional knockdown mice expressed reduced levels of CSPG biosynthetic enzymes (XT-1 and C4st), CSPG core proteins (brevican, neurocan and aggrecan), collagens 2a1 and 4a1, and GFAP, a marker of astrocyte activation, in the injured spinal cord compared to controls. These changes in gene expression were accompanied by improved hind limb function and locomotor recovery as evaluated by the Basso Mouse Scale (BMS) and rodent activity boxes. Histological assessments confirmed reduced CSPG deposition and collagenous scarring at the lesion of *Sox9* conditional knockdown mice, and demonstrated increased neurofilament-positive fibers in the lesion penumbra and increased serotonin immunoreactivity caudal to the site of injury. These results suggest that SOX9 inhibition is a potential strategy for the treatment of SCI.

2.1 Introduction

Damaged axons have a limited capacity for regeneration following adult mammalian spinal cord injury (SCI) [1]. This limited capacity for repair has been attributed, in part, to the nonpermissive environment of the glial scar that forms in the penumbra surrounding the lesion site [2-6]. This glial scar is predominantly formed from extracellular matrix (ECM) molecules expressed by reactive astrocytes although macrophages, microglia, oligodendrocytes, invading Schwann cells and meningeal fibroblasts all contribute to production of the scar matrix [6]. Chief of the many ECM molecules that serve to inhibit axonal regeneration are the chondroitin sulfate proteoglycans (CSPGs) [7, 8] that have greatly increased expression following SCI [4, 9]. CSPGs are a class of ECM macromolecules that share a common structure composed of a central core protein and a number of chondroitin sulfate side chains [10]. Both *in vitro* and *in vivo* studies have shown that axons do not extend into CSPG-rich ECM [4, 5, 11-13], and specific CSPGs which inhibit neurite outgrowth have been identified including: aggrecan [14], neurocan [15], phosphocan [16], brevican [17], versican [18], and NG2 [19].

Strategies designed to target CSPGs at the spinal lesion have resulted in improved axonal regeneration after SCI. Enzymatic digestion of the chondroitin sulfate side chains, found on all CSPGs, by intrathecal chondroitinase treatment resulted in increased regeneration of ascending and descending tracts after SCI [20]. The combination of chondroitinase ABC with peripheral nerve grafts [21, 22], rehabilitation [23, 24], or neural precursor cell transplantation [25] have all led to improved axonal regeneration and recovery.

We have previously argued that genes with related function are regulated together as classes or batteries after SCI [26] and that, in astrocytes, genes that promote axon regeneration

and genes that inhibit axon regeneration would be regulated as gene classes. We predicted that the transcription of genes involved in CSPG production, the genes encoding CSPG core proteins, and genes encoding the enzymes responsible for generating the chondroitin sulfate side chains such as xylosyltransferase-I (XT-I), XT-II and chondroitin-4-sulfotransferase-1 (C4st-1), would be coordinately regulated after SCI. Using bioinformatics we identified putative binding sites for the transcription factor SOX9 (sex-determining region Y-box 9) in the promoter sequences of XT-I, XT-II and C4st-1 in rats, mice and humans. We subsequently used gain of function and loss of function experiments to demonstrate that SOX9 positively regulates the expression of XT-I, XT-II, and C4st-1 in primary astrocyte cultures [27]. Thus we hypothesized that conditional ablation of *Sox9* in mice would result in reduced expression of CSPGs and improved recovery after SCI. We herein report improved hindlimb locomotor recovery after SCI in a line of conditional *Sox9* knockdown mice that correlates with reduced expression of CSPGs and related ECM proteins in the lesion penumbra and at sites more distant to the lesion epicenter.

2.2 Materials and Methods

Mouse breeding and *Sox9* conditional knockdown

Conventional *Sox9* knockdown mice have been generated but are unsuitable for studies of SCI as both *Sox9* knockdown (*Sox9*$^{-/-}$) and heterozygote (*Sox9*$^{+/-}$) embryos do not survive to birth [28]. To evaluate SOX9 loss-of-function after SCI, in a nervous system that developed with normal levels of SOX9 activity, a tamoxifen-inducible conditional *Sox9* knockdown strategy was used. We bred a mouse strain that carries floxed *Sox9* (exons 2 and 3 of *Sox9* surrounded by loxP sites) alleles [29] (*Sox9*$^{flox/flox}$) with a transgenic mouse line that expresses Cre recombinase fused

to the mutated ligand binding domain of the human estrogen receptor (ER) under the control of a chimeric cytomegalovirus immediate-early enhancer/chicken β–actin promoter (B6.Cg-Tg(CAG-Cre/Esr1)5Amc/J)[30] (Jackson Laboratories, Bar Harbor, Maine). The mutated ER ligand binding domain of the fusion protein does not bind endogenous estradiol but is highly sensitive to nanomolar concentrations of tamoxifen [31]. The Cre-ER fusion protein remains trapped in the cytoplasm of all cells until tamoxifen administration allows its transport to the nucleus where it excises *loxP*-flanked *Sox9* DNA [30]. The resulting *Sox9$^{flox/flox}$;CAGGCreER (Sox9$^{flox/flox}$;Cre)* offspring served as tamoxifen inducible *Sox9* knockdown animals, and *Sox9$^{flox/flox}$* offspring served as control animals expressing normal levels of SOX9. Animals were genotyped by PCR analysis using the following primers:

Sox9^{flox} allele: 5'-ACACAGCATAGGCTACCTG-3' and

5'-TGGTAATGAGTCATACACAGTAC-3'.

Sox9^{wildtype} allele: 5'-GGGGCTTGTCTCCTTCAGAG-3' and

5'- TGGTAATGAGTCATACACAGTAC-3'.

Sox9^{knockdown} allele: 5'-GTCAAGCGACCCATG-3' and

5'-TGGTAATGAGTCATACACAGTAC-3'.

Cre^{+} allele: 5'-CAATTTACTGACCGTACAC-3' and 5'-AGCTGGCCCAAATGTTGCTG-3'.

Tamoxifen (Sigma Aldrich, St. Louis, Missouri) was administered at 3 mg/20 g mouse by oral gavage to all *Sox9$^{flox/flox}$;Cre* and *Sox9$^{flox/flox}$* littermates once per day for 7 days. Following the final day of tamoxifen oral gavage, the animals were housed for 7 days without treatment to allow time for Cre-mediated recombination and tamoxifen clearance prior to subsequent SCI.

Primary astrocyte culture

Primary astrocyte cultures were prepared from newborn $Sox9^{flox/flox};Cre$ or $Sox9^{flox/flox}$ control mice at postnatal day 1. The upper portion of the skull was removed and the meninges carefully dissected away to avoid contamination of the culture with fibroblasts. The neocortices were removed, individually placed into serum-free Eagle Minimum Essential Medium (EMEM) (Lonza, Walkersville, Maryland), homogenized by trituration, and gravity-filtered through a 40-μm cell strainer (Becton Dickinson and Company, Toronto, Ontario). The cells were plated in EMEM + 20% FBS (Invitrogen, Carlsbad, California), penicillin/streptomycin (Invitrogen, Carlsbad, California); each animal's cells were divided into two wells each of a 6-well dish (Becton Dickinson and Company, Toronto, Ontario). After 2 days, media was changed to EMEM + 10% FBS, penicillin/streptomycin, and was changed three times per week thereafter. After 2 weeks in culture 1 μM 4-hydroxytamoxifen (Sigma Aldrich, St. Louis, Missouri) was administered in three changes of media over 1 week. Following 4-hydroxytamoxifen administration the cells were cultured in normal media for 1 more week. The percentage of GFAP-expressing cells in these cultures was found to be >95%.

Real time PCR

RNA was extracted from *Sox9* conditional knockdown and *Sox9* positive control primary astrocyte cultures 1 week post tamoxifen administration, and from the lesion epicentre of *Sox9* conditional knockdown and *Sox9* positive control mice 1 week post-SCI, using the RNA-Easy kit according to the manufacturer's instructions (Qiagen, Valencia, California). First strand cDNA was synthesized from 1 μg RNA per sample using the High Capacity cDNA Archive Kit

according to the manufacturer instructions (Applied Biosystems, Carlsbad, California). The primer probe sets, optical adhesive covers, and PCR plates were purchased from Applied Biosystems (Carlsbad, California). All primer probes were labeled with 5'FAM and with 3'TAMRA as quencher with the exception of the 18s ribosomal probe, which was labeled with 5' VIC. TaqMan assays were conducted using the Applied Biosystems gene expression assay primer probe sets listed in Table 1.

Table 1. List of TaqMan Real-Time PCR Primer Probe Sets

Primer Probe	Catalog number	PCR Ct range
18s	4308329	*14.72–16.07*
Sox9	Mm00448840_m1	*21.88–23.64*
XT-I	Mm00558690_m1	*27.34–29.57*
XT-II	Mm00461181_m1	*24.72–25.87*
C4st-1	Mm00517563_m1	*21.72–23.01*
Aggrecan	Mm00545807_m1	*24.53–27.07*
Brevican	Mm00476090_m1	*18.35–21.70*
Neurocan	Mm00484007_m1	*17.31–20.73*
Collagen 2A1	Mm01309562_g1	*23.40–27.33*
Collagen 4A1	Mm00802377_m1	*20.73–21.39*
GFAP	Mm01253033_m1	*19.96–22.16*
Cartilage link protein	Mm00488952_m1	*28.35–29.94*

TaqMan (Applied Biosystems, Carlsbad, California) gene expression assays were conducted on a 7900HT fast real time PCR apparatus (Applied Biosystems, Carlsbad, California) using thermal cycler conditions set as follows; 10 min at 95°C followed by 40 cycles of 30 s at 95°C followed by 30 s at 60°C. Cycle thresholds (Ct) for all target genes were kept below 30 as indicated in Table 1. A standard curve of cycle thresholds using cDNA serial dilutions was established and used to calculate mRNA expression. Target gene mRNA expression was normalized to the amount of 18S mRNA present in each sample. The ratio of knockdown to control sample normalized target gene mRNA was analyzed by Student's T-test.

Western blotting

Protein was isolated from the lesion site (0.45 cm) in tamoxifen-treated *Sox9* conditional knockdown and *Sox9* positive control mice 2 weeks post-SCI. The spinal cord tissue was lysed in modified RIPA buffer (1% nonidet P-40, 150 mM NaCl, 0.5% sodium deoxycholate, 0.1% SDS, 50 mM Tris, 1 mM EDTA, pH 7.5, plus 1 complete Mini protease inhibitor tablet/7mL RIPA buffer (Roche Molecular Biochemicals, Indianapolis, Indiana) on ice using a ground glass homogenizer. The protein mixture was centrifuged at 13,000 x g for 5 min and the supernatant collected, and diluted in reducing PAGE loading buffer. Protein samples were loaded on reducing SDS-PAGE gels at 10 μg/well. The membrane was blocked in 10% nonfat powdered milk and then incubated with primary antibodies; anti-SOX9 (AB 5535, Millipore, Billerica, Massachusetts used at 1:1000), anti-GFAP (MAB360, Millipore, Billerica, Massachusetts, used at 1:1000), and anti-β-actin (A1978, Sigma, St. Louis, Missouri, used at 1:10,000) for protein

expression assessed by western blot. HRP conjugated anti-mouse IgG (715-035-151, Jackson ImmunoResearch Laboratories, West Grove, Pennsylvania) and HRP conjugated anti-rabbit IgG (711-035-152, Jackson ImmunoResearch Laboratories, West Grove, Pennsylvania) secondary antibodies were used at 1:20,000 dilution to detect SOX9, GFAP, and β-actin protein expression. SOX9 and GFAP protein expression was normalized to β-actin protein expression by densitometry using the EpiChemi[3] Darkroom (UVP Bioimaging Systems, Upland, California) and LabWorks software (Media Cybernetics Inc, Bethesda, Maryland). Protein samples were also loaded in parallel at 3 μg/well into a Bio-Rad Slot-blot apparatus (BioRad, Mississauga, Ontario) and vacuum transferred onto a nitrocellulose membrane (BioRad, Mississauga, Ontario). The membrane was blocked in 10% nonfat powdered milk and then incubated with primary antibody at 1:200 dilution overnight for anti-CS-56 (C8035, Sigma, St. Louis, Missouri) or 1:10,000 dilution for anti-β-actin (A1978, Sigma, St. Louis, Missouri). HRP conjugated anti-mouse IgM (62-6820, Invitrogen, Carlsbad, California) and anti-mouse IgG (715-035-151, Jackson ImmunoResearch Laboratories, West Grove, Pennsylvania) secondary antibodies were used at 1:20,000 dilutions to detect CS56 and β-actin protein expression. CS56 protein expression was normalized to β-actin protein expression by densitometry using the EpiChemi[3] Darkroom (UVP Bioimaging Systems, Upland, California) and LabWorks software (Media Cybernetics Inc, Bethesda, Maryland).

Spinal cord injury

All protocols for these experiments were approved by the University of Western Ontario Animal Care Committee in accordance with the policies established in the Guide to Care and Use of Experimental Animals prepared by the Canadian Council on Animal Care. One week after the last tamoxifen oral gavage, 13 female *Sox9^{flox/flox};Cre* and 16 female *Sox9^{flox/flox}* mice were anesthetized with 100 mg/kg ketamine: 5 mg/kg xylazine. The T9 spinal cord segment was exposed by a dorsal laminectomy. The spinal cord was stabilized at T7 and T9 with forceps. The T9 spinal segment was injured by a 70 kdyne contusion delivered with a 1s dwell time by computer controlled Infinite Horizons Impactor (displacement range: 500-900 μM) (Precision Systems and Instrumentation, Fairfax, Virginia). Following SCI the mice were housed individually. Baytril (25 mg/kg, Bayer, Toronto, Ontario, Canada) and buprenorphine (0.01 mg/kg, Schering-Plough, Hertfordshire, UK) were injected subcutaneously for 3 days post-SCI. Bladders were manually emptied twice daily for the duration of the experiment.

Behavioral testing

Locomotor recovery of the animals was assessed by two blinded observers using the Basso Mouse Scale (BMS) open field locomotor score [32]. The day following SCI, all mice were evaluated for any signs of locomotor recovery in their hindlimbs and mice that had BMS scores > 0.5 were excluded from further analyses (4 *Sox9* conditional knockdowns and 5 controls). Animals were evaluated once per week for 14 weeks after SCI. Left and right hind limb scores were averaged to generate a composite score. In addition, locomotion was evaluated at 14 weeks post-SCI by rodent activity box (Accuscan Instruments Inc, Columbus, Ohio). The

activity box records distance traveled by detecting breaks in a series of infrared light beams. The total distance the mice traveled was measured over a 2 hour period at night (during their normal awake circadian cycle).

Spinal cord sectioning

Protein expression levels of SOX9 target genes were assessed at 14 weeks post-SCI. Animals were deeply anesthetized with 100 mg/kg ketamine: 5 mg/kg xylazine, and cardiac perfusion was carried out with 20 ml of saline at pH 7.4 followed by 20 ml 4% paraformaldehyde (4% PFA in 0.1 M phosphate buffer at pH 7.4). Spinal cords were dissected and post-fixed for 2 h in 4% PFA followed by cryoprotection in 20% sucrose in 0.1 M phosphate buffer at pH 7.4 at 4 ˚C overnight. Spinal cords were embedded in Tissue-Tek O.C.T. Compound (Sakura Finetek U.S.A. Inc, Torrance, California), frozen over dry ice, and stored at -80 ˚C overnight. Frozen cords were then cross-sectioned at 16 µm using a cryostat, and serially thaw-mounted on Superfrost^{TM} glass slides (Fisher Scientific Company, Ottawa, Canada).

Immunohistochemistry and trichrome staining

Immunohistochemistry was conducted using the primary antibodies listed in Table 2. Cryosectioned slides were rinsed in PBS and treated with 5% normal goat serum and 0.1% triton-X-100 in PBS at room temperature for 1 h. Slides were incubated with the appropriate dilutions of primary antibodies in a humidified chamber at 4˚C overnight. Sections were stained for CSPG expression using the monoclonal antibody CS56 that recognizes the terminal portions

of chondroitin sulfate-4 or -6 side chains and thus detects a variety of CSPGs [33] and a biotinylated goat anti-mouse IgM (Vector laboratories, Burlingame, California) secondary antibody (1:200). Sections were then incubated for 45 min with avidin-peroxidase conjugate (Elite Kit, Vector laboratories, Burlingame, California) at room temperature, and the signal visualized by peroxidase diaminobenzine (DAB, Invitrogen, Carlsbad, California). Sections to be stained for perineuronal nets (PNNs) were washed in PBS 3 x 10 min, and incubated with biotinylated Wisteria Floribunda Lectin (WFA, Sigma Aldrich, St. Louis, Missouri) (1:1000) for 1 h at room temperature. Sections were then incubated for 45 min with avidin-peroxidase conjugate (Elite Kit, Vector laboratories, Burlingame, California) at room temperature, and the signal visualized by peroxidase diaminobenzine (DAB, Invitrogen, Carlsbad, California). All DAB staining was conducted with a 2 min DAB reagent incubation time for all *Sox9* conditional knockdown and control cord sections, and were completed at the same time. Immunofluorescent labeling of the remaining proteins was performed using the following secondary antibodies; Alexa-Fluor 488-conjugated goat anti-mouse IgG (1:500, Invitrogen, Carlsbad, California), Alexa-Fluor 488-conjugated goat anti-rabbit IgG (1:500, Invitrogen, Carlsbad, California), or Alexa-Fluor 594-conjugated goat anti-rabbit IgG (1:500, Invitrogen, Carlsbad, California), for 1 h at room temperature. Slides were then washed in PBS and coverslips were attached with ProLong Gold Anti-Fade mounting medium (Invitrogen, Carlsbad, California). Gomori's Trichrome staining was used to stain for collagen according to the manufacturer's instructions (HT10316, Sigma Aldrich, St. Louis, Missouri).

Table 2. List of primary antibodies and stains used for spinal cord staining

Antibody	Dilution	Isotype	Source
Anti-GFAP	1:500	Mouse IgG	Millipore, Billerica, Massachusetts
Anti-CS56	1:300	Mouse IgM	Sigma Aldrich, St. Louis, Missouri
Anti-NF200	1:1000	Rabbit IgG	Sigma Aldrich, St. Louis, Missouri
Anti-5HT	1:500	Rabbit IgG	ImmunoStar, Hudson, Wisconsin
WFA	1:1000		Sigma Aldrich, St. Louis, Missouri

Quantification of GFAP, CS56, trichrome, NF-200, 5-HT, and WFA staining

GFAP, CS56, trichrome, and NF-200 staining were analyzed as follows. Cross-sections 16 μm thick and 160 μm apart between 1.6 mm rostral through 1.6 mm caudal to the epicentre of injury were analyzed for positive staining using Image Pro Plus software (Media Cybernetics Inc, Bethesda, Maryland). A threshold was set for each stain that identified positive signal (staining above background levels). The area of positive staining was normalized to total cord area. Staining results were grouped into 5 bins based on position relative to the lesion epicentre that was arbitrarily set as zero. The bin set as the epicenter encompassed 0.65 mm rostral and 0.65 mm caudal to the epicenter. The 1.3 mm included in the "epicenter" bin that approximates the size of the head of the impactor. The rostral bins encompassed two directly adjacent segments of spinal cord rostral to the lesion (0.8 mm each) and the two caudal bins encompassed two directly adjacent segments of spinal cord rostral to the lesion (0.8 mm each).

The area of 5-HT immunoreactivity (area per area of interest) was quantified in the intermediolateral cell column (IML) and in the ventral horns in 16 μm thick cross-sections 160 μm apart obtained 0.8-1.6 mm caudal to the injury site using Image Pro Plus Software (Media Cybernetics Inc, Bethesda, Maryland). A single pre-set area was used to define all IML or ventral horn regions in all cords across both *Sox9* conditional knockdown and control animal sections. The area of positive 5-HT immunoreactivity was quantified within this set area defined as the IML or ventral horn. The area of WFA immunoreactivity to identify PNNs was analyzed using 16 μm thick cross-sections 160 μm apart sampled at T10. Positive staining was quantified using Image Pro Plus Software (Media Cybernetics Inc, Bethesda, Maryland) using a threshold which identified positive signal (staining above background levels).

Statistical analysis

Mean values are expressed ± SE. Both *in vitro* and *in vivo* mRNA analyses were subjected to statistical analysis using Student's T-test. 5-HT and WFA quantification was subjected to statistical analysis using Student's T-test. CS56, trichrome, GFAP, and NF-200 immunohistochemical quantification was subjected to statistical analysis using two-way ANOVA with Neuman-Keuls post-hoc test at each binned region of the cord, rostral, epicenter, and caudal to the site of injury. BMS results were subjected to statistical analysis using two-way repeated measures ANOVA with Neuman-Keuls post-hoc test. Activity Box locomotion was subjected to statistical analysis using one-way ANOVA with Neuman-Keuls post hoc test. Analyses were conducted with GraphPad Prism software (GraphPad Software Inc, La Jolla, California), except for two-way ANOVAs which were conducted with SigmaStat software

(Systat Software Inc, San Jose, California), and significance was accepted at $p<0.05$. A two-way ANOVA summary table is provided as Supplementary Table 1.

2.3 Results

Changes in gene expression in primary astrocytes isolated from *Sox9* conditional knockdowns

Astrocyte cultures were isolated from *Sox9* conditional knockdown and from control mice to evaluate the effects of *Sox9*-ablation on gene expression in primary astrocytes. All cultures were treated with 4-hydroxytamoxifen for 1 week and then cultured free of tamoxifen for an additional week before harvesting for RNA isolation. Using quantitative-PCR (Q-PCR) we measured the mRNA levels of *Sox9*, *XT-I*, *XT-II*, *C4st-1*, *Col2a1*, *Col4a1*, cartilage link protein (*Crtl)*, and aggrecan *(Agc)* (Fig. 1). The mRNA levels of glial fibrillary acidic protein (*GFAP*), a marker of astrocyte activation, and brevican and neurocan (two CSPG core proteins) were also measured as we predicted that SOX9 would regulate genes broadly associated with astrocyte activation and scar production. Quantitative PCR demonstrated that administration of 4-hydroxytamoxifen resulted in a 72% ± 4% reduction in *Sox9* mRNA expression compared to control mouse astrocyte cultures. Reduced *Sox9* expression was associated with a statistically significant reduction in the expression of *XT-I*, *Agc*, brevican, neurocan, *Col2a1*, and *GFAP*, in comparison to control astrocyte cultures (Fig. 1).

Figure 1. Astrocytes from *Sox9* conditional knockdown mice demonstrate reduced glial scar gene expression compared to control mice. Treating *Sox9$^{flox/flox}$;Cre* astrocyte cultures with 1 μM 4-hydroxytamoxifen for one week results in a 72% ± 4% reduction in *Sox9* mRNA levels and is accompanied by a statistically significant reduction in *XT-1*, *aggrecan* (Agc), *brevican* (B-can), *neurocan* (N-can), *Col2A1*, and *GFAP* mRNA levels compared to *Sox9$^{flox/flox}$* astrocytes treated with 1 μM 4-hydroxytamoxifen, ($p<0.05$, Student's T-test; n=4 per group).
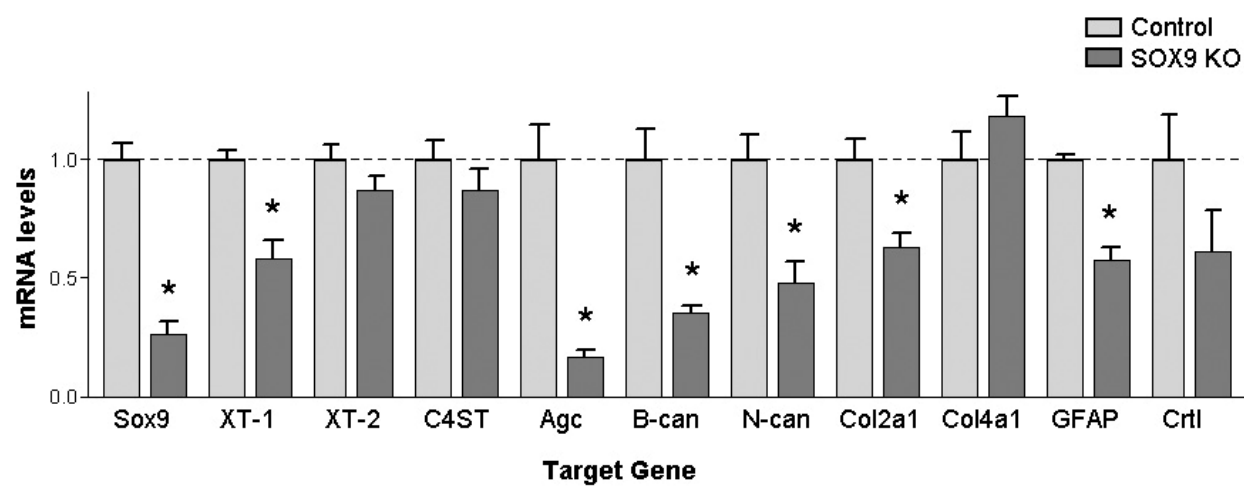
Changes in gene expression in the injured spinal cord in *Sox9* conditional knockdowns

To determine if the reductions in gene expression observed in the *Sox9*^{flox/flox}*;Cre* primary astrocyte cultures would also be observed after SCI we evaluated mRNA expression levels at the lesion in *Sox9* conditional knockdown and control mouse spinal cords one week after a 70 kdyne SCI. Q-PCR demonstrated a 62% ± 11% reduction in *Sox9* mRNA levels in the *Sox9* conditional knockdown mice compared to controls (Fig. 2). This reduction in *Sox9* mRNA levels was associated with a statistically significant reduction in *XT-I, C4st-1*, *Agc*, brevican, neurocan, *Col2a1*, *Col4a1*, and *GFAP* mRNA expression as compared to control mice (Fig. 2). To determine if these changes in mRNA levels result in parallel changes in protein levels we evaluated protein expression by western and slot blot analysis. *Sox9* conditional knockdown mice displayed significantly reduced SOX9, GFAP and CSPG protein expression 2 weeks post-SCI (Fig. 3).

Sox9 conditional knockdown mice demonstrate improved locomotor recovery after SCI

As the glial scar in general and CSPGs in particular have been identified as inhibitors of axonal regeneration after SCI we predicted that the reduction in CSPG and collagen expression at the spinal lesion observed at 1-2 weeks post-injury would lead to improved locomotor recovery in *Sox9* conditional knockdown mice. *Sox9*^{flox/flox}*;Cre* and control mice were administered tamoxifen for one week and allowed a week for tamoxifen washout before undergoing a 70 kdyne SCI using the Infinite Horizon impactor. Hind limb function was evaluated weekly for 14 weeks post-SCI. On day one following SCI all mice displayed paralyzed hind limbs, scoring a zero on the Basso Mouse Scale (BMS).   In both *Sox9*

Figure 2. ***Sox9* conditional knockdown mice demonstrate reduced glial scar gene expression compared to control mice.** Spinal cord-injured, tamoxifen-treated *Sox9$^{flox/flox}$;Cre* mice demonstrate a 62% ± 11% reduction in *Sox9* mRNA expression compared to spinal cord-injured, tamoxifen-treated *Sox9$^{flox/flox}$* mice one week post-SCI. This reduction in *Sox9* expression is associated with a statistically significant reduction in *XT-1*, *C4st*-1, *Agc*, brevican (B-can), neurocan (N-can), *Col2A1* and *4A1*, and *GFAP* mRNA levels ($p < 0.05$, Student's T-test; n=5 per group).
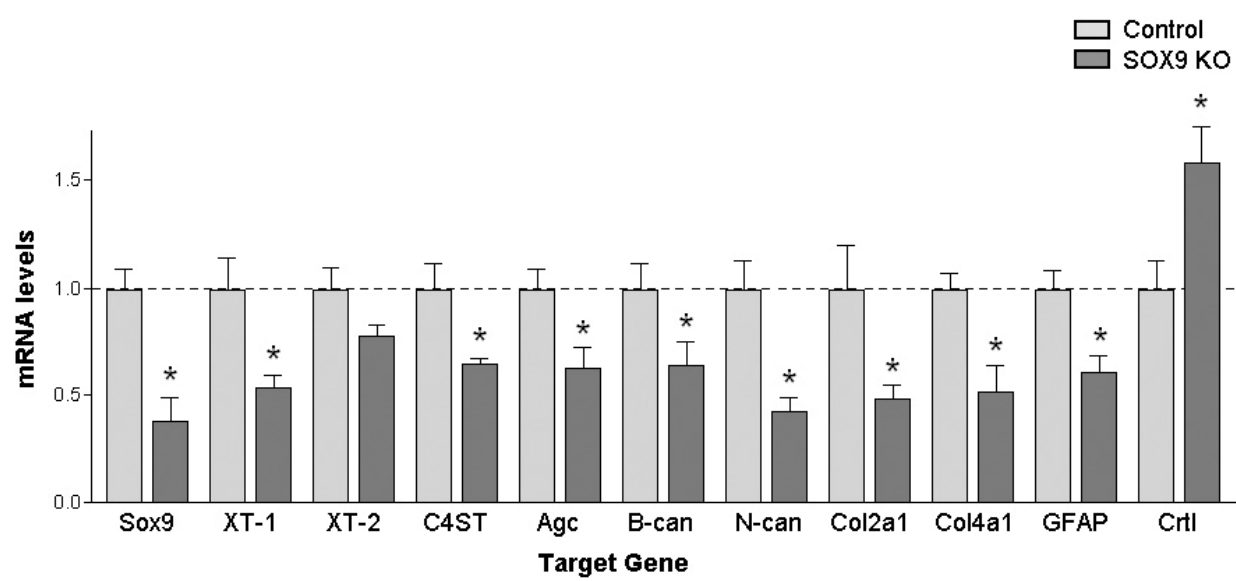
Figure 3. *Sox9* conditional knockdown mice demonstrate reduced SOX9, GFAP, and CSPG protein 2 weeks post-SCI. A) Western blot analysis and subsequent densitometry (B, C) demonstrate reduced SOX9 and GFAP levels in *Sox9* conditional knockdown mice in comparison to control mice (normalized to β-actin levels) ($p=<0.05$, Student's T-test; n=3). D) Slot blot and subsequent densitometry (E) demonstrates reduced CSPG expression in *Sox9* conditional knockdown mice compared to controls (normalized to β-actin levels) ($p=<0.05$, Student's T-test; n=3).

A

Controls   SOX9 KO

SOX9

GFAP

β-ACTIN

D

Control   Sox9 KO   Control   Sox9 KO

CSPG   β-ACTIN

B

SOX9 levels
2 weeks post-SCI

Protein Levels

1.5

1.0

0.5

0.0

Control   SOX9 KO

*

C

GFAP levels
2 weeks post-SCI

Protein Levels

1.5

1.0

0.5

0.0

Control   SOX9 KO

*

E

CSPG levels
2 weeks post-SCI

Protein Levels

1.5

1.0

0.5

0.0

Control   SOX9 KO

*
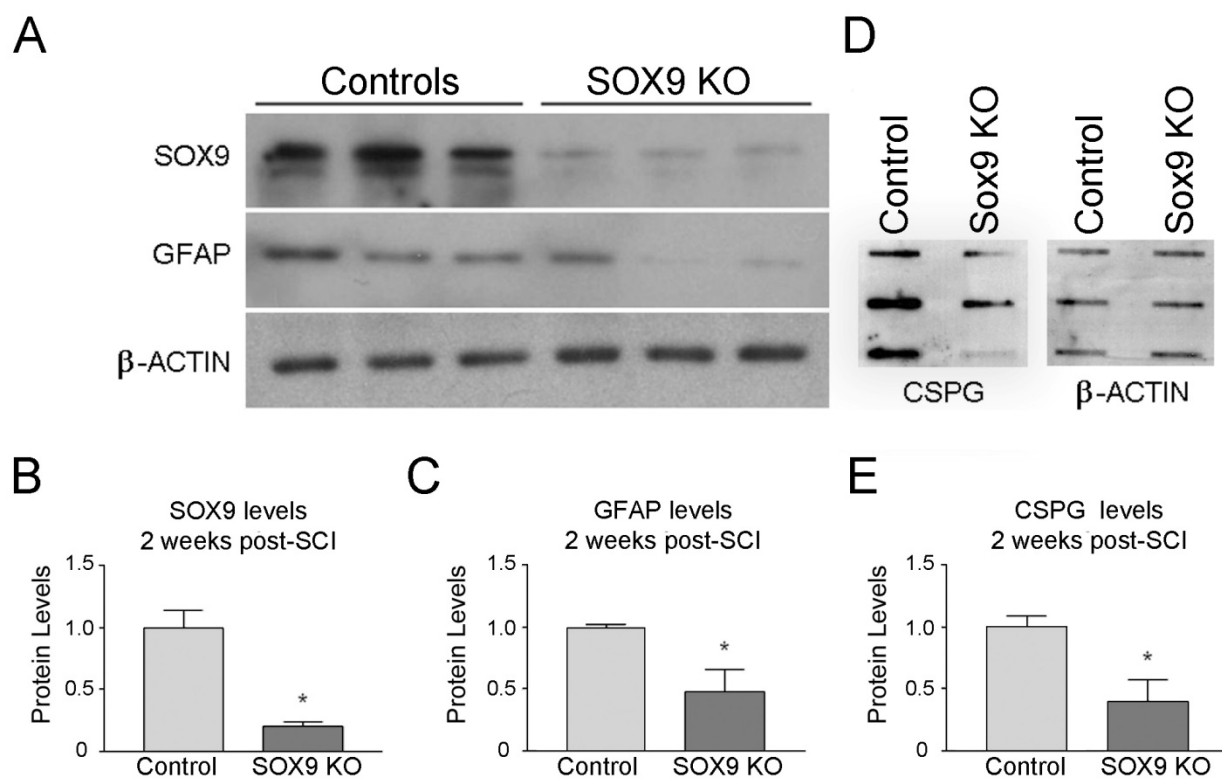
conditional knockdown and control mice hind limb locomotion gradually improved over time. Locomotor BMS scoring in control mice reached a plateau of 0.63 ± 0.21 at 4 weeks post-SCI, (Fig. 4a). The median BMS score in this group of 0.5 indicates slight (less than 90˚) movement in one ankle. In contrast, the BMS scores of the *Sox9* conditional knockdown mice continued to improve past 4 weeks and did not reach a plateau until 11 weeks post-SCI, achieving an average BMS score of 1.81 ± 0.19. The median BMS score for *Sox9* conditional knockdown mice of 2 indicates extensive (greater than 90˚) movement in both ankles. The significantly higher scores of the *Sox9* conditional knockdown mice were accompanied by a statistically significant increase in ability to achieve plantar placement of their hind limbs (Chi squared test p=0.005); six of nine *Sox9* conditional knockdown mice displayed at least one limb capable of plantar placement compared to one of eleven control mice which were capable of plantar placement. Finally, *Sox9* conditional knockdown mice and controls were placed in a computer-monitored rodent activity box to record total distance traversed over a 2 h period. Fourteen weeks after SCI, control mice covered a total distance of 1414 ± 269 cm in 2 h, whereas *Sox9* conditional knockdown mice covered a total distance of 3481 ± 814 cm in 2 h. The distance traversed by the *Sox9* conditional knockdown mice was significantly greater than that in the injured control animals and was not significantly different from uninjured *Sox9$^{flox/flox}$* mice (3330 ± 402 cm in 2 h) or uninjured control mice (3452 ± 526.5 cm in 2 h) (p=0.027 by 1-way ANOVA with Neuman-Keuls post hoc test) (Fig. 4b) .

Figure 4. *Sox9* **conditional knockdown mice demonstrate improved locomotor recovery after SCI.** A) *Sox9* conditional knockdown mice display increased hind limb functional recovery in comparison to control mice. Both *Sox9* conditional knockdown and control mice display hind limb paralysis immediately following SCI on day 1 post-SCI. *Sox9* conditional knockdown mice score higher (increased hind limb function) on the Basso Mouse Scale (BMS) in comparison to control mice every week between 1 and 14 weeks after SCI ($p<0.05$, 2 way repeated measures ANOVA, Newman-Keuls post-hoc tests ($p<0.05$); n=9 SOX9 KO, n= 11 control). B) *Sox9* conditional knockdown mice demonstrate increased distance traveled in comparison to control injured mice measured over a 2 h period in a rodent activity box ($p<0.05$, 1-way ANOVA; n=9 SOX9 KO, n= 11 controls).
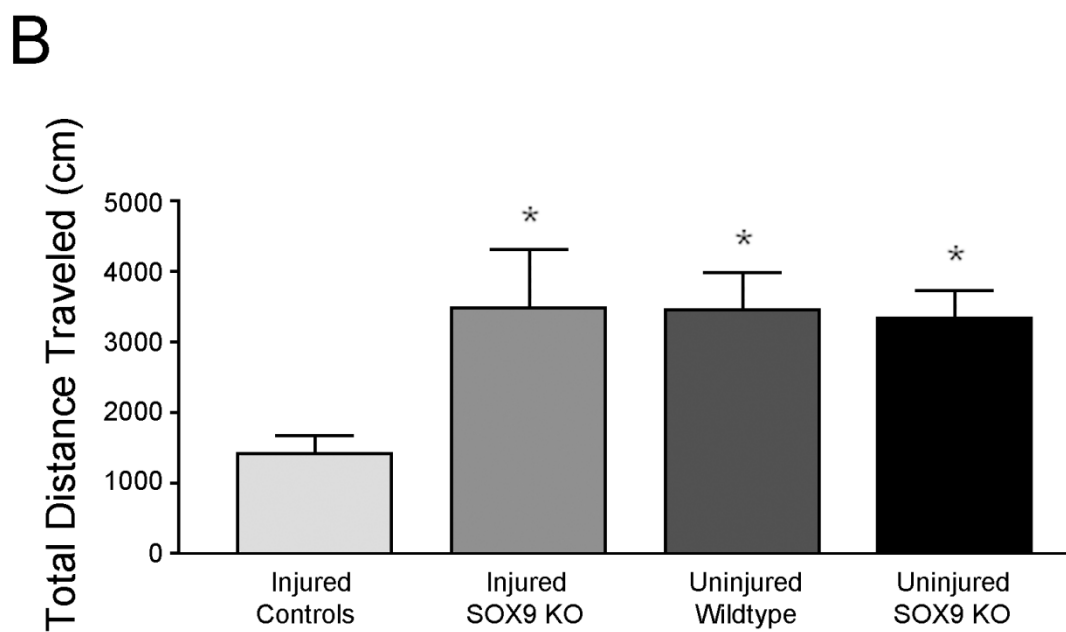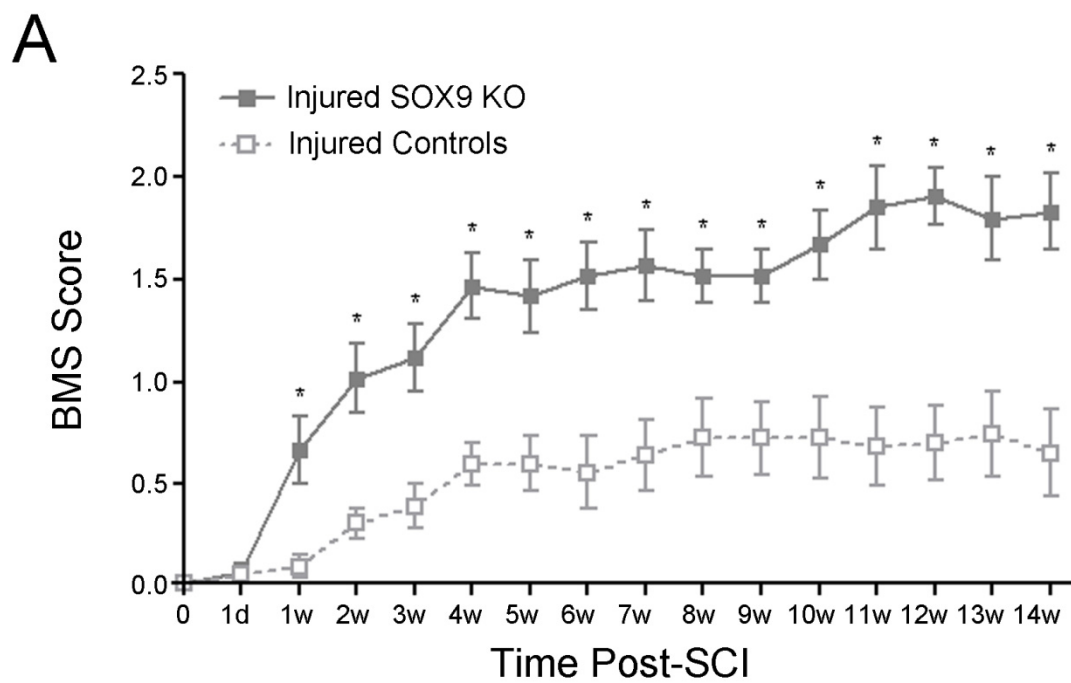
Sox9 conditional knockdown mice display reduced CSPG, collagen and GFAP expression at the lesion site 14 weeks following SCI

Since the *Sox9* conditional knockdown animals had reduced levels of *XT-I, C4st-1, Agc,* brevican, neurocan, *Col2a1, Col4a1,* and *GFAP* mRNA at 1 week post-SCI and concomitant reductions in CSPG and GFAP protein levels at the lesion 2 weeks post-SCI, we anticipated that these animals would display reduced evidence of a glial scar at 14 weeks post-SCI. Spinal cord sections from *Sox9* conditional knockdown mice at 14 weeks after SCI demonstrated a significant reduction in CSPG immunoreactivity (area immunoreactivity per cord area) rostral to, caudal to and at the lesion epicenter compared to controls (Fig. 5). Decreased CSPG staining correlated with increased BMS scores by linear regression analysis ($r^2 = 0.69$). Quantifying the area of positive trichrome staining for collagen (blue stain in Fig. 6) demonstrated reduced amounts of collagen (area immunoreactivity per cord area) in the lesion epicenter in *Sox9* conditional knockdown mice compared to controls. Finally, in agreement with the Q-PCR data at 1 week post-SCI and the protein quantitation at 2 weeks post-SCI, immunohistochemistry demonstrated reduced expression of GFAP (area immunoreactivity per cord area) in *Sox9* conditional knockdown mice rostral to, caudal to and at the lesion epicenter 14 weeks post-injury (Fig. 7). Together these data indicate that at 14 weeks post-injury, the lesion of spinal cord injured *Sox9* conditional knockdown animals contains fewer reactive astrocytes and less glial and collagenous scarring than that of the control animals.

Figure 5. *Sox9* conditional knockdown mice display reduced CSPG expression 14 weeks post-SCI. Representative photomicrographs of anti-CSPG DAB immunohistochemical staining approximately 1 mm rostral to the lesion epicenters (A) at the epicenters (B) and 1 mm caudal to the lesion epicenters (C) from *Sox9* conditional knockdowns and controls as indicated. D) Quantification of area of CSPG immunoreactivity in *Sox9* conditional knockdown and control sections. The area of immunostaining per cross-sectional area of spinal cord was quantified using ImageProPlus software on sections spaced 160 μm apart. The area per area measurements were then grouped into bins centered on the positions indicated. The bin representing epicenter in each animal extended 0.65 mm rostral and caudal to the center of the lesion. The bins rostral and caudal to the epicenter were centered on the positions shown relative to the epicenter and included sections 0.4 mm rostral and caudal. * indicates statistically significantly different from controls (p<0.05, 2 way ANOVA, Newman-Keuls post-hoc test (p<0.05); n = 9 *Sox9* KO, n =11 controls). Bars = 100 μm.

A **Rostral**

Control   SOX9 KO

B **Epicenter**

Control   SOX9 KO

C **Caudal**

Control   SOX9 KO

D **CSPG**

Area of immunoreactivity / cord area

☐ Control
■ SOX9 KO

| 1.85 | 1.05 | 0 | -1.05 | -1.85 |

Rostral   Epicenter   Caudal

Position relative to lesion (mm)
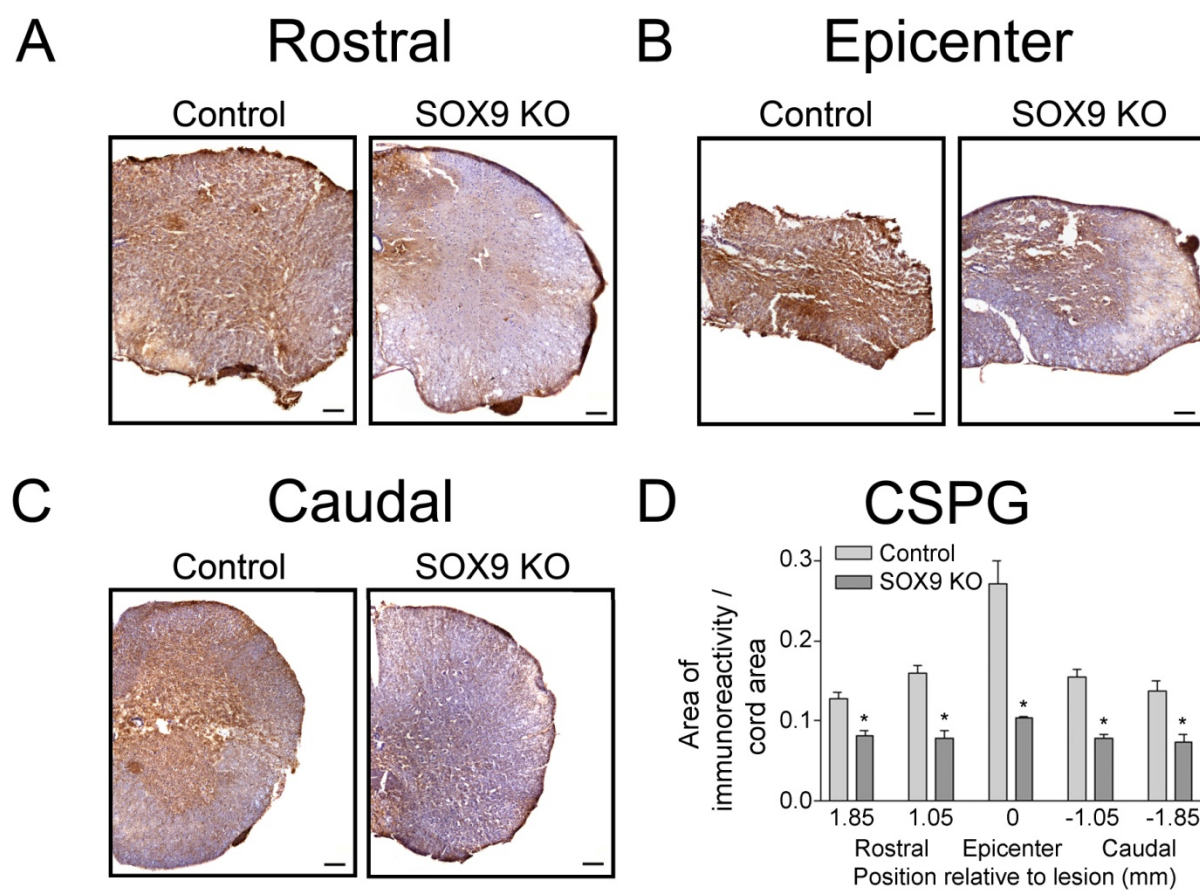
Figure 6. *Sox9* conditional knockdown mice demonstrate reduced collagen at the lesion epicenter 14 weeks post-SCI. A) Representative photomicrographs of Trichrome-stained spinal cord sections from the lesion epicenters of *Sox9* conditional knockdown and control mice.   B) High power magnifications of boxed areas in A). C) Quantification of area of collagen (blue) staining in *Sox9* conditional knockdown and control sections.   Areas of collagen staining were quantified as explained in legend to Figure 5. * indicates statistically significantly different from controls (p<0.05, 2 way ANOVA, Newman-Keuls post-hoc test (p<0.05); n=9 *Sox9* KO, n = 11 control). Bars = 100 μm.
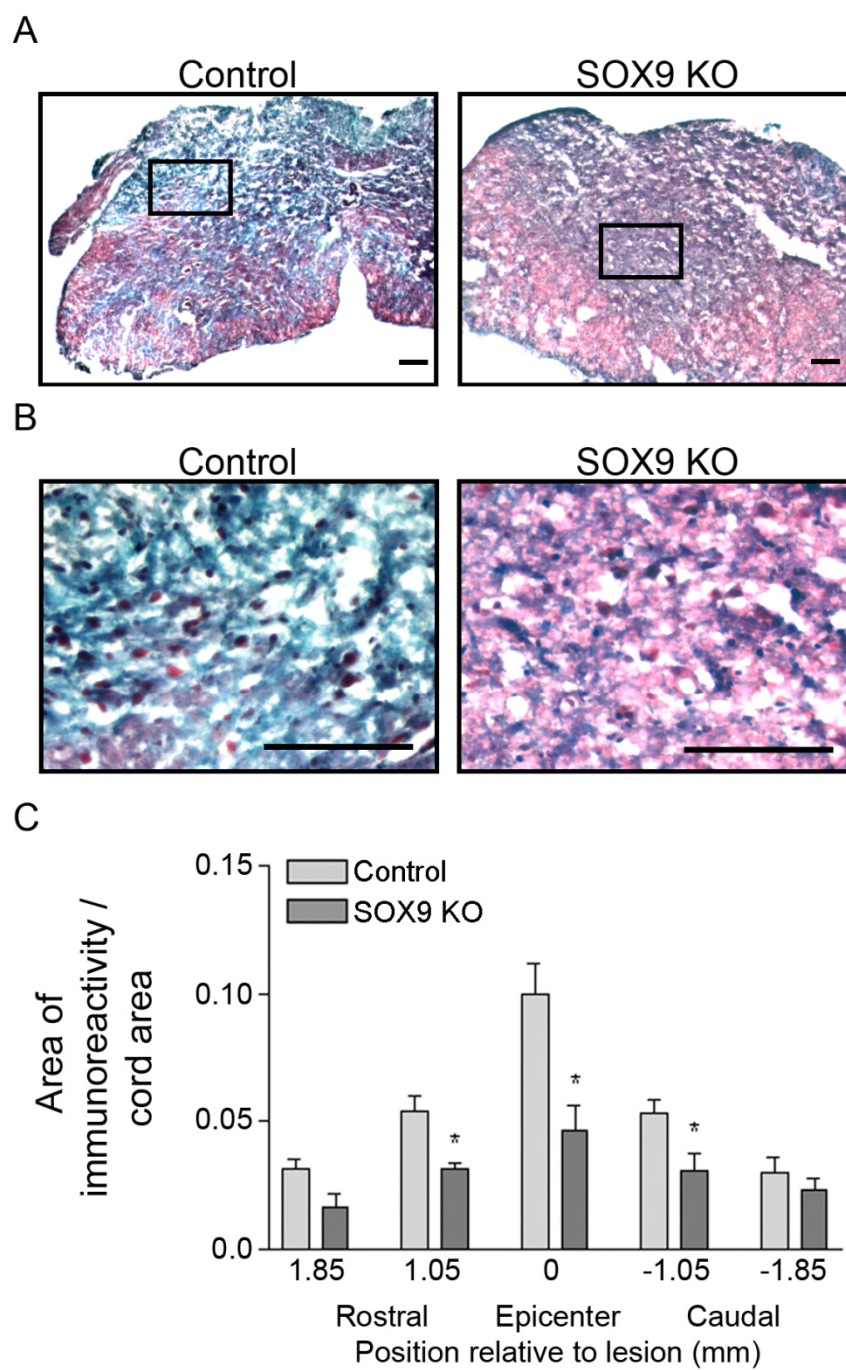
Figure 7. *Sox9* **conditional knockdown mice demonstrate reduced GFAP expression 14 weeks post-SCI.** A) Representative photomicrographs of anti-GFAP immuno-staining from spinal cord sections approximately 1 mm rostral to the lesion epicenters (A) at the epicenters (B) and 1 mm caudal to the lesion epicenters C) from *Sox9* conditional knockdowns and controls as indicated. D) Quantification of area of GFAP immunoreactivity (area per area) in *Sox9* conditional knockdown and control sections. Areas of GFAP immuno-staining were quantified as explained in legend to Figure 5. * indicates statistically significantly different from controls ($p < 0.05$, 2 way ANOVA, Newman-Keuls post-hoc test ($p < 0.05$); n=9 *Sox9* KO, n = 11 controls). Bars = 100 µm.

A **Rostral**
Control   SOX9 KO

B **Epicenter**
Control   SOX9 KO

C **Caudal**
Control   SOX9 KO

D **GFAP**
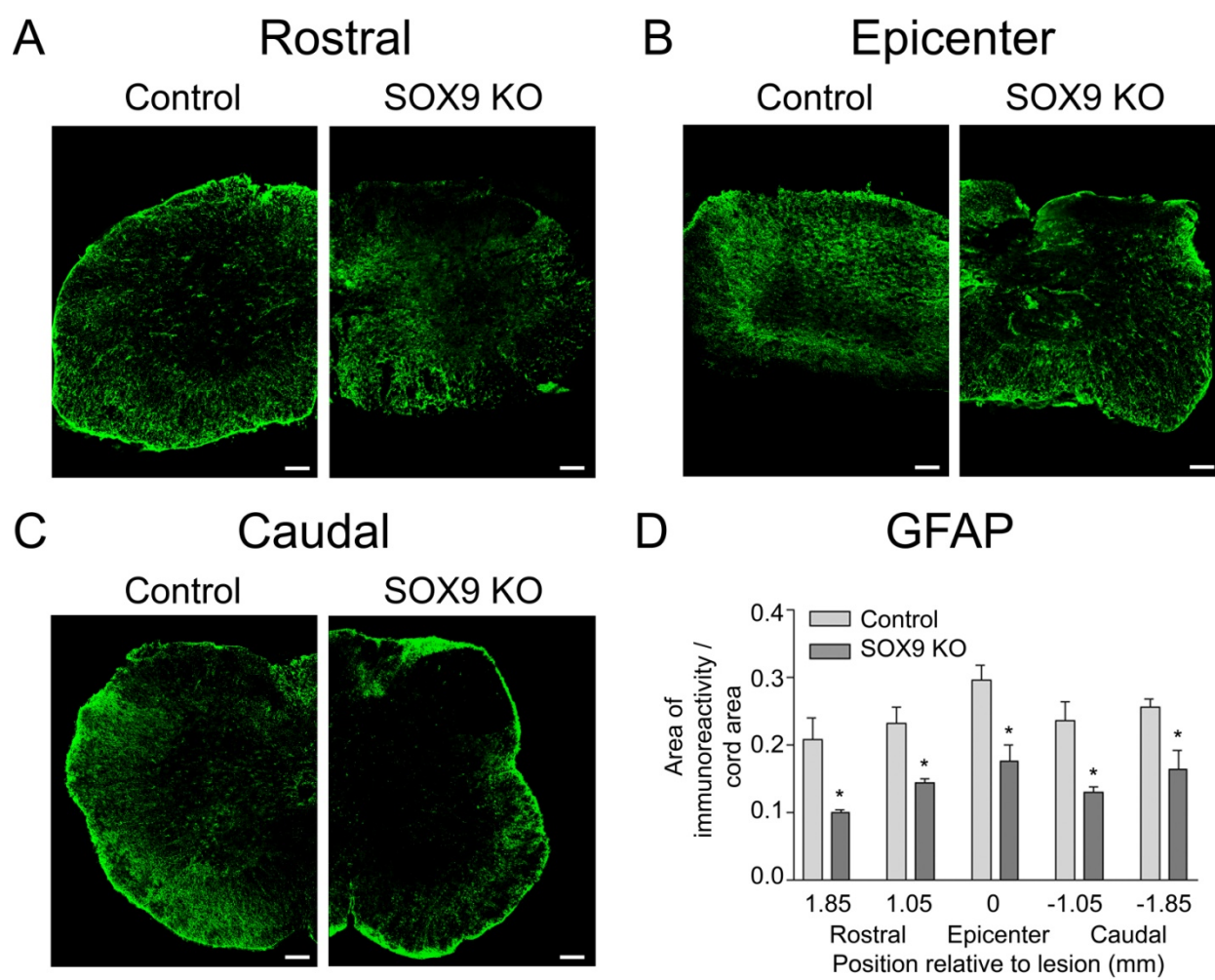
***Sox9* conditional knockdown mice have increased neurofilament-positive fibers in the penumbra of the lesion site following SCI**

As the reduced CSPG and collagen levels in the *Sox9* conditional knockdown lesions would be predicted to correlate with an environment more permissive to axonal growth and sprouting, we expected to observe an increased number of neurofilament-positive fibers in the spinal lesions of the *Sox9* conditional knockdown mice compared to controls. Immuno-stained spinal cord sections from *Sox9* conditional knockdowns and controls demonstrated significant reductions in neurofilament at the lesion epicenter (Fig. 8). Whereas the area of neurofilament immunoreactivity (area immunoreactivity per cord area) in the *Sox9* conditional knockdown mice was not significantly different from controls at the lesion epicenter, neurofilament immunoreactivity was increased in the bins 0.8 mm rostral and caudal to the lesion epicenter in *Sox9* conditional knockdowns compared to controls (Fig. 8).

***Sox9* knockdown mice display increased 5-HT immunoreactivity caudal to the lesion site following SCI**

Descending serotonergic (5-HT positive) projections from the raphe nuclei control a variety of normal body functions. Serotonergic projections synapsing in the dorsal horn modulate pain sensation [34, 35], serotonergic projections targeting sympathetic preganglionic neurons in the intermediolateral cell column (IML) contribute to autonomic regulation [36], and serotonergic projections synapsing in the ventral horn provide excitatory input to motor neurons, the loss of which correlates with locomotor dysfunction [37]. To evaluate whether the improved recovery achieved by the *Sox9* conditional knockdown mice could be attributed to increased

Figure 8. *Sox9* **conditional knockdown mice demonstrate increased neurofilament immunoreactivity rostral and caudal to their lesion epicenters 14 weeks post-SCI.** A) Representative photomicrographs of anti-neurofilament immuno-staining from spinal cord sections approximately 0.5 mm rostral to the lesion epicenters (A) at the epicenters (B) and 0.5 mm caudal to the lesion epicenters C) from *Sox9* conditional knockdowns and controls as indicated. D) Quantification of area of neurofilament immunoreactivity (area per area) in *Sox9* conditional knockdown and control sections. Areas of neurofilament immuno-staining were quantified as explained in legend to Figure 5. * indicates statistically significantly different from controls ($p<0.05$, 2 way ANOVA, Newman-Keuls post-hoc test ($p<0.05$); n=9 *Sox9* KO, n = 11 control). Bars = 100 µm.

A Rostral

Control | SOX9 KO

B Epicenter

Control | SOX9 KO

C Caudal

Control | SOX9 KO

D Neurofilament-200
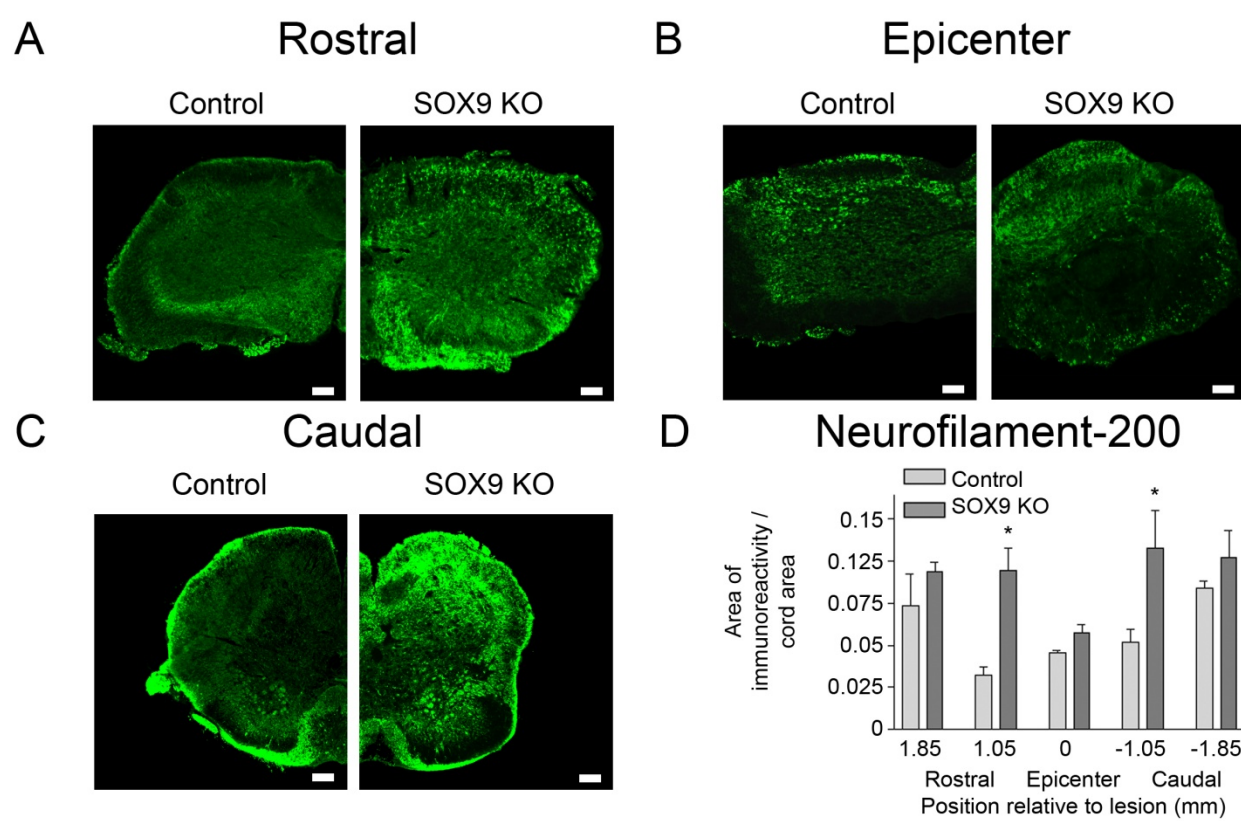
Figure 9. *Sox9* conditional knockdown mice display increased 5-HT immunoreactivity caudal to the lesion. Immunohistochemistry was used to detect serotonin in the spinal cord 14 weeks post-SCI. A) Representative photomicrographs of sections stained for 5-HT immunoreactivity ~1.2 mm caudal to the lesion epicenter from *Sox9* conditional knockdown and control mice. Almost no 5-HT immunoreactivity was observed caudal to the lesion in control mice, however 5-HT immunoreactivity was observed caudal to the lesion in SOX9 conditional knockdown mice. B) High power magnifications of boxed areas in A). C) Quantification of 5-HT immunoreactivity. 5-HT-immunoreactivity was significantly increased in intermediolateral cell column and the ventral horn of *Sox9* conditional knockdown mice in comparison to control mice. * indicates statistically significantly different from controls (Student's T-test, p=<0.05; n=9 *Sox9* KO, n = 11 controls). Bars = 100 μm.

A Control SOX9 KO

B Control SOX9 KO

IML

VH

C Serotonin (5-HT) staining in the IML caudal to epicenter

D Serotonin (5-HT) staining in the ventral horn caudal to epicenter
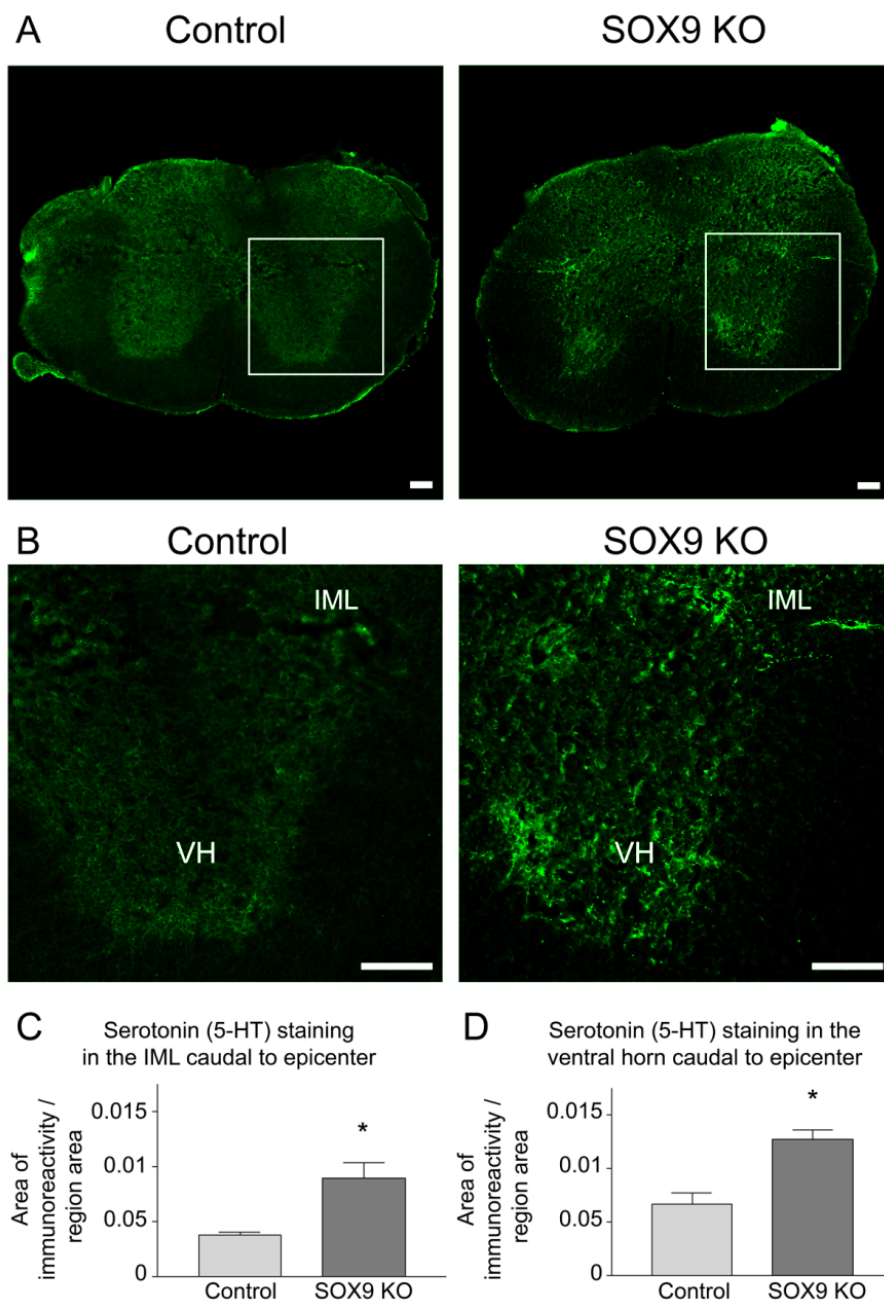
5-HT inputs onto targets caudal to the injury we performed immunostaining for 5-HT on cross-sections from *Sox9* conditional knockdowns and controls 14 weeks after SCI. Between 0.8 mm - 1.6 mm caudal to the lesion epicenter *Sox9* conditional knockdown mice displayed a statistically significant increase in 5-HT immunoreactivity in the IML and ventral horn, compared to control mice (Fig. 9).

Sox9 conditional knockdown mice display decreased WFA caudal to the lesion site following SCI

In addition to their contribution to the glial scar matrix CSPGs are also a major component of the PNN ECM that stabilize synapses during development [38] and limit plasticity in the adult nervous system. Since *Sox9* conditional knockdowns demonstrated reduced levels of CSPGs and other ECM components at the glial scar we evaluated whether they may also demonstrate reductions in the ECM in their PNNs. Cross-sections from *Sox9* conditional knockdowns and controls were stained with biotinylated Wisteria floribunda agglutinin (WFA). WFA binds N-acetylgalactosamine side chains in proteoglycans including CSPGs [39, 40]. Cross-sections $1.6 - 3.2$ mm caudal of the lesion epicenter were selected for WFA-staining to determine whether conditional *Sox9* ablation might lead to a reduction in PNN ECM distal to the lesion. WFA staining revealed a reduction in PNNs in the *Sox9* knockdown mice caudal to the lesion compared to control mice 14 weeks post-SCI (Fig. 10). This suggests that ablation of Sox9 creates a more growth-permissive environment in the mouse spinal cord, possibly contributing to improved motor function after spinal cord injury.

Figure 10. Perineuronal net matrix is reduced in *Sox9* conditional knockdown mice caudal to lesion 14 weeks post-SCI. WFA staining was used to detect PNN matrix caudal to lesion epicenter in control and *Sox9* conditional knockdown mice. A) Representative photomicrographs of sections stained for WFA caudal to the lesion epicenter from *Sox9* conditional knockdown and control mice. B) High power magnifications of boxed areas in A. C) Quantification of area of WFA staining in *Sox9* conditional knockdown and control sections. The area of WFA stained tissue per cross-sectional area of spinal cord was quantified using ImageProPlus software on sections spaced 160 μm apart from 1.6 to 3.2 mm caudal to the epicenters. * indicates statistically significantly different from controls (Student's T-test, p=<0.05; n=9 *Sox9* KO, n = 11 controls). Bars = 100 μm.

A   Control   SOX9 KO

B   Control   SOX9 KO

C   WFA staining 1.6-3.2mm
caudal to epicenter
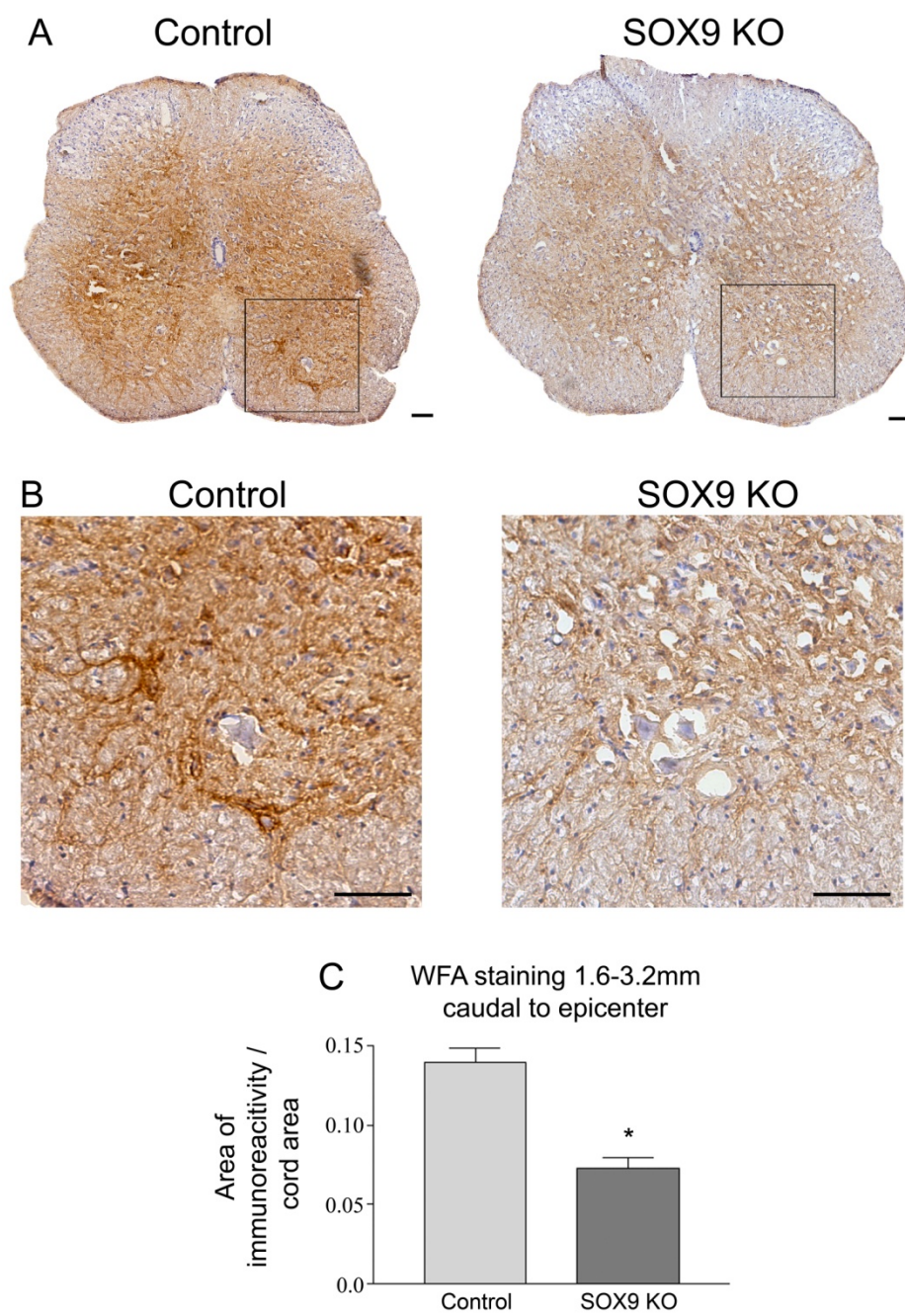
2.4 Discussion

Although the glial scar plays a key role in the acute response to SCI by sealing the lesion site, restoring homeostasis, and modulating immunity, it also presents an obstacle to recovery [41]. In the adult mammalian CNS, glial scarring is a major constraint to successful axonal regeneration. The scar impedes axonal growth through the lesion and leads to either misrouting or growth arrest, both ultimately resulting in chronic denervation [42-45]. These anti-

regenerative properties of the glial scar are predominantly caused by the build-up of various proteoglycans and collagens after injury [46-48]. Having previously demonstrated that siRNA knock-down of the transcription factor SOX9 down-regulates the expression of CSPG-synthetic enzymes in astrocyte cultures [27], we investigated the effect of *in vivo Sox9* conditional knockdown on gene expression, glial scarring and functional recovery after SCI.

In addition to our siRNA work demonstrating SOX9 regulation of xylosyltransferase-I and II and C4st-1[27] , others have shown that SOX9 also regulates the expression of *Col2a1* [49, 50], *Col4a1* [51], the CSPG core protein *Agc* [52], and *Crtl* [53]. 4-hydroxytamoxifen-induced knock-down of SOX9 expression in astrocyte cultures was accompanied by reduced mRNA expression of most of the predicted SOX9 target genes. In the injured spinal cord of tamoxifen-treated $Sox9^{flox/flox}$;*Cre* mice the mRNA expression of these same genes with the addition of *C4st-1*, *Col4a1* were also significantly reduced compared to controls; this was paralleled by reductions in SOX9, GFAP and CSPG protein levels. These results largely confirm the anti-*Sox9* siRNA results in rat primary astrocytes previously reported [27] and demonstrate that the SOX9 target genes identified in astrocyte cell culture experiments are also regulated by SOX9 *in vivo* in the injured spinal cord.

Some predicted SOX9 target genes did not show reduced expression in *Sox9* knockdown astrocyte cultures or spinal cord-injured mice. *XT-II* expression was not reduced in either the *Sox9$^{flox/flox}$;Cre* astrocyte cultures or spinal cord injured mice, suggesting that SOX9 activity is not necessary for the expression of this isoform of xylosyltransferase. The reduction of *XT-II* expression that we previously described in rat primary astrocyte cultures may simply reflect a minor species difference in SOX9 activities between rats and mice. Whereas *C4st-1*expression was not reduced in *Sox9$^{flox/flox}$;Cre* astrocyte cultures it was reduced in the injured spinal cords of *Sox9$^{flox/flox}$;Cre* mice. This may reflect *in vitro* versus *in vivo* differences in the regulation of *C4st-1* gene expression. The greater dependence *C4st-1* expression on SOX9 activity in the injured spinal cord may be due to the large increase in SOX9 expression that occurs within the first 12 hours of SCI that may mask the effects of other regulators that are important to *C4st-1* expression *in vitro*. Expression of *Col4a1,* like *C4st-1*, was not reduced in the *Sox9* conditional knockdown astrocyte cultures but was reduced in the spinal lesions of *Sox9* conditional knockdown mice after SCI. Others have shown that collagen 4 is expressed in the lesion epicenter in a directly adjacent but non-overlapping pattern with the GFAP-positive astrocytes in the surrounding penumbra [54]. Together this suggests that SOX9 is required for the expression of *Col4a1* in the cells (likely meningeal fibroblasts) that produce collagen 4 in the lesion epicenters. Finally *Crtl* expression was not reduced in the *Sox9* conditional knockdown cultures or in the *Sox9* conditional knockdown mice after SCI suggesting that SOX9 activity is not necessary for *Crtl* expression.   This result was surprising as others have demonstrated that anti-*Sox9* siRNA transfection into a human chondrosarcoma cell line, OUMS-27, resulted in reduced levels of *Crtl* expression [53]. However this same group also demonstrated the presence of a SOX9-independent enhancer element in the 5'-UTR of the *Crtl* gene. Thus we suggest that this

SOX9 independent enhancer element may be regulating expression of *Crtl* in astrocyte cultures and in the injured spinal cord.

The *Sox9* conditional knockdown mice achieved significantly higher BMS scores than controls, improved rates of plantar placement and traversed 2-3 times the distance traversed by controls 14 weeks post-SCI. The strong correlation ($r^2 = 0.61$) between BMS scores at 14 weeks post-SCI and decreased area of CSPG staining at the lesion site suggests that the improved locomoter function in the *Sox9* conditional knockdowns is due to the decreased CSPG expression in these mice following SCI. The reduced expression of *XT-I, C4st-1*, *Agc*, brevican, neurocan, *Col2a1* and *Col4a1* would be expected to produce a less fibrous scar with less CSPG content. Gomori's trichrome staining 14 weeks post-injury confirmed that the *Sox9* conditional knockdown lesions had less collagen than controls. Immunohistochemistry further demonstrated that there was less CSPG content in the *Sox9* conditional knockdown lesions than controls. Neurofilament immuno-staining showed that the area of neurofilament immunoreactivity at the lesion epicenter did not differ significantly between *Sox9* conditional knockdowns and controls. This suggests that the improved locomotor recovery in *Sox9* conditional knockdowns is not due to a greater degree of axonal sparing in these mice nor is it likely due to greater numbers of axons traversing the lesion site to connect caudal to the lesion. However neurofilament immuno-staining rostral and caudal to the lesion epicenters was increased in the *Sox9* conditional knockdown mice, consistent with the suggestion that the reduced CSPG content in the penumbra of the *Sox9* conditional knockdowns permits greater amounts of axonal sprouting. Axonal sprouting rostral and caudal to the lesion may allow the formation of connections with spared propriospinal neurons and underlie the improved locomotor behavior in the *Sox9* conditional knockdowns.

CSPG immunoreactivity and WFA-staining demonstrate reduced CSPG expression and PNN matrix rostral and caudal to the penumbra 14 weeks post-SCI in the *Sox9* conditional knockdowns. Evidence suggests that CSPGs are up-regulated within PNNs both near and far from a CNS lesion [55]. PNNs are produced by both neurons and astrocytes and surround synapses throughout the nervous system [39]. CSPG expression in PNNs is low during the initial stages of synaptogenesis, and dramatically increases toward the end of developmental plasticity [56, 57]. Enzymatic digestion of PNNs by chondroitinase ABC leads to reactivation of plasticity in adult animals [57, 58] , and enhances spared fiber collateral sprouting and synapse formation in injured animals [59]. Thus reduced SOX9 expression may open a window for increased plasticity following SCI at denervated sites within and remote to the lesion. In the *Sox9* conditional knockdowns, reduced PNNs and CSPG content in the PNNs may have permitted spared propriospinal or descending supraspinal axons to synapse on deafferented targets caudal to the lesion. Evidence in support of this comes from the 5-HT immuno-staining which clearly showed increased 5-HT immunoreactivity caudal to the lesion around the IML and ventral horn in *Sox9* conditional knockdowns.

The postulate that reduced CSPGs in the PNNs distal to the lesion may account for the improved locomotor recovery observed in the *Sox9* conditional knockdowns might explain other facets of the recovery in these mice. For example the *Sox9* conditional knockdowns have higher BMS scores than controls starting at one week post-SCI. This improvement in locomotor activity seems to occur too quickly to be explained by long-range regeneration of inputs rostral to the lesion. Furthermore the absence of increased neurofilament immunoreactivity at the lesion epicenter also argues against any significant amount of regeneration across the lesion epicenter. However short-range sprouting of spared axons onto deafferented targets promoted by reduced

CSPGs in PNNs would be expected to occur rapidly. This type of repair may also be less prone to mis-wiring of circuits as the most likely axons to form new synapses on a target will be those that are already innervating adjacent neurons in the same field. This type of repair may be far less demanding on axonal growth and targeting than long range regeneration.

A second possible explanation for improved locomotor recovery of the *Sox9* conditional knockdowns may be the reduced GFAP expression in these mice after SCI. Unlike the other SOX9 target genes that are involved in ECM production, GFAP is a cytoskeletal protein and used most often as a marker of astrocyte activation [60]. Its identification as part of a battery of genes up-regulated by SOX9 after SCI suggests that SOX9 not only up-regulates the expression of ECM-related genes but also regulates the overall state of astrocyte activation and response to injury.   In addition to being a major producer of the glial scar, astrocytes also play an important role in inflammation. In response to TGF-β1 astrocytes up-regulate expression of the pro-inflammatory genes nitric oxide synthase-2 (NOS-2) and cyclooxygenase-2 (COX-2) [61]. IL-1β and TNF-α also increase astrocyte production of nitric oxide [61, 62]. In the *Sox9* conditional knockdown mice, reduced GFAP expression might indicate less astrocyte activation and perhaps less production of pro-inflammatory mediators. Thus a muted inflammatory response may account for some of the improved recovery observed in the *Sox9* conditional knockdowns.

A third possible explanation for improved locomotor recovery of the *Sox9* conditional knockdowns rests on evidence that SOX9 may play a role in neural stem differentiation. Expression studies have shown that SOX9 is expressed by neuroepithelial cells in the ventricular zone of the developing spinal cord, by oligodendrocytes and by astrocytes but not by neurons [63]. Knocking out *Sox9* in the developing mouse spinal cord results in perinatal lethality,

decreased numbers of oligodendrocyte progenitors and astrocytes and an increased number of motor neurons [63] and neuroblasts [64]. MicroRNA studies also suggest that SOX9 is gliogenic, promoting neural stem cells to adopt an astrocyte or oligodendrocyte fate [65]. Following injury, neural stem cells proliferate and differentiate almost exclusively into astrocytes [66, 67] that generate scar, but not into neurons [66]. These results are consistent with the hypothesis that, in neural stem cells, SOX9 expression promotes a glial rather than a neuronal cell fate and that, in *Sox9* conditional knockdowns, neural stem cells activated by the injury may adopt a neuronal as opposed to a glial fate. If astrocytes newly-born after injury contribute to CSPG production, or if newly-born neuroblasts are able to generate new neurons or produce growth factors that support neuronal survival [68-70], then the effect of *Sox9* ablation on neural stem cell behavior (decreasing the number of newborn astrocytes and increasing the number of neuroblasts or neurons) may explain the improved recovery of *Sox9* conditional knockdown mice after SCI. This possibility is being evaluated by fate mapping studies in the *Sox9* conditional knockdowns after SCI.

In summary, *Sox9* conditional knockdown improved hind limb motor function in mice following T9 SCI. The improved recovery in the *Sox9* conditional knockdowns correlated with reduced GFAP, collagen, and CSPG expression at the lesion and at sites distant from the lesion. We suggest that the reduced CSPG expression at the glial scar and in PNNs distant to the injury opened up a window of opportunity for increased local plasticity possibly allowing for the formation of new propriospinal connections or sprouting from spared axons onto deafferented targets below the lesion. This explanation is consistent with the neurofilament immunoreactivity showing increased fiber sprouting in the lesion penumbra but no increase in fibers that traverse the lesion epicenter. It is also consistent with the demonstrated reduction in PNNs caudal to the

lesion and increased 5-HT immunoreactivity demonstrating more serotonergic inputs onto IML and ventral horn targets caudal to the lesion. These results suggest that inhibition of SOX9 activity may be a novel therapeutic strategy for the treatment of SCI.

2.5 Acknowledgments

2.6 Author Disclosure Statement

A.B. holds a patent on SOX9 inhibition as a target for regeneration in the nervous system. No competing financial interests exist for W.M.M.

2.7 Supplementary Table 1. Two Way ANOVA Summary Table

Experiment	Source	DF	SS	MS	F	P
BMS	Genotype	1	53.355	53.355	25.151	<0.001
	Time	15	55.027	3.668	28.615	<0.001
	Interaction	15	10.116	0.674	5.26	<0.001
CS56	Position	4	0.0483	0.0121	12.426	<0.001
	Genotype	1	0.133	0.133	136.651	<0.001
	Interaction	4	0.0231	0.00577	5.941	<0.001
Trichrome	Position	4	0.0135	0.00338	15.497	<0.001
	Genotype	1	0.00629	0.00629	28.886	<0.001
	Interaction	4	0.00267	0.000666	3.06	0.029
GFAP	Position	4	0.041	0.0102	4.027	0.007
	Genotype	1	0.145	0.145	57.079	<0.001
	Interaction	4	0.00184	0.00046	0.181	0.947
NF-200	Position	4	0.0121	0.00304	4.007	0.007
	Genotype	1	0.0157	0.0157	20.669	<0.001
	Interaction	4	0.00597	0.00149	1.969	0.115

2.8 References

1. David, S. and S. Lacroix, *Molecular approaches to spinal cord repair.* Annu Rev Neurosci, 2003. **26**: p. 411-40.
2. Bahr, M., C. Przyrembel, and M. Bastmeyer, *Astrocytes from adult rat optic nerves are nonpermissive for regenerating retinal ganglion cell axons.* Exp Neurol, 1995. **131**(2): p. 211-20.
3. Reier, P.J. and J.D. Houle, *The glial scar: its bearing on axonal elongation and transplantation approaches to CNS repair.* Adv Neurol, 1988. **47**: p. 87-138.
4. McKeon, R.J., et al., *Reduction of neurite outgrowth in a model of glial scarring following CNS injury is correlated with the expression of inhibitory molecules on reactive astrocytes.* J Neurosci, 1991. **11**(11): p. 3398-411.
5. Davies, S.J., et al., *Robust regeneration of adult sensory axons in degenerating white matter of the adult rat spinal cord.* J Neurosci, 1999. **19**(14): p. 5810-22.
6. Fawcett, J.W. and R.A. Asher, *The glial scar and central nervous system repair.* Brain Res Bull, 1999. **49**(6): p. 377-91.
7. Eddleston, M. and L. Mucke, *Molecular profile of reactive astrocytes--implications for their role in neurologic disease.* Neuroscience, 1993. **54**(1): p. 15-36.
8. Silver, J. and J.H. Miller, *Regeneration beyond the glial scar.* Nat Rev Neurosci, 2004. **5**(2): p. 146-56.
9. Lemons, M.L., D.R. Howland, and D.K. Anderson, *Chondroitin sulfate proteoglycan immunoreactivity increases following spinal cord injury and transplantation.* Exp Neurol, 1999. **160**(1): p. 51-65.

10. Morgenstern, D.A., R.A. Asher, and J.W. Fawcett, *Chondroitin sulphate proteoglycans in the CNS injury response.* Prog Brain Res, 2002. **137**: p. 313-32.

11. Zuo, J., et al., *Degradation of chondroitin sulfate proteoglycan enhances the neurite-promoting potential of spinal cord tissue.* Exp Neurol, 1998. **154**(2): p. 654-62.

12. Davies, S.J., et al., *Regeneration of adult axons in white matter tracts of the central nervous system.* Nature, 1997. **390**(6661): p. 680-3.

13. Meiners, S., E.M. Powell, and H.M. Geller, *A distinct subset of tenascin/CS-6-PG-rich astrocytes restricts neuronal growth in vitro.* J Neurosci, 1995. **15**(12): p. 8096-108.

14. Condic, M.L., D.M. Snow, and P.C. Letourneau, *Embryonic neurons adapt to the inhibitory proteoglycan aggrecan by increasing integrin expression.* Journal of Neuroscience, 1999. **19**(22): p. 10036-43.

15. Friedlander, D.R., et al., *The neuronal chondroitin sulfate proteoglycan neurocan binds to the neural cell adhesion molecules Ng-CAM/L1/NILE and N-CAM, and inhibits neuronal adhesion and neurite outgrowth.* J Cell Biol, 1994. **125**(3): p. 669-80.

16. Milev, P., et al., *Interactions of the chondroitin sulfate proteoglycan phosphacan, the extracellular domain of a receptor-type protein tyrosine phosphatase, with neurons, glia, and neural cell adhesion molecules.* J Cell Biol, 1994. **127**(6 Pt 1): p. 1703-15.

17. Yamada, H., et al., *The brain chondroitin sulfate proteoglycan brevican associates with astrocytes ensheathing cerebellar glomeruli and inhibits neurite outgrowth from granule neurons.* J Neurosci, 1997. **17**(20): p. 7784-95.

18. Schmalfeldt, M., et al., *Brain derived versican V2 is a potent inhibitor of axonal growth.* J Cell Sci, 2000. **113 (Pt 5)**: p. 807-16.

19. Dou, C.L. and J.M. Levine, *Inhibition of neurite growth by the NG2 chondroitin sulfate proteoglycan.* J Neurosci, 1994. **14**(12): p. 7616-28.

20. Bradbury, E.J., et al., *Chondroitinase ABC promotes functional recovery after spinal cord injury.* Nature, 2002. **416**(6881): p. 636-40.

21. Alilain, W.J., et al., *Functional regeneration of respiratory pathways after spinal cord injury.* Nature, 2011. **475**(7355): p. 196-200.

22. Houle, J.D., et al., *Combining an autologous peripheral nervous system "bridge" and matrix modification by chondroitinase allows robust, functional regeneration beyond a hemisection lesion of the adult rat spinal cord.* Journal of Neuroscience, 2006. **26**(28): p. 7405-15.

23. Garcia-Alias, G., et al., *Chondroitinase ABC treatment opens a window of opportunity for task-specific rehabilitation.* Nature Neuroscience, 2009. **12**(9): p. 1145-51.

24. Wang, D., et al., *Chondroitinase combined with rehabilitation promotes recovery of forelimb function in rats with chronic spinal cord injury.* Journal of Neuroscience, 2011. **31**(25): p. 9332-44.

25. Karimi-Abdolrezaee, S., et al., *Synergistic effects of transplanted adult neural stem/progenitor cells, chondroitinase, and growth factors promote functional repair and plasticity of the chronically injured spinal cord.* Journal of Neuroscience, 2010. **30**(5): p. 1657-76.

26. Gris, P., et al., *Differential gene expression profiles in embryonic, adult-injured and adult-uninjured rat spinal cords.* Molecular and cellular neurosciences, 2003. **24**(3): p. 555-67.

27. Gris, P., et al., *Transcriptional regulation of scar gene expression in primary astrocytes.* Glia, 2007. **55**(11): p. 1145-55.

28.   Bi, W., et al., *Haploinsufficiency of Sox9 results in defective cartilage primordia and premature skeletal mineralization.* Proc Natl Acad Sci U S A, 2001. **98**(12): p. 6698-703.

29.   Akiyama, H., et al., *The transcription factor Sox9 has essential roles in successive steps of the chondrocyte differentiation pathway and is required for expression of Sox5 and Sox6.* Genes Dev, 2002. **16**(21): p. 2813-28.

30.   Hayashi, S. and A.P. McMahon, *Efficient recombination in diverse tissues by a tamoxifen-inducible form of Cre: a tool for temporally regulated gene activation/inactivation in the mouse.* Dev Biol, 2002. **244**(2): p. 305-18.

31.   Danielian, P.S., et al., *Modification of gene activity in mouse embryos in utero by a tamoxifen-inducible form of Cre recombinase.* Current Biology, 1998. **8**(24): p. 1323-6.

32.   Basso, D.M., M.S. Beattie, and J.C. Bresnahan, *A sensitive and reliable locomotor rating scale for open field testing in rats.* J Neurotrauma, 1995. **12**(1): p. 1-21.

33.   Avnur, Z. and B. Geiger, *Immunocytochemical localization of native chondroitin-sulfate in tissues and cultured cells using specific monoclonal antibody.* Cell, 1984. **38**(3): p. 811-22.

34.   Calejesan, A.A., M.H. Ch'ang, and M. Zhuo, *Spinal serotonergic receptors mediate facilitation of a nociceptive reflex by subcutaneous formalin injection into the hindpaw in rats.* Brain Research, 1998. **798**(1-2): p. 46-54.

35.   Bardin, L., et al., *Effect of intrathecal administration of serotonin in chronic pain models in rats.* European Journal of Pharmacology, 2000. **409**(1): p. 37-43.

36.   Allen, G.V. and D.F. Cechetto, *Serotoninergic and nonserotoninergic neurons in the medullary raphe system have axon collateral projections to autonomic and somatic cell groups in the medulla and spinal cord.* Journal of Comparative Neurology, 1994. **350**(3): p. 357-66.

37.   Saruhashi, Y., W. Young, and R. Perkins, *The recovery of 5-HT immunoreactivity in lumbosacral spinal cord and locomotor function after thoracic hemisection.* Exp Neurol, 1996. **139**(2): p. 203-13.

38.   Galtrey, C.M. and J.W. Fawcett, *The role of chondroitin sulfate proteoglycans in regeneration and plasticity in the central nervous system.* Brain Res Rev, 2007. **54**(1): p. 1-18.

39.   Celio, M.R. and I. Blumcke, *Perineuronal nets--a specialized form of extracellular matrix in the adult nervous system.* Brain research. Brain research reviews, 1994. **19**(1): p. 128-45.

40.   Hartig, W., K. Brauer, and G. Bruckner, *Wisteria floribunda agglutinin-labelled nets surround parvalbumin-containing neurons.* Neuroreport, 1992. **3**(10): p. 869-72.

41.   Rolls, A., R. Shechter, and M. Schwartz, *The bright side of the glial scar in CNS repair.* Nat Rev Neurosci, 2009. **10**(3): p. 235-41.

42.   Frisen, J., et al., *Growth of ascending spinal axons in CNS scar tissue.* International Journal of Developmental Neuroscience, 1993. **11**(4): p. 461-75.

43.   Kruger, S., et al., *Three morphologically distinct types of interface develop between adult host and fetal brain transplants: implications for scar formation in the adult central nervous system.* Journal of Comparative Neurology, 1986. **249**(1): p. 103-16.

44.   Li, Y. and G. Raisman, *Sprouts from cut corticospinal axons persist in the presence of astrocytic scarring in long-term lesions of the adult rat spinal cord.* Exp Neurol, 1995. **134**(1): p. 102-11.

45.   Schnell, L. and M.E. Schwab, *Sprouting and regeneration of lesioned corticospinal tract fibres in the adult rat spinal cord.* European Journal of Neuroscience, 1993. **5**(9): p. 1156-71.

46.   Stichel, C. and H. Muller, *Experimental strategies to promote axonal regeneration after traumatic central nervous system injury.* Progress in Neurobiology, 1998. **56**: p. 119-148.

47.   Stichel, C.C., et al., *Inhibition of collagen IV deposition promotes regeneration of injured CNS axons.* Eur J Neurosci, 1999. **11**(2): p. 632-46.

48.   Stichel, C.C., et al., *Scar modulation in subacute and chronic CNS lesions: Effects on axonal regeneration.* Restor Neurol Neurosci, 1999. **15**(1): p. 1-15.

49.   Lefebvre, V., et al., *SOX9 is a potent activator of the chondrocyte-specific enhancer of the pro alpha1(II) collagen gene.* Mol Cell Biol, 1997. **17**(4): p. 2336-46.

50.   Lefebvre, V., P. Li, and B. de Crombrugghe, *A new long form of Sox5 (L-Sox5), Sox6 and Sox9 are coexpressed in chondrogenesis and cooperatively activate the type II collagen gene.* Embo J, 1998. **17**(19): p. 5718-33.

51.   Sumi, E., et al., *SRY-related HMG box 9 regulates the expression of Col4a2 through transactivating its enhancer element in mesangial cells.* American Journal of Pathology, 2007. **170**(6): p. 1854-64.

52.   Sekiya, I., et al., *SOX9 enhances aggrecan gene promoter/enhancer activity and is up-regulated by retinoic acid in a cartilage-derived cell line, TC6.* J Biol Chem, 2000. **275**(15): p. 10738-44.

53.   Kou, I. and S. Ikegawa, *SOX9-dependent and -independent transcriptional regulation of human cartilage link protein.* J Biol Chem, 2004. **279**(49): p. 50942-8.

54.   Klapka, N. and H.W. Muller, *Collagen matrix in spinal cord injury.* Journal of Neurotrauma, 2006. **23**(3-4): p. 422-35.

55.   Massey, J.M., et al., *Chondroitinase ABC digestion of the perineuronal net promotes functional collateral sprouting in the cuneate nucleus after cervical spinal cord injury.* Journal of Neuroscience, 2006. **26**(16): p. 4406-14.

56.   Lander, C., et al., *A family of activity-dependent neuronal cell-surface chondroitin sulfate proteoglycans in cat visual cortex.* J Neurosci, 1997. **17**(6): p. 1928-39.

57.   Pizzorusso, T., et al., *Reactivation of ocular dominance plasticity in the adult visual cortex.* Science, 2002. **298**(5596): p. 1248-51.

58.   Corvetti, L. and F. Rossi, *Degradation of chondroitin sulfate proteoglycans induces sprouting of intact purkinje axons in the cerebellum of the adult rat.* Journal of Neuroscience, 2005. **25**(31): p. 7150-8.

59.   Tropea, D., M. Caleo, and L. Maffei, *Synergistic effects of brain-derived neurotrophic factor and chondroitinase ABC on retinal fiber sprouting after denervation of the superior colliculus in adult rats.* Journal of Neuroscience, 2003. **23**(18): p. 7034-44.

60.   Pekny, M. and M. Nilsson, *Astrocyte activation and reactive gliosis.* Glia, 2005. **50**(4): p. 427-34.

61.   Hamby, M.E., J.A. Hewett, and S.J. Hewett, *TGF-beta1 reduces the heterogeneity of astrocytic cyclooxygenase-2 and nitric oxide synthase-2 gene expression in a stimulus-independent manner.* Prostaglandins and Other Lipid Mediators, 2008. **85**(3-4): p. 115-24.

62.   Hewett, S.J., et al., *Interferon-gamma and interleukin-1 beta induce nitric oxide formation from primary mouse astrocytes.* Neuroscience Letters, 1993. **164**(1-2): p. 229-32.

63. Stolt, C.C., et al., *The Sox9 transcription factor determines glial fate choice in the developing spinal cord.* Genes Dev, 2003. **17**(13): p. 1677-89.

64. Scott, C.E., et al., *SOX9 induces and maintains neural stem cells.* Nature neuroscience, 2010. **13**(10): p. 1181-9.

65. Cheng, L.C., et al., *miR-124 regulates adult neurogenesis in the subventricular zone stem cell niche.* Nature neuroscience, 2009. **12**(4): p. 399-408.

66. Johansson, C.B., et al., *Identification of a neural stem cell in the adult mammalian central nervous system.* Cell, 1999. **96**(1): p. 25-34.

67. Meletis, K., et al., *Spinal cord injury reveals multilineage differentiation of ependymal cells.* PLoS Biol, 2008. **6**(7): p. e182.

68. Behrstock, S., et al., *Human neural progenitors deliver glial cell line-derived neurotrophic factor to parkinsonian rodents and aged primates.* Gene Therapy, 2006. **13**(5): p. 379-88.

69. Llado, J., et al., *Neural stem cells protect against glutamate-induced excitotoxicity and promote survival of injured motor neurons through the secretion of neurotrophic factors.* Molecular and Cellular Neurosciences, 2004. **27**(3): p. 322-31.

70. Madhavan, L., V. Ourednik, and J. Ourednik, *Neural stem/progenitor cells initiate the formation of cellular networks that provide neuroprotection by growth factor-modulated antioxidant expression.* Stem Cells, 2008. **26**(1): p. 254-65.

Chapter 3: Conditional ablation of *Sox9* after spinal cord injury reduces chondroitin sulfate proteoglycan expression and improves locomotor recovery

William M McKillop[a,b], Elisa M. York[a], Arthur Brown[a,b]

Corresponding Author: Dr. Arthur Brown

Robarts Research Institute, Schulich School of Medicine,

University of Western Ontario

100 Perth Drive, London, Ontario, Canada, N6A 5K8

Email: abrown@robarts.ca

Telephone: 519-663-3776 ext. 24308

[a] Robarts Research Institute, University of Western Ontario, London, Canada

[b] Department of Anatomy and Cell Biology, University of Western Ontario, London, Canada

3.0 Abstract

Chondroitin sulfate proteoglycans (CSPGs) limit neuroplasticity during development and following spinal cord injury (SCI). We have previously identified SOX9 as a transcription factor that up-regulates the expression of CSPGs and have demonstrated that *Sox9* ablation prior to SCI leads to reduced CSPG expression and improved locomotor recovery. The present study sought to determine whether *Sox9* ablation would reduce CSPG levels in the injured cord and improve locomotor recovery if initiated a week after injury. $Sox9^{flox/flox}$ (control) and $Sox9^{flox/flox}$;*Cre* (*Sox9* knockdown) mice were subjected to a 70 kdyne contusion SCI at thoracic spinal cord level 9. One week after injury, tamoxifen was administered to ablate *Sox9*. Quantitative-PCR demonstrated that this experimental protocol caused *Sox9* mRNA levels to decline at 13 days post-SCI. Six weeks post-SCI mice with delayed *Sox9* knockdown expressed reduced levels of CSPG core proteins (neurocan and aggrecan), and glial fibrillary acidic protein (a marker of astrocyte activation) in the injured spinal cord compared to controls. These changes in gene expression were accompanied by improved hind limb function and locomotor recovery as evaluated by the Basso Mouse Scale (BMS) and rodent activity boxes. Histological assessments confirmed reduced CSPG deposition at the lesion site and in perineuronal nets of mice with delayed *Sox9* knockdown, and demonstrated increased serotonin immunoreactivity caudal to the injury site. Improved recovery following *Sox9* knockdown delayed for 1 week after SCI highlights the clinical potential of an anti-SOX9 treatment for SCI.

3.1 Introduction

The limited spontaneous recovery from spinal cord injury (SCI) observed in humans [1, 2] and adult animals [3, 4] has been attributed, in part, to injury-induced neuroplasticity. Axon growth that underlies structural neuroplasticity has been shown to be limited by chondroitin sulfate proteoglycans (CSPGs) *in vitro* [5-7] and *in vivo* [8-13]. CSPGs are a family of proteins composed of a core protein with chondroitin sulfate side chains [14]. In the injured spinal cord CSPGs are a major component of the glial scar that is mostly produced by reactive astrocytes [15, 16], with contributions from macrophages, microglia, oligodendrocytes, invading Schwann cells and meningeal fibroblasts [17]. Enzymatic removal of chondroitin sulfate side chains from CSPGs at the lesion site using chondroitinase ABC has been demonstrated to increase axon sprouting and neurological recovery [8, 9]. CSPGs are also found in extracellular matrix structures called perineuronal nets (PNNs) that surround the cell bodies and dendrites of some classes of neurons [18]. CSPGs in PNNs have been suggested to stabilize synapses by preventing axonal sprouting onto inappropriate targets after appropriate connections have been made during development [11]. Enzymatic digestion of PNNs by chondroitinase leads to reactivation of plasticity in adult animals [19, 20].

For several years our laboratory has been studying the molecular mechanisms that control CSPG production by reactive astrocytes with the goal of developing a strategy to reduce CSPG expression after SCI. This work led us to the identification of SOX9 as a transcription factor that up-regulates the expression of CSPGs in primary astrocytes [21]. Using a line of tamoxifen-inducible conditional *Sox9* knockdown mice, we subsequently demonstrated that SOX9 regulates the expression of a battery of genes involved in astrocyte activation and CSPG production and that SOX9 ablation reduces CSPG levels at the lesion site and in PNNs distant to the SCI [22].

We also demonstrated that conditional SOX9 ablation leads to improved locomotor outcomes after SCI. One of the difficulties in this previous study was that we elected to ablate *Sox9* before carrying out the SCI. Tamoxifen was administered once per day for one week, two weeks prior to SCI in order to allow one week for the Cre-mediated recombination to occur and one week for tamoxifen wash-out. This experimental design allowed us to maximize the effects of SOX9 ablation on scar formation but did not answer the more clinically relevant question - whether SOX9 ablation after scar formation has already begun could appreciably reduce CSPG levels in the injured cord and improve neurological outcomes. In the present study we report that ablating *Sox9* during the second week after SCI results in reduced levels of CSPGs at the lesion site and in PNNs in the lumbar enlargement. These reductions in CSPGs are accompanied by improved locomotor recovery in the spinal cord-injured Sox9 conditional knockdown mice.

3.2 Materials and Methods

Sox9 conditional knockdown mice

Mice carrying floxed *Sox9* (exons 2 and 3 of *Sox9* surrounded by loxP sites) alleles [23] (*Sox9$^{flox/flox}$*) were crossed with a transgenic mouse line that expresses Cre recombinase fused to the mutated ligand binding domain of the human estrogen receptor (ER) under the control of a chimeric cytomegalovirus immediate-early enhancer/chicken β–actin promoter (B6.Cg-Tg(CAG-Cre/Esr1)5Amc/J)[24] (Jackson Laboratories, Bar Harbor, Maine). The mutated ER ligand binding domain of the fusion protein binds tamoxifen [25]. The Cre-ER fusion protein remains trapped in the cytoplasm of all cells due to interactions with Hsp90. Tamoxifen binds to the mutated ER portion of the fusion protein releasing it from Hsp90 allowing its transport to the

nucleus where it excises *loxP*-flanked *Sox9* DNA [24]. Tamoxifen-treated *Sox9*^{flox/flox};*CAGGCreER (Sox9*^{flox/flox};*Cre)* mice served as inducible *Sox9* knockdown animals and their tamoxifen-treated *Sox9*^{flox/flox} littermates (not carrying the Cre transgene) served as control animals (expressing normal levels of SOX9). Tamoxifen (Sigma Aldrich, St. Louis, Missouri) was administered at 3 mg/20 g mouse by oral gavage to all *Sox9*^{flox/flox};*Cre* and *Sox9*^{flox/flox} littermates starting 7 days post-SCI, once per day, for 7 days.

Animals were genotyped by polymerase chain reaction (PCR) analysis using the following primers:

Sox9^{flox} allele: 5'-ACACAGCATAGGCTACCTG-3' and

5'-TGGTAATGAGTCATACACAGTAC-3'.

Sox9^{wildtype} allele: 5'-GGGGCTTGTCTCCTTCAGAG-3' and

5'- TGGTAATGAGTCATACACAGTAC-3'.

Sox9^{knockdown} allele: 5'-GTCAAGCGACCCATG-3' and

5'-TGGTAATGAGTCATACACAGTAC-3'.

Cre⁺ allele: 5'-CAATTTACTGACCGTACAC-3' and 5'-AGCTGGCCCAAATGTTGCTG-3'.

Spinal cord injury

All protocols for these experiments were approved by the University of Western Ontario Animal Care Committee in accordance with the policies established in the Guide to Care and

Use of Experimental Animals prepared by the Canadian Council on Animal Care. *Sox9^{flox/flox};Cre* and *Sox9^{flox/flox}* mice were anesthetized with 100 mg/kg ketamine: 5 mg/kg xylazine. The spinal cord was stabilized at vertebra T7 and T9 with forceps, and a T8 dorsal laminectomy was performed to expose spinal segment T9. The Infinite Horizons Impactor was used to deliver a 70 kdyne contusion injury with a 1 s dwell time (displacement range: 500-900 μM) to spinal segment T9 (Precision Systems and Instrumentation, Fairfax, Virginia). Following SCI the mice were housed individually. Baytril (25 mg/kg, Bayer, Toronto, Ontario, Canada) and buprenorphine (0.01 mg/kg, Schering-Plough, Hertfordshire, UK) were injected subcutaneously twice daily for 3 days post-SCI. Bladders were emptied manually twice daily for the duration of the experiment. The experimental timeline is shown in Figure 1.

Quantitative-PCR

RNA was extracted from a 5 mm segment of spinal cord centered on the lesion of delayed *Sox9* knockdown and control mice 6 weeks post-SCI, using the RNA-Easy kit according to the manufacturer's instructions (Qiagen, Valencia, California). First strand cDNA was synthesized from 1 μg RNA per sample using the High Capacity cDNA Archive Kit according to the manufacturer instructions (Applied Biosystems, Carlsbad, California). The primer probe sets, optical adhesive covers, and quantitative-PCR (q-PCR) plates were purchased from Applied Biosystems. All primer probes were labeled with 5'FAM and with 3'TAMRA as quencher. TaqMan assays were conducted using the Applied Biosystems gene expression assay primer probe sets listed in Table 1.

Figure 1. Experimental timeline. *Sox9^{flox/flox};Cre* and *Sox9^{flox/flox}* control mice were subjected to a SCI at T9 using the infinite Horizons Impactor. Beginning at 7 days post-SCI all mice received daily administrations of tamoxifen for one week. Changes in *Sox9* mRNA levels at the lesion were monitored by Q-PCR in a subset of animals on days 2, 4 and 6 after initiating tamoxifen administration (corresponding to days 9, 11 and 13 after SCI). Changes in SOX9 target gene protein and mRNA expression levels at the lesion by Western blot analyses and Q-PCR was carried out 6 weeks post-SCI. Hind limb function was assessed using the BMS on the day following SCI and then at weekly intervals until 14 weeks post-SCI. Locomotor activity was assessed using rodent activity boxes at 1 week, 6 weeks and 14 weeks post-SCI. After sacrificing the mice at 14 weeks post-SCI their spinal cords were removed for immunohistochemical analyses.
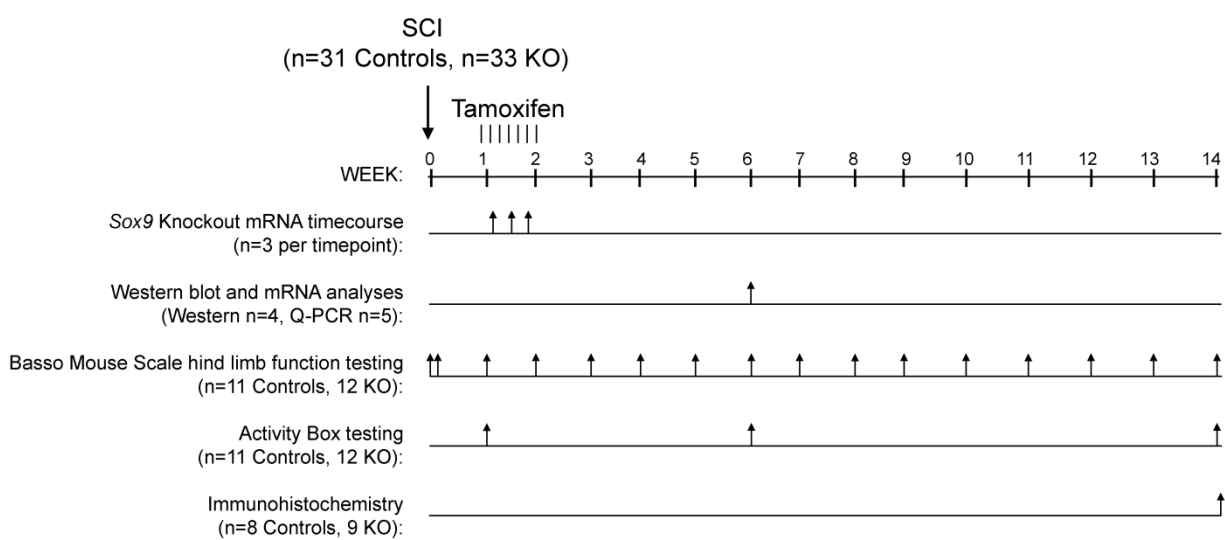
Table 1. List of TaqMan Real-Time PCR Primer Probe Sets

Primer Probe	Catalog Number	PCR Ct Range
GAPDH	Mm99999915_g1	*17.04-18.65*
Sox9	Mm00448840_m1	*22.10-25.97*
Aggrecan	Mm00545807_m1	*23.47-25.97*
Neurocan	Mm00484007_m1	*23.48-29.98*
GFAP	Mm01253033_m1	*17.04-18.97*

TaqMan (Applied Biosystems) gene expression assays were conducted on a 7900HT fast q-PCR apparatus (Applied Biosystems) using thermal cycler conditions set as follows; 10 min at 95°C followed by 40 cycles of 30 s at 95°C followed by 30 s at 60°C. Cycle thresholds (Ct) for all target genes were kept below 30 as indicated in Table 1. Target gene mRNA expression was normalized to the amount of GAPDH mRNA present in each sample and analyzed using the comparative Ct method [26]. The ratio of knockdown to control sample normalized target gene mRNA was analyzed by Student's T-test.

Time course of *Sox9* expression after tamoxifen administration

Sox9^{flox/flox};Cre and *Sox9^{flox/flox}* control mice underwent SCI as described above. Tamoxifen administration began 1 week after SCI. Mice were sacrificed at 2, 4, and 6 days after

the start of tamoxifen administration and Q-PCR was carried out to characterize the time course with which *Sox9* mRNA levels decline following tamoxifen administration in *Sox9*$^{flox/flox}$;*Cre* mice.

Western blotting

Protein was isolated from a 5 mm segment of spinal cord tissue centered on the lesion site in delayed *Sox9* knockdown and control mice 6 weeks post-SCI. The spinal cord tissue was lysed in modified RIPA buffer (1% nonidet P-40, 150 mM NaCl, 0.5% sodium deoxycholate, 0.1% SDS, 50 mM Tris, 1 mM EDTA, pH 7.5, plus 1 complete Mini Protease Inhibitor tablet/7mL RIPA buffer (Roche Molecular Biochemicals, Indianapolis, Indiana) on ice using a ground glass homogenizer. The protein mixture was centrifuged at 13,000 x g for 5 min and the supernatant collected. For the neurocan and aggrecan analyses the protein aliquots (at a concentration of 2–3 mg/ml) were treated with 0.3 U/ml chondroitinase ABC (Sigma-Aldrich) for 8 h at 37 °C. The protein samples were diluted in reducing PAGE loading buffer, and loaded on reducing SDS-PAGE gels at 10 μg/well. The membrane was blocked in 10% nonfat powdered milk and then incubated with primary antibodies; anti-SOX9 (AB 5535, Millipore, Billerica, Massachusetts used at 1:1000), anti-glial fibrillary acidic protein (GFAP; MAB360, Millipore, Billerica, Massachusetts used at 1:1000), anti-neurocan (MAB5212, Millipore, Billerica, Massachusetts used at 1:1000), anti-aggrecan (WH0000176M1, Sigma, St. Louis, Missouri, used at 1:1000), and anti-β-actin (A1978, Sigma, St. Louis, Missouri, used at 1:10,000) for protein expression assessed by western blot. Horse radish peroxidase (HRP)-conjugated anti-mouse IgG (715-035-151, Jackson ImmunoResearch Laboratories, West Grove, Pennsylvania) and HRP conjugated

anti-rabbit IgG (711-035-152, Jackson ImmunoResearch Laboratories, West Grove, Pennsylvania) secondary antibodies were used at 1:20,000 dilution to detect protein expression. SOX9, GFAP, neurocan, and aggrecan protein expression was normalized to β-actin protein expression by densitometry using the EpiChemi[3] Darkroom (UVP Bioimaging Systems, Upland, California) and LabWorks software (Media Cybernetics Inc, Bethesda, Maryland).

Behavioral testing

All aspects of the behavioral testing and data analyses completed in this study were done using a blinded experimental design. Locomotor recovery of the mice was assessed by two observers, blinded to animal genotypes, using the Basso Mouse Scale (BMS) open field locomotor score [27]. The day following SCI, all mice were evaluated for any signs of locomotor recovery in their hindlimbs, and mice that had BMS scores > 0.5 were excluded from further analyses (3 delayed *Sox9* knockdowns and 2 controls). Animals were evaluated once per week for 14 weeks after SCI. Left and right hind limb scores were averaged to generate a composite score. In addition, locomotion was evaluated using rodent activity boxes (Accuscan Instruments Inc, Columbus, Ohio). The activity boxes use infrared sensors to track the animal's movements. The total distance the mice traveled was measured over a 2 h period at night (during their normal awake circadian cycle) at 1, 6, and 14 weeks post-SCI.

Spinal cord sectioning

Fourteen weeks post-SCI the animals were deeply anesthetized with 50 mg/kg ketamine: 5 mg/kg xylazine, and cardiac perfusion was carried out with 20 ml of saline at pH 7.4 followed by 20 ml 4% paraformaldehyde (4% PFA in 0.1 M phosphate buffer at pH 7.4). Spinal cords were dissected and post-fixed for 2 h in 4% PFA followed by cryoprotection in 20% sucrose in 0.1 M phosphate buffer at pH 7.4 at 4 ˚C overnight. Spinal cords were embedded in Tissue-Tek O.C.T. Compound (Sakura Finetek U.S.A. Inc, Torrance, California), frozen over dry ice, and stored at -80 ˚C overnight. Frozen cords were then sectioned at 16 μm using a cryostat, and serially thaw-mounted on Superfrost^{TM} glass slides (Fisher Scientific Company, Ottawa, Canada).

Immunohistochemistry

Immunohistochemistry was conducted using the primary antibodies listed in Table 2. Slides were rinsed in PBS and treated with 5% normal goat serum and 0.1% triton-X-100 in phosphate buffered saline (PBS) at room temperature for 1 h and then incubated with the primary antibodies in a humidified chamber at 4 ˚C overnight. Sections were immunostained for CSPG expression using the monoclonal antibody CS56 that recognizes the terminal portions of chondroitin sulfate-4 or -6 side chains and thus detects a variety of CSPGs [28]. CS56 was detected with a biotinylated goat anti-mouse IgM (Vector laboratories, Burlingame, California) secondary antibody (1:200). Sections were then incubated for 45 min with avidin-peroxidase conjugate (Elite Kit, Vector laboratories, Burlingame, California) at room temperature, and the signal visualized by peroxidase diaminobenzine (DAB, Invitrogen, Carlsbad, California). All

DAB staining was conducted with a 2-min DAB reagent incubation time for spinal cord sections from all delayed *Sox9* knockdown and control mice, and were processed at the same time. Sections to be stained for perineuronal nets were washed in PBS 3 x 10 min, and incubated with biotinylated Wisteria Floribunda agglutinin (WFA, Sigma Aldrich, St. Louis, Missouri) (1:1000) for 1 h at room temperature. Sections were then incubated for 45 min with streptavidin conjugated Alexa-Fluor 594 (1:500 Invitrogen, Carlsbad, California) at room temperature, and counter-stained with a fluorescent Nissl stain, N-21479 (Invitrogen) (1:100) for 1 h at room temperature. Sections were stained for serotonin with an antibody against 5-hydroxytryptamine (5-HT) and for GFAP. Anti-5-HT and anti-GFAP antibodies were detected by Alexa-Fluor 488-conjugated goat anti-rabbit IgG (1:500, Invitrogen, Carlsbad, California), or Alexa-Fluor 488-conjugated goat anti-mouse IgG (1:500, Invitrogen, Carlsbad, California), for 1 h at room temperature. Slides were then washed in PBS and coverslips applied with ProLong Gold Anti-Fade mounting medium (Invitrogen, Carlsbad, California).

Table 2. List of primary antibodies and stains used for spinal cord staining

Antibody	Dilution	Isotype	Source
Anti-GFAP	1:500	Mouse IgG	Millipore, Billerica, Massachusetts
Anti-CS56	1:300	Mouse IgM	Sigma Aldrich, St. Louis, Missouri
Anti-5HT	1:500	Rabbit IgG	ImmunoStar, Hudson, Wisconsin
WFA	1:1000		Sigma Aldrich, St. Louis, Missouri
Nissl	1:100		Invitrogen, Carlsbad, California

Quantification of GFAP, CS56, 5-HT, and WFA staining

For GFAP and CS56 immunostaining, six 16 μm thick longitudinal sections, 160 μm apart were analyzed using ImagePro Plus software (Media Cybernetics Inc, Bethesda, Maryland). A threshold was set for each immunostain that identified positive signal (staining above background levels). For GFAP and CS56 immunoreactivity the area of positive staining was quantified within an area of interest that was centered on, and spanned 3.5 mm rostral and caudal to the lesion epicenter. This area of interest was kept constant for all sections. The area of 5-HT immunoreactivity (area per area of interest) was quantified in the ventral horns in 16 μm thick cross-sections 160 μm apart obtained 0.8-1.6 mm caudal to the injury site. A single pre-set area of interest was used to define all ventral horn regions in all cords in both the *Sox9* knockdown and control animal sections. The area of 5-HT staining was quantified using ImagePro Plus Software (Media Cybernetics Inc, Bethesda, Maryland) using a threshold which identified positive signal (staining above background levels). The area of WFA immunoreactivity in the lumbar enlargement was analyzed using 16 μm thick cross-sections 160 μm apart sampled at the L2 spinal level. A single pre-set area of interest was used to define all ventral horn regions in all cords across sections from both *Sox9* knockdown and control animals. Positive WFA staining was quantified using ImagePro Plus Software (Media Cybernetics Inc, Bethesda, Maryland) using a threshold which identified positive signal (staining above background levels).

Statistical analysis

Mean values are expressed ± SE. mRNA levels were subjected to statistical analyses using Student's T-test. GFAP, CS56, 5-HT and WFA levels were compared between delayed knockdown mice and controls using a Student's T-test. BMS and activity box results were subjected to statistical analysis using a two-way repeated measures ANOVA followed by a Neuman-Keuls post-hoc test when a significant interaction term was achieved. Analyses were conducted with GraphPad Prism software (GraphPad Software Inc, La Jolla, California), except for two-way ANOVAs which were conducted with SigmaStat software (Systat Software Inc, San Jose, California). Statistical significance was accepted at $p<0.05$. A two way ANOVA summary table is provided as Supplementary Table 1.

3.3 Results

Tamoxifen administration requires 6 days to knock down *Sox9* mRNA levels

In this study we initiated delayed *Sox9* ablation by administering tamoxifen for a period of 7 days starting 1 week after SCI. A time course study was carried out to determine how rapidly *Sox9* mRNA levels might decline following tamoxifen administration. *Sox9* knockdown and control mice were sacrificed at 2, 4 and 6 days after the first tamoxifen administration (corresponding to days 9, 11 and 13 after SCI, respectively) and RNA from a 5 mm segment of their spinal cords centered on the lesion epicenter was isolated and evaluated for SOX9 mRNA levels by Q-PCR. *Sox9* knockdown and control mice displayed similar *Sox9* mRNA levels until the 6th day after the first tamoxifen administration (13 days after SCI) when *Sox9* mRNA expression was significantly reduced in *Sox9* knockdown mice compared to controls (Fig. 2).

Figure 2. Tamoxifen administration 1 week post-SCI requires 6 days to achieve significant *Sox9* knockdown. Spinal cord-injured *Sox9^{flox/flox}* and *Sox9^{flox/flox};Cre* mice were administered tamoxifen daily for one week beginning at 7 days post-injury. *Sox9^{flox/flox}* and *Sox9^{flox/flox};Cre* mice were sacrificed at 2, 4 and 6 days after initiating the tamoxifen administration and RNA from a 5 mm segment of spinal cord centered on the lesion was analyzed for *Sox9* mRNA levels by Q-PCR. A decrease in *Sox9* mRNA levels is not observed until 6 days after the first tamoxifen dose (13 days after SCI). Values are means +/- S.E. * significantly different from control at the same time point (p <0.05, two-tailed Student t-test, n=3/group).

Sox9 mRNA expression following the onset of tamoxifen administration post-SCI
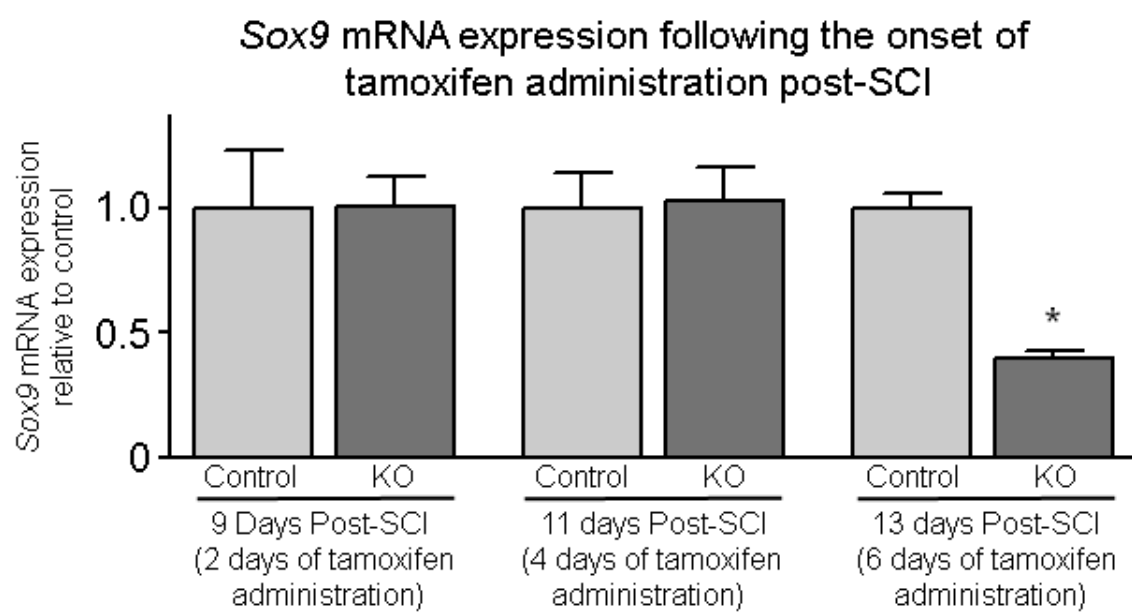
Delayed *Sox9* ablation results in reduced scar gene expression

We previously demonstrated that *Sox9* ablation prior to SCI causes a decrease in the mRNA and protein levels for a variety of genes involved in CSPG biosynthesis and astrocyte activation when measured 1 week after injury [22]. To evaluate whether *Sox9* ablation in the second week after SCI would yield similar reductions in SOX9 target gene expression, a subset of spinal cord-injured control and *Sox9* knockdown mice were sacrificed at 6 weeks post-SCI. From these mice, 5 mm spinal cord segments centered on the lesions were harvested for mRNA and protein expression analyses. Six weeks after SCI (5 weeks after the first dose of tamoxifen) *Sox9* knockdown mice displayed a 72% reduction in *Sox9* mRNA, a 25% reduction in GFAP mRNA, a 36% reduction in neurocan mRNA and a 33% reduction in aggrecan mRNA levels (Fig. 3). To determine if the observed reductions in mRNA expression were accompanied by parallel reductions in protein levels, we investigated SOX9, GFAP, neurocan, and aggrecan protein levels by western blot analysis 6 weeks post-SCI. The spinal lesions of *Sox9* knockdown mice displayed a 72% reduction in Sox9 protein, a 33% reduction in GFAP protein, a 51% reduction in neurocan protein and an 83% reduction in aggrecan protein (Fig. 3).

Delayed *Sox9* knockdown mice show improved hind limb function

We have previously shown that knocking out *Sox9* in an adult mouse prior to SCI results in improved hind limb recovery [22]. To investigate whether SOX9 ablation beginning 1 week after SCI also leads to improved hind limb locomotor function after SCI, we evaluated the delayed *Sox9* knockdown and control mice weekly in an open field test using the Basso mouse scale (BMS) scoring [29] for locomotor activity for 14 weeks after SCI. Immediately after injury, all mice showed complete or near complete paralysis of the hind limbs, represented by a

Figure 3. ***Sox9*, *GFAP*, *neurocan* and *aggrecan* mRNA and protein expression levels are reduced 6 weeks post-SCI following Sox9 ablation initiated at 1 week after injury.** Spinal cord-injured *Sox9$^{flox/flox}$* and *Sox9$^{flox/flox}$;Cre* mice were administered tamoxifen daily for one week beginning at 7 days post-injury. *Sox9$^{flox/flox}$* and *Sox9$^{flox/flox}$;Cre* mice were sacrificed at 6 weeks post-SCI and either protein (n=4/group) or RNA (n=5 per group) was isolated from a 5 mm segment of spinal cord centered on the lesion epicenter. A) SOX9 protein levels (as measured by Western blot analyses) and mRNA levels (as measured by Q-PCR) are reduced in the *Sox9* knockdown mice (p<0.05, Student's t-test). The *Sox9* knockdown mice demonstrate similar reduction in the protein and mRNA levels of GFAP (B), neurocan (C) and aggrecan (D).
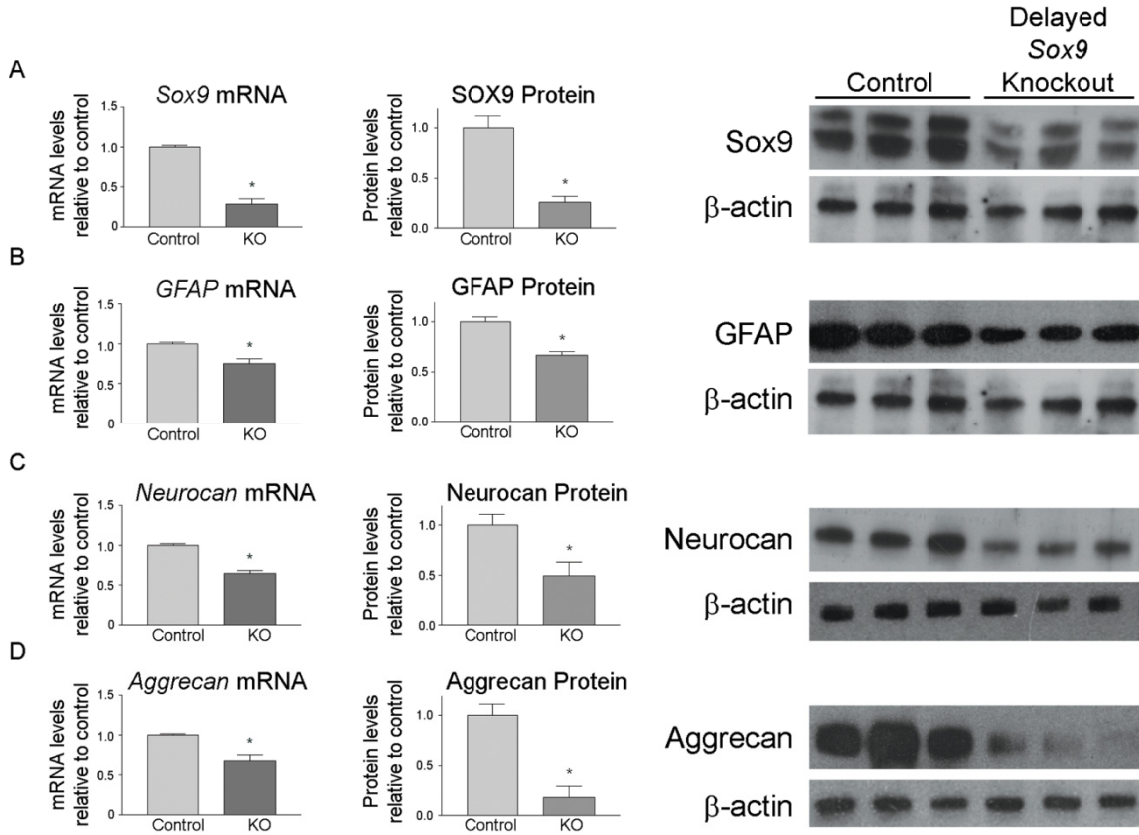
score of 0, and on day one following SCI all mice displayed a score of < 0.5. Whereas hind limb function in both delayed *Sox9* knockdown mice and controls gradually improved over time the delayed *Sox9* knockdowns demonstrated a statistically significant improvement over their control littermates. Locomotor BMS scoring in control mice reached a plateau of 0.63 ± 0.15 at 4 weeks post-SCI, (Fig. 4A). The median BMS score in this group of 0.5 indicates slight (less than 90˚) movement in only one of the two hindlimb ankles. In contrast, the BMS scores of the delayed *Sox9* knockdown mice continued to improve past 4 weeks and did not reach a plateau until 10 weeks post-SCI, achieving an average BMS score of 1.48 ± 0.21. The median BMS score for delayed *Sox9* knockdown mice of 1.5 indicates an extensive (greater than 90˚) movement in one ankle, and a slight (less than 90˚) movement in the other ankle.

***Sox9* knockdown mice display improved locomotor activity**

As a second measure of locomotor recovery we evaluated the delayed *Sox9* knockdown and control mice for their overall level of mobility by tracking their locomotion over a 2-h time period using rodent activity boxes. The total distance traversed in a 2-h period was recorded for each mouse during their normal wake period (at night) on 2 consecutive nights and averaged. One week after SCI, and before tamoxifen administration, the $Sox9^{flox/flox}$ control mice (Cre-negative) traversed an average distance of 1412 ± 191 cm in 2 h (Fig. 4B), which was not significantly different from the distance traversed by the $Sox9^{flox/flox};Cre$ mice (1456 ± 252 cm in 2 h). At 6 weeks post-SCI (5 weeks after the first tamoxifen administration) no significant differences in total distance traversed between control mice that traversed an average distance of 1393 ± 235 cm in 2 h, and delayed *Sox9* knockdown mice that averaged 1906 ± 451 cm in 2 h.

Figure 4. *Sox9* **knockdown mice demonstrate improved locomotor recovery compared to control mice.** A) Both delayed *Sox9* knockdown and control mice display hind limb paralysis immediately following SCI, and on day 1 post-SCI (first time point before week 1). *Sox9* knockdown mice score higher (increased hind limb function) on the Basso Mouse Scale (BMS) beginning on the sixth week post-SCI (one week after first tamoxifen administration) in comparison to control mice as determined by a 2-way repeated measures ANOVA followed by a Neuman-Keuls post-hoc test (p<0.05; n=12 *Sox9* knockdown mice and n=11 controls). B) *Sox9* conditional knockdown mice demonstrate increased locomotion in comparison to control mice. Over a 2 h period in a rodent activity box *Sox9* knockdown mice demonstrate increased locomotion in comparison to littermate controls at 14 weeks post-SCI as determined by a 2-way repeated measures ANOVA followed by a Neuman-Keuls post-hoc test (p<0.05; n=12 *Sox9* knockdown mice and n=11 controls).
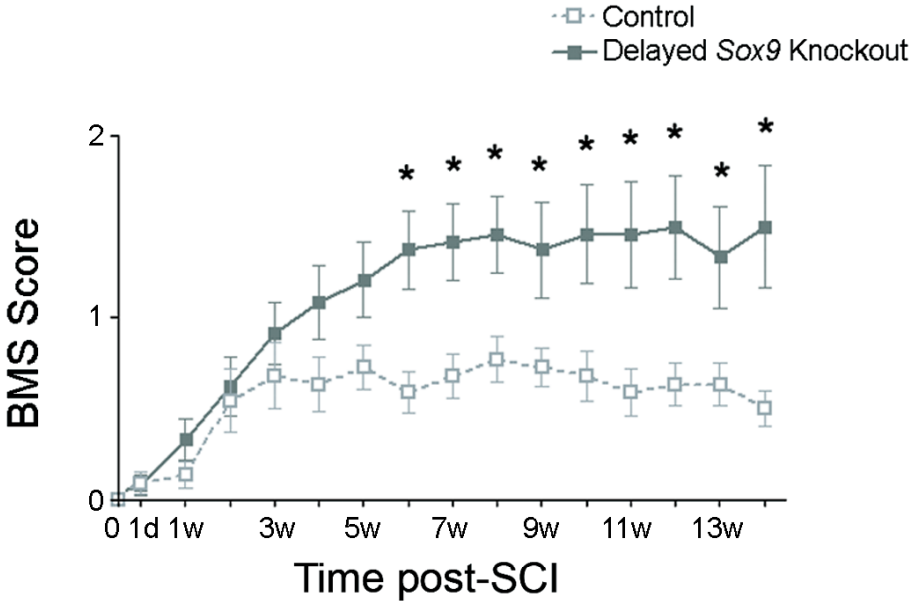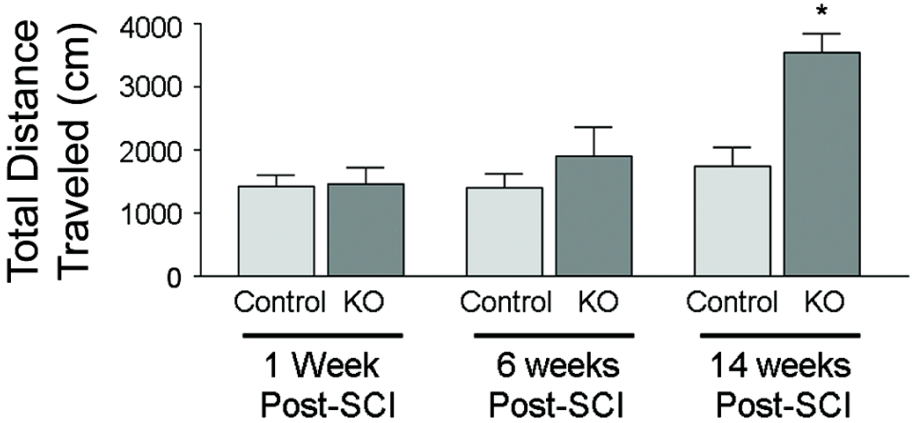
At 14 weeks after SCI, control mice traversed an average distance of 1731 ± 300 cm in 2 h, whereas the delayed *Sox9* knockdown mice traversed an average distance of 3537 ± 301 cm in 2 h. The distance traversed by the injured delayed *Sox9* knockdown mice was significantly greater than that traversed by the injured control animals and was not significantly different from tamoxifen-treated uninjured *Sox9^{flox/flox};Cre* mice (3446 ± 543 cm in 2 h, n=4) or uninjured control mice (3287 ± 396 cm in 2 h, n=4).

Delayed *Sox9* knockdown mice demonstrate decreased CSPG, GFAP and PNN protein expression 14 weeks following SCI

To investigate CSPG and GFAP expression at the lesion, immunohistochemistry was carried out on spinal cords harvested from *Sox9* knockdown and control mice at the end of behavioral testing, 14 weeks post-SCI. Spinal cord sections from delayed *Sox9* knockdown mice at 14 weeks after SCI had significant reductions in CSPG (Fig. 5) and GFAP (Fig. 6) immunoreactivity (area immunoreactivity per area of interest). In addition to their contribution to the glial scar matrix, CSPGs are also a major component of the PNN that stabilizes synapses during development [11] and limits plasticity in the adult nervous system. Since delayed *Sox9* knockdowns had reduced levels of CSPGs at the lesion site we evaluated whether they may also have reductions in their PNNs distant to the lesion. Cross-sections from the lumbar enlargement of delayed *Sox9* knockdowns and controls were stained with biotinylated Wisteria floribunda agglutinin (WFA) that binds N-acetylgalactosamine side chains in proteoglycans including CSPGs [18, 30]. WFA staining revealed a reduction in PNN proteoglycans in the delayed *Sox9* knockdown mice caudal to the lesion compared to control mice 14 weeks post-SCI, with the

Figure 5. Reduced CSPG expression levels in *Sox9* knockdown mice 14 weeks post-SCI. (A,B) Representative photomicrographs of CS56 immunostaining of longitudinal spinal cord sections centered at the T9 spinal lesion. (A) CSPG expression in control mice shown at low (left panel) and high magnification (right panel). (B) CSPG expression in *Sox9* knockdown mice shown at low (left panel) and high magnification (right panel). (C) Quantification of area of CS56 immunoreactivity (area per area) in *Sox9* conditional knockdown and control spinal cords. * indicates statistically significantly different from controls (p<0.05, Student's t-test; n=6 for *Sox9* knockdown mice and n=5 for controls). Scale Bars = 100 µm.

A Control

B Delayed *Sox9* Knockout

C CS56 Quantification
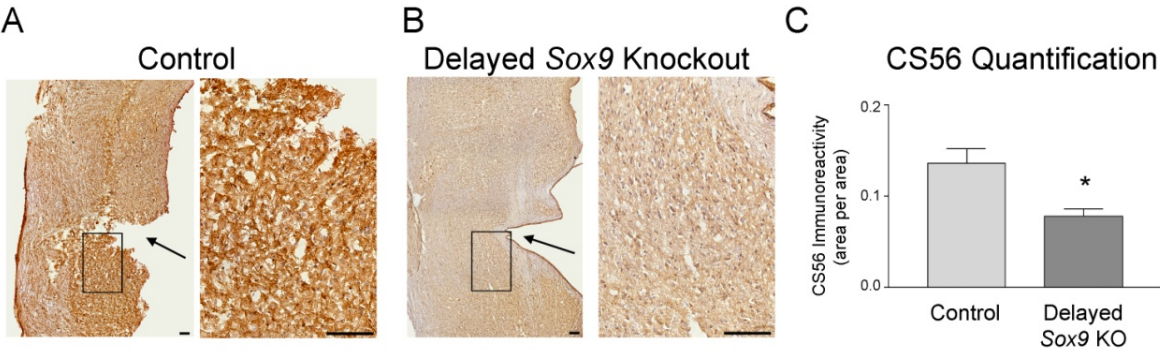
Figure 6. Reduced GFAP expression levels in *Sox9* knockdown mice 14 weeks post-SCI.
(A-D) Representative photomicrographs of anti-GFAP immunostaining of longitudinal spinal cord sections centered at the T9 spinal lesion. (A) Control mice have abundant GFAP immunoreactivity at the lesion. (B) High magnification photomicrograph of boxed area in panel A. (C) *Sox9* knockdown mice have low levels of GFAP immunoreactivity at the lesion. (D) High magnification photomicrograph of boxed area in panel C. (E) Quantification of area of GFAP immunoreactivity (area per area) in *Sox9* conditional knockdown and control spinal cords. * indicates statistically significantly different from controls (p<0.05, Student's t-test; n=6 for Sox9 knockdown mice and n=5 for controls). Scale Bars = 100 μm.

Control

Delayed *Sox9* Knockout

GFAP Quantification
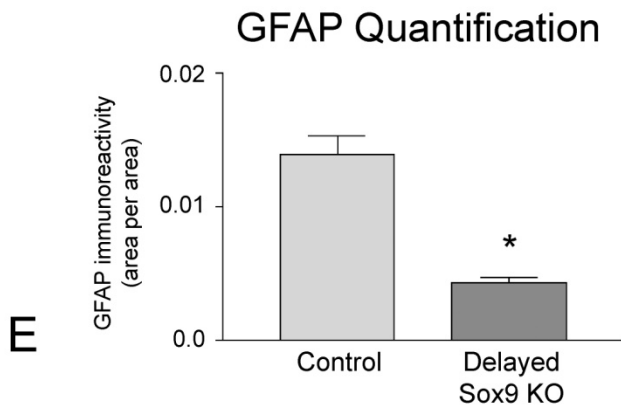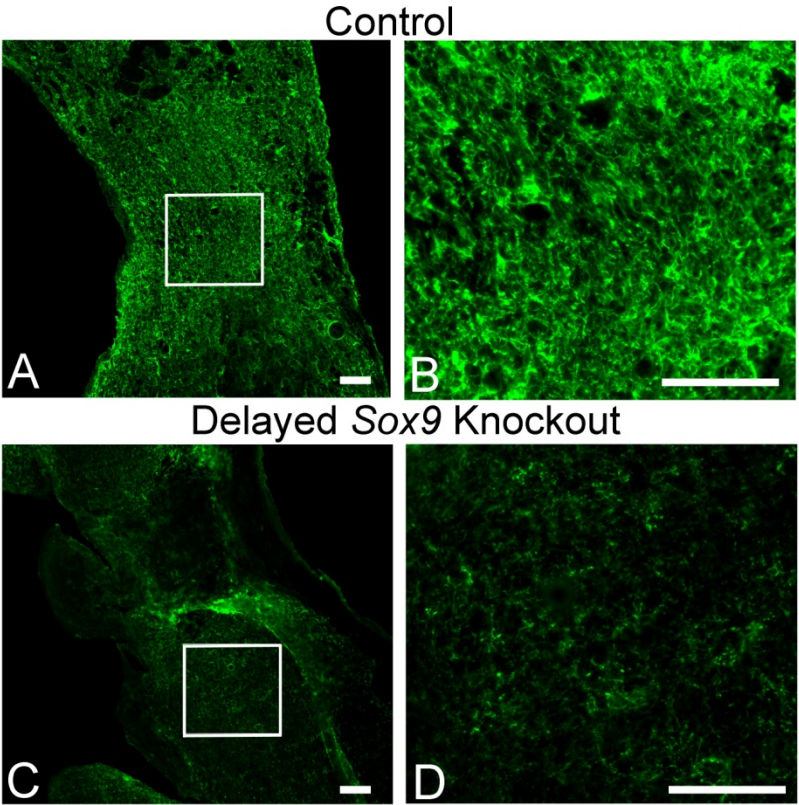
most notable reduction occurring in the layer VIII interneuron pool of the lumbar enlargement (Fig. 7).

Delayed *Sox9* knockdown mice display increased 5-HT immunoreactivity caudal to the lesion site following SCI

Serotonergic projections from the Raphe Nuclei synapse in the ventral horn to modulate motor activity [31], and the loss of these serotonergic inputs to the ventral horn leads to decreased motor function [31]. To evaluate whether the improvements in hind limb function seen in the delayed S*ox9* knockdown mice could be attributed to increased ventral horn serotonergic input in comparison to control mice, we performed 5-HT immunostaining on spinal cord cross-sections sections taken from 0.8 mm - 1.6 mm caudal to the lesion epicenter in the delayed *Sox9* knockdowns and controls 14 weeks after SCI. The delayed *Sox9* knockdown mice demonstrated a statistically significant increase in 5-HT immunoreactivity in the ventral horn, compared to control mice (Fig. 8).

Figure 7. Reduced WFA staining in *Sox9* knockdown mice 14 weeks post-SCI. WFA staining (red) is reduced in the lumbar enlargement ventral horn of *Sox9* knockdown mice (B) compared to controls (A) 14 weeks after SCI. Sections have been counterstained a fluorescent Nissl stain, N-21479 (green). C) Quantification of area of WFA staining (area per area of interest) in *Sox9* conditional knockdown and control spinal cords. * indicates statistically significant difference from controls (p<0.05, Student's t-test; n=6 for *Sox9* knockdown mice and n=5 for controls). Scale Bars = 100 µm.

Control

Delayed
***Sox9* Knockout**

WFA Quantification
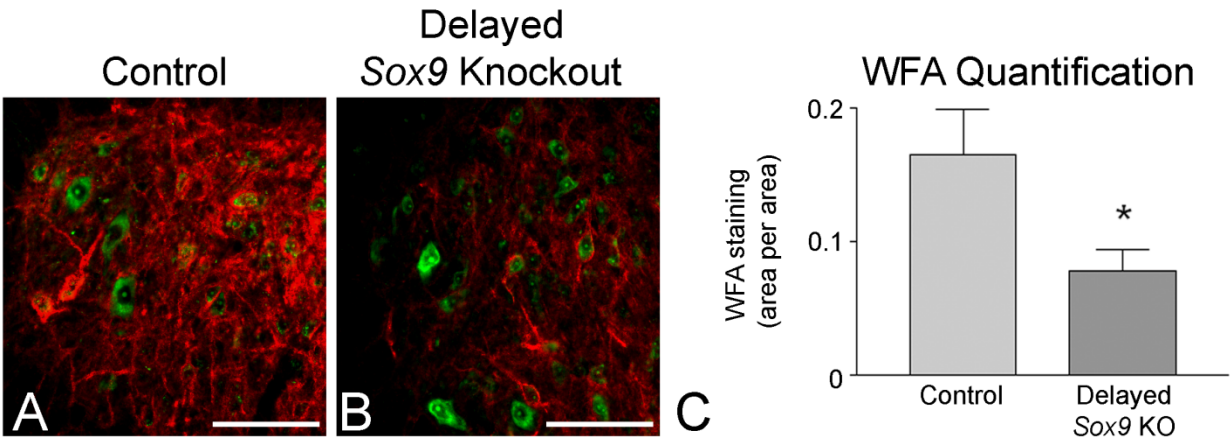
Figure 8. Increased 5-HT immunoreactivity caudal to the lesion in *Sox9* knockdown mice 14 weeks post-SCI. Immunohistochemistry was used to detect serotonin in the spinal cord 14 weeks post-SCI. (A, B) Representative photomicrographs of sections stained for 5-HT immunoreactivity 1.2 mm caudal to the lesion epicenter from *Sox9* conditional knockdown and control mice. (A) Almost no 5-HT immunoreactivity was observed caudal to the lesion in control mice. (B) 5-HT immunoreactivity was readily observed caudal to the lesion in the ventral horn and intermediolateral cell column of *Sox9* knockdown mice. Insets are high power magnifications of the boxed areas in A and B. (C) Quantification of area of 5-HT immunoreactivity (area per area) in *Sox9* conditional knockdown and control spinal cords. * indicates statistically significantly different from controls (p<0.05, Student's t-test; n=3). Scale Bars = 100 µm.

Control

Delayed
Sox9 Knockout

Serotonin (5-HT)
Quantification
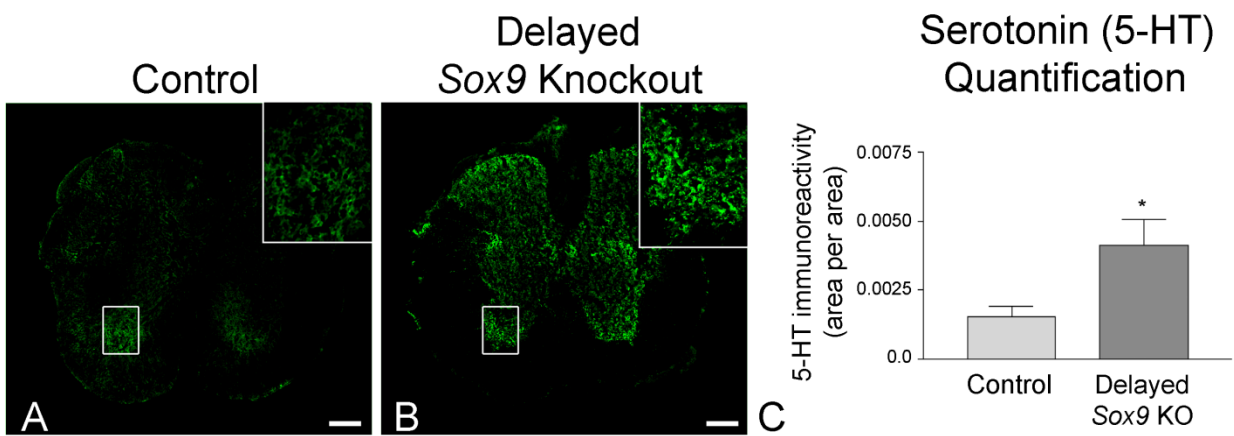
3.4 Discussion

CSPGs are present in the adult CNS [32], and following injury their expression levels increase greatly [5, 33]. In the uninjured adult CNS, CSPGs are key components of PNNs [18] whereas, in the injured CNS, CSPGs are also key components of the glial scar [14, 34] . A demonstration that PNN CSPGs limit plasticity comes from studies in the development of ocular dominance columns. Depriving rats of visual input from one eye by lid suturing until adulthood skews ocular dominance toward the non-deprived eye. Reverse lid suturing when coupled with chondroitinase treatment of the visual cortices of these rats allows normalization of ocular dominance columns and visual function [35]. The inhibitory effect of glial scar CSPGs on recovery has been provided by numerous studies that demonstrate that chondroitinase treatment at the scar increases structural plasticity in the lesion and improves neurological outcomes in rodent models of SCI [8, 9, 13, 36]. The inhibitory effect of PNN CSPGs distant to the lesion has been demonstrated by the application of chondroitinase at the level of the cuneate nucleus in the brain stem following an ipsilateral dorsal column transection at C6-C7. This chondroitinase treatment resulted in reduced PNN CSPGs and enhanced collateral sprouting of spared afferents [37]. Thus, CSPGs in the uninjured and injured nervous system limit plasticity.

Using a tamoxifen-inducible line of *Sox9* knockdown mice we previously demonstrated that *Sox9* ablation prior to SCI leads to significant reduction in CSPG levels at the lesion epicenter and in PNN matrix distant to the lesion [22]. These changes in CSPG levels correlated with improved locomotor recovery in the delayed *Sox9* knockdown mice. In this previous study we administered tamoxifen daily by gavage for one week and then allowed one week for tamoxifen to clear the system. This experimental protocol avoided any confounding effects of tamoxifen on recovery from SCI, and maximized the possible effects of reduced SOX9

expression by employing a pre-injury ablation strategy. However the disadvantage of this protocol was that it did not test the potential clinical value of an anti-SOX9 strategy as that requires an experimental protocol that ablates or inhibits *Sox9* expression after SCI.

In the present study we administered tamoxifen daily for 1 week beginning at 7 days after SCI. Our time course evaluation of *Sox9* mRNA levels in the injured spinal cords of tamoxifen-treated control and knockdown mice indicates that significant decreases in *Sox9* mRNA levels were not achieved until 6 days after the first tamoxifen administration. This probably reflects the time taken for Cre activation by tamoxifen, and the half-life of *Sox9* mRNA. We note that *Sox9* mRNA levels continued to decline relative to controls from 13 days after SCI to 6 weeks after SCI indicating that maximal *Sox9* ablation was reached sometime after 13 days post-injury. As SOX9 protein levels would not be expected to decline before *Sox9* mRNA levels, SOX9 activity probably began to decline at approximately 2 weeks post-SCI. This is a time after astrocyte activation and scar deposition has begun, and thus is a rigorous test of whether *Sox9* ablation can reduce CSPG levels in the glial scar after its formation has commenced. Since this subacute time period after SCI is a window of time at which SCI patients might reasonably be expected to undergo therapeutic interventions, this experimental protocol enabled us to evaluate whether potential SOX9 inhibitors could yield beneficial effects when applied within a clinically achievable time frame.

To evaluate the effect of *Sox9* ablation after SCI on SOX9 target gene expression, we measured the mRNA levels of *Sox9*, *gfap*, neurocan and aggrecan in a 5 mm section of spinal cord centered on the lesion at 6 weeks post-SCI. As expected Sox9 mRNA levels were approximately 75% lower in the lesions of delayed knockdown mice compared to controls. The reduction in *Sox9* mRNA levels was accompanied by a similar reduction in SOX9 protein in

these lesions. The reduction in SOX9 levels were also accompanied by reduction in the mRNA and protein levels of GFAP, neurocan and brevican. Thus despite the delayed time course of *Sox9* ablation, by 6 weeks post-SCI the delayed knockdown lesions had significantly lower CSPG and GFAP levels compared to controls suggesting that these lesions had less astrocyte activation and less scar deposition.

To evaluate the effect of *Sox9* ablation after SCI on locomotor recovery we performed open field locomotor testing weekly and quantified hind limb function using the BMS [29]. In addition, as a more general indication of mobility, we also measured the total distance traveled by each mouse in a 2 h period using rodent activity boxes at 1, 6 and 14 weeks after SCI. The open field testing demonstrated that whereas the locomotor recovery in spinal cord-injured *Sox9^{flox/flox}* and *Sox9^{flox/flox}*;*Cre* mice were indistinguishable for the first two weeks of recovery (i.e. before tamoxifen administration) *Sox9^{flox/flox}*;*Cre* mice began to show improved hind limb function thereafter. The rodent activity box data supported these findings and indicated that at 14 weeks post-SCI the delayed *Sox9* knockdown mice traverse about twice the distance of control mice and are not different from uninjured *Sox9* ablated or wild type mice. The degree of improvement in locomotor function as assessed by the BMS scores may seem modest and stands in contrast to the more obvious improvement in mobility as measured using the rodent activity boxes. This indicates that whereas the spinal cord-injured *Sox9* knockdown mice are much more mobile than the spinal cord-injured controls their method for ambulation is abnormal and does not fully translate into greater BMS scores.

We have previously suggested that improved locomotor recovery in conditional *Sox9* knockdown mice could potentially be explained by one or more of the following: a muted inflammatory response, altered neural stem cell behavior or increased structural neuroplasticity

[22] . We suggested that the muted inflammatory response could be due to reduced astrocyte activation in the *Sox9* knockdown mice as evidenced by their reduced GFAP expression. However as the most damaging inflammatory response in SCI is found to occur within the first hours and days of SCI [38] it would seem unlikely that a muted inflammatory response commencing at about 2 weeks after SCI could likely account for the improved recovery observed in the delayed *Sox9* knockdowns described in the present study. The possibility that improved locomotor recovery observed in *Sox9* knockdown mice is due to altered neural stem cell behavior rests on studies demonstrating that SOX9 directs stem cell fate down a glial lineage [39, 40] . Thus, *Sox9* ablation could result in the generation of fewer astrocytes and more neurons after SCI and lead to better outcomes. We are currently testing this hypothesis using a tamoxifen-inducible neural stem cell-specific line of *Sox9* knockdown mice.

The most likely explanation for improved locomotor recovery in *Sox9* conditional knockdown mice is that the reductions in SOX9 activity resulted in lower CSPG levels in the glial scar and in PNNs which permitted increased structural neuroplasticity. The importance of developing methods to reduce CSPG expression both at and far from the lesion site has been suggested by others based on increased CSPG expression at these sites after SCI [41] .We have shown that *Sox9* ablation by tamoxifen administration starting at 1 week after SCI results in reduced *Sox9* mRNA levels as early as 13 days after SCI and reduced levels of Sox9, GFAP, neurocan and aggrecan mRNA and protein levels at the lesion by 6 weeks after SCI. Immunohistochemistry demonstrated reduced levels of GFAP and CSPGs at the lesion site in delayed *Sox9* knockdowns at 14 weeks post-SCI. Reductions in PNN matrix in delayed *Sox9* knockdown mice was demonstrated in the ventral horn of the lumbar enlargement by staining with WFA, a lectin that binds N-acetylgalactosamine side chains in proteoglycans including

CSPGs [18, 30]. We suggest that the reductions in CSPG levels in the *Sox9* conditional knockdown mice removes the limits on neuroplasticity that these matrix molecules normally impose and accounts for the improved outcomes in the *Sox9* conditional knockdown mice. We further suggest that the reduction in PNN CSPGs, more than the reduction in glial scar CSPGs, underlies the improved outcomes as long-range axonal growth from above to below the lesion is less likely to result in functional, productive circuitry than short range reactive sprouting of spared fibers. Evidence for increased neuroplasticity in delayed *Sox9* knockdown mice comes from the demonstration of increased 5-HT immunoreactivity at the lumbar enlargement in the ventral horns of these animals.

We have previously shown that *Sox9* ablation before SCI results in reduced CSPG levels in the spinal cord and improvements in motor function post-SCI [22]. The present study extends our previous work by demonstrating that *Sox9* ablation in the subacute period after SCI also reduces CSPG levels in the injured spinal cord and yields improvements in locomotor function. These findings are supported by previous work demonstrating that chondroitinase treatment 2 weeks after SCI improves recovery in spinal cord-injured mice [42]. Thus, as a general approach, increasing neuroplasticity may be a therapeutic option well after SCI. These results suggest that *Sox9* inhibition is a clinically viable and practical therapeutic strategy for the treatment of SCI.

3.5 Acknowledgments

The *Sox9flox/flox* mice were kindly provided by Dr. Andreas Schedl. This work was supported by grants from the Canadian Institutes of Health Research (CIHR) and the International Foundation of Research in Paraplegia (IFP). WMM was supported by a doctoral scholarship from the Natural Sciences and Engineering Research Council of Canada (NSERC).

3.6 Author Disclosure Statement

A.B. holds a patent on SOX9 inhibition as a target for regeneration in the nervous system. No competing financial interests exist for W.M.M., or E.M.Y.

3.7 Supplementary Table 1. Two Way ANOVA Summary Table

Experiment	Source	DF	SS	MS	F	P
BMS	Genotype	1	25.067	25.067	5.766	0.026
	Time	15	46.542	3.103	22.150	<0.001
	Interaction	15	8.204	0.547	3.904	<0.001
Activity Box	Position	1	6808374.969	6808374.969	11.213	0.003
	Genotype	2	7553409.742	3776704.871	8.544	0.002
	Interaction	2	4619599.870	2309799.935	5.226	0.015

3.8 References

1.   Dietz, V., et al., *Locomotor pattern in paraplegic patients: training effects and recovery of spinal cord function.* Spinal Cord, 1998. **36**(6): p. 380-90.
2.   Wernig, A. and S. Muller, *Laufband locomotion with body weight support improved walking in persons with severe spinal cord injuries.* Paraplegia, 1992. **30**(4): p. 229-38.
3.   Rossignol, S., et al., *Locomotor performance and adaptation after partial or complete spinal cord lesions in the cat.* Progress in Brain Research, 1999. **123**: p. 349-65.
4.   Schwab, M.E. and D. Bartholdi, *Degeneration and regeneration of axons in the lesioned spinal cord.* Physiological Reviews, 1996. **76**(2): p. 319-70.
5.   McKeon, R.J., et al., *Reduction of neurite outgrowth in a model of glial scarring following CNS injury is correlated with the expression of inhibitory molecules on reactive astrocytes.* J Neurosci, 1991. **11**(11): p. 3398-411.
6.   Zuo, J., et al., *Degradation of chondroitin sulfate proteoglycan enhances the neurite-promoting potential of spinal cord tissue.* Exp Neurol, 1998. **154**(2): p. 654-62.
7.   Meiners, S., E.M. Powell, and H.M. Geller, *A distinct subset of tenascin/CS-6-PG-rich astrocytes restricts neuronal growth in vitro.* J Neurosci, 1995. **15**(12): p. 8096-108.
8.   Barritt, A.W., et al., *Chondroitinase ABC promotes sprouting of intact and injured spinal systems after spinal cord injury.* J Neurosci, 2006. **26**(42): p. 10856-67.
9.   Bradbury, E.J., et al., *Chondroitinase ABC promotes functional recovery after spinal cord injury.* Nature, 2002. **416**(6881): p. 636-40.
10.   Fry, E.J., et al., *Corticospinal tract regeneration after spinal cord injury in receptor protein tyrosine phosphatase sigma deficient mice.* Glia, 2010. **58**(4): p. 423-33.
11.   Galtrey, C.M. and J.W. Fawcett, *The role of chondroitin sulfate proteoglycans in regeneration and plasticity in the central nervous system.* Brain Res Rev, 2007. **54**(1): p. 1-18.
12.   Grimpe, B. and J. Silver, *A novel DNA enzyme reduces glycosaminoglycan chains in the glial scar and allows microtransplanted dorsal root ganglia axons to regenerate beyond lesions in the spinal cord.* J Neurosci, 2004. **24**(6): p. 1393-7.
13.   Huang, W.C., et al., *Chondroitinase ABC promotes axonal re-growth and behavior recovery in spinal cord injury.* Biochem Biophys Res Commun, 2006. **349**(3): p. 963-8.
14.   Morgenstern, D.A., R.A. Asher, and J.W. Fawcett, *Chondroitin sulphate proteoglycans in the CNS injury response.* Prog Brain Res, 2002. **137**: p. 313-32.
15.   Eddleston, M. and L. Mucke, *Molecular profile of reactive astrocytes--implications for their role in neurologic disease.* Neuroscience, 1993. **54**(1): p. 15-36.
16.   Silver, J. and J.H. Miller, *Regeneration beyond the glial scar.* Nat Rev Neurosci, 2004. **5**(2): p. 146-56.
17.   Fawcett, J.W. and R.A. Asher, *The glial scar and central nervous system repair.* Brain Res Bull, 1999. **49**(6): p. 377-91.
18.   Celio, M.R. and I. Blumcke, *Perineuronal nets--a specialized form of extracellular matrix in the adult nervous system.* Brain research. Brain research reviews, 1994. **19**(1): p. 128-45.
19.   Pizzorusso, T., et al., *Reactivation of ocular dominance plasticity in the adult visual cortex.* Science, 2002. **298**(5596): p. 1248-51.

20.   Corvetti, L. and F. Rossi, *Degradation of chondroitin sulfate proteoglycans induces sprouting of intact purkinje axons in the cerebellum of the adult rat.* Journal of Neuroscience, 2005. **25**(31): p. 7150-8.

21.   Gris, P., et al., *Transcriptional regulation of scar gene expression in primary astrocytes.* Glia, 2007. **55**(11): p. 1145-55.

22.   McKillop, W.M., et al., *Conditional Sox9 ablation reduces chondroitin sulfate proteoglycan levels and improves motor function following spinal cord injury.* Glia, 2013. **61**(2): p. 164-77.

23.   Bi, W., et al., *Sox9 is required for cartilage formation.* Nat Genet, 1999. **22**(1): p. 85-9.

24.   Hayashi, S. and A.P. McMahon, *Efficient recombination in diverse tissues by a tamoxifen-inducible form of Cre: a tool for temporally regulated gene activation/inactivation in the mouse.* Dev Biol, 2002. **244**(2): p. 305-18.

25.   Danielian, P.S., et al., *Modification of gene activity in mouse embryos in utero by a tamoxifen-inducible form of Cre recombinase.* Current Biology, 1998. **8**(24): p. 1323-6.

26.   Schmittgen, T.D. and K.J. Livak, *Analyzing real-time PCR data by the comparative C(T) method.* Nat Protoc, 2008. **3**(6): p. 1101-8.

27.   Basso, D.M., M.S. Beattie, and J.C. Bresnahan, *A sensitive and reliable locomotor rating scale for open field testing in rats.* J Neurotrauma, 1995. **12**(1): p. 1-21.

28.   Avnur, Z. and B. Geiger, *Immunocytochemical localization of native chondroitin-sulfate in tissues and cultured cells using specific monoclonal antibody.* Cell, 1984. **38**(3): p. 811-22.

29.   Basso, D.M., et al., *Basso Mouse Scale for locomotion detects differences in recovery after spinal cord injury in five common mouse strains.* J Neurotrauma, 2006. **23**(5): p. 635-59.

30.   Hartig, W., K. Brauer, and G. Bruckner, *Wisteria floribunda agglutinin-labelled nets surround parvalbumin-containing neurons.* Neuroreport, 1992. **3**(10): p. 869-72.

31.   Saruhashi, Y., W. Young, and R. Perkins, *The recovery of 5-HT immunoreactivity in lumbosacral spinal cord and locomotor function after thoracic hemisection.* Exp Neurol, 1996. **139**(2): p. 203-13.

32.   Bignami, A., R. Asher, and G. Perides, *The extracellular matrix of rat spinal cord: a comparative study on the localization of hyaluronic acid, glial hyaluronate-binding protein, and chondroitin sulfate proteoglycan.* Exp Neurol, 1992. **117**(1): p. 90-3.

33.   Lemons, M.L., D.R. Howland, and D.K. Anderson, *Chondroitin sulfate proteoglycan immunoreactivity increases following spinal cord injury and transplantation.* Exp Neurol, 1999. **160**(1): p. 51-65.

34.   Asher, R.A., et al., *Chondroitin sulphate proteoglycans: inhibitory components of the glial scar.* Prog Brain Res, 2001. **132**: p. 611-9.

35.   Pizzorusso, T., et al., *Structural and functional recovery from early monocular deprivation in adult rats.* Proc Natl Acad Sci U S A, 2006. **103**(22): p. 8517-22.

36.   Caggiano, A.O., et al., *Chondroitinase ABCI improves locomotion and bladder function following contusion injury of the rat spinal cord.* J Neurotrauma, 2005. **22**(2): p. 226-39.

37.   Massey, J.M., et al., *Chondroitinase ABC digestion of the perineuronal net promotes functional collateral sprouting in the cuneate nucleus after cervical spinal cord injury.* Journal of Neuroscience, 2006. **26**(16): p. 4406-14.

38.   Geremia, N.M., et al., *CD11d Antibody Treatment Improves Recovery in Spinal Cord-Injured Mice.* Journal of Neurotrauma, 2012. **29**(3): p. 539-50.

39.   Cheng, L.C., et al., *miR-124 regulates adult neurogenesis in the subventricular zone stem cell niche.* Nature neuroscience, 2009. **12**(4): p. 399-408.

40.   Stolt, C.C., et al., *The Sox9 transcription factor determines glial fate choice in the developing spinal cord.* Genes Dev, 2003. **17**(13): p. 1677-89.

41.   Andrews, E.M., et al., *Alterations in chondroitin sulfate proteoglycan expression occur both at and far from the site of spinal contusion injury.* Experimental Neurology, 2011.

42.   Bukhari, N., et al., *Axonal regrowth after spinal cord injury via chondroitinase and the tissue plasminogen activator (tPA)/plasmin system.* Journal of Neuroscience, 2011. **31**(42): p. 14931-43.

Chapter 4: *Sox9* knockdown promotes neuroplasticity after spinal cord injury

William M McKillop[a,b], Todd Hryciw[a], Kathy Xu[a], Nicole Geremia[a], Arthur Brown[a,b]

Corresponding Author: Dr. Arthur Brown

Robarts Research Institute, Schulich School of Medicine,

University of Western Ontario

100 Perth Drive, London, Ontario, Canada, N6A 5K8

Email: abrown@robarts.ca

Telephone: 519-663-3776 ext. 24308

[a] Robarts Research Institute, University of Western Ontario, London, Canada

[b] Department of Anatomy and Cell Biology, University of Western Ontario, London, Canada

Running title: *Sox9* knockdown promotes neuroplasticity after spinal cord injury

Keywords: SOX9, spinal cord injury, neuroplasticity, CSPG, regeneration, perineuronal nets

4.0 Abstract

The absence of axonal regeneration after spinal cord injury (SCI) has been attributed to the up-regulation of axon-repelling molecules present in the glial scar that forms post-SCI. Amongst the most important of the inhibitory molecules in the scar are chondroitin sulfate proteoglycans (CSPGs) produced by reactive astrocytes that respond to the injury. We have previously identified the transcription factor SOX9 as a key regulator of CSPG production both *in vitro* and *in vivo*. *Sox9* conditional knockdown (KO) mice display decreased CSPG expression and improved hind limb function post-SCI. Herein we investigated sparing, long-range regeneration and reactive sprouting as possible explanations for the improved locomotor outcomes in *Sox9* KO mice after SCI. Retrograde tract-tracing studies failed to reveal any evidence of increased sparing or of long-range regeneration in the *Sox9* KO mice compared to controls. However caudal to the lesion site we found evidence of increased neuroplasticity as indicated by increased levels of the presynaptic markers synaptophysin and vesicular glutamate 1 transporter (VGLUT1) and by increased serotonin immunoreactivity. These findings were supported by anterograde tract-tracing experiments that demonstrated increased reactive sprouting caudal to the lesion after SCI. The increased neuroplasticity after SCI in *Sox9* KO mice highlights the clinical potential of SOX9 antagonists as a treatment strategy for SCI.

4.1 Introduction

Spinal cord injury (SCI) is a catastrophic event that often results in the loss of mobility and sensation below the injury site, as well as impaired organ function and sensitivity to pain. The up-regulation of axon-repelling molecules in the glial scar that forms post-SCI leads to an absence of axonal regeneration. One of the key inhibitory factors preventing regeneration in this glial scar is the chondroitin sulfate proteoglycan (CSPG) family of extracellular matrix molecules [1-3]. CSPGs inhibit axonal regeneration by imposing both a physical and molecular barrier preventing axonal passage. CSPGs sterically inhibit access to substrate adhesion molecules [4], and receptor protein tyrosine phosphatase sigma (RPTPσ) present on axonal growth cones causes growth cone collapse on interaction with CSPGs [5-7]. CSPGs also play a critical role in the development of the central nervous system (CNS) as key components of perineuronal nets (PNNs). PNNs are highly condensed extracellular matrix structures which surround the cell bodies and dendrites of some classes of neurons [8]. The function of CSPGs in PNNs is to stabilize synapses during development by preventing axonal sprouting onto inappropriate targets after appropriate connections have been made, and thus modulate neuroplasticity [1, 9-12]. Following SCI, expression levels of CSPGs dramatically increase both in the glial scar at the site of injury and in distant PNNs [3, 13, 14].

Specific CSPGs have been shown to inhibit neurite outgrowth including; NG2 [15], versican [16], neurocan [17], brevican [18] and phosphocan [19]. All of these CSPGs rely on the same enzymes, xylosyltransferase-I and -II (XT-I, XT-II) and chondroitin 4-sulfotransferase (C4ST), to add the axon-repelling chondroitin sulfate side chains to their core proteins [2, 20, 21]. These chondroitin sulfate side chains play a crucial role in axon repulsion as their digestion by treatment with the enzyme chondroitinase [22], or interference with their synthesis by

inhibiting XT-I [23], increases axonal regeneration in rodent models of SCI. Thus, CSPGs are a potential target for therapeutics focused on improving recovery post SCI.

We have previously identified SOX9 as a transcription factor that up-regulates the expression of CSPG synthesizing enzymes XT-I, XT-II and C4ST in reactive astrocytes [24], and hypothesized that SOX9 inhibition would lead to decreased CSPG expression, a lesion microenvironment more permissive to neuroregeneration, and improved neurological recovery after CNS injury. We have demonstrated that following SCI, *Sox9* KO mice exhibit reduced expression of known SOX9 target genes including: XT-I, Collagen 2a, GFAP (glial fibrillary acidic protein, a marker of astrocyte activation) and three CSPG core proteins (aggrecan, brevican and neurocan) [24, 25]. This reduction in mRNA expression was accompanied by reductions in CSPG protein levels both in the glial scar and in peri-neuronal nets distant to the injury [25]. In addition to reduced CSPG levels, *Sox9* KO mice also displayed improved hindlimb functional recovery as assessed by the Basso Motor Scale (BMS) and overall locomotor activity as assessed by activity boxes [25]. Finally, the *Sox9* KO mice displayed increased serotonin immunostaining caudal to the injury site in the intermediolateral cell column as well as the ventral horn.

In the present study we investigated sparing, long-range regeneration and reactive sprouting as possible explanations for the improved locomotor outcomes in *Sox9* KO mice after SCI. We herein report that retrograde tract-tracing studies failed to reveal any evidence of increased sparing or of long-range regeneration in the corticospinal, rubrospinal, reticulospinal, vestibulospinal tracts or long descending propriospinal projections in the *Sox9* KO mice. However, *Sox9* KO mice displayed increased synaptic plasticity caudal to the lesion as *Sox9* KO mice displayed increased levels of the presynaptic markers synaptophysin and vesicular

glutamate 1 transporter (VGLUT1), as well as increased serotonin immunoreactivity. Anterograde tract tracing studies support the immunohistochemical evidence for increased reactive sprouting below the level of the lesion. The data presented herein describes the mechanism by which conditional *Sox9* KO mice display improved hind limb function and locomotor activity post SCI, and suggest the potential utility of an anti-SOX9 treatment for SCI.

4.2 Materials and Methods

Sox9 conditional knockdown (KO) mice

Mice homozygous for floxed *Sox9* (exons 2 and 3 of *Sox9* surrounded by loxP sites) alleles [26] and heterozygous for Cre recombinase fused to the mutated ligand binding domain of the human estrogen receptor (ER) under the control of a chimeric cytomegalovirus immediate-early enhancer/chicken β–actin promoter [27] (*Sox9^{flox/flox}*;*CAGGCreER* refered to as *Sox9^{flox/flox}*;*Cre*) were used as *Sox9* KO animals. The mutated ER ligand binding domain of the fusion protein binds tamoxifen [28] allowing for Cre transport into the nucleus where it excises *loxP*-flanked *Sox9* DNA [27]. Tamoxifen-treated *Sox9^{flox/flox}* littermates (not carrying the Cre transgene) served as control animals (expressing normal levels of *Sox9*). Tamoxifen (Sigma Aldrich, St. Louis, Missouri) was administered at 3 mg/20 g mouse by oral gavage to all *Sox9^{flox/flox}*;*Cre* and *Sox9^{flox/flox}* littermates starting 14 days prior to SCI, once per day, for 7 days.

Animals were genotyped by polymerase chain reaction (PCR) analysis using the following primers:

Sox9^{flox} allele: 5'-ACACAGCATAGGCTACCTG-3' and

5'-TGGTAATGAGTCATACACAGTAC-3'.

Sox9^{wildtype} allele: 5'-GGGGCTTGTCTCCTTCAGAG-3' and

5'- TGGTAATGAGTCATACACAGTAC-3'.

Sox9^knockdown allele: 5'-GTCAAGCGACCCATG-3' and

5'-TGGTAATGAGTCATACACAGTAC-3'.

Cre^+ allele: 5'-CAATTACTGACCGTACAC-3' and 5'-AGCTGGCCCAAATGTTGCTG-3'.

Spinal cord injury

All protocols for these experiments were approved by the University of Western Ontario Animal Care Committee in accordance with the policies established in the Guide to Care and Use of Experimental Animals prepared by the Canadian Council on Animal Care. *Sox9^flox/flox;Cre* and *Sox9^flox/flox* mice were anesthetized with 100 mg/kg ketamine: 5 mg/kg xylazine. The spinal cord was stabilized at vertebra T7 and T9 with forceps, and the 9th thoracic spinal cord segment (T9) was exposed by a T8 dorsal laminectomy. The T9 spinal segment was injured using the Infinite Horizon Impactor to deliver a 70 kdyne contusion injury with a 1 s dwell time (displacement range: 500-900 μM) (Precision Systems and Instrumentation, Fairfax, Virginia). Following SCI the mice were housed individually. Baytril (25 mg/kg, Bayer, Toronto, Ontario, Canada) and buprenorphine (0.01 mg/kg, Schering-Plough, Hertfordshire, UK) were injected subcutaneously twice daily for 3 days post-SCI. Bladders were emptied manually twice daily for the duration of the experiment. The experimental timeline is shown in Figure 1.

Figure 1. Experimental Timeline. *Sox9^{flox/flox};Cre* and *Sox9^{flox/flox}* control mice received daily administrations of tamoxifen for one week. Following a week for cre mediated recombination and tamoxifen clearance the mice were subjected to a SCI at T9 using the infinite Horizons Impactor. 1 week post-SCI a subset of mice underwent a second T10 spinal cord transection along with the insertion of fluorogold soaked gel foam. These mice were sacrificed at week 3 to assess axonal sparing post-SCI. 8 weeks post-SCI a subset of mice underwent a second T10 spinal cord transection along with the insertion of fluorogold soaked gel foam. These 8 week flourogold mice were sacrificed at week 10 to assess long range regeneration post-SCI. 8 weeks post-SCI a subset of mice underwent BDA injections into the primary motor cortex. These 8 week BDA mice were sacrificed at week 10 to assess reactive sprouting caudal to the lesion. The BDA mice were also used for WFA, synaptophysin, VGLUT1, VGAT, and serotonin immunohistochemical analyses.

SCI

Tamoxifen

WEEK: -2   -1   0   1   2   3   4   5   6   7   8   9   10

Fluorogold 1w experiment start:
Fluorogold 1w experiment end point:
Fluorogold 8w experiment start:
Fluorogold 8w experiment end point:
BDA anterograde tacer experiment start:
BDA anterograde tacer experiment end point:
WFA immunostaining:
Synaptophysin, VGLUT1, VGAT immunostaining:
Serotonin immunostaining:
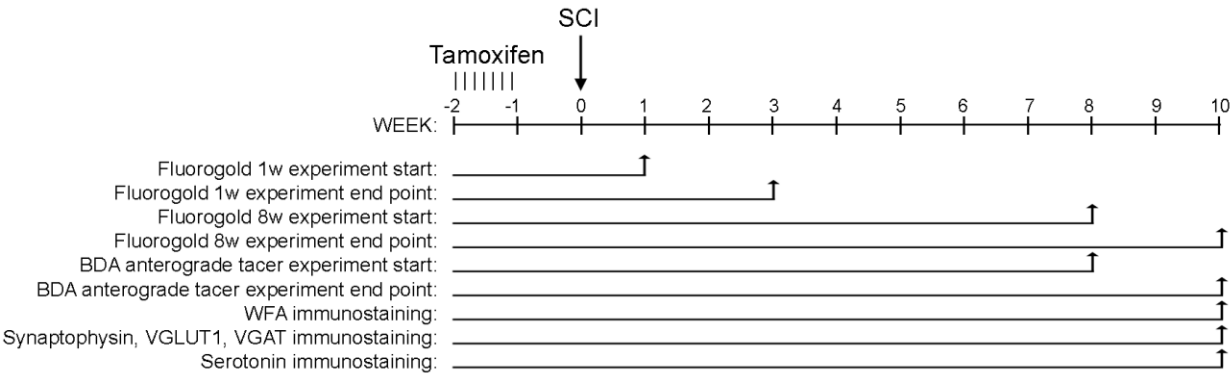
Spinal cord sectioning

Groups of mice were sacrificed over the 10 week post-SCI timeline by deep anesthesia with 50 mg/kg ketamine: 5 mg/kg xylazine, and cardiac perfusion with 20 ml of saline at pH 7.4 followed by 20 ml 4% paraformaldehyde (4% PFA in 0.1 M phosphate buffer at pH 7.4). Spinal cords were dissected and post-fixed for 2 h in 4% PFA followed by cryoprotection in 20% sucrose in 0.1 M phosphate buffer at pH 7.4 at 4 ˚C overnight. Spinal cords were embedded in Tissue-Tek O.C.T. Compound (Sakura Finetek U.S.A. Inc, Torrance, California), frozen over dry ice, and stored at -80 ˚C overnight. Frozen cords were then sectioned at 16 μm using a cryostat, and serially thaw-mounted on Superfrost^{TM} glass slides (Fisher Scientific Company, Ottawa, Canada).

Immunohistochemistry

Immunohistochemistry was conducted at the end of the study, 10 weeks post SCI, using the primary antibodies listed in Table 1. Slides were rinsed in PBS and treated with 5% normal goat serum and 0.1% triton-X-100 in phosphate buffered saline (PBS) at room temperature for 1 h and then incubated with the primary antibodies in a humidified chamber at 4 ˚C overnight. Sections to be stained for PNNs were washed in PBS 3 x 10 min, and incubated with biotinylated Wisteria Floribunda Agglutinin (WFA at 1:1000, Sigma Aldrich) for 1 h at room temperature. Biotinylated WFA was detected by streptavidin conjugated Alexa-Fluor 594 (1:500 Invitrogen, Carlsbad, California) for 45 min at room temperature. Sections were stained for serotonin with an antibody against 5-hydroxytryptamine (5-HT) (1:500 ImmunoStar, Hudson, Wisconsin). Anti-5-HT was detected by Alexa-Fluor 488-conjugated goat anti-rabbit IgG (1:500, Invitrogen) for 1 h at room temperature. Sections were stained for synaptophysin (1:150 Sigma Aldrich). Anti-

synaptophysin was detected by Alexa-Fluor 488-conjugated goat anti-mouse IgG (1:500, Invitrogen) for 1 h at room temperature. Sections were stained for VGLUT1 (1:200 Synaptic Systems, Goettingen, Germany). Anti-VGLUT1 was detected by Alexa-Fluor 488-conjugated goat anti-rabbit IgG (1:500, Invitrogen) for 1 h at room temperature. Sections were stained for VGAT (1:200 Synaptic Systems). Anti-VGAT was detected by Alexa-Fluor 488-conjugated goat anti-mouse IgG (1:500, Invitrogen) for 1 h at room temperature. All fluorescently labeled slides were washed in PBS and coverslips applied with ProLong Gold Anti-Fade mounting medium (Invitrogen).

Table 1. List of primary antibodies and stains used for spinal cord staining

Antibody	Dilution	Isotype	Source
WFA	1:1000		Sigma Aldrich, St. Louis, Missouri
Synaptophysin	1:150	Mouse IgG	Sigma Aldrich, St. Louis, Missouri
VGLUT1	1:200	Rabbit IgG	Synaptic Systems, Goettingen, Germany
VGAT	1:200	Mouse IgG	Synaptic Systems, Goettingen, Germany
NeuN	1:300	Mouse IgG	Millipore, Billerica, Massachusetts
5HT	1:500	Rabbit IgG	ImmunoStar, Hudson, Wisconsin

Retrograde labeling study

Either 1 week or 8 weeks post-SCI mice were anaesthetized and underwent a second dorsal laminectomy one segment caudal to the original dorsal contusion, a T9 dorsal laminectomy exposing the 10th thoracic spinal cord segment (T10). The T10 spinal cord was fully transected by scalpel and a gel foam pledget soaked in 4% hydroxystilbamidine (a

fluorescent molecule responsible for retrograde transport in the common retrograde tracer Fluoro-Gold [29]) (4% w/v in saline; Invitrogen) was inserted into the T10 site. The incisions were sutured and the mice returned to animal housing. Two weeks later the mice underwent cardiac perfusion with 4% paraformaldehyde after which their spinal cords were cryosectioned in cross section (16 μm thick sections) at the cervical enlargement, and their brains were cryosectioned in coronal section (30 μm thick sections). Sections from the cervical enlargement as well as several areas of the brain (primary motor cortex, red nucleus, reticular formation, and vestibular formation), were directly visualized for retrograde tracer labeling.

Anterograde labeling study

Eight weeks post-injury mice were re-anesthetized and their heads stabilized in a stereotaxic frame. A burr hole (1.5 mm in diameter) was made in the skull overlying the left sensorimotor cortex. BDA (biotinylated dextran amine, 10,000 d, Molecular Probes, Invitrogen) was injected by Hamilton syringe with a 33G needle (0.4 μl of 10% BDA suspended in PBS) at a depth of 0.5 mm from the cortical surface in the hindlimb area of the motor cortex at 4 sites centered on +1.5mm lateral, -1mm posterior to bregma (+1mm lateral, -0.5mm posterior, +2mm lateral, -0.5mm posterior, +1mm lateral, -1.5mm posterior; +2mm lateral, -1.5mm posterior) [30] to label corticospinal neurons. The syringe remained in position for 1 min after BDA injection. Two weeks after BDA injections, mice underwent cardiac perfusion with 4% paraformaldehyde and their spinal cords were cut in cross section (16 μm thick sections) at C4, and in the lumbar enlargement (L1). Sections for BDA fiber staining in the cervical enlargement were incubated for 45 min with avidin-peroxidase conjugate (Elite Kit, Vector laboratories, Burlingame, California) at room temperature, and the signal visualized by peroxidase diaminobenzine (DAB,

Invitrogen). All DAB staining was conducted with a 2-min DAB reagent incubation time and processed at the same time. The number of BDA-labeled fibers at C4 were counted in both uninjured and SCI mice, and used to assess sprouting rostal to injury as well as BDA labeling efficiency. Sections for the quantification of BDA puncta surrounding motor neurons in the ventral horn cervical enlargement or lumbar enlargement by high magnification confocal imaging were stained for 45 min with streptavidin conjugated Alexa-Fluor 594 (1:500 Invitrogen, Carlsbad, California) at room temperature, and co-stained with anti-VGLUT1 and anti-NeuN. BDA and VGLUT1 labeled puncta surrounding motor neurons in the ventral horn of the cervical and lumbar enlargements were compared between *Sox9* KO and control mice to assess reactive sprouting both rostral and caudal to the injury site.

Quantification of retrograde tracer, anterograde tracer, WFA, Serotonin, Synaptophysin, VGLUT1, and VGAT immunostaining

Retrograde tracer labeled neurons were counted individually in the primary motor cortex, red nucleus, reticular formation, and vestibular formation using 30 μm thick cross-sections spaced 300 μm apart spanning the relevant structures (~1.8mm bregma - ~0.3mm bregma, ~3mm bregma - ~3.9mm bregma, ~-5.1mm bregma - ~-7.2mm bregma and ~-6mm bregma - ~-6.9mm bregma for the primary motor cortex, red nucleus, reticular formation, and vestibular formation respectively). Long range pro-priospinal neuron retrograde tracer labeling was evaluated in the cervical enlargement (C4) using ten 16 μm thick spinal cord cross-sections spaced 160 μm apart from each area.

The number of BDA labeled fibers were counted across ten 16 μm thick spinal cord cross-sections each spaced 160 μm apart from the cervical enlargement (C4). BDA labeling was

assessed throughout the grey matter, and fibers measuring at least 5 μm in length were counted as real BDA labeled fiber staining. BDA labeling was robust at C4 in both uninjured and injured mice, with no statistical difference between *Sox9* KO and control mouse labeling. BDA puncta surrounding motor neurons was evaluated in both the cervical enlargement and the lumbar enlargement by imaging five high magnification z-stacks (10 slices 0.2 μm apart) per mouse taken at NeuN stained motor neurons defined by their position in Rexed laminae layer 8 or 9, as well as their size and appearance, at 63x with a 3x zoom by a Zeiss LSM-510-Meta confocal microscope. Positive staining was identified as individual puncta measuring at least 1.5 μm in diameter as quantified by the spots algorithm in the Imaris x64 7.0 software package (Bitplane USA, South Windsor, CT).

The area of WFA and 5-HT immunoreactivity was examined just caudal to the lesion site (T10) as well as in the lumbar enlargement (L1) using ten 16 μm thick spinal cord cross-sections spaced 160 μm apart from each area. A single pre-set area of interest was used to define all ventral horn regions in all cords across sections from both *Sox9* KO and control animals. Positive WFA and 5-HT staining was quantified using ImagePro Plus Software (Media Cybernetics Inc, Bethesda, Maryland) using a threshold which identified positive signal (staining above background levels).

Synaptophysin, VGLUT1, and VGAT were examined at the lumbar enlargement (L1) using ten 16 μm thick cross-sections 160 μm apart captured by Zeiss LSM-510 confocal microscope. A single pre-set area of interest was used to define all ventral horn regions in all cords across sections from both *Sox9* KO and control animals. Positive staining was quantified using ImagePro Plus Software (Media Cybernetics Inc, Bethesda, Maryland) using a threshold which identified positive signal (staining above background levels). Five high magnification

ventral horn motor neuron z-stack images (10 slices 0.2 μm apart) per mouse were taken at 63x

with a 3x zoom by a Zeiss LSM-510-Meta confocal microscope. Positive staining was identified

as individual puncta measuring at least 1.5 μm in diameter as quantified by the spots algorithm in

the Imaris x64 7.0 software package (Bitplane USA, South Windsor, CT). All microscopy was

completed using a Olympus BX-50 epifluorescence microscope except when a Zeiss LSM-510-

Meta confocal was used as indicated.

Statistical analysis

WFA, Synaptophysin, VGLUT1, VGAT, and 5-HT areas of immunoreactivity, as well as

retrograde tracer neuronal labeling, were compared between *Sox9* KO and controls using a one

way ANOVA with a Neuman Keuls post hoc test. Synaptophysin, VGLUT1, VGAT, and BDA

positive individual puncta counts were compared between *Sox9* KO and controls using Student's

T-test. Analyses were conducted with GraphPad Prism software (GraphPad Software Inc, La

Jolla, California). Statistical significance was accepted at $p<0.05$. Mean values are expressed ±

SE.

4.3 Results

Sox9 KO mice demonstrate decreased PNN matrix post-SCI

CSPGs are a major component of the PNN that stabilizes synapses during development

and limits plasticity in the adult central nervous system [1]. As *Sox9* KO mice demonstrate

reduced CSPG levels throughout the injury site [25], we evaluated whether they may also have

reductions in their PNNs directly caudal to the injury, as well as at the distant lumbar

enlargement where descending axons synapse on the motor neurons that innervate the hind limb musculature. Cross-sections from T10 and the lumbar enlargement of both uninjured and SCI *Sox9* KO and control mice were stained with biotinylated Wisteria floribunda agglutinin (WFA). WFA binds N-acetylgalactosamine side chains in proteoglycans including CSPGs [8, 31]. WFA staining revealed that spinal cord-injured *Sox9* KO mice had significantly lower levels of PNN matrix in their ventral horns at T10 (a 56% reduction) and in the distant lumbar enlargement (a 58% reduction) compared to the PNN matrix in control mice 10 weeks post SCI (p<0.05 by one-way ANOVA, Figure 2). WFA staining of PNN matrix was not different between uninjured control, uninjured *Sox9* KO mice or spinal cord-injured *Sox9* KO mice.

Sox9 KO mice display no evidence of altered axonal sparing or of long range axonal regeneration post-SCI

Retrograde labeling was carried out to examine axonal sparing and long range regeneration in the *Sox9* KO mice. At 1 week or 8 weeks after T9 SCI control and *Sox9* KO mice underwent retrograde labeling by placing a hydroxystilbamidine-soaked pledget caudal to the lesion (at T10). Since axons can not regenerate a full segment (~3 mm) caudal to the lesion within a week of injury, the neurons labeled at 1 week after injury must have axons that were spared from injury [32, 33]. We examined retrograde labeling in the cervical enlargement for long range propriospinal neurons, as well as in the motor cortex for corticospinal tract neurons, the red nucleus for rubrospinal tract neurons, the reticular formation for reticular spinal tract neurons, and the vestibular formation for vestibulospinal tract neurons. At 1 week post SCI both *Sox9* KO and control mice displayed similar significant reductions in retrograde tracer-labeled corticospinal, and reticulospinal neurons when compared to uninjured controls (Figure 3). To

Figure 2. WFA staining is reduced both just caudal to the injury site, as well as in the lumbar enlargement in *Sox9* KO mice 10 weeks post-SCI. A) Perineuronal net staining in uninjured control mice at T10. B) Perineuronal net staining in uninjured *Sox9* KO mice at T10. C) Perineuronal net staining in control mice just caudal to the injury site (T10). D) Perineuronal net staining in *Sox9* KO mice just caudal to the injury site (T10). E) *Sox9* KO mice display reduced WFA staining just caudal to the injury site ($p<0.05$, one way ANOVA). F) Perineuronal net staining at the ventral horn of the lumbar enlargement (L1) in uninjured control mice. G) Perineuronal net staining in the ventral horn of the lumbar enlargement (L1) in uninjured *Sox9* KO mice. H) Perineuronal net staining in the ventral horn of the lumbar enlargement (L1) in control mice post-SCI. I) Perineuronal net staining in *Sox9* KO mice in the ventral horn of the lumbar enlargement (L1) post-SCI. J) *Sox9* KO mice display reduced WFA staining in the ventral horn of the lumbar enlargement post-SCI ($p<0.05$, one way ANOVA). This suggests the potential for increased plasticity in *Sox9* KO mice. Scale bars = 100μm.

Thoracic Cord
Control   Sox9 KO

Lumbar Enlargement Cord
Control   Sox9 KO

Uninjured

SCI

E

WFA quantification immediately caudal to injury
in the thoracic cord (T10)

J

WFA quantification in the ventral horn
of the lumbar enlargement
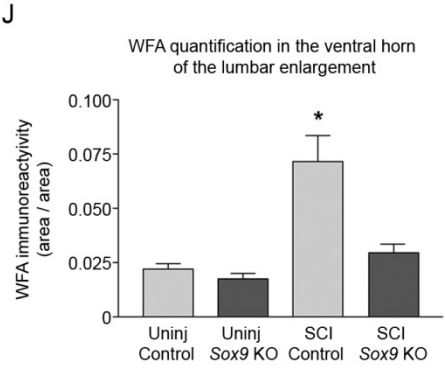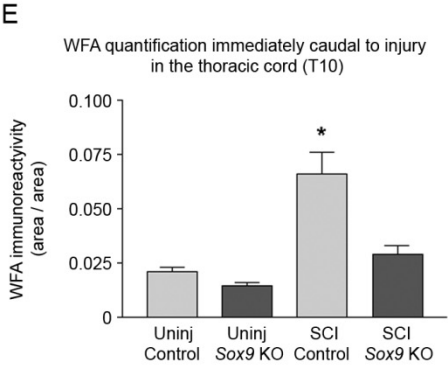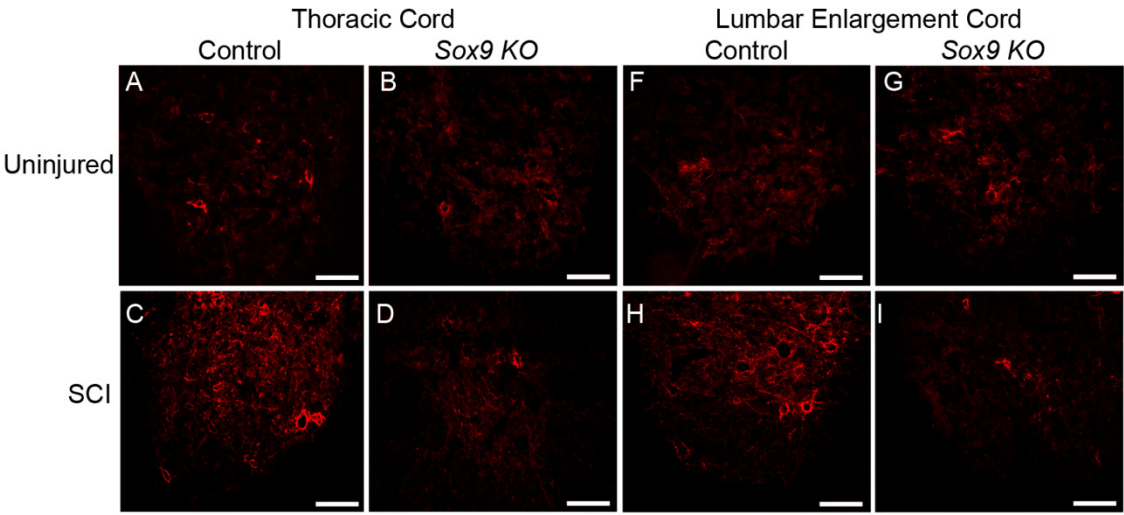
evaluate whether long-range regeneration of corticospinal, and reticulospinal axons through the lesion site might occur in the *Sox9* KO mice we investigated retrograde labeling after allowing sufficient time for axonal regrowth (8 weeks after SCI). This analysis failed to demonstrate any increase in retrogradely labeled neurons (Figure 3). Similar results were obtained both 1 week and 8 weeks after SCI when evaluating retrogradely-labeled rubrospinal, vestibulospinal or propriospinal interneurons (Supplementary Figure 1).

Sox9 KO mice display increased levels of presynaptic protein markers caudal to the lesion site post-SCI

We predicted that increased neuroplasticity in spinal cord injured *Sox9* KO mice would be most evident around lumbar motor neurons as they demonstrate reduced levels of PNN CSPGs and are deafferented by the spinal lesion. Thus we evaluated the area of immunoreactivity of presynaptic markers in the ventral horn of the lumbar enlargement in control and *Sox9* KO mice. Synaptophysin has been used as a marker of synaptic density [34]. At 48 h after SCI both *Sox9* KO and control mice demonstrated a similar large reduction in synaptophysin area of immunoreactivity caudal to the lesion when compared to uninjured mice (Figure 4). At 10 weeks post-injury the *Sox9* KO mice demonstrated a significant 31% increase in the area of synaptophysin immunoreactivity compared to injured controls.

To characterize this neuroplasticity further, we evaluated the area of immunoreactivity of the presynaptic markers VGLUT1 and VGAT. At 48 h after SCI, spinal cord sections from both *Sox9* KO and control mice had approximately the same amount of VGLUT1+ and VGAT+ area of immunoreactivity, but by 10 weeks post-SCI sections from *Sox9* KO mice demonstrated a significant 39% increase in VGLUT1 immunoreactivity compared to controls (Figure 5). No

Figure 3. *Sox9* **KO mice do not display increased axonal sparing or long range axonal regeneration post-SCI.** Uninjured mice display more fluorogold labeled corticospinal and reticulospinal tract neurons, than injured mice. Control and *Sox9* KO mice do not display differing fluorogold labeling at 1 week after SCI indicating that *Sox9* KO does not improve sparing post-SCI in these tracts. Control and *Sox9* KO mice do not display differing fluorogold labeling at 8 weeks post-SCI indicating that *Sox9* KO does not result in increased long range (at least 1 spinal segment) axonal regeneration after SCI in these tracts ($p = <0.05$, one way ANOVA. * indicates significantly different from the injured groups. a, b, c indicates significantly different from each other). Scale bars = 100μm. Supplementary Figure 1 contains fluorogold labeling data depicting that *Sox9* KO mice also do not display increased sparing or long range axonal regeneration in cervical spinal cord propriospinal interneurons, the rubrospinal tract or the vestibular spinal tract post-SCI.

Motor Cortex
Corticospinal Tract
Control | Sox9 KO

Reticular Formation
Reticular Spinal Tract
Control | Sox9 KO

Uninjured

1 week post SCI

8 weeks post SCI

Motor Cortex neurons retrogradely labeled
by fluorogold in control and *Sox9* KO mice

Reticular nuclei retrogradely labeled
by fluorogold in control and *Sox9* KO mice
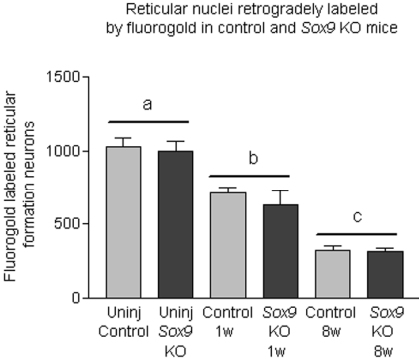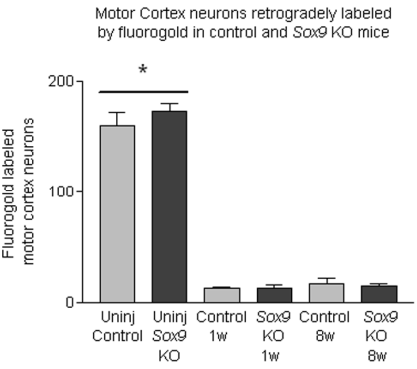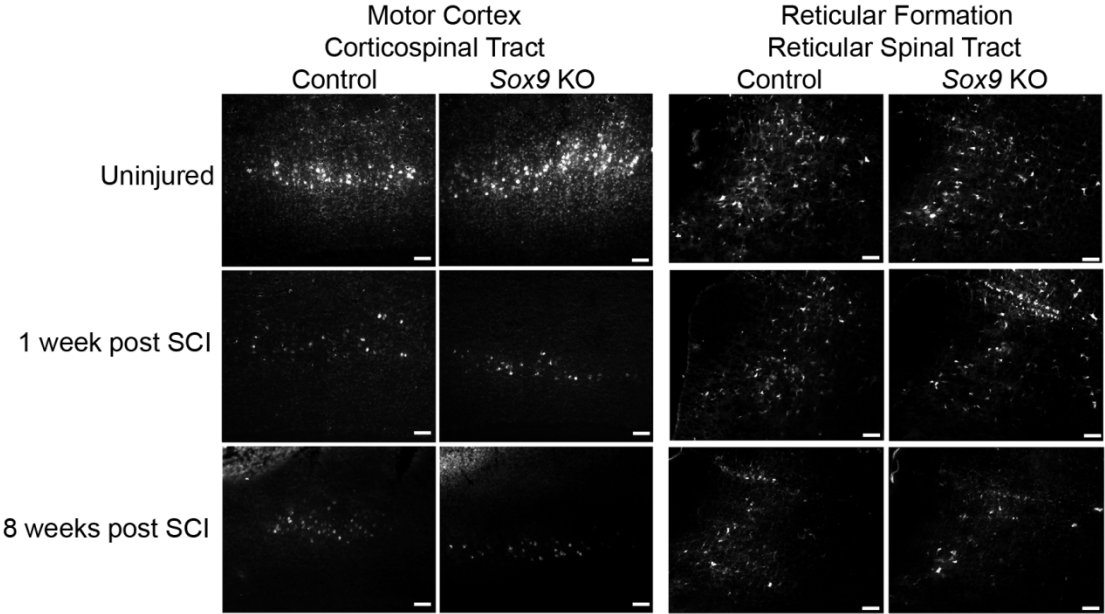
Figure 4. *Sox9* KO mice display increased synaptophysin immunoreactivity in the ventral horn of the lumbar enlargement 10 weeks post-SCI. A) Synaptophysin immunoreactivity in uninjured control mice. B) Synaptophysin immunoreactivity in uninjured *Sox9* KO mice. C) Synaptophysin immunoreactivity in control mice 48 hrs post-SCI. D) Synaptophysin immunoreactivity in *Sox9* KO mice 48 hrs post-SCI. E) Synaptophysin immunoreactivity in control mice 10 weeks post-SCI. F) Synaptophysin immunoreactivity in *Sox9* KO mice 10 weeks post-SCI. G) Both control and *Sox9* KO mice display increased synaptophysin immunoreactivity at 10 weeks post-SCI in comparison to 48 hr post-SCI, and *Sox9* KO mice display significantly increased synaptophysin immunoreactivity 10 weeks post-SCI compared to control mice ($p < 0.05$ by one way ANOVA with Neuman Keuls post-hoc test, a,b,c,* each significantly different from each other). Dotted line separates GM (grey matter) from WM (white matter). Scale bars indicate 100μm.

Control   *Sox9* KO

A   B   G

Uninjured

GM
WM

C   D

48 hr. post-SCI

E   F

10 weeks post-SCI

Synaptophysin quantification in the ventral horn of the lumbar enlargement

Synaptophysin immunoreactivity (area / area)

0.04

0.03 — a

0.02

0.01 — b   c   *

0.00

Uninj Control   Uninj *Sox9* KO   48hr Control   48hr *Sox9* KO   10w Control   10w *Sox9* KO
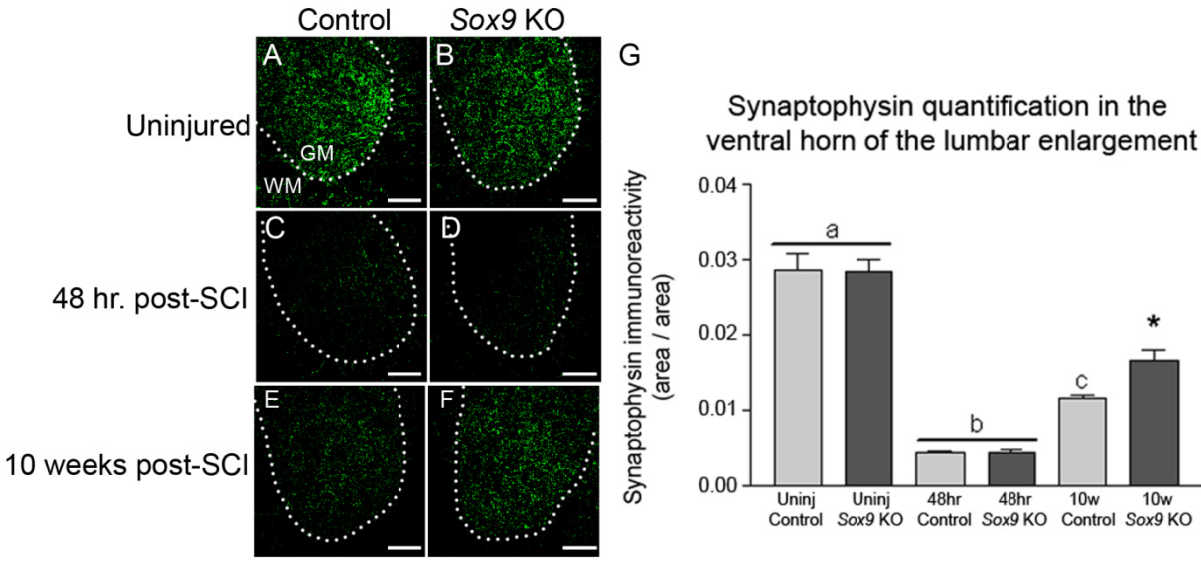
Figure 5. *Sox9* **KO mice display increased VGLUT1 immunoreactivity in the ventral horn of the lumbar enlargement 10 weeks post-SCI.** A) VGLUT1 immunoreactivity in uninjured control mice. B) VGLUT1 immunoreactivity in uninjured *Sox9* KO mice. C) VGLUT1 immunoreactivity in control mice 48 hrs post-SCI. D) VGLUT1 immunoreactivity in *Sox9* KO mice 48 hrs post-SCI. E) VGLUT1 immunoreactivity in control mice 10 weeks post-SCI. F) VGLUT1 immunoreactivity in *Sox9* KO mice 10 weeks post-SCI. G) Both control and *Sox9* KO mice display increased VGLUT1 immunoreactivity at 10 weeks post-SCI in comparison to 48 hr post-SCI, and *Sox9* KO mice display significantly increased VGLUT1 immunoreactivity 10 weeks post-SCI compared to control mice ($p < 0.05$ by one way ANOVA with Neuman Keuls post-hoc test, a,b,c,* each significantly different from each other). Dotted line separates GM (grey matter) from WM (white matter). Scale bars indicate 100μm.

Control   *Sox9* KO

Uninjured

48 hr. post-SCI

10 weeks post-SCI

VGLUT1 quantification in the ventral horn of the lumbar enlargement
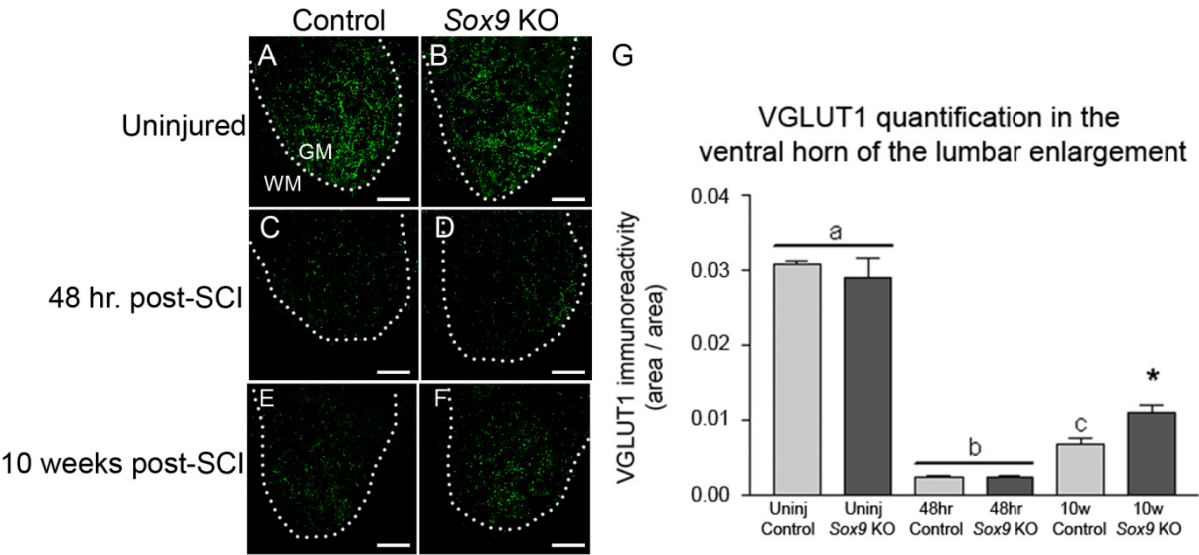
Figure 6. Control and *Sox9* KO mice display similar VGAT immunoreactivity in the ventral horn of the lumbar enlargement 10 weeks post-SCI. A) VGAT immunoreactivity in uninjured control mice. B) VGAT immunoreactivity in uninjured *Sox9* KO mice. C) VGAT immunoreactivity in control mice 48 hrs post-SCI. D) VGAT immunoreactivity in *Sox9* KO mice 48 hrs post-SCI. E) VGAT immunoreactivity in control mice 10 weeks post-SCI. F) VGAT immunoreactivity in *Sox9* KO mice 10 weeks post-SCI. G) Both control and *Sox9* KO mice display increased VGAT immunoreactivity at 10 weeks post-SCI in comparison to 48 hr post-SCI ($p<0.05$ by one way ANOVA with Neuman Keuls post-hoc test, a,b,c each significantly different from each other). Dotted line separates GM (grey matter) from WM (white matter). Scale bars indicate 100μm.

Control   *Sox9* KO

Uninjured

48 hr. post-SCI

10 weeks post-SCI

GM
WM

**VGAT quantification in the
ventral horn of the lumbar enlargement**
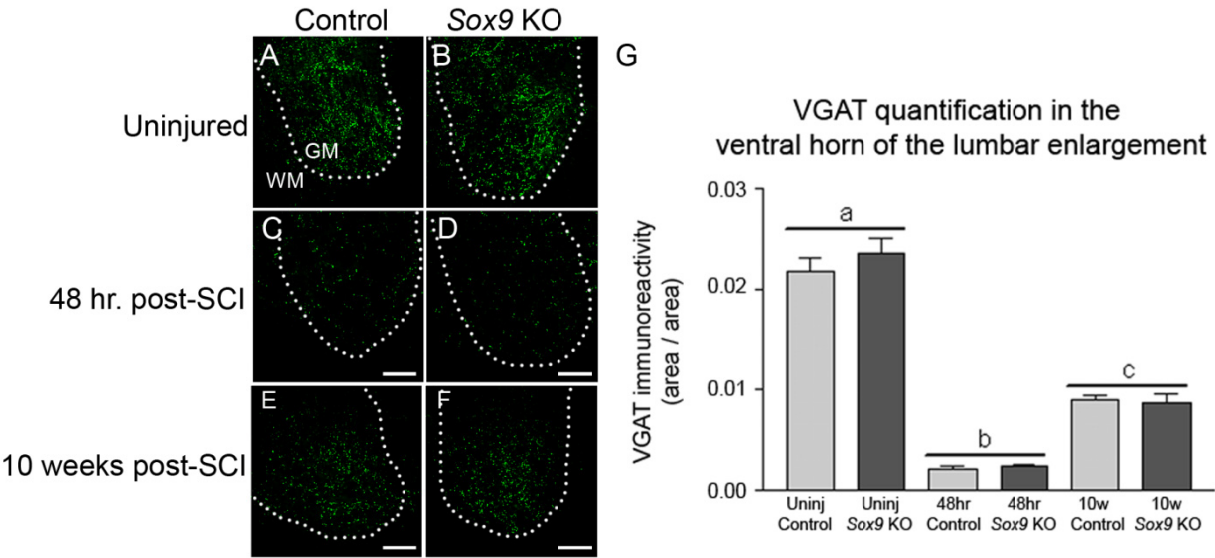
differences were found in VGAT immunostaining between controls and *Sox9* KO mice 10 weeks post SCI (Figure 6).

To investigate whether the increased areas of synaptophysin and VGLUT1 immunoreactivities might indicate increased number of presynaptic release sites, the number of synaptophysin and VGLUT1 immunoreactive puncta were counted 10 weeks after injury in the ventral horns of sections from the lumbar enlargements of *Sox9* KO and control spinal cords using high-power magnification. Increased individual synaptophysin+ (a 52% increase, Figure 7) and VGLUT1+ (a 2.34 fold increase, Figure 8) puncta were noted in *Sox9* KO mice in comparison to controls, whereas individual VGAT+ (Figure 9) puncta were found to be similar in both *Sox9* KO and control mice 10 weeks post SCI.

Sox9 KO mice display increased reactive sprouting caudal to the lesion site post-SCI

The increased presynaptic marker immunoreactivity and puncta density observed in the lumbar enlargement of *Sox9* KO mice could theoretically be explained by an increased level of protein expression or by an increased level of reactive sprouting. To investigate reactive sprouting in the spinal cord anterograde labeling experiments were performed. BDA was injected into the motor cortex of control and *Sox9* KO mice at 8 weeks after SCI and then after allowing 2 weeks for anterograde transport the mice were sacrificed and BDA labeling at cervical and lumbar spinal levels was evaluated. Counting individual BDA labeled puncta around motor neurons in the lumbar enlargement demonstrated a greater than two-fold increase in BDA labeling in *Sox9* KO mice compared to controls (a 2.28 fold increase, Figure 10). In support of the prediction that the increased sprouting of corticospinal axons might underlie the improved locomotor recovery, in comparison to controls the *Sox9* KO mice displayed a greater

Figure 7. *Sox9* KO mice display increased pre-synaptic terminal synaptophysin positive boutons in layer IX of ventral horn at the lumbar enlargement 10 weeks post-SCI. A) Confocal micrograph of synaptophysin+ pre-synaptic boutons in control mice 10 weeks post-SCI. B) Confocal micrograph of synaptophysin+ pre-synaptic boutons with Imaris identified individual puncta overlayed in control mice 10 weeks post-SCI. C) Imaris identified individual synaptophysin+ puncta alone in control mice 10 weeks post-SCI. D) Confocal micrograph of synaptophysin+ pre-synaptic boutons in *Sox9* KO mice 10 weeks post-SCI. E) Confocal micrograph of synaptophysin+ pre-synaptic boutons with Imaris identified individual puncta overlayed in *Sox9* KO mice 10 weeks post-SCI. F) Imaris identified individual synaptophysin+ puncta alone in *Sox9* KO mice 10 weeks post-SCI. G) *Sox9* KO mice display significantly increased synaptophysin+ pre-synaptic boutons 10 weeks post-SCI compared to control mice (p<0.05 by Student's T-test). Visualized with a 63x magnification objective, scale bar = 25 μm.

Confocal Overlay Individual Puncta

Control

Sox9 KO

G Quantification of individual synaptophysin+ puncta
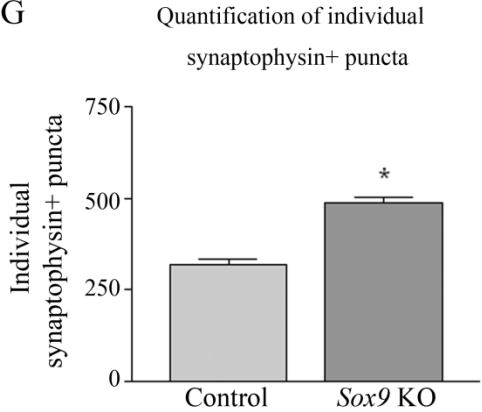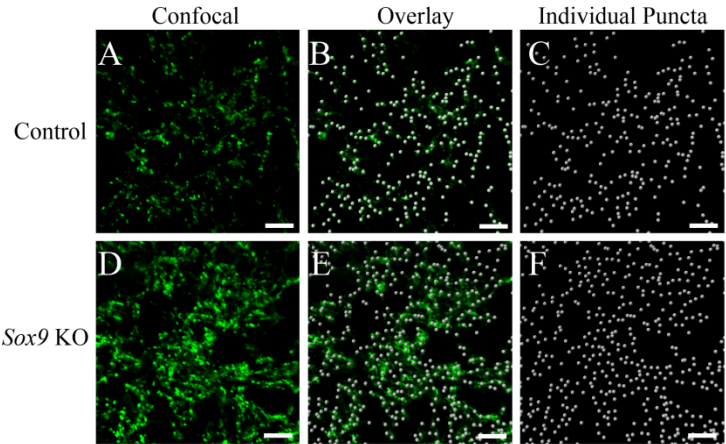
Figure 8. *Sox9* **KO mice display increased pre-synaptic terminal VGLUT1 positive boutons in layer IX of ventral horn at the lumbar enlargement 10 weeks post-SCI.** A) Confocal micrograph of VGLUT1+ pre-synaptic boutons in control mice 10 weeks post-SCI. B) Confocal micrograph of VGLUT1+ pre-synaptic boutons with Imaris identified individual puncta overlayed in control mice 10 weeks post-SCI. C) Imaris identified individual VGLUT1+ puncta alone in control mice 10 weeks post-SCI. D) Confocal micrograph of VGLUT1+ pre-synaptic boutons in *Sox9* KO mice 10 weeks post-SCI. E) Confocal micrograph of VGLUT1+ pre-synaptic boutons with Imaris identified individual puncta overlayed in *Sox9* KO mice 10 weeks post-SCI. F) Imaris identified individual VGLUT1+ puncta alone in *Sox9* KO mice 10 weeks post-SCI. G) *Sox9* KO mice display significantly increased VGLUT1+ pre-synaptic boutons 10 weeks post-SCI compared to control mice ($p < 0.05$ by Student's T-test). Visualized with a 63x magnification objective, scale bar = 25 μm.

Confocal	Overlay	Individual Puncta

Control: A, B, C

Sox9 KO: D, E, F

G — Quantification of individual VGLUT1+ puncta
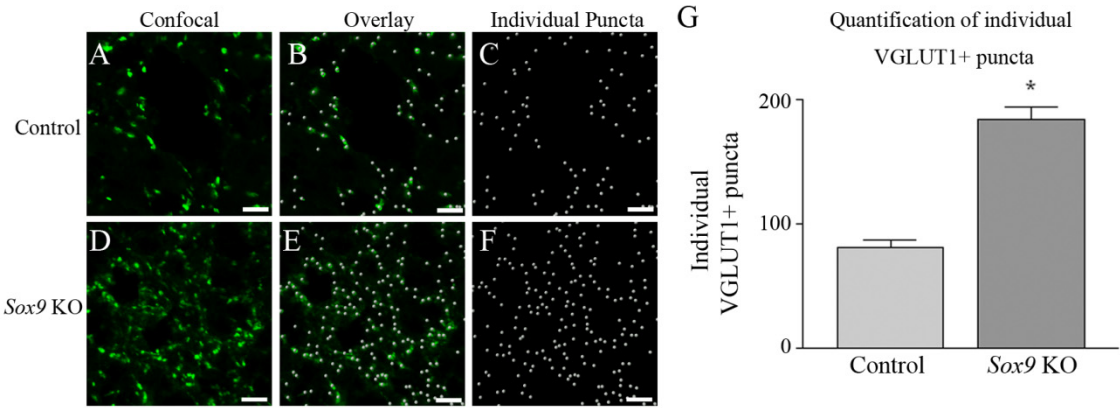
Figure 9. Control and *Sox9* KO mice display similar pre-synaptic terminal VGAT positive boutons in layer IX of ventral horn at the lumbar enlargement 10 weeks post-SCI. A) Confocal micrograph of VGAT+ pre-synaptic boutons in control mice 10 weeks post-SCI. B) Confocal micrograph of VGAT+ pre-synaptic boutons with Imaris identified individual VGAT+ puncta overlayed in control mice 10 weeks post-SCI. C) Imaris identified individual VGAT+ puncta alone in control mice 10 weeks post-SCI. D) Confocal micrograph of VGAT+ pre-synaptic boutons in *Sox9* KO mice 10 weeks post-SCI. E) Confocal micrograph of VGAT+ pre-synaptic boutons with Imaris identified individual VGAT+ puncta overlayed in *Sox9* KO mice 10 weeks post-SCI. F) Imaris identified individual VGAT+ puncta alone in *Sox9* KO mice 10 weeks post-SCI. G) *Sox9* KO mice display significantly increased VGAT+ pre-synaptic boutons 10 weeks post-SCI compared to control mice (p<0.05 by Student's T-test). Visualized with a 63x magnification objective, scale bar = 25 μm.
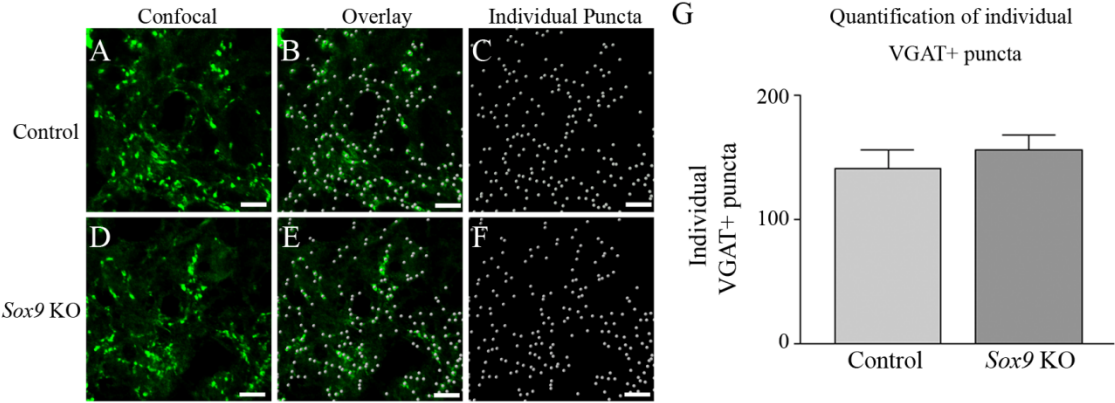
Figure 10. High magnification images display increased BDA and VGLUT1 positive puncta around ventral horn motor neurons in the lumbar enlargement in *Sox9* KO mice. Motor neurons in the ventral horn of the lumbar enlargement stained for BDA+ puncta, VGLUT1+ puncta, and BDA-VGLUT1 co-localized puncta viewed by confocal z-stack. BDA confocal z-stack (A) and Imaris identified individual BDA+ puncta (B) in control mice. BDA confocal z-stack (C) and Imaris identified individual BDA+ puncta (D) in *Sox9* KO mice. E) Motor neurons in the ventral horn of the lumbar enlargement displayed increased BDA+ puncta in *Sox9* KO mice ($p = <0.05$, Student's t-test). VGLUT1 confocal z-stack (F) and Imaris identified individual VGLUT1+ puncta (G) in control mice. VGLUT1 confocal z-stack (H) and Imaris identified individual VGLUT1+ puncta (I) in *Sox9* KO mice. J) Motor neurons in the ventral horn of the lumbar enlargement displayed increased VGLUT1+ puncta in *Sox9* KO mice ($p = <0.05$, Student's t-test). NeuN (blue) BDA-VGLUT1 confocal z-stack (K) and Imaris identified individual BDA-VGLUT1+ co-localized puncta (L) in control mice. NeuN (blue) BDA-VGLUT1 confocal z-stack (M) and Imaris identified individual BDA-VGLUT1+ co-localized puncta (N) in *Sox9* KO mice. O) Motor neurons in the ventral horn of the lumbar enlargement displayed increased numbers of BDA-VGLUT1 co-localized puncta in *Sox9* KO mice ($p = <0.05$, Student's t-test). Scale bars indicate 10μm.

BDA Confocal Photomicrograph

BDA Imaris Identified Individual puncta

VGLUT1 Confocal Photomicrograph

VGLUT1 Imaris Identified Individual puncta

BDA-VGLUT1 Confocal Photomicrograph

BDA-VGLUT1 Co-localized Imaris Identified Individual puncta

Control mice

Sox9 KO mice

Average number of BDA+ puncta around ventral horn motor neurons sampled in the lumbar enlargement

Average number of VGLUT1+ puncta around ventral horn motor neurons sampled in the lumbar enlargement

Average number of BDA-VGLUT1 co-localized puncta around ventral horn motor neurons sampled in the lumbar enlargement

than three-fold increase in the number of BDA-labeled puncta that were co-localized with VGLUT1 (a 3.03 fold increase, Figure 10).

BDA labeling in the cervical enlargement of uninjured *Sox9* KO and control mice was investigated to evaluate whether *Sox9* ablation on its own (without an accompanying injury) might lead to increased reactive sprouting. BDA labeling of axons in uninjured mice was found to be the same in both *Sox9* KO and control mice (Supplemental Figure 2). To evaluate BDA labeling distant to a denervated site we investigated BDA labeling around ventral horn motor neurons in the cervical enlargement following SCI. In comparison to control mice, *Sox9* KO mice did not display altered BDA+ puncta, VGLUT1+ puncta, or BDA-VGLUT1 co-localized puncta, around ventral horn motor neurons in the cervical enlargement following SCI (Supplementary Figure 3).

Sox9 KO mice display increased 5-HT immunoreactivity caudal to the lesion site after SCI

Serotonergic projections from the Raphe Nuclei synapse in the ventral horn and are believed to directly modulate motor activity [35]. Injuries which lead to a reduction in these serotonergic inputs to the ventral horn result in decreased motor function [36]. To evaluate whether the improvements in hind limb function seen in S*ox9* KO mice could be the result of increased ventral horn serotonergic input, we investigated serotonin immunoreactivity in spinal cord cross-sections sections taken from T10 and the lumbar enlargement of both uninjured and SCI *Sox9* KO and control mice. Following injury both *Sox9* KO and control mice demonstrate decreased serotonin immunoreactivity compared to uninjured controls, however, *Sox9* KO mice demonstrate a statistically significant increase in serotonin immunoreactivity in the ventral horn

at spinal levels T10 (a 2.19 fold increase) and L1 (a 2.39 fold increase), compared to control mice 10 weeks post SCI ($p<0.05$ by one-way ANOVA, Figure 11).

Figure 11. *Sox9* **KO mice display increased serotonin immunoreactivity both just caudal to the injury site and in the ventral horn of the lumbar enlargement 10 weeks post-SCI.** A) Serotonin immunoreactivity in uninjured control mice at T10. B) Serotonin immunoreactivity in uninjured *Sox9* KO mice at T10. C) Serotonin immunoreactivity in control mice just caudal to the injury site (T10). D) Serotonin immunoreactivity in *Sox9* KO mice just caudal to the injury site (T10). E) Just caudal to the injury site, *Sox9* KO mice display increased serotonin immunoreactivity in comparison to control mice post-SCI ($p<0.05$, one way ANOVA). F) Serotonin immunoreactivity at the ventral horn of the lumbar enlargement (L1) in uninjured control mice. G) Serotonin immunoreactivity in the ventral horn of the lumbar enlargement (L1) in uninjured *Sox9* KO mice. H) Serotonin immunoreactivity in the ventral horn of the lumbar enlargement (L1) in control mice post-SCI. I) Serotonin immunoreactivity in *Sox9* KO mice in the ventral horn of the lumbar enlargement (L1) post-SCI. J) *Sox9* KO mice display increased serotonin immunoreactivity in the ventral horn of the lumbar enlargement post-SCI ($p<0.05$, one way ANOVA, a,b,c are significantly different from each other). Scale bars = 100μm.

Thoracic Cord
Control   *Sox9* KO

Lumbar Enlargement Cord
Control   *Sox9* KO

Uninjured

SCI

E

Serotonin quantitation immediately cuadal to injury in the thoracic cord (T10)

J

Serotonin quantitation in the ventral horn of the lumbar enlargement
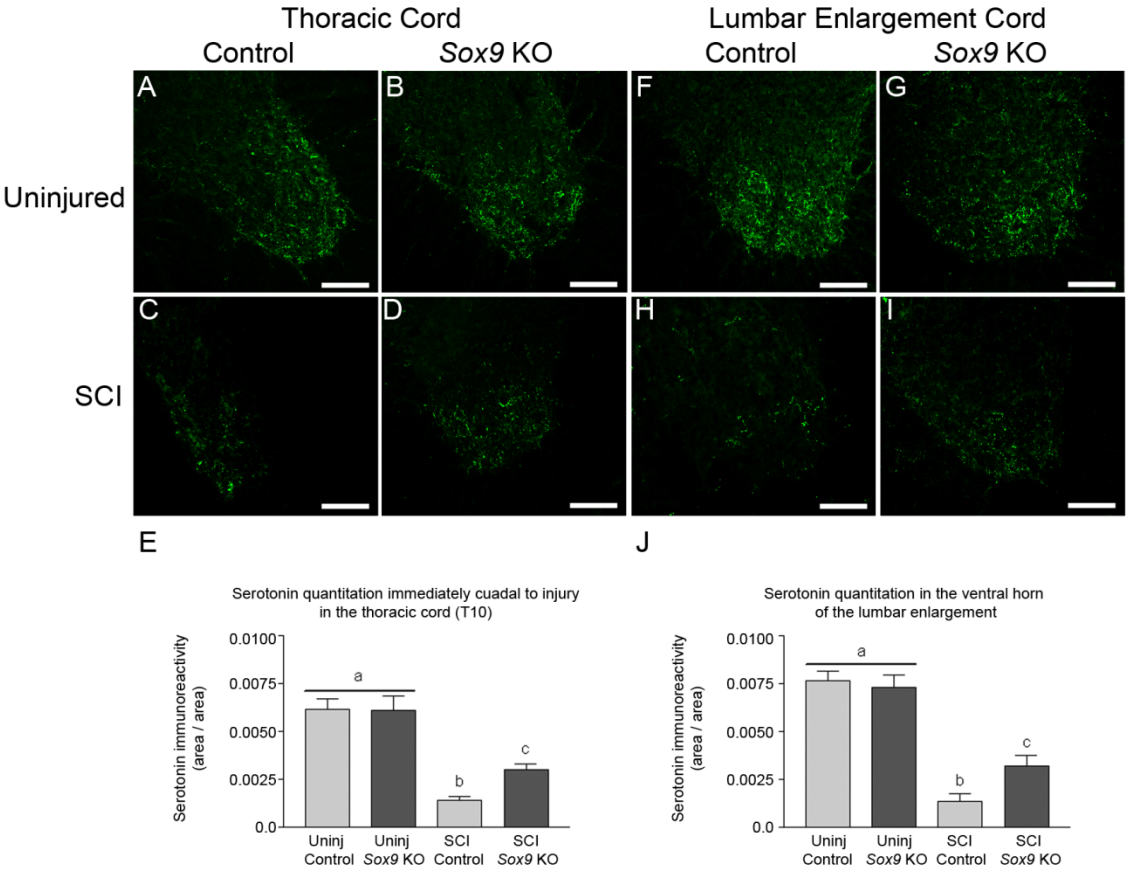
4.4 Discussion

Recovery following SCI is significantly impeded by the CSPG-rich inhibitory extracellular matrix that serves to prevent neuroplasticity both at the lesion site as well as distant to the lesion [37-39]. Degradation of CSPG side chains by administration of the bacterial enzyme chondroitinase results in enhanced regeneration following SCI in rodents [4, 13, 22, 40], as well as improved skilled locomotor function in adult cats following T10 hemisection [41]. We previously proposed that SOX9 inhibition could serve as an alternate strategy for reducing CSPG levels in the injured spinal cord by reducing the expression of CSPG biosynthetic enzymes and core proteins [24, 25]. This proposition was supported by our previous study demonstrating that conditional *Sox9* ablation reduces CSPG levels in the injured spinal cord and improves hind limb function after SCI [25]. However that study did not address the mechanism through which *Sox9* ablation resulted in improved locomotor recovery.

Sox9 ablation could lead to better locomotor outcomes after SCI for a variety of reasons. First, we have previously demonstrated that *Sox9* KO is associated with a concomitant reduction in GFAP expression [25]. Astrocytes activated at the time of SCI display upregulated GFAP as well as increased cytokine production and stimulate the inflammatory response [42, 43]. As *Sox9* KO mice display reduced GFAP, they may have a reduced inflammatory response post-SCI compared to controls. This could result in increased sparing of descending axons at the time of injury, and perhaps the preservation of injured nervous tissue. Alternatively, reduced CSPG levels at the glial scar [25] could create an environment more permissive to long-range axonal regeneration through the lesion site. Finally reduced CSPG levels in PNNs [25] could provide an environment that promotes reactive sprouting. Herein we evaluated each of these potential mechanisms of neuroplasticity in the *Sox9* KO mice.

We assessed neuronal sparing by labeling axons with retrograde tracer one segment caudal to the original injury site one week after SCI.   It has been estimated that roughly 5 days are required for the proximal stump of a severed axon to prepare for growth, and axonal growth rates are suggested to be 0.25 mm/day through an injury site [32, 33]. Thus, 1 week of recovery is not enough time for regeneration through the lesion to the site of retrograde tracer labeling (a distance of ~3mm). Thus at 1 week post-SCI only axons spared from injury should be available for retrograde labeling. The absence of significant difference in the number of neurons with descending projections labeled in this way between *Sox9* KO and control mice suggests that increased sparing of axons through the lesion site in *Sox9* KO mice is not the explanation for their improved locomotor recovery after SCI.

To assess the possibility of long-range regeneration in spinal cord-injured mice we carried out retrograde labeling at 8 weeks post-SCI, a time point at which one would predict that sufficient time has elapsed from the injury to allow for regeneration through the lesion [32, 33]. This labeling study failed to reveal any evidence for long range regeneration in the corticospinal, reticulospinal, rubrospinal, vestibulospinal or long range propriospinal tracts within the *Sox9* KO mice. This may not be all that surprising as a considerable number of anti-regenerative molecules likely still remain at the lesion site. Semaphorins, ephrins, netrins, slit, Nogo, myelin-associated glycoprotein, repulsive guidance molecule, and oligodendrocyte myelin glycoprotein are all expressed after injury in the glial scar and induce axonal growth cone collapse [3, 44-50]. Thus the failure to demonstrate long-range regeneration in the *Sox9* KO mice after SCI may be due to the expression of various inhibitors to axon growth that are not affected by *Sox9* ablation. With that said, perhaps the reason that long range regeneration does not contribute to natural recovery post-SCI is the difficulty a regenerating axon would have in travelling the distance to its intended

target site and in making a functional synapse on its correct target while ignoring all the incorrect potential targets.

In contrast to the difficulty posed by long range axonal regeneration, there are forms of neuroplasticity that normally occur post-CNS trauma for which appropriate targeting may be less problematic. Spontaneous re-wiring of limb somatotopic maps occurs in the somatosensory and motor cortices as well as within the brainstem post-neurotrauma [51-53]. Rat corticospinal tract axons cut in the thoracic dorsal funiculus sprout rostrally into the cervical spinal cord gray matter resulting in novel forelimb whisker and trunk activation evoked by hindlimb motor cortex stimulation [54]. After unilateral pyramidotomy, axons originating on the uninjured side of the corticospinal tract sprout and grow into the denervated side of the cord [55, 56]. Following a lesion of the dorsal corticospinal tract, a small proportion of ventral corticospinal fibers sprout into the denervated dorsal spinal cord [57]. Hindlimb corticospinal tract axons were found to sprout into the cervical gray matter and connect with long propriospinal neurons which bridged the lesion site and innervated lumbar spinal cord motorneurons, and electrophysiological stimulation of the hindlimb motor cortex revealed these circuits to be functional [58]. All of these are examples of naturally occurring axonal plasticity post SCI. The reduction in CSPG expression seen in *Sox9* KO mice may improve these endogenous reactive sprouting mechanisms, allowing newly formed collateral sprouts from spared axons traversing the lesion to make functional connections on motor neuron targets in the same field as the original targets of the injured axons.

If the spinal cord injured *Sox9* KO mice displayed increased neuroplasticity we reasoned that it would be most evident around deafferented lumbar motor neurons demonstrating reduced PNN CSPGs. Thus, we investigated synaptic plasticity by examining acute and chronic changes

in pre-synaptic markers in the ventral horn of the lumbar enlargement in control and *Sox9* KO mice after SCI. After SCI, synaptic inputs in the ventral horn are decreased acutely and then, over time some synaptic inputs return [59]. This return of synaptic inputs is attributed to neuroplasticity within the spinal cord. At 48 h post SCI, *Sox9* KO mice and controls had approximately the same number of pre-synaptic synaptophysin vesicle markers remaining, supporting our finding that *Sox9* KO does not result in sparing of axons. However, at 10 weeks post-SCI *Sox9* ablated mice displayed increased synaptophysin immunoreactivity as well as increased synaptophysin+ individual puncta.

The synaptic losses observed at 48 hours after injury are likely due to substantial reductions in glutamatergic and GABAergic inputs, like those occurring in autonomic circuits [60]. As the majority of inputs onto spinal motor neurons are either glutamatergic or GABAergic [61, 62], densities of VGLUT1+ and VGAT+ presynaptic vesicles have been used to reveal changes in synaptic input due to remodeling after injury [61] as they reflect the number of synapses on cell bodies [34, 63, 64]. We thus investigated VGLUT1 and VGAT pre-synaptic markers in the *Sox9* KO mice. At 48 h post SCI, *Sox9* KO mice and controls had approximately the same number of VGLUT1+ and VGAT+ pre-synaptic vesicle markers remaining but by 10 weeks post-SCI *Sox9* ablated mice displayed increased VGLUT1 immunoreactivity as well as VGLUT1+ individual puncta compared to controls, and similar levels of VGAT immunoreactivity and individual puncta compared to controls. Thus following SCI the VGLUT1 pre-synaptic marker increases more quickly in the *Sox9* KO mice than in controls.

The increased presynaptic markers displayed in *Sox9* KO lumbar enlargements could indicate an increased number of neuronal synapses, an increased number of neurotransmitter release sites, or an increased number of presynaptic vesicles per release site. Each of these

possibilities are examples of neuroplasticity, and each would indicate increased synaptic strength in the lumbar enlargements of *Sox9* KO mice 10 weeks post-SCI. As *Sox9* KO mice did not display evidence of long-range axonal regeneration, this increase in presynaptic markers is likely due to the sprouting of spared fibers below the spinal lesion.

To investigate reactive sprouting in *Sox9* KO mice we carried out an anterograde labeling study. Anterograde labeling demonstrated an increased number of BDA+ puncta around ventral horn motor neurons below the lesion in *Sox9* KO mice in comparison to controls. Since we did not observe an increase in neuronal sparing in the *Sox9* KO mice the increased BDA labelling indicates that fibers spared from injury undergo reactive sprouting to a greater extent in *Sox9* KO mice than in controls. Our data also demonstrated that more anterogradely labeled pre-synaptic terminals co-localize with the VGLUT1 pre-synaptic marker in *Sox9* KO mice than in control mice. This suggests that many of the reactive sprouts found in *Sox9* KO mice terminate in VGLUT1+ pre-synaptic boutons near motor neurons, and are likely to be at least partly responsible for the improved functional recovery seen in these mice.

Others have shown that the limited recovery after SCI is likely due to remodeling of existing circuits rather than to the re-growth of descending supraspinal inputs [58, 65]. Thus we were not surprised to see an increase in reactive sprouting as opposed to long-range regeneration of damaged descending spinal tracts. As we did not find increased BDA+ puncta or VGLUT1+ puncta around ventral horn motor neurons in the cervical enlargement, we suggest that the increased reactive sprouting in *Sox9* KO mice occurs due to two signals: deafferentation of target neurons and reduced levels of CSPGs in the PNNs of those target neurons.

Most spinal cord injuries in humans are in fact incomplete injuries where a proportion of axonal projections running through the lesion site remain intact post injury [66]. Thus, a

therapeutic strategy that promotes sprouting of these surviving spared axons may greatly improve functional outcome post SCI. It has been suggested that increased collateral sprouting in cervical level injuries might increase spared lower cervical level fiber innervation and improve control of the triceps, thus affording improved control over a wheelchair [67], and that increased innervation by spared serotonergic fibers might yield improved bladder control [68] or reduced pain [69].

We have previously shown that *Sox9* ablation both before SCI and in the subacute period after SCI results in reduced CSPG levels in the spinal cord and improvements in motor function post-SCI. The present study extends our previous work by demonstrating that *Sox9* ablation leads to increased reactive sprouting caudal to the lesion post-SCI. Taken together, increasing neuroplasticity by way of SOX9 inhibition is a promising therapeutic strategy for the treatment of SCI.

Supplementary Figure 1. *Sox9* **KO mice also do not display increased sparing or long range axonal regeneration in propriospinal interneurons, the rubrospinal tract or the vestibular spinal tract post-SCI.** Uninjured mice display more fluorogold labeled propriospinal interneurons, rubrospinal tract neurons or vestibular spinal tract neurons, than in injured mice. Control and *Sox9* KO mice do not display differing fluorogold labeling at 1 week post-SCI indicating that *Sox9* KO does not improve sparing post-SCI in these tracts. Control and *Sox9* KO mice do not display differing fluorogold labeling at 8 weeks post-SCI indicating that *Sox9* KO does not result in increased long range (at least 1 spinal segment) axonal regeneration post-SCI in these tracts. ($p=<0.05$, one way ANOVA. * indicates significantly different from the injured groups. a, b, c indicates significantly different from each other). Scale bars = 100μm.

Cervical enlargement
Propriospinal interneurons
Control   Sox9 KO

Red Nucleus
Rubrospinal Tract
Control   Sox9 KO

Vestibular Formation
Vestibular Spinal Tract
Control   Sox9 KO

Uninjured

1 week post-SCI

8 weeks post-SCI

Propriospinal interneurons retrogradely labeled
by fluorogold in control and Sox9 KO mice

Red nucleus retrogradely labeled
by fluorogold in control and Sox9 KO mice

Vestibular nuclei retrogradely labeled
by fluorogold in control and Sox9 KO mice
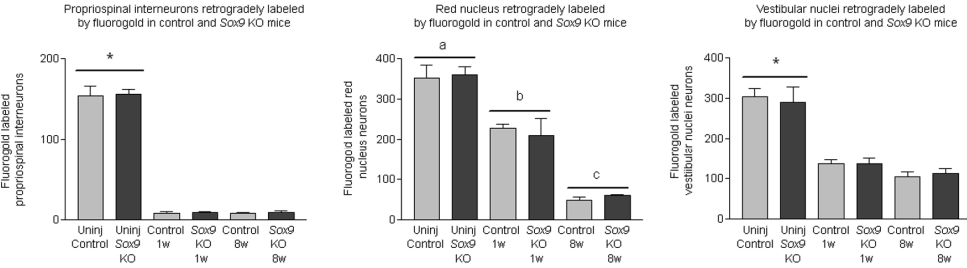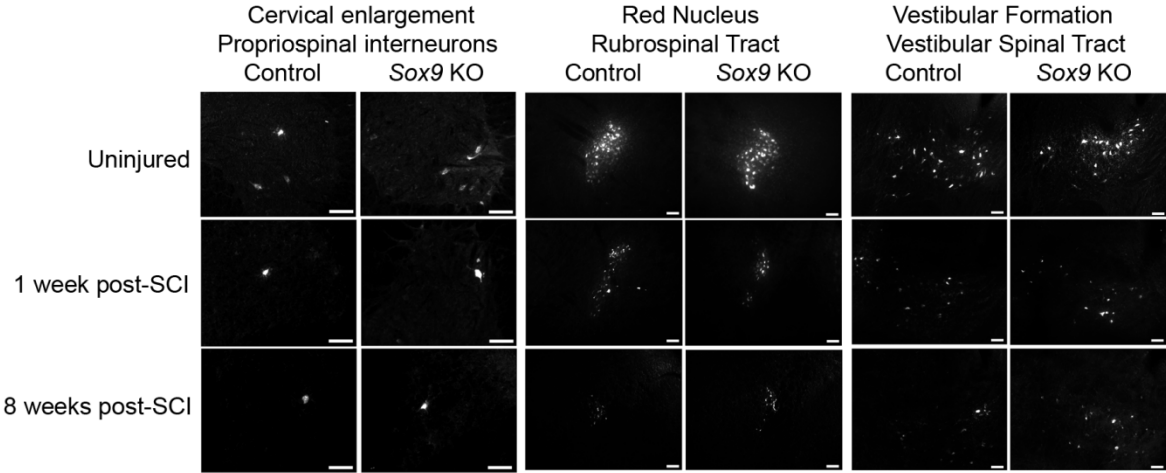
Supplementary Figure 2. Control and *Sox9* KO mice display similar numbers of BDA labeled fibers in the cervical enlargement in both uninjured mice as well as 10 weeks post-SCI. A) BDA labeling in the cervical enlargement of uninjured control mice. B) BDA labeling in the cervical enlargement of uninjured Sox9 KO mice. C) The cervical enlargements in uninjured Sox9 KO and control mice display equal BDA labeling (p=>0.05, Student's t-test). D) BDA labeling in the cervical enlargement of control mice post-SCI. E) BDA labeling in the cervical enlargement of Sox9 KO post-SCI. F) In the cervical enlargement (rostral to the injury site) Sox9 KO and control mice display equal BDA labeling (p=>0.05, Student's t-test). Scale bars = 100μm.

Control   *Sox9* KO

Cervical enlargement in uninjured mice

Cervical enlargement in injured mice

BDA positive fibers in the cervical enlargement of uninjured mice

BDA positive fibers in the cervical enlargement rostral to SCI

Number of BDA labeled fibers
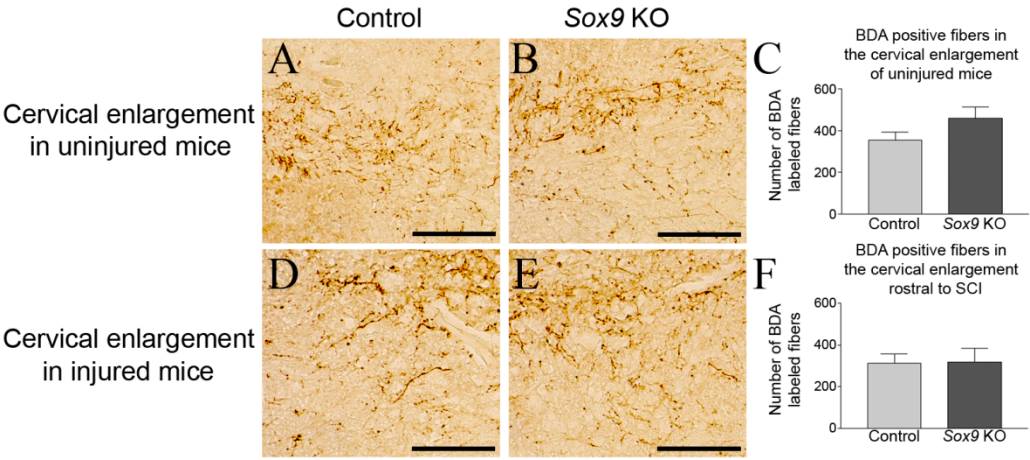
Supplementary Figure 3. High magnification images display similar numbers of BDA and VGLUT1 positive puncta around ventral horn motor neurons in the cervical enlargement in *Sox9* KO mice. Motor neurons in the ventral horn of the cervical enlargement stained for BDA+ puncta, VGLUT1+ puncta, and BDA-VGLUT1 co-localized puncta viewed by confocal z-stack. BDA confocal z-stack (A) and Imaris identified individual BDA+ puncta (B) in control mice. BDA confocal z-stack (C) and Imaris identified individual BDA+ puncta (D) in *Sox9* KO mice. E) Motor neurons in the ventral horn of the lumbar enlargement displayed similar numbers of BDA+ puncta in control and *Sox9* KO mice (p=<0.05, Student's t-test). VGLUT1 confocal z-stack (F) and Imaris identified individual VGLUT1+ puncta (G) in control mice. VGLUT1 confocal z-stack (H) and Imaris identified individual VGLUT1+ puncta (I) in *Sox9* KO mice. J) Motor neurons in the ventral horn of the lumbar enlargement displayed similar numbers of VGLUT1+ puncta in control and *Sox9* KO mice (p=<0.05, Student's t-test). NeuN (blue) BDA-VGLUT1 confocal z-stack (K) and Imaris identified individual BDA-VGLUT1+ co-localized puncta (L) in control mice. NeuN (blue) BDA-VGLUT1 confocal z-stack (M) and Imaris identified individual BDA-VGLUT1+ co-localized puncta (N) in *Sox9* KO mice. O) Motor neurons in the ventral horn of the lumbar enlargement displayed similar numbers of BDA-VGLUT1 co-localized puncta in control and *Sox9* KO mice (p=<0.05, Student's t-test). Scale bars indicate 10μm.

BDA Confocal Photomicrograph · BDA Imaris Identified Individual puncta · VGLUT1 Confocal Photomicrograph · VGLUT1 Imaris Identified Individual puncta · BDA-VGLUT1 Confocal Photomicrograph · BDA-VGLUT1 Co-localized Imaris Identified Individual puncta

Control mice

Sox9 KO mice

E — Average number of BDA+ puncta around ventral horn motor neurons sampled in the cervical enlargement

J — Average number of VGLUT1+ puncta around ventral horn motor neurons sampled in the cervical enlargement

O — Average number of BDA-VGLUT1 co-localized puncta around ventral horn motor neurons sampled in the cervical enlargement

4.5 Acknowledgments

4.6 Author Disclosure Statement

A.B. holds a patent on SOX9 inhibition as a target for regeneration in the nervous system. No competing financial interests exist for W.M.M., T.H. K.X, or N.G.

4.7 References

1. Galtrey, C.M. and J.W. Fawcett, *The role of chondroitin sulfate proteoglycans in regeneration and plasticity in the central nervous system.* Brain research reviews, 2007. **54**(1): p. 1-18.
2. Morgenstern, D.A., R.A. Asher, and J.W. Fawcett, *Chondroitin sulphate proteoglycans in the CNS injury response.* Prog Brain Res, 2002. **137**: p. 313-32.
3. McKeon, R.J., et al., *Reduction of neurite outgrowth in a model of glial scarring following CNS injury is correlated with the expression of inhibitory molecules on reactive astrocytes.* J Neurosci, 1991. **11**(11): p. 3398-411.
4. McKeon, R.J., A. Hoke, and J. Silver, *Injury-induced proteoglycans inhibit the potential for laminin-mediated axon growth on astrocytic scars.* Experimental neurology, 1995. **136**(1): p. 32-43.
5. Johnson, K.G. and D. Van Vactor, *Receptor protein tyrosine phosphatases in nervous system development.* Physiological reviews, 2003. **83**(1): p. 1-24.
6. Dunah, A.W., et al., *LAR receptor protein tyrosine phosphatases in the development and maintenance of excitatory synapses.* Nature neuroscience, 2005. **8**(4): p. 458-67.
7. Rashid-Doubell, F., et al., *Chick PTPsigma regulates the targeting of retinal axons within the optic tectum.* J Neurosci, 2002. **22**(12): p. 5024-33.
8. Celio, M.R., et al., *Perineuronal nets: past and present.* Trends Neurosci, 1998. **21**(12): p. 510-5.

9. Berardi, N., et al., *Molecular basis of plasticity in the visual cortex.* Trends in neurosciences, 2003. **26**(7): p. 369-78.

10. Lander, C., et al., *A family of activity-dependent neuronal cell-surface chondroitin sulfate proteoglycans in cat visual cortex.* J Neurosci, 1997. **17**(6): p. 1928-39.

11. Pizzorusso, T., et al., *Reactivation of ocular dominance plasticity in the adult visual cortex.* Science, 2002. **298**(5596): p. 1248-51.

12. Pizzorusso, T., et al., *Structural and functional recovery from early monocular deprivation in adult rats.* Proc Natl Acad Sci U S A, 2006. **103**(22): p. 8517-22.

13. Lemons, M.L., D.R. Howland, and D.K. Anderson, *Chondroitin sulfate proteoglycan immunoreactivity increases following spinal cord injury and transplantation.* Exp Neurol, 1999. **160**(1): p. 51-65.

14. Andrews, E.M., et al., *Alterations in chondroitin sulfate proteoglycan expression occur both at and far from the site of spinal contusion injury.* Exp Neurol, 2011.

15. Dou, C.L. and J.M. Levine, *Inhibition of neurite growth by the NG2 chondroitin sulfate proteoglycan.* J Neurosci, 1994. **14**(12): p. 7616-28.

16. Schmalfeldt, M., et al., *Brain derived versican V2 is a potent inhibitor of axonal growth.* J Cell Sci, 2000. **113 (Pt 5)**: p. 807-16.

17. Friedlander, D.R., et al., *The neuronal chondroitin sulfate proteoglycan neurocan binds to the neural cell adhesion molecules Ng-CAM/L1/NILE and N-CAM, and inhibits neuronal adhesion and neurite outgrowth.* J Cell Biol, 1994. **125**(3): p. 669-80.

18. Yamada, H., et al., *The brain chondroitin sulfate proteoglycan brevican associates with astrocytes ensheathing cerebellar glomeruli and inhibits neurite outgrowth from granule neurons.* J Neurosci, 1997. **17**(20): p. 7784-95.

19. Milev, P., et al., *Interactions of the chondroitin sulfate proteoglycan phosphacan, the extracellular domain of a receptor-type protein tyrosine phosphatase, with neurons, glia, and neural cell adhesion molecules.* J Cell Biol, 1994. **127**(6 Pt 1): p. 1703-15.

20. Gotting, C., et al., *Molecular cloning and expression of human UDP-d-Xylose:proteoglycan core protein beta-d-xylosyltransferase and its first isoform XT-II.* J Mol Biol, 2000. **304**(4): p. 517-28.

21. Yamauchi, S., et al., *Molecular cloning and expression of chondroitin 4-sulfotransferase.* J Biol Chem, 2000. **275**(12): p. 8975-81.

22. Bradbury, E.J., et al., *Chondroitinase ABC promotes functional recovery after spinal cord injury.* Nature, 2002. **416**(6881): p. 636-40.

23. Grimpe, B. and J. Silver, *A novel DNA enzyme reduces glycosaminoglycan chains in the glial scar and allows microtransplanted dorsal root ganglia axons to regenerate beyond lesions in the spinal cord.* J Neurosci, 2004. **24**(6): p. 1393-7.

24. Gris, P., et al., *Transcriptional regulation of scar gene expression in primary astrocytes.* Glia, 2007. **55**(11): p. 1145-55.

25. McKillop, W.M., et al., *Conditional Sox9 ablation reduces chondroitin sulfate proteoglycan levels and improves motor function following spinal cord injury.* Glia, 2013. **61**(2): p. 164-77.

26. Bi, W., et al., *Sox9 is required for cartilage formation.* Nat Genet, 1999. **22**(1): p. 85-9.

27. Hayashi, S. and A.P. McMahon, *Efficient recombination in diverse tissues by a tamoxifen-inducible form of Cre: a tool for temporally regulated gene activation/inactivation in the mouse.* Dev Biol, 2002. **244**(2): p. 305-18.

28.   Danielian, P.S., et al., *Modification of gene activity in mouse embryos in utero by a tamoxifen-inducible form of Cre recombinase.* Curr Biol, 1998. **8**(24): p. 1323-6.

29.   Wessendorf, M.W., *Fluoro-Gold: composition, and mechanism of uptake.* Brain Research, 1991. **553**(1): p. 135-48.

30.   Pronichev, I.V. and D.N. Lenkov, *Functional mapping of the motor cortex of the white mouse by a microstimulation method.* Neuroscience and behavioral physiology, 1998. **28**(1): p. 80-5.

31.   Hartig, W., K. Brauer, and G. Bruckner, *Wisteria floribunda agglutinin-labelled nets surround parvalbumin-containing neurons.* Neuroreport, 1992. **3**(10): p. 869-72.

32.   Tuszynski, M.H. and O. Steward, *Concepts and methods for the study of axonal regeneration in the CNS.* Neuron, 2012. **74**(5): p. 777-91.

33.   Steward, O., B. Zheng, and M. Tessier-Lavigne, *False resurrections: distinguishing regenerated from spared axons in the injured central nervous system.* J Comp Neurol, 2003. **459**(1): p. 1-8.

34.   Chou, A.K., et al., *Altered synaptophysin expression in the rat spinal cord after chronic constriction injury of sciatic nerve.* Neuroscience letters, 2002. **333**(3): p. 155-8.

35.   Murray, K.C., et al., *Recovery of motoneuron and locomotor function after spinal cord injury depends on constitutive activity in 5-HT2C receptors.* Nature medicine, 2010. **16**(6): p. 694-700.

36.   Saruhashi, Y., W. Young, and R. Perkins, *The recovery of 5-HT immunoreactivity in lumbosacral spinal cord and locomotor function after thoracic hemisection.* Exp Neurol, 1996. **139**(2): p. 203-13.

37.   Stichel, C. and H. Muller, *Experimental strategies to promote axonal regeneration after traumatic central nervous system injury.* Progress in Neurobiology, 1998. **56**: p. 119-148.

38.   Stichel, C.C., et al., *Inhibition of collagen IV deposition promotes regeneration of injured CNS axons.* Eur J Neurosci, 1999. **11**(2): p. 632-46.

39.   Stichel, C.C., et al., *Scar modulation in subacute and chronic CNS lesions: Effects on axonal regeneration.* Restor Neurol Neurosci, 1999. **15**(1): p. 1-15.

40.   Barritt, A.W., et al., *Chondroitinase ABC promotes sprouting of intact and injured spinal systems after spinal cord injury.* J Neurosci, 2006. **26**(42): p. 10856-67.

41.   Tester, N.J. and D.R. Howland, *Chondroitinase ABC improves basic and skilled locomotion in spinal cord injured cats.* Experimental neurology, 2008. **209**(2): p. 483-96.

42.   Sofroniew, M.V., *Molecular dissection of reactive astrogliosis and glial scar formation.* Trends Neurosci, 2009. **32**(12): p. 638-47.

43.   Sofroniew, M.V. and H.V. Vinters, *Astrocytes: biology and pathology.* Acta Neuropathol, 2010. **119**(1): p. 7-35.

44.   Davies, S.J., et al., *Robust regeneration of adult sensory axons in degenerating white matter of the adult rat spinal cord.* J Neurosci, 1999. **19**(14): p. 5810-22.

45.   Reier, P.J. and J.D. Houle, *The glial scar: its bearing on axonal elongation and transplantation approaches to CNS repair.* Adv Neurol, 1988. **47**: p. 87-138.

46.   Bahr, M., C. Przyrembel, and M. Bastmeyer, *Astrocytes from adult rat optic nerves are nonpermissive for regenerating retinal ganglion cell axons.* Exp Neurol, 1995. **131**(2): p. 211-20.

47.   Jones, L.L., et al., *NG2 is a major chondroitin sulfate proteoglycan produced after spinal cord injury and is expressed by macrophages and oligodendrocyte progenitors.* J Neurosci, 2002. **22**(7): p. 2792-803.

48. Eddleston, M. and L. Mucke, *Molecular profile of reactive astrocytes--implications for their role in neurologic disease.* Neuroscience, 1993. **54**(1): p. 15-36.

49. Fawcett, J.W. and R.A. Asher, *The glial scar and central nervous system repair.* Brain Res Bull, 1999. **49**(6): p. 377-91.

50. Davies, S.J., et al., *Regeneration of adult axons in white matter tracts of the central nervous system.* Nature, 1997. **390**(6661): p. 680-3.

51. Fouad, K. and A. Tse, *Adaptive changes in the injured spinal cord and their role in promoting functional recovery.* Neurological research, 2008. **30**(1): p. 17-27.

52. Raineteau, O. and M.E. Schwab, *Plasticity of motor systems after incomplete spinal cord injury.* Nature reviews. Neuroscience, 2001. **2**(4): p. 263-73.

53. Kaas, J.H., et al., *Cortical and subcortical plasticity in the brains of humans, primates, and rats after damage to sensory afferents in the dorsal columns of the spinal cord.* Experimental neurology, 2008. **209**(2): p. 407-16.

54. Fouad, K., et al., *Cervical sprouting of corticospinal fibers after thoracic spinal cord injury accompanies shifts in evoked motor responses.* Current biology : CB, 2001. **11**(22): p. 1766-70.

55. Barth, T.M. and B.B. Stanfield, *The recovery of forelimb-placing behavior in rats with neonatal unilateral cortical damage involves the remaining hemisphere.* J Neurosci, 1990. **10**(10): p. 3449-59.

56. Kuang, R.Z. and K. Kalil, *Specificity of corticospinal axon arbors sprouting into denervated contralateral spinal cord.* J Comp Neurol, 1990. **302**(3): p. 461-72.

57. Weidner, N., et al., *Spontaneous corticospinal axonal plasticity and functional recovery after adult central nervous system injury.* Proc Natl Acad Sci U S A, 2001. **98**(6): p. 3513-8.

58. Bareyre, F.M., et al., *The injured spinal cord spontaneously forms a new intraspinal circuit in adult rats.* Nature neuroscience, 2004. **7**(3): p. 269-77.

59. Beattie, M.S., M.G. Leedy, and J.C. Bresnahan, *Evidence for alterations of synaptic inputs to sacral spinal reflex circuits after spinal cord transection in the cat.* Experimental neurology, 1993. **123**(1): p. 35-50.

60. Llewellyn-Smith, I.J. and L.C. Weaver, *Changes in synaptic inputs to sympathetic preganglionic neurons after spinal cord injury.* J Comp Neurol, 2001. **435**(2): p. 226-40.

61. Apostolova, I., A. Irintchev, and M. Schachner, *Tenascin-R restricts posttraumatic remodeling of motoneuron innervation and functional recovery after spinal cord injury in adult mice.* J Neurosci, 2006. **26**(30): p. 7849-59.

62. Houk, J.C., J. Keifer, and A.G. Barto, *Distributed motor commands in the limb premotor network.* Trends in neurosciences, 1993. **16**(1): p. 27-33.

63. Cabalka, L.M., T.C. Ritchie, and J.D. Coulter, *Immunolocalization and quantitation of a novel nerve terminal protein in spinal cord development.* J Comp Neurol, 1990. **295**(1): p. 83-91.

64. Masliah, E., et al., *Reactive synaptogenesis assessed by synaptophysin immunoreactivity is associated with GAP-43 in the dentate gyrus of the adult rat.* Experimental neurology, 1991. **113**(2): p. 131-42.

65. Courtine, G., et al., *Recovery of supraspinal control of stepping via indirect propriospinal relay connections after spinal cord injury.* Nat Med, 2008. **14**(1): p. 69-74.

66. Kakulas, B.A., *A review of the neuropathology of human spinal cord injury with emphasis on special features.* J Spinal Cord Med, 1999. **22**(2): p. 119-24.

67.   Hagg, T., *Collateral sprouting as a target for improved function after spinal cord injury.* Journal of neurotrauma, 2006. **23**(3-4): p. 281-94.

68.   Burgard, E.C., M.O. Fraser, and K.B. Thor, *Serotonergic modulation of bladder afferent pathways.* Urology, 2003. **62**(4 Suppl 1): p. 10-5.

69.   Hains, B.C., et al., *Changes in serotonin, serotonin transporter expression and serotonin denervation supersensitivity: involvement in chronic central pain after spinal hemisection in the rat.* Experimental neurology, 2002. **175**(2): p. 347-62.

Chapter 5: Discussion

5.0 *Sox9* knockdown, a potential pro-regenerative treatment for SCI

The ultimate goal of post-SCI nervous system repair strategies is to reestablish the required neuronal connections for recovery of neurological function. Such connections may occur by way of retracted axons undergoing long-distance regeneration through the lesion site followed by proper synapse formation on downstream motor neurons. For this type of regeneration to occur, damaged axons would need not only to survive near the post-injury lesion epicenter, but would also need to extend through the inhibitory lesion site to the caudal spinal cord and make functional synapses on correct targets while choosing from millions of potentially incorrect targets. Although there have been no confirmed reports of such regeneration in humans, there is reason to believe pro-regenerative treatments for chronic SCI can be developed.

The initiation of walking is handled by the brain that sends a message down spinal cord axons to initiate walking [1]. This message needs to be received by a center in the lumbar spinal cord referred to as the central pattern generator (CPG) that initiates and coordinates the muscles required for proper walking motion [2]. The CPG region contains neural circuits that produce self-sustaining patterns of muscle activation independently of sensory input [3]. CPG activity has been observed in newborn children including anencephalic newborns suggesting that CPGs are likely to exist in adult humans as well [4, 5]. It is possible to exogenously stimulate the lumbar enlargement in the lower spinal cord and activate a walking motion [2, 6]. In humans with significantly impaired ability to move their legs, epidural spinal cord stimulation of lumbar segment 2 results in improved locomotion as well as recruitment of more muscle fibers and

improved gait post incomplete SCI [7-9]. A significant challenge then is to ensure the brain can send the required initiation of walking signal through the spinal cord to this central pattern generator machinery. While considering this, it is important to note that rats and cats can walk normally with less than 10% of their spinal cord intact at a lesion site [10], and spinal surgeons have suggested that this may be true for humans as well [11]. If only 10% of the axons in the spinal cord are necessary and sufficient to initiate locomotor activity, it is not unreasonable to think pro-regenerative treatments for chronic SCI could be developed. In this thesis I investigated one such potential pro-regenerative treatment, the effect of *Sox9* knockdown on hind limb function and neuroplasticity post-SCI in the mouse.

5.1 Obstacles to regeneration, activation of SOX9 post-SCI

Many animals found low on the evolutionary tree such as teleost fish, the salamander, and newt display profound axonal regeneration throughout life whereas more evolved animals such as mammals do not [12]. In fact, the CNS of mammals develops early in ontogeny, and once the critical period of plasticity closes in early adulthood mammals only display regeneration of their PNS [12, 13]. Thus, it may be more feasible to reprogram the local environment of an adult mammal to be more reminiscent of early life so as to activate pro-regenerative genetic programs native to the CNS as opposed to trying to activate regenerative programs native to the PNS or those found in more primitive animals. Unfortunately there are significant cellular and molecular differences between the adult-injured spinal cord and the embryonic spinal cord [14], not the least of which being that the development of the spinal cord takes place in an environment devoid of inflammation, and that the inflammatory response is dramatically up-

regulated post-SCI resulting in a complete change in the local microenvironment. One of the key outcomes of increased inflammation is a cytokine and chemokine storm that contains many molecules capable of activating the transcription factor SOX9. Pro-inflammatory cytokines including transforming growth factors β1 and 3, interleukin-6, and platelet-derived growth factor all work to activate SOX9 [15, 16]. Thus the inflammatory environment post-SCI provides ample opportunity for SOX9 activation, increased glial scarring, and amplified expression of anti-regenerative CSPGs. We hypothesized that inhibition of SOX9 would combat these environmental changes.

5.2 *Sox9* knockdown results in improved hind limb motor function post-SCI

Our contusion model of SCI results in paralysis of the hind limbs immediately post-injury. Injured mice recover a minimal degree of hind limb function over time. In our initial proof of principle study we knocked down SOX9 expression in a group of mice prior to SCI. These *Sox9* knockdown mice displayed remarkably quick recovery of hind limb function post contusion, scoring statistically higher than control mice expressing normal levels of SOX9 on the Basso Mouse Scale by 1 week post-SCI. This statistically significant improvement continued throughout the 14 weeks of our initial proof of principle study. The obvious caveat to this study was that the experiment occurred in mice which had already had *Sox9* knocked out prior to SCI. This type of experimental design works well to demonstrate the potential of a SOX9 inhibition based therapy, but does not speak toward the clinical feasibility of such a treatment. To address this we conducted a follow up study where our contusion injury occurred 1 week prior to tamoxifen administration. As it requires roughly 6 days of tamoxifen administration for

appreciable *Sox9* knockdown to occur this second study investigated the effect of *Sox9* knockdown almost two weeks post-SCI. In this model *Sox9* knockdown mice performed statistically better than control mice on the Basso Mouse Scale from 6 weeks post-SCI. This study demonstrates not only a clinical relevance and potential of an anti-SOX9 treatment for SCI, but suggests that the mechanism leading to recovery seems to be effective even after glial scar formation in *Sox9* knockdown mice. We next investigated the anatomic mechanism behind this functional improvement.

5.3 *Sox9* knockdown reduces anti-regenerative CSPG expression post-SCI

Following SCI damaged axons retreat a short distance before they attempt to grow back towards the injury site. Contact with CSPGs rich inhibitory extracellular matrix throughout the lesion site leads to growth cone collapse and axonal dystrophy, however these dystrophic axons are surprisingly dynamic and continually attempt to cross the lesion site [17]. Some invade the lesion area but do not exit on the distal side, but the great majority stop at the border of injury and appear to wait there even years post-SCI [18, 19]. If provided an avenue for growth through the inhibitory extracellular matrix, spinal axons do possess the ability to not only grow in the spinal cord but to form functional synapses on novel targets. David & Aguayo used peripheral nerves to bridge a spinal lesion and found spinal axons would grow into and through these nerves [20, 21]. These axons were found to innervate muscle at the distal end of the inserted peripheral nerve [22], and form functional glutamatergic synapses on their new targets [23, 24]. These studies emphasized how the inhibitory matrix in the local tissue microenvironment plays a key role in regulating axonal growth post-SCI [25]. It is also pertinent to note that lampreys, teleost

fish, and the urodele amphibians that can regenerate an injured spinal cord throughout their lifespan do not develop a CSPG rich glial scar [26]. *Sox9* knockdown mice consistently display a reduction in CSPG expression both at the mRNA and protein level at the lesion epicenter and in the lesion penumbra. Our prediction was that the reduction in inhibitory matrix in *Sox9* knockdown mice would provide a needed avenue for growth through the glial scar and allow dystrophic axons to finally traverse the lesion. *Sox9* knockdown mice also display reduced PNN matrix throughout the lesion site, and at the distant lumbar enlargement. Enzymatic digestion of PNNs by chondroitinase results in reactivation of plasticity [27, 28], and enhances spared fiber reactive sprouting and synapse plasticity [29], in injured adult animals. We therefore investigated whether the *Sox9* knockdown mice displayed increased neuroplasticity that could account for their improved hind limb motor function following SCI.

5.4 Investigating neuroplasticity post-SCI; axonal regeneration, reactive sprouting, and synapse plasticity

There are three main types neuroplasticity leading to recovery post injury; axonal regeneration, axonal sprouting, and synaptic plasticity. Axonal regeneration refers to the growth of an injured axon over long distances across, and extending beyond, the lesion site [30, 31]. Successful regeneration would thus require a damaged axonal fiber to grow several millimeters or more along its original trajectory toward its original synaptic partner [30]. Axonal sprouting applies to growth from either a damaged or intact axonal fiber over shorter distances [30, 31]. There is no precise definition as to the required length at which axonal growth transitions from sprouting to regeneration [30]. Reactive sprouting occurs in response to the injury when an uninjured fiber sprouts and makes new connections in an attempt to re-connect damaged tracts

[31]. Synaptic plasticity is the re-organization of existing synapses, or the creation of new synapses which would result in correct activation of the original targets which lost connectivity as a result of SCI [32].

Due to reduced glial scar CSPGs and lumbar enlargement PNNs, *Sox9* knockdown CNS axons damaged at the time of SCI should have a more hospitable growth environment through the lesion, and the lumbar enlargement environment should be more permissive to reactive sprouts finding motor neuron targets. We thus predicted that increased long range regeneration would occur through the glial scar, and that increased reactive sprouting and increased synaptic plasticity would occur in the ventral horn of the lumbar enlargement.

5.5 *Sox9* knockdown does not promote axonal sparing post-SCI

Prior to assessing axonal plasticity we must ensure that we rule out the possibility of axonal sparing in the *Sox9* knockdown mice so as to not confuse increased axonal sparing with increased axonal growth. We saw no evidence of descending axonal sparing in *Sox9* knockdown mice. We observed similar amounts of neurofilament traversing the lesion site in *Sox9* knockdown and control mice post-SCI. Our 1 week post-SCI fluorogold labeling study confirmed the absence of increased sparing in the *Sox9* knockdown mice by demonstrating equal numbers of retrogradely labeled neurons post-SCI in *Sox9* knockdown and control mice. Thus, *Sox9* knockdown mice do not display increased axonal sparing post-SCI. As the *Sox9* knockdown mice did not display evidence of axonal sparing, but did display reduced anti-regenerative extracellular matrix, we turned our attention to an investigation of axonal plasticity.

5.6 *Sox9* knockdown does not promote long range axonal regeneration post-SCI

Although we hypothesized that successful reduction in CSPG expression throughout the lesion environment would result in improved long range axonal regeneration, we saw no evidence of this. The lesion epicenter in injured *Sox9* knockdown mice 14 weeks post-SCI did not display increased neurofilament immunoreactivity arguing against significant regeneration across the lesion site. Secondly, our retrograde labeling study demonstrated a significant loss of labeled axonal tracts 1 week post-SCI, and that none of the injured tracts studied displayed long range axonal regeneration 8 weeks post-SCI.

The *Sox9* knockdown mice do however display improved locomotor function in comparison to controls post-SCI. Long range regeneration may not be occurring in our *Sox9* knockdown mice, but there are other potential mechanisms for regeneration known to occur endogenously post-SCI that are based on smaller neuronal changes that could potentially be improved by *Sox9* knockdown. Thus, we investigated short range reactive sprouting of spared axons as well as axonal synapse plasticity.

5.7 *Sox9* knockdown results in increased short range reactive sprouting and synapse plasticity post-SCI

An endogenously occurring compensatory and functional response to denervation post-SCI, termed reactive sprouting, has been studied for over 50 years. In 1958 McCouch et al. demonstrated that sensory afferents undergo sprouting in the spinal cord after SCI in both cats

and monkeys [33]. CSPGs restrict this reactive sprouting as chondroitinase injection into the brainstem post-cervical SCI resulted in digestion of PNNs and anatomical evidence of sprouting by spinal cord afferents in the cuneate nucleus [34]. Further studies on combined BDNF and chondroitinase treatment induced significant sprouting of undamaged retinal afferents into the denervated superior colliculus after a partial retinal lesion in the adult rat [29], and anti-synapsin antibody staining demonstrated increased synapse plasticity at the ends of the newly sprouted axons [29]. Beneficial alterations to the strength of existing neural connections may also occur post-SCI. An increased density of postsynaptic neurotransmitter receptors, increased excitatory neurotransmitter release, decreased inhibitory neurotransmitter release, or the removal of inhibition from excitatory input would all be beneficial to recovery from SCI [35, 36]. It is these types of short range plasticity we believe *Sox9* knockdown facilitates, and are in fact much easier to imagine occurring in a human than the aforementioned long range regeneration.

Recovery in the *Sox9* knockdown mice occurred quickly, within 1 week in the proof of principle model. It would thus seem unlikely that long range regeneration would be the mechanism behind such quick recovery, and therefore it was not surprising that we did not see evidence of long range regeneration in the *Sox9* knockdown mice. Short-range sprouting of spared axons onto deafferented targets due to the profound reduction in PNN burden in the *Sox9* knockdown mice would be expected to occur rapidly. This type of repair may also be less prone to mis-wiring of circuits as the most likely axons to form new synapses on a target will be those that are already innervating adjacent neurons in the same target field. We hypothesized that PNN reduction in the distant lumbar enlargement would allow for increased reactive sprouting and synapse plasticity in the ventral horn of the lumbar enlargement.

Our neurofilament immunostaining suggests the same amount of axonal matter crosses the lesion site in both controls and *Sox9* knockdown mice, however significantly more neurofilament was noted just rostral and just caudal to the injury penumbra. This suggests local sprouting of spared axons and potentially bridging connections created to circumvent the lesion site. Our BDA labeling data confirm these hypotheses as significantly increased BDA labeling was noted in the distant lumbar enlargement. As more BDA positive puncta were found in the lumbar enlargement, and PNNs in the lumbar enlargement were found to be down regulated in *Sox9* knockdown mice we were not surprised to see increased synaptic plasticity in these animals' lumbar enlargements. We noted increased synaptophysin expression in the ventral horn of *Sox9* knockdown mice lumbar enlargements. Synaptophysin was increased not only in total immunostaining, but also in the number of individual synaptophysin+ puncta, suggesting either increased synaptic release sites, increased vesicles per release site, or increased number of individual synapses. Each of these possibilities would indicate increased synaptic plasticity in these animals. Our data thus suggest that spared descending supraspinal and/or propriospinal axons sprout beneath the lesion and form synapses on ventral horn layer VIII and IX targets, probably motor neurons. We also investigated excitatory and inhibitory input in the ventral horn by assessing vesicular glutamate transporter VGLUT1 (excitatory neurotransmitter of the corticospinal tract) and vesicular GABA transporter VGAT (inhibitory neurotransmitter of the corticospinal tract) neurotransmitter expression [37]. We found increased VGLUT1 excitatory input and unchanged VGAT inhibitory input in *Sox9* knockdown mice in comparison to controls post-SCI.

The majority of human SCI are incomplete [19], and it has been suggested that these incomplete SCI may be more permissive to regeneration as cortical and subcortical structures, as

well as distant spinal cord circuitry, remain largely intact, while the damaged local spinal cord circuitry still remains partially connected by unlesioned axonal fibers [32]. Reactive sprouting as described herein would fit this model as a potential mechanism to stimulate beneficial neuroplasticity in the human post-SCI.

It is important to note that untargeted sprouting might lead to abnormally formed reflexes and detrimental sprouting of uninjured sensory afferents. However, the BDA labeling experiment described herein found no evidence for sprouting in the cervical enlargement away from the injury site. *Sox9* knockdown mice did not display altered numbers of BDA fibers identified in the cervical enlargement. We also investigated BDA labeling as well as VGLUT1 expression around ventral horn motor neurons in the cervical enlargement, but did not find increased BDA positive puncta or VGLUT1 staining. Thus, we suggest that the neuroplasticiy displayed by *Sox9* knockdown mice described herein requires not only a decrease in anti-regenerative CSPG and PNN expression, but also the loss of synaptic input and creation of free synaptic space. Given our T9 SCI model, it would be expected that motor neurons of the lumbar enlargement would display significant denervation whereas those in the cervical cord would likely be undamaged. This lack of denervation in the cervical enlargement may not have allowed the reactive sprouting or synaptic plasticity demonstrated in the lumbar enlargement. Thus, it is possible that the great majority of functional connections that are made due to increased plasticity after reduction of CSPG expression occur near the injury site. They likely serve as positive forms of neuroplasticity allowing restored functionality rather than detrimental improperly formed connections. Adding credence to the belief is data from chondroitinase treated animals suggesting that, despite the increased growth, sprouting and connectivity displayed following chondroitinase treatment there has been no reported evidence of increased sensitivity to pain in

these animals [38-40]. However, previous studies have demonstrated that, following a hemisection at T13 and a complete transection at T5, sensory afferents sprouted in the dorsal horn and are believed to have contributed to the development of mechanical allodynia and autonomic dysreflexia [41, 42]. Although we see no evidence of such changes through day to day handling and visual observation of *Sox9* knockdown mice, a thorough investigation of pain and sensory function is an important study that needs to be conducted. The presence of mechanical allodynia (a pain syndrome in which innocuous stimuli are perceived as painful) could be assessed by stimulating the backs of injured mice with a Semmes Weinstein monofilament at, and rostral, to the level of SCI. The number of avoidance responses (attempts to escape, vocalization, jumping, flinching and/or attempting to bite the filament) due to the stimulation over a number of trials would be recorded and compared between control and *Sox9* knockdown mice. Autonomic function could be assessed by measuring autonomic dysreflexia (episodic hypertension triggered by sensory stimulation below the level of the spinal lesion) in the mice. Autonomic dysreflexia is thought to be due to the loss of descending inhibitory inputs and the generation of abnormal reflexes in the injured spinal cord [43]. Autonomic dysreflexia can be assessed by measuring increases in blood pressure in response to colon distension [44], the extent of which correlates with the degree of SCI [45]. Blood pressure increases due to the stimulation over a number of trials could be recorded and compared between control and *Sox9* knockdown mice.

5.8 Combination therapies may be required to produce maximal beneficial effect post-SCI

The reduction in the inhibitory CSPG barrier which results from SOX9 inhibition creates an environment permissive to neuroplasticity, but optimal axonal regeneration may require exogenous administration of other growth factors, and perhaps inhibition of other anti-growth factors. Molecularly, the signaling pathways which regulate neurite and axonal growth are complex. Addition of neurotrophins [46], and inhibition of myelin-associated inhibitory molecules such as Nogo, myelin associated glycoprotein or myelin oligodendrocyte glycoprotein, may prove beneficial in promotion of reactive sprouting. For a review see Hagg et al. [47]. Recent studies suggest that combining pharmacological and activity based therapies may yield the best results post-SCI. Chondroitinase administration in concert with activity training resulted in improved rat forelimb function and locomotion recovery post-SCI [48]. Rats were assigned to one of two rehabilitation paradigms, the first receiving only skilled reaching training, and the second receiving only locomotion training. Chondroitinase treatment resulted in increased sprouting of corticospinal axons in both rehabilitation groups. Rats receiving the combination of chondroitinase and reaching training displayed increased reaching ability. Rats that received chondroitinase and locomotor training displayed improved locomotor abilities. Importantly, a major caveat appeared in this study. The rats that underwent the locomotor training scored worse on reaching tests than rats that received no specific activity training. The authors conclude that, although reducing CSPG burden opens a window of plasticity during which rehabilitation can promote recovery, only specifically trained skills appeared to improve, and other functions may in fact be negatively affected. Thus, combination therapies that emphasize a particular type of activity may eventually prove beneficial, but significant work needs to be undertaken to characterize the full effect of activity training on neuroplasticity and

recovery post-SCI. Regardless, we recognize that in the future combined therapies that target more than one axon-repelling molecule or make use of physical training may yield the best results post-SCI.

5.9 Complete *Sox9* knockdown is unlikely to be optimal for recovery post-SCI; beneficial role of astrocytes post-SCI

One of the benefits of a SOX9 targeted approach is the coinciding reduction in astrocyte activation (GFAP expression). It is however important to note that it is likely unwise to completely eliminate astrocyte activation and glial scarring post-SCI. Thus close regulation of SOX9 activity will be required in any future anti-SOX9 therapy devised for treatment of SCI.

Astrocytes do not only express molecules known to block axonal regeneration, but have also been shown to secrete extracellular matrix molecules conducive to axonal growth such as laminin, N-cadherin [49], neural cell adhesion molecule [50], and fibronectin [51]. Laminin and fibronectin have been shown to be good substrates for neurite extension in various in vitro models [52]. In neuron-astrocyte co-cultures, the ability of astrocytes to support neurite outgrowth depends upon astrocyte expression of laminin [53]. Neonatal rats regenerate transected connections and recover locomotor function after SCI [54], perhaps because glial tissue from lesioned neonates is rich in laminin and fibronectin and adequately supports neurite extension [55]. In general, astocyte cell lines that support neurite outgrowth produce an ECM rich in laminin and fibronectin while astrocyte lines producing ECM rich in CSPGs are nonpermissive to neurite extension [56]. *In vivo*, the regeneration of microtransplanted sensory neurons through inhibitory CNS myelin has been shown to be dependent on astrocyte-associated

fibronectin [51, 57, 58] and intrathecal administration of laminin promoted regeneration in a rat model of SCI [59]. Astrocytes provide trophic support including required metabolites, nutrients, and growth factors, brain-derived neurotrophic factor and neurotrophin 3, to the injury site which may help preserve spared neurons [60, 61]. Astrocytes play a key role in molecular scavenging and are thus important in regulating excessive levels of glutamate, potassium, and other ions post-SCI. In fact, astrocytes can directly protect neurons from nitric oxide toxicity through a glutathione-dependent mechanism [62]. The glial scar itself may be crucial for the survival of spared axons as it helps create a scaffold for the vasculature. Astrocytes and extracellular matrix components recruit endothelial cells and fibroblasts to the lesion site and induce the formation of new capillaries [63]. Recent studies suggest that complete removal of astrocytes results in significantly larger lesions, local tissue disruption, demyelination, and local neuron and oligodendrocyte death [64-67]. Thus, it is not optimal to completely inhibit astrocyte activation post-SCI.

5.10 Complete *Sox9* knockdown is unlikely to be optimal for recovery post-SCI; beneficial role of CSPGs post-SCI

It is also important to consider the possibility that CSPGs may be physiologically necessary to minimize inflammation and provide a scaffold for remodeling post-SCI [68, 69]. Thus, completely ablating CSPG presence at the site of injury may in fact exacerbate SCI rather than promote recovery. Michal Schwartz's group has shown that inhibition of CSPG expression immediately following SCI results in increased leukocyte infiltration, a dramatic change in microglia/macrophage organization at the lesion, decreased growth promoting insulin-like

growth factor 1 production, and increased pro-inflammatory tumor necrosis factor alpha production, by microglia/macrophages. This contributed to impaired functional motor recovery, and increased tissue loss. Inhibiting CSPG expression 2 days post-injury resulted in significantly improved outcome [70]. Their conclusion was that, in the acute stages of SCI, CSPGs appear to be beneficial for repair and subsequent recovery of function, but that chronic CSPG production does in fact inhibit axonal regeneration [70]. Thus, maximal recovery and improvements in quality of life for those with a nervous system injury may require careful modulation of CSPG levels over time.

5.11 Why do we our *Sox9* knockdown mice only display ~65% *Sox9* reduction?

Given that astrocytes and CSPGs undoubtedly make some beneficial contribution to wound healing and recovery post-SCI, it is likely wise to allow a moderate degree of astrocyte activation and CSPG production post-SCI. Thus, our conditional knockdown strategy may have significant advantages over a complete knockout model. As we only see ~65% *Sox9* knockdown following tamoxifen administration a significant amount of SOX9 remains to carry out its normal function. With this said, it is interesting to contemplate why we have not seen more complete *Sox9* knockdown post tamoxifen administration. In the animals used for these experiments *Sox9* knockdown occurs due to Cre recombinase acting on loxP sites flanking exons 2 and 3 of the *Sox9* gene. Researchers in the Brown laboratory have investigated Cre recombinase activity in ROSA-YFP mice in which tamoxifen administration activates YFP expression by removing a STOP codon in front of the *YFP* gene. As both the *Sox9* recombination, and the ROSA-YFP recombination, events are based on Cre activity, they should

occur equally under the same tamoxifen administration schedule. However, in practice these recombination events do not occur with equal frequencies. While we see ~65% *Sox9* knockdown, we see ~90% YFP expression as assessed by immunohistochemistry and flow cytometry. In a neural stem cell-specific *Sox9* knockdown mouse model that also contains the ROSA-YFP allele ~20% of the YFP positive cells found in the ependymal layer (those that were affected by tamoxifen and had a recombination event) still expressed SOX9 (unpublished observation in the Brown Laboratory). This indicates that when a cell receives tamoxifen the Cre enzyme is more efficient at excising the STOP codon in front of the ROSA-YFP than the *Sox9* loxP flanked locus. In the mouse the ROSA locus resides on chromosome 6, and the *Sox9* locus resides on chromosome 11 (Genbank). We hypothesize that the Cre recombinase has easier access to the loxP sites flanking the STOP codon preceding the ROSA locus than to the loxP sites flanking *Sox9*. Such a situation would account for the reduced Cre recombination efficiency seen in *Sox9* knockdown mice in comparison to the ROSA-YFP mice.

5.12 Alternative competing strategies, chondroitinase ABC

Chondroitinase is a very promising strategy currently being investigated for treatment of human SCI. There are however significant caveats with chondroitinase treatment which must be addressed. First, there are inherent dangers associated with treating humans with bacterial enzymes due to the potential for eliciting a damaging immune response. Chondroitinase also loses its enzymatic activity at body temperature [71] and must be repeatedly administered by intrathecal injection or infusion, an administration strategy that is not only invasive but also prone to inducing infection. Chondroitinase also does not diffuse far within the cord and thus

only acts on CSPGs at the local injection site. Finally, chondroitinase attempts to cleave carbohydrate stubs off of the large CSPG core proteins, but small inhibitory stubs remain as do the large core proteins themselves, thus axonal regeneration and functional recovery is limited [72, 73].

5.13 Alternative competing strategies, decorin

Another strategy being investigated is the use of decorin, a small proteoglycan with high affinity for binding transforming growth factor β. This interaction prevents transforming growth factor β from interacting with its receptors and thereby inhibits its signaling. As transforming growth factor β is a key inducer of CSPG biosynthesis, decorin has been used to inhibit glial scarring at the site of injury. Significant reduction of inhibitory proteoglycans neurocan, NG2, phosphacan and brevican was seen following pump infusion of recombinant decorin into acute stab injuries in the adult rat spinal cord [74]. Decorin also allowed transplanted adult sensory axons to grow across the acute stab injuries [74]. Decorin treatment resulted in an increase in plasminogen and plasmin protein expression, molecules which cleave CSPGs and activate neurotrophins and thereby seem a likely candidate for promoting axonal plasticity post-SCI. However, until now no reports have suggested that decorin confers a functional benefit post-SCI.

5.14 Alternative competing strategies, inhibition of *N-acetylgalactosaminyltransferase-1*

A third strategy aims to reduce CSPG expression while increasing heparan sulphate proteoglycan (HSPG) expression. HSPGs are structurally similar to CSPGs, but have been

shown to promote axonal growth. The assembly of HSPGs and CSPGs rely on the same initial enzymatic activity by XT-I and XT-II, thus by inhibiting XT-I and XT-II activity by way of *Sox9* knockdown we may be inhibiting not only CSPG synthesis but HSPG synthesis as well. An interesting competing strategy to the one presented herein made use of inhibitors to the downstream enzyme *N-acetylgalactosaminyltransferase-1* which will specifically block CSPG synthesis but allow HSPG synthesis. Following SCI, *N-acetylgalactosaminyltransferase-1* knockdown mice display significantly increased functional recovery [75]. As *Sox9* knockdown mice appear to display a reduced scarring phenotype in general, it is possible that *Sox9* knockdown mice may display reductions in *N-acetylgalactosaminyltransferase-1* post-SCI. As *Sox9* knockdown does not completely eliminate XT-I and XT-II expression it is still possible that HSPGs are being synthesized. Therefore, it would be interesting to investigate *N-acetylgalactosaminyltransferase-1* and HSPG expression in *Sox9* knockdown mice.

5.15 Alternative competing strategies, inhibition of *Nogo-A*

Nogo-A is a neurite growth inhibitory molecule expressed by differentiated oligodendrocytes and found in high concentrations in CNS myelin [76]. The interaction between myelin based *Nogo-A* and the *Nogo-66 receptor* on the axon surface restricts neuronal growth through negative modulation of growth cone actin dynamics [77]. Following SCI in the rat, inhibiting *Nogo-A* with an antibody resulted in improved CNS axon regeneration [78], and inhibiting the *Nogo-66 receptor* with a competitive antagonist resulted in significant corticospinal tract regeneration, and improved functional recovery [79]. Targeting *Nogo-A* has proven beneficial in primates as well as the recovery of manual dexterity and sprouting of

corticospinal tract axons were improved post-SCI in monkeys treated with anti-*Nogo-A* antibody [80, 81].

Early phase clinical trials targeting *Nogo-A* are currently in progress for the treatment of SCI. The pharmaceutical company Novartis AG created a humanized anti-*Nogo-A* antibody which has been used for a Phase I clinical trial. The antibody was delivered intrathecally via a pump for time periods ranging from 24 h to 4 weeks. The drug was tolerated well with no reported side effects. A Phase II study is currently underway and aims to test the efficacy of the anti-*Nogo-A* antibody treatment in paraplegic and quadraplegic SCI patients [82].   The authors admit that dosing will be particularly challenging as completely inhibiting *Nogo-A* activity is in fact detrimental as seen in *Nogo-A* KO mice which do not display increased neuronal growth or recovery due to a compensatory up-regulation of other inhibitory factors such as *ephrinA3*, *ephrinA4*, *Sema 4D* and *3F* and *plexin B2* [83].

5.16 Alternative competing strategies, inhibition of *Rho*

Another potential treatment for SCI focuses on the inhibition of the small GTPase *Rho*. Following SCI there is an up-regulation of *Rho* activity due to the release of growth inhibitory proteins and inflammatory cytokines whose receptors signal to *Rho* [84]. Activated *Rho* inhibits axonal growth by acting on the actin cytoskeleton and thus collapsing the neuronal growth cone [85, 86]. *Rho* normally cycles between the cytosolic compartment and the cell membrane where it interacts with its receptors. Clostridium botulinum exoenzyme C3 (C3) leads to sequestration of *Rho* in the cytosolic compartment, preventing its interaction with receptors on the cell

membrane [87]. Local application of C3 to the injury site in a mouse hemi-section model of SCI resulted in long-distance regeneration of cortico-spinal neurons, and improved functional recovery as assessed by locomotor scores and limb coordination [88, 89].

Cethrin is a cell-permeable derivative of Clostridium botulinum exoenzyme C3 (C3) which has been investigated in a Phase I/IIa clinical trial. In a group of thoracic or cervical SCI patients Cethrin was delivered as a gel topically to the spinal cord at the time of decompression surgery by placement on the dura mater of the spinal cord at the end of the surgical procedure, a delivery mechanism shown to be effective in rodents [84]. Motor recovery scores displayed a trend suggestive of neurological recovery [90]. However, the authors compared their motor outcomes to historical controls, thus a larger scale trial comparing Cethrin to placebo treatment will need to be conducted so as to properly assess efficacy. The authors also suggest increasing the Cethrin dosage for a follow up study. Of course, increased dosage would need to be closely monitored for safety.

5.17 Alternative explanations for functional recovery post *Sox9* knockdown

All of the above strategies hold promise as potential future treatments for SCI. However, all of the above strategies also focus on combating anti-regenerative molecules up-regulated following SCI. There are several alternative explanations for the recovery seen in *Sox9* knockdown mice that do not focus on combating anti-regenerative CSPG molecules. These alternative mechanisms have not as of yet been thoroughly studied, but may contribute to improved functional recovery post-SCI in *Sox9* knockdown mice. Such versatility and the

potential to promote regeneration and recovery through multiple avenues may be the biggest advantage of an anti-SOX9 based therapy for SCI.

A reduction in CSPG expression leading to an environment more permissive to axonal regeneration is not the only potential route by which functional recovery could be occurring in *Sox9* knockdown mice. Inflammation is one of the key causes of secondary SCI, and is at least partially the result of leukocyte recruitment by activated astrocytes, thus as a result of decreased astrocyte activation *Sox9* knockdown might lead to reduced inflammation at the site of injury. SOX9 may also play a role in neural precursor cell differentiation down a glial lineage, thus *Sox9* knockdown might lead to reduced gliogenesis and increased neurogenesis. It is probable that the functional recovery seen in *Sox9* knockdown mice is due to a combination of these potentially contributing mechanisms.

5.18 Alternative explanations for functional recovery post *Sox9* knockdown; the effect of *Sox9* knockdown on inflammation

The inflammatory response is one of the major contributors to secondary injury after SCI. Following SCI, endothelial cells up-regulate vascular cell adhesion molecules and reactive astrocytes express cytokine pro-inflammatory and chemoattractant molecules which attract inflammatory leukocytes to extravasation from the blood to the injured tissue. Leukocytes recruited to the site of injury may play a phagocytic role cleansing the area of bacterial infection; however, such activity can be detrimental to the spinal cord. The release of oxygen free radicals and reactive nitrogen species during phagocytosis can lead to neuronal damage through demyelination and scarring of spinal tissue [91, 92]. In addition, the release of pro-inflammatory

cytokines from activated phagocytes promotes further inflammation. Ongoing damage to neurons and the area surrounding the primary lesion contributes to increased lesion size and further neurological dysfunction [92, 93]. Inhibiting the inflammatory response by macrophage depletion following SCI decreases cavitation size and improves axonal regeneration [93, 94].

Sox9 knockdown mice display reduced GFAP expression. However, we have noted similar levels of glutamine synthetase positive cells in *Sox9* knockdown and control mice (unpublished observation). In the brain, glutamine synthetase is expressed predominantly in astrocytes. Thus *Sox9* knockdown mice display the same numbers of astrocytes as measured by glutamine synthetase, but a reduced astrocyte activation state as indicated by reduced GFAP expression. Reduced astrocyte activation may translate into reduced pro-inflammatory chemokine and cytokine production by astrocytes, and thus *Sox9* knockdown mice may display a muted inflammatory response to SCI.

A pilot study was conducted finding that in comparison to control mice *Sox9* knockdown mice demonstrate reduced macrophage numbers at the lesion site 14 weeks post-SCI (unpublished observation). This opens an interesting avenue for the future investigation of the effect of *Sox9* knockdown on the inflammatory response. As we have only investigated macrophage present at the lesion site at the end point of our study (14 weeks post-SCI), a complete time course of leukocyte infiltration must be conducted, as well as evaluation of reactive oxygen and nitrogen species, and determination of a complete pro-inflammatory cytokine profile at the lesion site post-SCI. If indeed anti-inflammatory, timing an anti-SOX9 based intervention would be critical as the inflammatory response operates in several phases, with an initial more destructive phase composed predominantly of neutrophil influx over the first 24 h post-SCI [95], followed by a pro-inflammatory phenotype macrophage influx between days

2 and 7 [95], and finally a more drawn out macrophage response over the second week of injury, thought to be beneficial for wound healing.

5.19 Alternative explanations for functional recovery post *Sox9* knockdown; the effect of *Sox9* knockdown on neural stem cells

Neural stem cells constantly self-renew and eventually differentiate into neurons, astrocytes, or oligodendrocytes [96]. Considerable research has been conducted investigating the transplantation of exogenous neural stem cells as a potential method to replace cells lost at the time of injury or to produce new neurons capable of building connections across the injury site and contributing to improved function [97]. One of the main findings of these works was that the majority of cells surviving the transplant differentiate into astrocytes and do not result in improved functional recovery [98, 99]. Perhaps the injury environment only supports glial neural stem cell differentiation. This is not surprising as neural stem cells differentiate into neurons when transplanted into hippocampal brain areas, but differentiate into astrocytes when transplanted into uninjured spinal cords [100]. It has been shown that by priming or genetically modifying neural stem cells it is possible to promote their neural differentiation once transplanted into the CNS [97, 101-104]. However, such strategies are not optimal clinical treatments as injecting highly proliferative cells may lead to tumor formation [105], and still rely on transplant allograft with a high likelihood of immunological rejection [106]. It may be safer and more efficient to alter the differentiation of the endogenous neural stem cells to produce more neurons and oligodendrocytes, and fewer astrocytes.

The developing CNS in *Sox9* knockdown mice displays altered neuronal/astroglial numbers. Twelve and one half days post conception *Sox9* deficient embryos displayed a 30% increase in motor neurons, and at 14.5 days post conception *Sox9* knockdown embryos displayed 25% as many oligodendrocyte progenitors as wild-type embryos and almost a complete lack of astrocytes in their spinal cords [107]. Together these findings suggest that during development SOX9 promotes neural stem cell differentiation down the astroglial lineage while inhibiting differentiation into new neurons. SOX9 is also required to maintain fully functioning neural stem cells as modulation of SOX9 expression results in altered neurosphere formation [108]. In both mouse and chick embryos neural stem cells appear just after up-regulation of SOX9 expression. Increasing SOX9 expression at an earlier time point before the normal appearance of neural stem cells resulted in early neurosphere formation and when *Sox9* was knocked out fewer neurospheres were found [108]. miRNA treatment has since confirmed the finding that inhibiting S*ox9* expression reduces neural stem cell function and proliferation as well as the formation of astroglia, while promoting neuronal differentiation [109].

In the *Sox9* knockdown mice described herein tamoxifen administration results in *Sox9* ablation in all cell types. Thus the improved locomotor recovery seen could be the result of reduced SOX9 expression in a variety of cell types, with astrocytes and neural stem cells known to be the two major cell types in the spinal cord that express SOX9 [110]. The improved functional recovery seen in these mice may not be due to just reduced CSPG expression leading to increased neuroplasticity of existing neurons, but perhaps due to changes in neural stem cell behavior as well. *Sox9* ablation in neural stem cells should generate new neurons and neuroblasts at the lesion site after spinal cord injury and may thus contribute to recovery.

Investigators in Dr. Brown's laboratory have knocked down *Sox9* specifically in neural stem cells and assessed hind limb functional recovery after a contusion SCI. Although the average BMS score for neural stem cell *Sox9* knockdown mice was 1.30, and only 0.65 for the control mice expressing wild type levels of SOX9, these scores were not significantly different. However, this does not mean that *Sox9* knockdown neural stem cells are not contributing any benefit leading to the functional recovery seen in the *Sox9* knockdown mice. Also, a mouse line expressing Cre recombinase only in astrocytes exists and could be bred to our $Sox9^{flox/flox}$;Cre mice. It would be interesting to know if the improvements in motor function described herein using a mouse line in which *Sox9* is knocked down throughout the CNS could be recapitulated by a combination of improvements seen in the neural stem cell *Sox9* knockdowns and astrocyte specific *Sox9* knockdowns.

5.20 Conclusion

Sox9 knockdown reduces the expression of anti-regenerative extracellular matrix genes, results in increased reactive sprouting and synaptic plasticity, and improves motor function in a mouse model of SCI. The data presented in this thesis demonstrate the potential anti-SOX9 strategies have for treatment of spinal cord injury, and the mechanism leading to anatomic CNS plasticity described herein suggests that anti-SOX9 strategies may in fact be beneficial for the treatment of other types of CNS neurotrauma.

5.21 References

1.   Duysens, J. and H.W. Van de Crommert, *Neural control of locomotion; The central pattern generator from cats to humans.* Gait & posture, 1998. **7**(2): p. 131-141.

2.   Dimitrijevic, M.R., Y. Gerasimenko, and M.M. Pinter, *Evidence for a spinal central pattern generator in humans.* Annals of the New York Academy of Sciences, 1998. **860**: p. 360-76.

3.   Jankowska, E., et al., *The effect of DOPA on the spinal cord. 5. Reciprocal organization of pathways transmitting excitatory action to alpha motoneurones of flexors and extensors.* Acta physiologica Scandinavica, 1967. **70**(3): p. 369-88.

4.   Yang, J.F., M.J. Stephens, and R. Vishram, *Infant stepping: a method to study the sensory control of human walking.* The Journal of physiology, 1998. **507 (Pt 3)**: p. 927-37.

5.   Forssberg, H.A., *Developmental Model of Human Locomotion*, ed. S. Grillner, et al.1986, London: Macmillan.

6.   Van de Crommert, H.W., T. Mulder, and J. Duysens, *Neural control of locomotion: sensory control of the central pattern generator and its relation to treadmill training.* Gait & posture, 1998. **7**(3): p. 251-263.

7.   Huang, H., et al., *Modulation effects of epidural spinal cord stimulation on muscle activities during walking.* IEEE transactions on neural systems and rehabilitation engineering : a publication of the IEEE Engineering in Medicine and Biology Society, 2006. **14**(1): p. 14-23.

8.   Carhart, M.R., et al., *Epidural spinal-cord stimulation facilitates recovery of functional walking following incomplete spinal-cord injury.* IEEE transactions on neural systems and rehabilitation engineering : a publication of the IEEE Engineering in Medicine and Biology Society, 2004. **12**(1): p. 32-42.

9.   Herman, R., et al., *Spinal cord stimulation facilitates functional walking in a chronic, incomplete spinal cord injured.* Spinal Cord, 2002. **40**(2): p. 65-8.

10.   Blight, A.R., *Cellular morphology of chronic spinal cord injury in the cat: analysis of myelinated axons by line-sampling.* Neuroscience, 1983. **10**(2): p. 521-43.

11.   Young, W., et al., *Somatosensory evoked potential changes in spinal injury and during intraoperative spinal manipulation.* The Journal of the American Paraplegia Society, 1982. **5**(4): p. 44-8.

12.   Lee-Liu, D., et al., *Spinal cord regeneration: lessons for mammals from non-mammalian vertebrates.* Genesis, 2013. **51**(8): p. 529-44.

13.   Avci, H.X., et al., *Thyroid hormone triggers the developmental loss of axonal regenerative capacity via thyroid hormone receptor alpha1 and kruppel-like factor 9 in Purkinje cells.* Proc Natl Acad Sci U S A, 2012. **109**(35): p. 14206-11.

14.   Gris, P., et al., *Differential gene expression profiles in embryonic, adult-injured and adult-uninjured rat spinal cords.* Molecular and cellular neurosciences, 2003. **24**(3): p. 555-67.

15.   Gris, P., et al., *Transcriptional regulation of scar gene expression in primary astrocytes.* Glia, 2007. **55**(11): p. 1145-55.

16.   Kawakami, Y., J. Rodriguez-Leon, and J.C. Izpisua Belmonte, *The role of TGFbetas and Sox9 during limb chondrogenesis.* Current opinion in cell biology, 2006. **18**(6): p. 723-9.

17. Tom, V.J., et al., *Studies on the development and behavior of the dystrophic growth cone, the hallmark of regeneration failure, in an in vitro model of the glial scar and after spinal cord injury*. J Neurosci, 2004. **24**(29): p. 6531-9.

18. Beattie, M.S., et al., *Endogenous repair after spinal cord contusion injuries in the rat*. Experimental neurology, 1997. **148**(2): p. 453-63.

19. Bunge, R.P., W.R. Puckett, and E.D. Hiester, *Observations on the pathology of several types of human spinal cord injury, with emphasis on the astrocyte response to penetrating injuries*. Adv Neurol, 1997. **72**: p. 305-15.

20. David, S. and A.J. Aguayo, *Axonal elongation into peripheral nervous system "bridges" after central nervous system injury in adult rats*. Science, 1981. **214**(4523): p. 931-3.

21. David, S. and A.J. Aguayo, *Axonal regeneration after crush injury of rat central nervous system fibres innervating peripheral nerve grafts*. Journal of neurocytology, 1985. **14**(1): p. 1-12.

22. Carlstedt, T., et al., *Restoration of hand function and so called "breathing arm" after intraspinal repair of C5-T1 brachial plexus avulsion injury. Case report*. Neurosurgical focus, 2004. **16**(5): p. E7.

23. Brunelli, G., et al., *Glutamatergic reinnervation through peripheral nerve graft dictates assembly of glutamatergic synapses at rat skeletal muscle*. Proc Natl Acad Sci U S A, 2005. **102**(24): p. 8752-7.

24. Pizzi, M., et al., *Glutamatergic innervation of rat skeletal muscle by supraspinal neurons: a new paradigm in spinal cord injury repair*. Current opinion in neurobiology, 2006. **16**(3): p. 323-8.

25. Aguayo, A.J., et al., *Degenerative and regenerative responses of injured neurons in the central nervous system of adult mammals*. Philosophical transactions of the Royal Society of London. Series B, Biological sciences, 1991. **331**(1261): p. 337-43.

26. Wujek, J.R. and P.J. Reier, *Astrocytic membrane morphology: differences between mammalian and amphibian astrocytes after axotomy*. J Comp Neurol, 1984. **222**(4): p. 607-19.

27. Corvetti, L. and F. Rossi, *Degradation of chondroitin sulfate proteoglycans induces sprouting of intact purkinje axons in the cerebellum of the adult rat*. J Neurosci, 2005. **25**(31): p. 7150-8.

28. Pizzorusso, T., et al., *Reactivation of ocular dominance plasticity in the adult visual cortex*. Science, 2002. **298**(5596): p. 1248-51.

29. Tropea, D., M. Caleo, and L. Maffei, *Synergistic effects of brain-derived neurotrophic factor and chondroitinase ABC on retinal fiber sprouting after denervation of the superior colliculus in adult rats*. J Neurosci, 2003. **23**(18): p. 7034-44.

30. Cafferty, W.B., A.W. McGee, and S.M. Strittmatter, *Axonal growth therapeutics: regeneration or sprouting or plasticity?* Trends in neurosciences, 2008. **31**(5): p. 215-20.

31. Tuszynski, M.H. and O. Steward, *Concepts and methods for the study of axonal regeneration in the CNS*. Neuron, 2012. **74**(5): p. 777-91.

32. Raineteau, O. and M.E. Schwab, *Plasticity of motor systems after incomplete spinal cord injury*. Nature reviews. Neuroscience, 2001. **2**(4): p. 263-73.

33. McCouch, G.P., et al., *Sprouting as a cause of spasticity*. Journal of neurophysiology, 1958. **21**(3): p. 205-16.

34.   Massey, J.M., et al., *Chondroitinase ABC digestion of the perineuronal net promotes functional collateral sprouting in the cuneate nucleus after cervical spinal cord injury.* J Neurosci, 2006. **26**(16): p. 4406-14.

35.   Chen, R., et al., *Mechanisms of cortical reorganization in lower-limb amputees.* J Neurosci, 1998. **18**(9): p. 3443-50.

36.   Jacobs, K.M. and J.P. Donoghue, *Reshaping the cortical motor map by unmasking latent intracortical connections.* Science, 1991. **251**(4996): p. 944-7.

37.   Du Beau, A., et al., *Neurotransmitter phenotypes of descending systems in the rat lumbar spinal cord.* Neuroscience, 2012. **227**: p. 67-79.

38.   Barritt, A.W., et al., *Chondroitinase ABC promotes sprouting of intact and injured spinal systems after spinal cord injury.* J Neurosci, 2006. **26**(42): p. 10856-67.

39.   Galtrey, C.M., et al., *Promoting plasticity in the spinal cord with chondroitinase improves functional recovery after peripheral nerve repair.* Brain : a journal of neurology, 2007. **130**(Pt 4): p. 926-39.

40.   Karimi-Abdolrezaee, S., et al., *Synergistic effects of transplanted adult neural stem/progenitor cells, chondroitinase, and growth factors promote functional repair and plasticity of the chronically injured spinal cord.* J Neurosci, 2010. **30**(5): p. 1657-76.

41.   Weaver, L.C., et al., *Autonomic dysreflexia and primary afferent sprouting after clip-compression injury of the rat spinal cord.* Journal of neurotrauma, 2001. **18**(10): p. 1107-19.

42.   Finnerup, N.B. and T.S. Jensen, *Spinal cord injury pain--mechanisms and treatment.* European journal of neurology : the official journal of the European Federation of Neurological Societies, 2004. **11**(2): p. 73-82.

43.   Brown, A. and J.E. Jacob, *Genetic approaches to autonomic dysreflexia.* Prog Brain Res, 2006. **152**: p. 299-313.

44.   Jacob, J.E., et al., *Autonomic dysreflexia in a mouse model of spinal cord injury.* Neuroscience, 2001. **108**(4): p. 687-93.

45.   Jacob, J.E., et al., *Autonomic dysreflexia after spinal cord transection or compression in 129Sv, C57BL, and Wallerian degeneration slow mutant mice.* Experimental neurology, 2003. **183**(1): p. 136-46.

46.   David, S. and S. Lacroix, *Molecular approaches to spinal cord repair.* Annu Rev Neurosci, 2003. **26**: p. 411-40.

47.   Hagg, T., *Collateral sprouting as a target for improved function after spinal cord injury.* Journal of neurotrauma, 2006. **23**(3-4): p. 281-94.

48.   Garcia-Alias, G., et al., *Chondroitinase ABC treatment opens a window of opportunity for task-specific rehabilitation.* Nat Neurosci, 2009. **12**(9): p. 1145-51.

49.   Tomaselli, K.J., et al., *N-cadherin and integrins: two receptor systems that mediate neuronal process outgrowth on astrocyte surfaces.* Neuron, 1988. **1**(1): p. 33-43.

50.   Neugebauer, K.M., et al., *N-cadherin, NCAM, and integrins promote retinal neurite outgrowth on astrocytes in vitro.* J Cell Biol, 1988. **107**(3): p. 1177-87.

51.   Tom, V.J., et al., *Astrocyte-associated fibronectin is critical for axonal regeneration in adult white matter.* J Neurosci, 2004. **24**(42): p. 9282-90.

52.   Rogers, S.L., et al., *Neurite extension by peripheral and central nervous system neurons in response to substratum-bound fibronectin and laminin.* Dev Biol, 1983. **98**(1): p. 212-20.

53. Costa, S., et al., *Astroglial permissivity for neuritic outgrowth in neuron-astrocyte cocultures depends on regulation of laminin bioavailability.* Glia, 2002. **37**(2): p. 105-13.

54. Wakabayashi, Y., et al., *Functional recovery and regeneration of descending tracts in rats after spinal cord transection in infancy.* Spine, 2001. **26**(11): p. 1215-22.

55. McKeon, R.J., et al., *Reduction of neurite outgrowth in a model of glial scarring following CNS injury is correlated with the expression of inhibitory molecules on reactive astrocytes.* J Neurosci, 1991. **11**(11): p. 3398-411.

56. Fok-Seang, J., et al., *An analysis of astrocytic cell lines with different abilities to promote axon growth.* Brain Res, 1995. **689**(2): p. 207-23.

57. Davies, S.J., et al., *Robust regeneration of adult sensory axons in degenerating white matter of the adult rat spinal cord.* J Neurosci, 1999. **19**(14): p. 5810-22.

58. Davies, S.J., et al., *Regeneration of adult axons in white matter tracts of the central nervous system.* Nature, 1997. **390**(6661): p. 680-3.

59. Wiksten, M., et al., *Regeneration of adult rat spinal cord is promoted by the soluble KDI domain of gamma1 laminin.* J Neurosci Res, 2004. **78**(3): p. 403-10.

60. White, R.E., F.Q. Yin, and L.B. Jakeman, *TGF-alpha increases astrocyte invasion and promotes axonal growth into the lesion following spinal cord injury in mice.* Exp Neurol, 2008. **214**(1): p. 10-24.

61. Wu, V.W., N. Nishiyama, and J.P. Schwartz, *A culture model of reactive astrocytes: increased nerve growth factor synthesis and reexpression of cytokine responsiveness.* J Neurochem, 1998. **71**(2): p. 749-56.

62. Chen, Y., et al., *Astrocytes protect neurons from nitric oxide toxicity by a glutathione-dependent mechanism.* J Neurochem, 2001. **77**(6): p. 1601-10.

63. Zonta, M., et al., *Neuron-to-astrocyte signaling is central to the dynamic control of brain microcirculation.* Nature neuroscience, 2003. **6**(1): p. 43-50.

64. Sofroniew, M.V., *Molecular dissection of reactive astrogliosis and glial scar formation.* Trends Neurosci, 2009. **32**(12): p. 638-47.

65. Bush, T.G., et al., *Leukocyte infiltration, neuronal degeneration, and neurite outgrowth after ablation of scar-forming, reactive astrocytes in adult transgenic mice.* Neuron, 1999. **23**(2): p. 297-308.

66. Faulkner, J.R., et al., *Reactive astrocytes protect tissue and preserve function after spinal cord injury.* J Neurosci, 2004. **24**(9): p. 2143-55.

67. Sofroniew, M.V. and H.V. Vinters, *Astrocytes: biology and pathology.* Acta Neuropathol, 2010. **119**(1): p. 7-35.

68. Rolls, A., R. Shechter, and M. Schwartz, *The bright side of the glial scar in CNS repair.* Nat Rev Neurosci, 2009. **10**(3): p. 235-41.

69. Okada, S., et al., *Conditional ablation of Stat3 or Socs3 discloses a dual role for reactive astrocytes after spinal cord injury.* Nature medicine, 2006. **12**(7): p. 829-34.

70. Rolls, A., et al., *Two faces of chondroitin sulfate proteoglycan in spinal cord repair: a role in microglia/macrophage activation.* PLoS medicine, 2008. **5**(8): p. e171.

71. Tester, N.J. and D.R. Howland, *Chondroitinase ABC improves basic and skilled locomotion in spinal cord injured cats.* Experimental neurology, 2008. **209**(2): p. 483-96.

72. Bradbury, E.J., et al., *Chondroitinase ABC promotes functional recovery after spinal cord injury.* Nature, 2002. **416**(6881): p. 636-40.

73. Lemons, M.L., et al., *Intact aggrecan and chondroitin sulfate-depleted aggrecan core glycoprotein inhibit axon growth in the adult rat spinal cord.* Exp Neurol, 2003. **184**(2): p. 981-90.

74. Davies, J.E., et al., *Decorin suppresses neurocan, brevican, phosphacan and NG2 expression and promotes axon growth across adult rat spinal cord injuries.* Eur J Neurosci, 2004. **19**(5): p. 1226-42.

75. Takeuchi, K., et al., *Chondroitin sulphate N-acetylgalactosaminyl-transferase-1 inhibits recovery from neural injury.* Nature communications, 2013. **4**: p. 2740.

76. Wang, X., et al., *Localization of Nogo-A and Nogo-66 receptor proteins at sites of axon-myelin and synaptic contact.* J Neurosci, 2002. **22**(13): p. 5505-15.

77. Montani, L., et al., *Neuronal Nogo-A modulates growth cone motility via Rho-GTP/LIMK1/cofilin in the unlesioned adult nervous system.* J Biol Chem, 2009. **284**(16): p. 10793-807.

78. Schnell, L. and M.E. Schwab, *Axonal regeneration in the rat spinal cord produced by an antibody against myelin-associated neurite growth inhibitors.* Nature, 1990. **343**(6255): p. 269-72.

79. GrandPre, T., S. Li, and S.M. Strittmatter, *Nogo-66 receptor antagonist peptide promotes axonal regeneration.* Nature, 2002. **417**(6888): p. 547-51.

80. Freund, P., et al., *Nogo-A-specific antibody treatment enhances sprouting and functional recovery after cervical lesion in adult primates.* Nature medicine, 2006. **12**(7): p. 790-2.

81. Freund, P., et al., *Anti-Nogo-A antibody treatment enhances sprouting of corticospinal axons rostral to a unilateral cervical spinal cord lesion in adult macaque monkey.* J Comp Neurol, 2007. **502**(4): p. 644-59.

82. Zorner, B. and M.E. Schwab, *Anti-Nogo on the go: from animal models to a clinical trial.* Annals of the New York Academy of Sciences, 2010. **1198 Suppl 1**: p. E22-34.

83. Kempf, A., et al., *Upregulation of axon guidance molecules in the adult central nervous system of Nogo-A knockdown mice restricts neuronal growth and regeneration.* Eur J Neurosci, 2013. **38**(11): p. 3567-79.

84. Dubreuil, C.I., M.J. Winton, and L. McKerracher, *Rho activation patterns after spinal cord injury and the role of activated Rho in apoptosis in the central nervous system.* The Journal of cell biology, 2003. **162**(2): p. 233-43.

85. Hall, A. and G. Lalli, *Rho and Ras GTPases in axon growth, guidance, and branching.* Cold Spring Harbor perspectives in biology, 2010. **2**(2): p. a001818.

86. Auer, M., B. Hausott, and L. Klimaschewski, *Rho GTPases as regulators of morphological neuroplasticity.* Annals of anatomy = Anatomischer Anzeiger : official organ of the Anatomische Gesellschaft, 2011. **193**(4): p. 259-66.

87. Genth, H., et al., *Entrapment of Rho ADP-ribosylated by Clostridium botulinum C3 exoenzyme in the Rho-guanine nucleotide dissociation inhibitor-1 complex.* J Biol Chem, 2003. **278**(31): p. 28523-7.

88. Ellezam, B., et al., *Inactivation of intracellular Rho to stimulate axon growth and regeneration.* Prog Brain Res, 2002. **137**: p. 371-80.

89. Lord-Fontaine, S., et al., *Local inhibition of Rho signaling by cell-permeable recombinant protein BA-210 prevents secondary damage and promotes functional recovery following acute spinal cord injury.* Journal of neurotrauma, 2008. **25**(11): p. 1309-22.

90.   McKerracher, L. and K.D. Anderson, *Analysis of recruitment and outcomes in the phase I/IIa Cethrin clinical trial for acute spinal cord injury.* Journal of neurotrauma, 2013. **30**(21): p. 1795-804.

91.   Taoka, Y. and K. Okajima, *Spinal cord injury in the rat.* Progress in neurobiology, 1998. **56**(3): p. 341-58.

92.   Gris, D., et al., *Transient blockade of the CD11d/CD18 integrin reduces secondary damage after spinal cord injury, improving sensory, autonomic, and motor function.* J Neurosci, 2004. **24**(16): p. 4043-51.

93.   Popovich, P.G., et al., *Depletion of hematogenous macrophages promotes partial hindlimb recovery and neuroanatomical repair after experimental spinal cord injury.* Experimental neurology, 1999. **158**(2): p. 351-65.

94.   Popovich, P.G., et al., *Hematogenous macrophages express CD8 and distribute to regions of lesion cavitation after spinal cord injury.* Experimental neurology, 2003. **182**(2): p. 275-87.

95.   Blight, A.R., *Macrophages and inflammatory damage in spinal cord injury.* Journal of neurotrauma, 1992. **9 Suppl 1**: p. S83-91.

96.   Johansson, C.B., et al., *Identification of a neural stem cell in the adult mammalian central nervous system.* Cell, 1999. **96**(1): p. 25-34.

97.   Li, J. and G. Lepski, *Cell transplantation for spinal cord injury: a systematic review.* BioMed research international, 2013. **2013**: p. 786475.

98.   Cao, Q.L., et al., *Pluripotent stem cells engrafted into the normal or lesioned adult rat spinal cord are restricted to a glial lineage.* Experimental neurology, 2001. **167**(1): p. 48-58.

99.   Webber, D.J., et al., *Transplanted neural progenitor cells survive and differentiate but achieve limited functional recovery in the lesioned adult rat spinal cord.* Regenerative medicine, 2007. **2**(6): p. 929-45.

100.   Shihabuddin, L.S., et al., *Adult spinal cord stem cells generate neurons after transplantation in the adult dentate gyrus.* J Neurosci, 2000. **20**(23): p. 8727-35.

101.   Tarasenko, Y.I., et al., *Human fetal neural stem cells grafted into contusion-injured rat spinal cords improve behavior.* Journal of neuroscience research, 2007. **85**(1): p. 47-57.

102.   Harper, J.M., et al., *Axonal growth of embryonic stem cell-derived motoneurons in vitro and in motoneuron-injured adult rats.* Proceedings of the National Academy of Sciences of the United States of America, 2004. **101**(18): p. 7123-8.

103.   Hwang, D.H., et al., *Transplantation of human neural stem cells transduced with Olig2 transcription factor improves locomotor recovery and enhances myelination in the white matter of rat spinal cord following contusive injury.* BMC neuroscience, 2009. **10**: p. 117.

104.   Bregman, B.S., et al., *Transplants and neurotrophic factors increase regeneration and recovery of function after spinal cord injury.* Progress in brain research, 2002. **137**: p. 257-73.

105.   Gordeeva, O.F., *Pluripotent cells in embryogenesis and in teratoma formation.* Journal of stem cells, 2011. **6**(1): p. 51-63.

106.   Preynat-Seauve, O., et al., *Neural progenitors derived from human embryonic stem cells are targeted by allogeneic T and natural killer cells.* Journal of cellular and molecular medicine, 2009. **13**(9B): p. 3556-69.

107.   Stolt, C.C., et al., *The Sox9 transcription factor determines glial fate choice in the developing spinal cord.* Genes Dev, 2003. **17**(13): p. 1677-89.

108. Scott, C.E., et al., *SOX9 induces and maintains neural stem cells.* Nature neuroscience, 2010. **13**(10): p. 1181-9.
109. Cheng, L.C., et al., *miR-124 regulates adult neurogenesis in the subventricular zone stem cell niche.* Nature neuroscience, 2009. **12**(4): p. 399-408.
110. Meletis, K., et al., *Spinal cord injury reveals multilineage differentiation of ependymal cells.* PLoS biology, 2008. **6**(7): p. e182.

Ethics Approval for Animal Usage on Protocol 2007-009-02

Western🛡️

2007-009-02::6:

AUP Number: 2007-009-02
AUP Title: Molecular and Cellular Studies of Spinal Cord Injury in Mice and Rats

Yearly Renewal Date: 06/01/2013

The YEARLY RENEWAL to Animal Use Protocol (AUP) 2007-009-02 has been approved, and will be approved for one year following the above review date.

1. This AUP number must be indicated when ordering animals for this project.
2. Animals for other projects may not be ordered under this AUP number.
3. Purchases of animals other than through this system must be cleared through the ACVS office.
   Health certificates will be required.

REQUIREMENTS/COMMENTS
Please ensure that individual(s) performing procedures on live animals, as described in this protocol, are familiar with the contents of this document.

The holder of this Animal Use Protocol is responsible to ensure that all associated safety components (biosafety, radiation safety, general laboratory safety) comply with institutional safety standards and have received all necessary approvals. Please consult directly with your institutional safety officers.

Submitted by: Mollard, Maureen
on behalf of the Animal Use Subcommittee

JOHN WILEY AND SONS LICENSE
TERMS AND CONDITIONS

Apr 10, 2014

This is a License Agreement between William M McKillop ("You") and John Wiley and Sons ("John Wiley and Sons") provided by Copyright Clearance Center ("CCC"). The license consists of your order details, the terms and conditions provided by John Wiley and Sons, and the payment terms and conditions.

All payments must be made in full to CCC. For payment instructions, please see information listed at the bottom of this form.

License Number	3365480633660
License date	Apr 10, 2014
Licensed content publisher	John Wiley and Sons
Licensed content publication	GLIA
Licensed content title	Conditional Sox9 ablation reduces chondroitin sulfate proteoglycan levels and improves motor function following spinal cord injury
Licensed copyright line	Copyright © 2012 Wiley Periodicals, Inc.
Licensed content author	William M. McKillop,Magdalena Dragan,Andreas Schedl,Arthur Brown
Licensed content date	Oct 1, 2012
Start page	164
End page	177
Type of use	Dissertation/Thesis
Requestor type	Author of this Wiley article
Format	Print and electronic
Portion	Full article
Will you be translating?	No
Title of your thesis / dissertation	Conditional Sox9 Ablation Reduces CSPG Expression, Increases Neuroplasticity, and Improves Motor Function Following Spinal Cord Injury
Expected completion date	Jun 2014
Expected size (number of pages)	200
Total	0.00 USD

Terms and Conditions

Terms and Conditions are not available at this time.

If you would like to pay for this license now, please remit this license along with your payment made payable to "COPYRIGHT CLEARANCE CENTER" otherwise you will be invoiced within 48 hours of the license date. Payment should be in the form of a check or money order referencing your account number and this invoice number RLNK501275270.
Once you receive your invoice for this order, you may pay your invoice by credit card. Please follow instructions provided at that time.

Make Payment To:
Copyright Clearance Center
Dept 001
P.O. Box 843006
Boston, MA 02284-3006

For suggestions or comments regarding this order, contact RightsLink Customer Support: customercare@copyright.com or +1-877-622-5543 (toll free in the US) or +1-978-646-2777.

Gratis licenses (referencing $0 in the Total field) are free. Please retain this printable license for your reference. No payment is required.

Curriculum Vitae

Name: William Montgomery McKillop

Place of Birth: Winnipeg, Manitoba, Canada

Date of Birth: April 26, 1983

Post-Secondary Education: The University of Western Ontario

London, Ontario, Canada

Ph.D. Anatomy and Cell Biology

2009-2014

The University of Western Ontario

London, Ontario, Canada

M. Sc. Microbiology and Immunology

2005-2008

The University of Western Ontario

London, Ontario, Canada

B. MSc. Biochemistry (Honors)

2001-2005

Honors and Awards: 1st Place: Anatomy and Cell Biology Research Day

PhD Competition

Conference Poster Presentation

Awarded 2013

2nd Place: CIHR National Poster Competition

National Conference Poster Presentation

Awarded 2013

1st Place: London Health Research Day

Conference Oral Presentation

Awarded 2013

Ontario Graduate Scholarship

Awarded 2012

Queen Elizabeth II Scholarship in Science and Technology

Declined 2012

1st Place: Anatomy and Cell Biology Research Day

PhD Competition

Conference Oral Presentation

Awarded 2012

1st Place: Taylor Prize Stem Cell and Rehabilitative Medicine

Conference Poster Presentation

Awarded 2011

1st Place: Anatomy and Cell Biology Research Day

Neuroscience Competition

Conference Poster Presentation

Awarded 2011

Schulich School of Medicine and Dentistry Graduate Scholarship

Awarded 2009-2013

NSERC Post Graduate Scholarship CGS D3

Awarded 2009

The cover article for the Journal of Leukocyte Biology

October 2009. J. Leukoc. Biol. 2009 Oct;86(4)

2nd Place: Canadian Society for Life Science Research

National Conference Poster Presentation

Awarded 2007

Schulich School of Medicine and Dentistry Graduate Scholarship

Awarded 2007

University of Western Ontario Graduate Research Scholarship

Awarded 2005-2007

1st Place: CIHR Infection and Immunity Research Day

Conference Poster Presentation

Awarded 2006

University of Western Ontario Laurene Patterson Estate
Scholarship

Awarded 2003

University of Western Ontario Scholar of Excellence Scholarship

Awarded 2001

Related Work Experience: Graduate Teaching Assistant

Anatomy and Cell Biology 9531 "Neuroscience for

Rehabilitation Sciences" Laboratory Instructor

The University of Western Ontario

2010 -2013

Research Technician

Laboratory of Dr. Arthur Brown

The University of Western Ontario

2009

Research Technician

Laboratory of Dr. Greg Dekaban

The University of Western Ontario

2009

Graduate Teaching Assistant

Microbiology and Immunology 220a "Biology of Prokaryotes"
Laboratory Instructor

The University of Western Ontario

2006

Research Technician

Laboratory of Dr. Greg Dekaban

The University of Western Ontario

2005

Laboratory Assistant

Laboratory of Dr. Susan Koval

The University of Western Ontario

2004

Founding Vice-President

Biology Undergraduate Society of the University of Western Ontario

2003

Invertebrate Field and Laboratory Assistant

Laboratories of Dr. Jack DuBois, Dr. Brian McKillop, and Dr. Graham Young

The Manitoba Museum of Man and Nature

1991-2001

Publications:

Papers: McKillop, W.M., Dragan, M., Schedl, A., Brown, A. 2013. Conditional Sox9 ablation reduces chondroitin sulfate proteoglycans levels and improves motor function following spinal cord injury. Glia 61:164-177.

McKillop, W.M., Barrett, J.W., Pasternak, S.H., Chan, B.M.C., Dekaban, G.A. 2009. The Extracellular Domain of CD11d Regulates

its Cell Surface Expression. The Journal of Leukocyte Biology 86(4):851-862.

Barrett, J.W., Werden, S.J., Wang, F., McKillop, W.M., Jimenez, J., Villeneuve, D., Dekaban, G.A., McFadden, G. 2009. Myxoma virus M130R is a novel virulence factor required for lethal myxomatosis in rabbits. Virus Research 144(1-2):258-265.

McKillop, W.B. and W.M. McKillop. Distribution records of the Threespine Stickleback, *Gasterosteus aculeatus* Linnaeus (Pisces:Gasterosteidae), in Manitoba. 1997. Canadian Field-Naturalist 111(4): 662-663.

McKillop,W.B., W.M. McKillop and A.C. Conroy. Observations on the life history and distribution of the Showy Pond Snail, *Bulimnea megasoma* (Say) (Gastropoda:Pulmonata) in southeastern Manitoba. 1993. Canadian Field-Naturalist 107(2): 192-195.

Abstracts:

McKillop, W.M., Pniak, A, Schedl, A, and A. Brown. Conditional SOX9 ablation reduces chondroitin sulfate proteoglycan expression and improves motor function following spinal cord injury. Society of Neuroscience Meeting Planner 2011: 462.23.

McKillop, W.M. and G.A. Dekaban. Characterization of CD11d Leukocyte Integrin Surface Expression. 2007. McGill Journal of Medicine 10(2): 169.

Presentations:

Poster:

McKillop, W.M. SOX9 knockdown reduced peri-neuronal net expression and increases neuroplasticity post spinal cord injury. Anatomy and Cell Biology Research Day, Poster Presentation. University of Western Ontario. 2013.

McKillop, W.M. Delayed SOX9 knockdown improves motor function following spinal cord injury. CIHR National Poster Competition, Winnipeg, Manitoba. 2013.

McKillop, W.M. Conditional SOX9 ablation reduces Chondroitin Sulfate Proteoglyan expression and improves motor function following spinal cord injury. London Health Research Day. 2012.

McKillop, W.M. Conditional SOX9 ablation reduces Chondroitin Sulfate Proteoglyan expression and improves motor function following spinal cord injury. Society for Neuroscience, Neuroscience 2011 Conference. 2011.

McKillop, W.M. Conditional SOX9 ablation reduces Chondroitin Sulfate Proteoglyan expression and improves motor function following spinal cord injury. Taylor Prize Stem Cell and Rehabilitative Medicine Day, Robarts Research Institute. 2011.

McKillop, W.M. Conditional SOX9 ablation reduces Chondroitin Sulfate Proteoglyan expression and improves motor function following spinal cord injury. Anatomy and Cell Biology Research Day, Poster Presentation. University of Western Ontario. 2011.

McKillop, W.M. Characterization of CD11d Leukocyte Integrin Surface Expression. 5th Annual Robarts Research Institute Research Day, Poster Presentation. University of Western Ontario. 2007.

McKillop, W.M. Characterization of CD11d Leukocyte Integrin Surface Expression. Infection and Immunity Research Day, Poster Presentation. University of Western Ontario. 2007.

McKillop, W.M. Characterization of CD11d Leukocyte Integrin Surface Expression. Canadian Society for Life Science Research 2nd Annual Conference, Poster Presentation. McGill University. 2007.

McKillop, W.M. Examination of CD11d Integrin Surface Expression. Margaret Moffit Research Day, Poster Presentation. University of Western Ontario. 2007.

McKillop, W.M. Examination of CD11d Integrin Surface Expression. 4th Annual Robarts Research Institute Research Day, Poster Presentation. Robarts Research Institute. 2007.

McKillop, W.M. Examination of CD11d Integrin Surface Expression. Infection and Immunity Research Day. Poster Presentation, University of Western Ontario. 2006.

Oral: McKillop, W.M. SOX9 knockdown reduces chondroitin sulfate proteoglycan expression, increases neuroplasticity, and improves motor function in a rodent model of spinal cord injury. Oral Presentation given to the Department of Anatomy and Cell Biology, U.W.O. 2014.

McKillop, W.M. SOX9 knockdown promotes reactive sprouting and synaptic plasticity post spinal cord injury. Oral Presentation given to the Molecular Medicince Research Group at the Robarts Research Institute. 2014.

McKillop, W.M. SOX9 knockdown promotes neuronal-plasticity and recovery of motor function post spinal cord injury. Oral Presentation given to the Molecular Medicine Research Group at the Robarts Research Institute. 2013.

McKillop, W.M. Delayed SOX9 knockdown improves motor function following spinal cord injury. London Health Research Day. 2013.

McKillop, W.M. Delayed SOX9 knockdown improves motor function following spinal cord injury. Oral Presentation given at the Department of Anatomy and Cell Biology Research Day, U.W.O. 2012.

McKillop, W. M. SOX9 knockdown improves functional recovery in a rodent model of spinal cord injury. Oral Presentation given to the Molecular Brain Research Group at the Robarts Research Institute. 2011.

McKillop, W. M. Putting the S.C.I. in SCIence: the role of SOX9 in spinal cord injury. Oral Presentation given at the Department of Anatomy and Cell Biology Recruitment Weekend, U.W.O. 2011.

McKillop, W. M. SOX9 knockdown reduces glial scarring and improves functional recovery in a rodent model of spinal cord injury. Oral Presentation given at the Department of Anatomy and Cell Biology Research Day, U.W.O. 2010.

McKillop, W. M. Putting the S.C.I. in SCIence: the role of SOX9 in spinal cord injury. Oral Presentation given at the Department of Anatomy and Cell Biology Recruitment Weekend, U.W.O. 2010.

McKillop, W. M. Intracellular Localization of the CD11d Integrin Alpha Chain. Oral Presentation given to the Biotherapeutics Research Group, Robarts Research Institute. 2008.

McKillop, W. M. Is There a Role for Casein Kinase 2 in CD11d Leukocyte Integrin Surface Expression? Oral Presentation given to the Spinal Cord Injury Team, Robarts Research Institute. 2006.